Integration of transport pathways in *Saccharomyces cerevisiae*

by

Jesper Johansen

Master of Science, University of Southern Denmark, 2008

Thesis Submitted in Partial Fulfillment of the
Requirements for the Degree of
Doctor of Philosophy

in the
Department of Molecular Biology and Biochemistry
Faculty of Science

SIMON FRASER UNIVERSITY

Spring 2017

Approval

Name: **Jesper Johansen**

Degree: **Doctor of Philosophy**

Title: ***Integration of transport pathways in Saccharomyces cerevisiae***

Examining Committee: **Chair:** Peter Unrau
Professor

Dr. Christopher Beh
Senior Supervisor
Associate Professor

Dr. Nicholas Harden
Supervisor
Professor

Dr. Michel Leroux
Supervisor
Professor

Dr. Michael Silverman
Internal Examiner
Associate Professor
Biological Sciences

Dr. Christopher Loewen
External Examiner
Associate Professor
Cell and Developmental Biology
University of British Columbia

Date Defended/Approved: February 28, 2017

Abstract

Plasma membrane (PM) homeostasis is essential for viability and depends on maintaining a constant balance between the amount of membrane material arriving at the cell cortex and the amount recycled. This membrane transport is mediated by two distinct mechanisms: (i) vesicular transport, utilizing membrane-enclosed vesicles for bulk transport of membrane proteins and lipids; and (ii) non-vesicular lipid transport. While the molecular mechanisms of these processes are well defined, they are generally considered independent events but how they are integrated is poorly understood. To gain insight into how these transport pathways are coordinated at the PM, three avenues of research were conducted using a combination of genetic, biochemical and live-cell microscopy assays. First, I showed that the Oxysterol-binding protein-related protein (ORP) Osh4p, implicated in non-vesicular sterol transfer, was found to associate with exocytic vesicles and formed complexes with regulators of polarized exocytosis, including the small GTPases Sec4p, Cdc42p, and Rho1p. Second, I tested the function of the evolutionarily conserved endoplasmic reticulum (ER)-associated protein Arv1p, also suggested to be involved in non-vesicular sterol transfer. Ultimately Arv1p was found to be dispensable for sterol exchange between the ER and PM but instead it was shown to play an important role in maintaining ER ultrastructure; Arv1p might be involved in regulating insertion of tail-anchored proteins into membranes. Finally, the essential yeast Rab GTPase Sec4p, principally known to be a key regulator of exocytosis, was shown to mechanistically couple polarized exocytosis with cortical actin polymerization, which activates Las17p (the yeast Wiskott–Aldrich syndrome [WASp])-dependent endocytosis. Las17p activation results in actin filament nucleation, which pulls the PM inward for endocytic vesicle biogenesis. Sec4p thereby represents the first direct regulatory link that couples exocytosis and endocytosis, which we termed "yeast compensatory endocytosis." By identifying novel mechanisms that coordinate intracellular transport pathways, these studies provided important new insights into how PM homeostasis is regulated and maintained.

Masters theses are a maximum of 150 words; doctorates, 350 words.

Keywords: Yeast compensatory endocytosis; Non-vesicular transport; Transport pathway integration; *SEC4*; *OSH4*; *ARV1*

Dedication

Til minde om Ann Margrethe Johansen

Acknowledgements

First, I would like to thank my senior supervisor, Dr. Christopher Beh. Without his mentorship and support throughout this project, with all its ups and downs, I may not have made it. I have really enjoyed our many conversations about science and will always remember the many lessons he has taught me. I also want to thank him for his unwavering support he has shown me during my darkest hours.

I also extend great gratitude towards Dr. Nancy Hawkins who has been an un-official supervisor during my thesis. She was always there with words of encouragement and support when needed and I have always valued our discussions during lab meetings and when really important results came along, she was often the fist to learn.

I would also like to thank my two supervising committee members, Dr. Nicholas Harden and Dr. Michel Leroux. They both provided extremely helpful advice throughout my project and were always ready to listen to crazy ideas or give support whenever that was needed. Without their guidance, the project may not have been finished in the manner it was.

I would also like to thank my Internal Examiner, Dr. Michael Silverman, who always has shown great interest in my work and was always ready with some non-yeast input on my progress.

Last but not least I would like to thank my External Examiner, Dr. Chris Loewen, for taking the time to lend his expertise on this project and for sharing a beer or two at loon lake and other enjoyable occasions. Talking science is always better with a cold beverage in hand.

This project would not have been completed without the endless support of the Hawkins/Beh lab, members past and present. Thank you for always helpful advice and making the lab an enjoyable place to work. I would specifically like to thank Dr. Gabriel Alfaro, Lauren Fullerton and Evan Quon for their contributions to this work and help with this thesis.

I also want to thank Dr. Kyla Hingwing and Hamida Safi for all of their support during the years. Without them life in the lab would have been a lot less enjoyable.

I'd like to thank Dr. Victor Jensen for helping with proofreading some of this thesis, the many many MANY scientific discussions we have had over the years, and mostly for his friendship. Looking forward to the next beer trip. Hopefully it will be in Calgary.

Lastly, I would like to thank my family for their unconditional love and support. Thanks to my father for flying across the globe for being here today. I also want to thank Mariam for giving me the final push through this process. Without her love and constant encouragement, I am not sure that I would have made it through the last stretch.

Table of Contents

Approval ii
Abstract iii
Dedication v
Acknowledgements vi
Table of Contents viii
List of Tables xii
List of Figures xiii

Chapter 1. Introduction 1
1.1. FOREWORD: Cell growth requires the integration of multiple transport pathways controlling cell surface expansion 1
1.2. PM homeostasis involves several distinct mechanisms for the trafficking molecular cargo to-and-from the cell cortex 2
1.2.1. Vesicular transport by exocytosis and endocytosis controls bulk lipid and membrane protein transport to-and-from the PM 3
1.2.2. Polarized exocytosis directs newly synthesized membrane components to the PM for the formation of the budding daughter cell. 4
1.2.3. Endocytosis provides a vesicular transport pathway to remove bulk lipids and proteins from the PM 12
1.2.4. Non-vesicular lipid transfer provides an alternative lipid transport mechanism to vesicular transport for moving lipids to-and-from the cell cortex 17
1.2.5. Sterols are transported to the PM by non-vesicular transfer forming PM microdomain lipid rafts with sphingolipids. 21
1.2.6. Phosphatidylserine concentration gradient between the PM and ER is maintained by non-vesicular trafficking 25
1.3. Mechanistic integration of membrane transport pathways is required for PM homeostasis 28
1.3.1. Integrating exocytosis with endocytosis by compensatory endocytosis 28
1.3.2. Compensatory endocytosis in Xenopus is mediated by stabilizing exocytic vesicles on the PM with an actin coat during Kiss-and-coat 29
1.3.3. Maintenance of constant cell volume at synapses active zones require rapid compensatory endocytosis 31
1.3.4. Compensatory endocytosis might be a general mechanism for PM homeostasis maintenance in all metazoan cells. 34
1.3.5. Preliminary evidence hints at the existence of compensatory endocytosis in yeast. 35
1.4. Lipids regulate both vesicular and non-vesicular trafficking directly 35
1.4.1. PIPs regulate both membrane structure and trafficking directly at the PM 36
1.4.2. Sterols and sphingolipids generate lipid rafts in the PM that affect membrane structure and regulate lipid trafficking events 41

1.4.3. Phospholipid asymmetry is essential for membrane function and may regulate transport at the PM 45
1.5. Lipid-binding proteins directly regulate vesicular and non-vesicular trafficking 46
1.5.1. ORPs are putative non-vesicular transport proteins implicated as regulators of vesicular transport 47
1.5.2. Sec14p: Proposed lipid transfer protein that regulates TGN vesicle biogenesis by regulating membrane lipid composition 49
1.5.3. Integral ER membrane protein Arv1p is proposed to mediate ER to PM sterol transfer 50
1.6. Potential transport integrators. What does it take for lipids or proteins to be considered transport integrators? 50
1.6.1. PIPs and lipid rafts regulate multiple transport pathways but are they transport integrators? 51
1.6.2. Lipid binding proteins and small Rab GTPase cascades integrate vesicular trafficking? 52

Chapter 2. The Sterol-Binding Protein Kes1/Osh4p is a Regulator of Polarized Exocytosis 54
2.1. Results 57
2.1.1. Docking of exocytic vesicles is defective in cells lacking functional Osh proteins 57
2.1.2. Osh4p associates with vesicles targeted to sites of polarized growth 61
2.1.3. Osh4p association with polarized exocytic vesicles is SEC6-dependent 63
2.1.4. Osh4p forms complexes with exocyst-associated proteins 64
2.1.5. The Osh4(Y97F)p sterol-binding mutant increases Osh4p activity causing lethality 68
2.1.6. The dependence of Sec4p and Osh4p localization on sterols 73
2.1.7. Sterols affect OSH4 regulation of SAC1 lipid signaling 75
2.2. Discussion 78
2.2.1. Osh4p is directly involved in exocyst-dependent vesicle docking 79
2.2.2. The role of sterols in Osh4p regulation of vesicular and nonvesicular transport 80
2.2.3. A model for Osh4p activities during vesicle docking 82
2.3. Materials and Methods 84
2.3.1. Strains, plasmids, microbial and genetic techniques 84
2.3.2. Fluorescence microscopy and live cell imaging 85
2.3.3. Analyses of yeast in vivo protein-protein interactions 86
2.4. Acknowledgments 88
2.5. Supporting Information 89
2.5.1. Supplemental Figures 92

Chapter 3. PM and ER membrane organization is affected by Arv1 but intracellular sterol transport is not 98
3.1. Results and Discussion 100

3.1.1. Arv1 is localized to the cortical ER 100
3.1.2. Characterization of S. cerevisiae arv1Δ cells 102
3.1.3. Dehydroergosterol (DHE) is transported from the PM to the ER and lipid droplets in arv1Δ cells 105
3.1.4. Ergosterol is transported from the ER to the PM in arv1Δ cells 108
3.1.5. Altered PM lipid organization in arv1Δ cells 110
3.1.6. Cortical and cytoplasmic ER defects in arv1Δ cells 112
3.2. Summary 115
3.3. Materials and Methods 117
3.3.1. General 117
3.3.2. Drug sensitivity tests 117
3.3.3. Fluorescence microscopy 118
3.3.4. Immunoblot analysis 118
3.4. Acknowledgements 119

Chapter 4. Polarized Exocytosis Induces Compensatory Endocytosis by Sec4p-Regulated Cortical Actin Polymerization 122
4.1. Abstract 122
4.2. Introduction 123
4.3. Results 126
4.3.1. Sec4p is Recruited to Nascent Cortical Actin Patches to Promote Their Assembly 126
4.3.2. Sec4p Interacts in vitro and in vivo With Actin Patch Subunits 131
4.3.3. Actin Patch Subunits Have Reciprocal Effects on Sec4p and Polarized Exocytosis 135
4.3.4. Sec4p Polarization Affects Actin Patch Polarization 137
4.3.5. Sec4p Overrides Sla1p Inhibition of Las17p-Dependent Actin Polymerization in vitro 141
4.4. Discussion 144
4.5. Materials and Methods 148
4.5.1. Strains and Plasmids 148
4.5.2. Fluorescence microscopy 148
4.5.3. Image analysis 149
4.5.4. BiFC protein interaction assays 150
4.5.5. in vitro protein binding assays and Bgl2p polarized exocytosis assay 151
4.5.6. in vitro pyrene-actin polymerization assay and affinity purification of fusion proteins 152
4.5.7. Statistical Analysis 153
4.6. Acknowledgements 153
4.7. Supporting Information 153
Supplemental Movies and Legends 156

Chapter 5. Discussion 159
5.1. ORPs are regulators of vesicular and non-vesicular transport but mechanisms remain elusive 159

5.2. Arv1p potentially regulates proper lipid raft formation by maintaining ER ultrastructure. 162
5.3. Implications of the discovery of yeast compensatory endocytosis and open questions 164
5.4. Concluding remarks 167

References 169

Appendix A: List of Genes 213

Appendix B: List of Video Files 234

List of Tables

Table 2.1S. *S. cerevisiae* strains used……89

Table 2.2S. Plasmids used……...91

Table 3.1S. Yeast strains used in this study……..……..120

Table 3.2S. Plasmids used in this study…….....121

Table 3.3S. Sterol, steryl ester and phospholipid content of wild-type and *arv1*Δ cells……..…….121

Table 4.1S. *S. cerevisiae* strains used in this study……153

Table 4.2S. Plasmids used in this study……155

List of Figures

Figure1.1. Cartoon showing major transport pathways affecting PM homeostasis and potential mechanistic integration of these pathways…….3

Figure 1.2 Schematic of yeast polarized exocytosis……5

Figure1.3. Temporal recruitment of proteins to actin patches results in membrane morphology modification, invagination and vesicle fission from the PM..13

Figure1.4. Proposed models of non-vesicular lipid transfer between the ER and the PM……...19

Figure 1.5 Cartoon of the proposed PM-ER tether in yeast…….20

Figure1.6. Osh protein structure and crystal structure of Osh4p in lipid-bound states....23

Figure 1.7. Proposed mechanism for PS and PI(4)P exchange at PM-ER membrane contact sites in yeast and mammals……..25

Figure1.8. Membrane mixing induces F-actin-dependent stabilization of cortical granules during kiss-and-coat compensatory endocytosis…….30

Figure 1.9. Neuronal compensatory endocytosis: one mechanism, two models……..32

Figure 1.10. Schematic of the primary PIP species at the yeast PM and the proteins regulating their levels……....37

Figure 1.11 Schematic model for the Ypt31/32p Rab GTPase cascade regulating vesicle transport in yeast……...40

Figure1.12. Model of lipid raft structures in the yeast PM…….41

Figure1.13 Phospholipid distribution of the PM……..45

Figure 2.1. Localization and lifespan of exocyst-associated subunits in cells lacking *OSH* gene function……60

Figure 2.2. Osh4p resides on vesicles targeted to sites of polarized growth……...62

Figure 2.3. Osh4p-YFP localization on motile (vesicle) particles was disrupted in *sec6-4*^{ts} cells……...64

Figure 2.4. Osh4p interacts with exocyst complex-associated proteins……67

Figure 2.5. Osh4(Y97F)p is constitutively active and dominant-lethal……...70

Figure 2.6. *OSH2*^{Y963F} is not dominant-lethal……72

Figure 2.7. GFP-Sec4p and Osh4p-YFP mislocalization after sterol depletion……74

Figure 2.8. *SAC1* deletion suppresses growth defects caused by increased *OSH4* expression or by the *OSH4*^{Y97F} dominant activated allele……..77

Figure 2.1S. Osh4p co-fractionates with markers of polarized exocytic vesicles in *sec6-4* cells……..92

Figure 2.2S. P^{MET3}-*OSH4*^{Y97F} expression from a low-copy (*CEN*) plasmid produced Osh4(Y97F)p at comparable levels to endogenous Osh4p……..95

Figure 2.3S. Increased dosage of *OSH4* exacerbated growth defects of conditional *MYO2* mutants……...96

Figure 2.4S. Anti-Bgl2p antibody production……97

Figure 3.1. Arv1 – membrane topology and subcellular localization……101

Figure 3.2. Characterization of *arv1*Δ cells……...103

Figure 3.3. DHE transport from PM to ER……106

Figure 3.4. Ergosterol transport from ER to PM.....109

Figure 3.5. Drug sensitivity tests……111

Figure 3.6. Cortical ER organization is disrupted in *arv1*Δ cells……113

Figure 3.7. Tail-anchored ER integral membrane proteins in *arv1*Δ cells……....115

Figure 4.1. Spatial and temporal co-localization of Sec4p with actin patch subunits during actin patch assembly……..128

Figure 4.2. Mutations in *SEC4* and *SEC2* disrupt actin patches assembly and proper endocytic internalization……130

Figure 4.3. Physical interaction of Sec4p with actin patch subunits……133

Figure 4.4. Reciprocal effects of endocytosis on polarized exocytosis……...136

Figure 4.5. Actin patch polarization is affected by Sec4p polarization……139

Figure 4.6. GTPγS-Sec4p overrides Sla1p inhibition of Las17p-dependent actin nucleation *in vitro*……143

Figure 4.7. Sec4p overrides the inhibition of cortical actin polymerization to induce compensatory endocytosis……144

Figure 5.1. Schematic of current understanding of transport pathway integration in yeast……..168

Chapter 1. Introduction

1.1. FOREWORD: Cell growth requires the integration of multiple transport pathways controlling cell surface expansion

Maintaining a constant cell size requires a balance between the flux of newly synthesized proteins and lipids going out to the PM, and those components being brought back into the cell for recycling. In addition to the secretory vesicles that move membrane cargo back and forth, other non-vesicular mechanisms transfer specific lipids directly between membranes. Despite functional links between these transport pathways, they are generally considered independent processes. How a balance is struck between all of these pathways, and whether it involves a direct regulatory mechanism to integrate these events, is unclear. Under specific conditions, some specialized cell types induce membrane internalization and recycling to compensate for the delivery of newly synthesized membrane material. Do these specialized examples extensions of other general regulatory mechanisms that coordinate PM trafficking pathways to control PM expansion? As detailed in this thesis, the goal of my research was to identify regulatory factors that coordinate vesicle trafficking pathways and to test candidate proteins to establish their role in how sterol lipids are exchanged between intracellular membranes. Using yeast molecular genetics, live cell microscopy, and *in vitro* and *in vivo* assays, novel regulators of membrane trafficking were identified and new mechanisms were determined for how seemingly separate transport pathways are integrated at the PM[1].

[1] A full list of genes discussed in this thesis can be found in Appendix A

1.2. PM homeostasis involves several distinct mechanisms for the trafficking molecular cargo to-and-from the cell cortex

Because lipids and membrane-bound proteins are insoluble in the aqueous cytoplasm, they depend on specific intracellular transport mechanisms to move them from their site of synthesis to their membrane destinations. To achieve this, membrane cargo is transported to and from the PM by two distinct general mechanisms: i) Vesicular trafficking, where membrane-enclosed vesicles transport lipids and proteins to-and-from the PM; or ii) Non-vesicular transport, which mediates lipid transfer independently of vesicles. Since PM homeostasis relies on the balance between these transport processes, it is crucial for cell viability that they are functionally and potentially mechanistically linked (figure 1.1). To identify protein or lipid factors that integrate these pathways, a detailed understanding of the molecular machinery involved in both vesicular and non-vesicular transport must be obtained.

Figure1.1. Cartoon showing major transport pathways affecting PM homeostasis and potential mechanistic integration of these pathways.

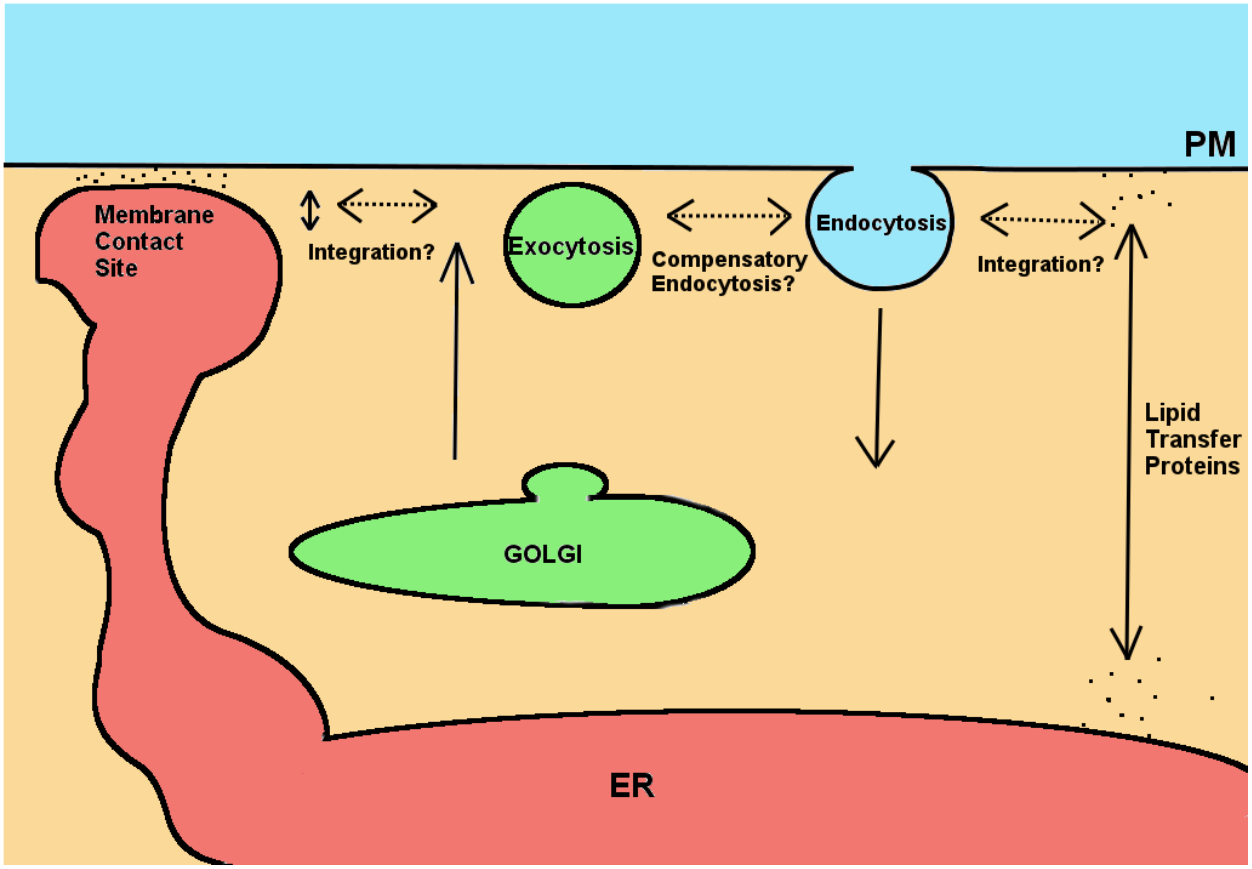

Potential integration of major transport routes at the PM in yeast. Solid arrows represent the direction of vesicular transport relative to the PM during endocytosis and exocytosis. Bidirectional arrows indicate proposed sites for non-vesicular transport affecting the PM mediated by proteins (black spots) between the ER and PM in the cytosol and at membrane contact sites. Dashed arrows represent potential mechanistic integration between transport pathways assayed in this thesis. This figure was drawn by J.J

1.2.1. Vesicular transport by exocytosis and endocytosis controls bulk lipid and membrane protein transport to-and-from the PM

Vesicular transport is the main mechanism for bulk lipid and protein transport between biological membranes. It involves a sequential series of regulated steps resulting in the generation, transport and fusion of membrane-enclosed vesicles with a cellular membrane of destination. Each transport step is mediated and regulated by distinct protein complexes, ensuring tight control of the process. First, proteins are

recruited to the site of vesicle biogenesis where lipids and proteins destined for transport are modified. These modifications result in membrane excision and release of these membrane protrusions result in vesicle formation. After vesicle biogenesis, small GTPases stimulate myosin motors to facilitate vesicular transport along the cytoskeleton to a destination, which is dictated by protein targeting complexes aboard the vesicle. Upon arrival, the vesicle docks and fuses with the acceptor membrane in a process that is facilitated by SNARE proteins and tethering complexes. For decades, yeast has been used to study vesicular transport of membrane material from the trans-Golgi network (TGN) to the PM (exocytosis) and the reciprocal internalization of excess membrane material during endocytosis. Decades of studies have provided a detailed understanding of the molecular machinery regulating these processes in yeast.

1.2.2. Polarized exocytosis directs newly synthesized membrane components to the PM for the formation of the budding daughter cell.

During yeast cell division, exocytic vesicles are specifically targeted to the tip of the growing bud by polarized exocytosis. This constitutes the major pathway for moving membrane material from the mother cell to the bud resulting in cellular growth. Polarized exocytosis is a tightly regulated process that can be divided into three steps: i) vesicle biogenesis at the TGN, ii) vesicle transport and targeting and iii) tethering and fusion of the vesicle to the PM (Figure 1.2). Each of these steps requires the activity of multiple proteins and lipid modifications.

Figure 1.2 Schematic of yeast polarized exocytosis.

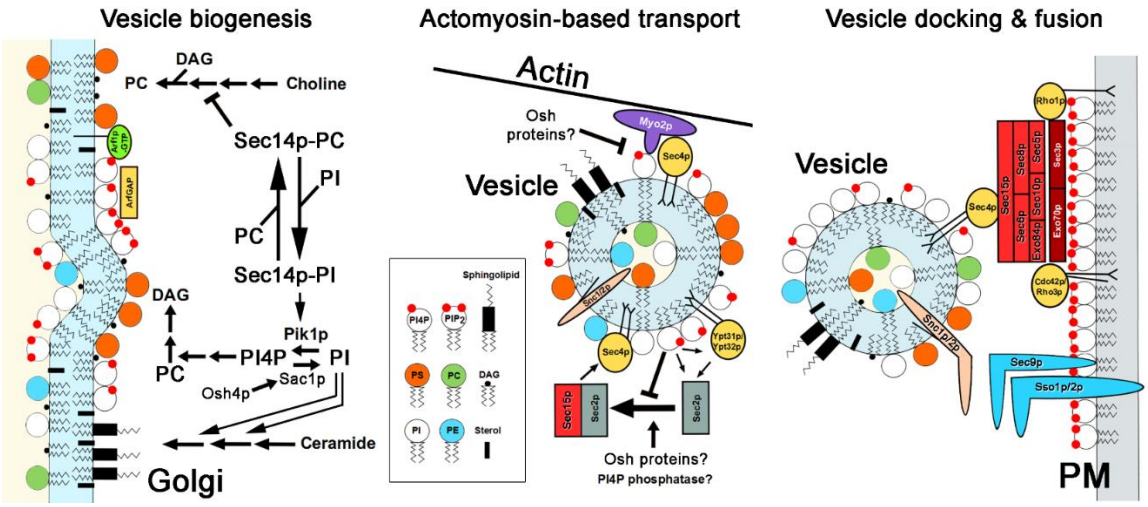

During vesicle biogenesis (left) Sec14p-dependent regulation of lipid metabolism both stimulates DAG synthesis and inhibits DAG consumption as a precursor in PC production. As a precursor for the synthesis of PI-containing complex sphingolipids, PI is used in complex sphingolipid production at the expense of DAG production. Concentrated with sterols, de novo synthesized sphingolipids form membrane microdomains that recruit membrane proteins for exocytosis. In transit between the Golgi and PM (center), vesicles move along actin filaments propelled by a type V myosin (Myo2p). Myo2p interaction with vesicles is dependent in part on PI(4)P as is the reconfiguration of small GTPases (yellow) required for the assembly of vesicle-associated exocyst complex subunits (light red). At the interface between the PM and vesicle membrane (right), Rho GTPases and exocyst complex subunits associated with the PM (dark red) via $PI(4,5)P_2$ assemble with the vesicle-bound exocyst complex subunits to facilitate vesicle docking at sites of polarized growth. Membrane fusion follows after v-SNAREs (tan) and t-SNAREs (blue) interactions. (Johansen, Ramanathan, & Beh, 2012)

Generally, vesicle biogenesis involves the assembly of a protein lattice which coats the forming vesicle during membrane deformation and vesicle scission (Figure 1.2) (Faini, Beck, Wieland, & Briggs, 2013). However, no coat protein has yet been identified during exocytic vesicle biogenesis at the TGN in yeast, making it unique amongst vesicular transport events (Paczkowski, Richardson, & Fromme, 2015). Instead, the ebb and flow of lipid precursors through competing biosynthetic pathways largely controls the generation of secretory vesicles emanating from the Golgi (Fig. 1.2). The structural changes in the Golgi bilayer that initiate membrane curvature for vesicle budding are dictated in part by the dynamic balance between DAG production and DAG consumption in the production of PC. Inclusion of membrane proteins into nascent vesicles is in part dependent on the balance of PI incorporation into complex sphingolipids versus the generation of PI(4)P and other phosphoinositides (PIPs). The PI/PC transfer protein

Sec14p plays a pivotal role acting as a traffic cop directing lipid flux through these metabolic pathways (Bankaitis, Aitken, Cleves, & Dowhan, 1990; Bankaitis, Malehorn, Emr, & Greene, 1989; Henneberry, Lagace, Ridgway, & McMaster, 2001; Kearns et al., 1997; Mousley, Tyeryar, Vincent-Pope, & Bankaitis, 2007; Routt & Bankaitis, 2004; Skinner et al., 1995). At the Golgi, Sec14p integrates PI, PC, DAG, and complex sphingolipid metabolism, and as a result Sec14p inactivation blocks exocytosis during post-Golgi vesicle biogenesis (Fig. 1.2).

Sec14p, which is essential for exocytosis and yeast growth, is dispensable if DAG is exogenously supplemented to cells (Henneberry et al., 2001; Kearns et al., 1997). This result suggests that Sec14p increases levels of DAG, but this simple outcome belies the complexity of Sec14p-dependent regulation. Sec14p is proposed to have a dual function in DAG production depending on whether it is bound to PI or PC (Fig. 1.2). When bound to PC, Sec14p appears to inhibit choline-phosphate cytidyl transferase (Pct1p), the rate-limiting enzyme in PC biosynthetic pathway that consumes DAG as a precursor for PC synthesis (Skinner et al., 1995). In this way, Sec14p might increase DAG, thought to be a “pro-secretory” lipid, while at the same time decreasing PC, an “anti-secretory” lipid (Mousley et al., 2007; Routt & Bankaitis, 2004). Due to its small head-group and long hydrophobic acyl chains, the cone-shape of DAG is predicted to affect the local curvature of the Golgi bilayer in proximity to DAG-enriched domains (Allen, Thomas, & Michell, 1978; Helfrich, 1973; Kearns, Alb Jr, & Bankaitis, 1998). The structural deformation of the membrane at these sites might promote vesicle membrane budding. In contrast, the cylindrical shape of PC is hypothesized to resist membrane deformation and inhibit vesicle formation. When bound to PI, Sec14p appears to stimulate the PI 4-kinase Pik1p to generate more PI(4)P for conversion into PI(4,5)P_2. PI(4,5)P_2 activates Spo14p, phospholipase D, which represents another mechanism for decreasing PC and its potentially anti-secretory effects (Xie et al., 1998). Spo14p hydrolyses PC to form choline and phosphatidic acid (PA), which can be metabolized into DAG. Thus, it is possible that Sec14p-PC and Sec14p-PI both tilt the dynamic balance of lipids towards DAG at the expense of PC (Sreenivas, Patton-Vogt, Bruno, Griac, & Henry, 1998).

An alternative mechanism by which DAG might affect vesicle formation is through the recruitment and activation of Gcs1p, an ARF-GAP (ADP-ribosylation factor GTPase-activating protein) implicated in vesicle scission from the Golgi. Gcs1p acts together with other ARF-GAPs, Age1p and Age2p, to regulate the small GTPase Arf1p (Poon, Nothwehr, Singer, & Johnston, 2001; Yanagisawa et al., 2002), which in turn "primes" vesicle formation by recruiting cargo and other regulators of vesicle transport (Springer, Spang, & Schekman, 1999). DAG stimulates the GAP activity of Age1p and Gcs1p *in vitro* (Benjamin et al., 2011; Yanagisawa et al., 2002), and exocytosis defects in *GCS1* and *AGE2* mutant cells are rescued by the exogenous addition of DAG (Wong et al., 2005). Based on these findings, it is proposed that DAG-induced membrane curvature might recruit and activate ARF-GAP activity at the Golgi (Wong et al., 2005).

Although it might appear that DAG is a key lipid regulator of Sec14p-dependent vesicle formation (Kearns et al., 1997), other reports suggest that the essential requirement for *SEC14* can be bypassed without increasing cellular DAG levels (Stock, Hama, DeWald, & Takemoto, 1999). On the other hand, PI(4)P levels are reduced by ~45% when *sec14*^{ts} cells are cultured at elevated temperature (Hama, Schnieders, Thorner, Takemoto, & DeWald, 1999). This result suggests that PI(4)P is an important lipid species for Sec14p-dependent vesicle biogenesis (Stock et al., 1999). Consistent with this suggestion, the deletion of *SAC1*, which encodes an ER/Golgi PI(4)P phosphatase, rescues the lethality of *SEC14*-inactivating mutations (A. E. Cleves, Novick, & Bankaitis, 1989; Kearns et al., 1997). In *SEC14*-defective cells, the elimination of *SAC1* results in elevated PI(4)P levels but, unexpectedly, cellular DAG levels are unchanged suggesting rescue of *SEC14* mutants is DAG-independent (Stock et al., 1999). (Although this finding does not preclude the possibility that localized increases in DAG levels within the Golgi membrane induce vesicle biogenesis). PI(4)P levels might also affect the ARF-GAPs Gcs1p and Age1p, which contain general lipid-binding domains that bind PIPs including PI(4)P (Benjamin et al., 2011; Wong et al., 2005), a homologous domain can also be found within Age2p. These results suggest that ARF-GAP activities might be affected by PIPs. In addition to PI(4)P, *SEC14*-defective cells accumulate ~3-fold more complex sphingolipid precursors, in which levels of very long chain ceramides are particularly elevated (Mousley et al., 2008). Given the broad changes in lipid composition in cells lacking *SEC14* function, it is likely that the observed

defects in vesicle formation is the collective effect of changes in the distribution and synthesis of several lipids.

In addition to regulated changes in lipid metabolism and membrane composition within specific membrane domains at the Golgi, vesicle formation also depends on the maintenance of trans-bilayer lipid asymmetry. Phosphatidylserine (PS) is synthesized within one leaflet of the ER bilayer but it equilibrates between leaflets (van Meer, Voelker, & Feigenson, 2008). When PS arrives at the Golgi membrane, it is restricted to the cytoplasmic membrane leaflet by the P-type ATPase phospholipid flippase Drs2p and its Cdc50p chaperone. Drs2p thereby maintains Golgi bilayer asymmetry, which is functionally linked to Arf1p-dependent vesicle budding; mutations in either *CDC50* or *DRS2* are synthetically lethal with *ARF1* (C. Y. Chen & Graham, 1998). Disruption of Drs2p or Cdc50p results in exocytosis and polarization defects and the accumulation of aberrant membrane structures (Sophie Chen et al., 2006; Gall et al., 2002). A possible mechanism for how PS asymmetry affects vesicle biogenesis involves the induction of localized membrane curvature, as predicted by the bilayer couple hypothesis (Sheetz & Singer, 1974). Membrane curvature might also promote ARF-GAP recruitment. Consistent with this model, the deletion of *DRS2* is synthetically lethal with *gcs1*Δ (M. Robinson et al., 2006), perhaps indicating a functional interaction required for post-Golgi vesicle formation. The involvement of a lipid flippase in the initial stages of exocytosis suggests that vesicle formation requires modulations in both *cis* and *trans* organization of the lipid bilayer.

Even before their release from the Golgi, nascent vesicles are attached to the type V myosin Myo2p, which is recruited via the Rab GTPases Ypt31p/32p and by PI(4)P (Fig. 1.2) (Jedd, Mulholland, & Segev, 1997; Y. Jin et al., 2011; Lipatova et al., 2008). As Myo2p-dependent transport proceeds and vesicles are moved along actin filaments to the bud, the small GTPase Sec4p displaces Ypt31p/32p (Y. Jin et al., 2011; Santiago-Tirado, Legesse-Miller, Schott, & Bretscher, 2011). Although important for the proper regulation of actomyosin transport, this GTPase cascade is dispensable if the interaction between Myo2p and PI(4)P is augmented. By replacing the GTPase-binding C-terminal tail of Myo2p with an additional PI(4)P-binding PH domain, small GTPases

are no longer required for Myo2p-dependent vesicle transport (Santiago-Tirado et al., 2011). Consistent with these results, increased PI(4)P levels can also negate the inhibitory effects of overexpressing the C-terminal tail of Myo2p. This tail region competes for Sec4p and Ypt31p/32p binding with the endogenous wild-type Myo2p but increasing Pik1p production of PI(4)P restores Myo2p association with vesicles (Santiago-Tirado et al., 2011).

In addition to the recruitment of Myo2p to vesicles, PI(4)P affects the protein interactions of Ypt31p/32p and Sec4p during the priming of the vesicle-associated subunits of the exocyst complex, which is required for subsequent vesicle docking with the PM (Mizuno-Yamasaki, Medkova, Coleman, & Novick, 2010). A critical event in this priming occurs when the Sec2p GEF (guanine-nucleotide exchange factor), originally recruited to vesicles and bound by Ypt31p/32p, switches its binding to the exocyst subunit Sec15p. With this exchange of binding partners, the Sec2p GEF is then free to activate Sec4p-GTP for the assembly of the other vesicle-associated exocyst complex subunits (Mizuno-Yamasaki et al., 2010; Ortiz, Medkova, Walch-Solimena, & Novick, 2002). Although it is not fully understood, a drop in vesicle PI(4)P levels triggers Ypt31p/32p release of Sec2p, and the subsequent Sec4p-dependent GTPase signaling cascade then ensues (Mizuno-Yamasaki et al., 2010). Sec4p and Sec2p recruiting Sec15p to the vesicle allows for subsequent assembly of the exocyst complex, which serves as a targeting complex, directing the vesicle to the PM (Salminen & Novick, 1989).

The exocyst complex is an evolutionary well-conserved multimeric protein complex composed of the eight subunits (Sec3p, Sec5p, Sec6p, Sec8p, Sec10p, Sec15p, Exo70p, and Exo84p) and plays an essential role in targeting exocytic vesicles to the PM (Guo, Roth, Walch-Solimena, & Novick, 1999; TerBush & Novick, 1995). The exocyst complex initially assembles in two distinct subcomplexes, one of which associates with the vesicle while the other is bound to the PM. The vesicle-bound exocyst complex is physically associated with the vesicle though Sec15p and consists of Sec5p, Sec6p, Sec8p, Sec10p, and Exo84p (He & Guo, 2009). The PM-bound exocyst serves as a targeting beacon for vesicle transport and ultimately serves as a docking site for the vesicle. The polarized localization of the PM-associated exocyst complex

subunits, Exo70p and Sec3p, is dependent on direct interactions with PI(4,5)P_2. Sec3p and Exo70p polarization is also dependent on the Rho GTPase Cdc42p, restricting the PM-bound exocyst to the tip of the bud (Fig. 1.2) (Boyd, Hughes, Pypaert, & Novick, 2004; Hamburger, Hamburger, West, & Weis, 2006; He, Xi, Zhang, Zhang, & Guo, 2007; J. Liu, Zuo, Yue, & Guo, 2007; Wu & Brennwald, 2010; Yamashita et al., 2010; Zhang et al., 2008). Overexpression of the PI(4)P 5-kinase Mss4p increases PI(4,5)P_2 levels and partially rescues the temperature-sensitive growth defects of *cdc42-6* cells at elevated temperatures, suggesting that PI(4,5)P_2 and Cdc42p define two independent mechanisms for recruiting exocyst complex subunits to the PM (Yakir-Tamang & Gerst, 2009). However, it is not known if increased PI(4,5)P_2 levels can completely bypass the Cdc42p requirement for recruiting Sec3p and/or Exo70p to the PM. In addition, the Sec14p-related PI-transfer protein Sfh5p promotes Cdc42p activity at the PM by extracting PI from exocytic vesicles then presenting it to Stt4p (PI 4-kinase) and Mss4p for conversion into PI(4,5)P_2 at the PM (Yakir-Tamang & Gerst, 2009). The PI(4,5)P_2 generated in this way is required for Cdc42p localization to sites of polarized exocytosis, though the exact mechanism is unclear (Yakir-Tamang & Gerst, 2009). In addition, PI(4,5)P_2 is required for localization of both Cdc24p, the PH domain-containing GEF that activates Cdc42p, and the Cdc42p effector Gic2p (G. C. Chen, Kim, & Chan, 1997; Orlando et al., 2008; J. W. Yu et al., 2004). PI(4,5)P_2 is, therefore, the key lipid at the PM for assembling exocytosis regulatory complexes.

Another Rho GTPase, Rho1p, also binds and promotes Sec3p polarized localization, whereas both Rho3p and Cdc42p bind Exo70p to mediate its polarization (Adamo et al., 2001; Adamo, Rossi, & Brennwald, 1999; He et al., 2007; N. G. Robinson et al., 1999; Wu & Brennwald, 2010; Wu, Turner, Gardner, Temple, & Brennwald, 2010; Zhang et al., 2001). Rom2p, the GEF for Rho1p, also binds PI(4,5)P_2 through a PH domain that is essential for Rom2p localization to sites of polarized growth and downstream activation of Rho1p (Anjon Audhya & Emr, 2002; Manning, Padmanabha, & Snyder, 1997). PI(4,5)P_2 is, therefore, a requirement for multiple different regulators and effectors for vesicle docking at the PM.

Like bilayer asymmetries in the Golgi membrane, lipid asymmetry across the PM bilayer also impacts exocytosis. PS is localized to incipient bud sites where it promotes

Cdc42p-dependent bud formation. Deletion of *CHO1*, encoding PS synthase, results in Cdc42p depolarized localization that is partially rescued by addition of lysoPS into the medium (G D Fairn, Hermansson, Somerharju, & Grinstein, 2011). PS, PI and PE are also required to initiate changes in the sites of polarized exocytosis during the yeast cell cycle, which are needed to support growth of the daughter bud. PS, PI and PE stimulate Cdc42p-GTP turn-over by the GAPs (GTPase-activating proteins) Rga1p/2p, which cause Cdc42p-GDP reorganization at the bud cortex to alter the direction of polarized growth and exocytosis (Saito et al., 2007). The Lem3p-Dnf1p and Lem3p-Dnf2p flippase complexes facilitate Cdc42p reorganization by flipping PE into the cytoplasmic leaflet of the PM bilayer, where PE activates Cdc42p GAPs (Saito et al., 2007). The flipping of PE into the cytoplasmic leaflet is also proposed to disrupt electrostatic interactions between a cationic region near the C-terminal end of Cdc42p and the negatively charged PS in the PM, thus aiding both Cdc42p extraction and its recycling from polarized membrane sites (Das et al., 2012). In contrast, $PI(4,5)P_2$ in the cytoplasmic leaflet of the PM bilayer appears to inactivate the Rga1p/2p GAPs, though it is not understood how (Saito et al., 2007).

The penultimate event in polarized exocytosis involves SNARE-mediated membrane fusion between the exocytic vesicle and its target at the PM. After arriving at the PM, the vesicle-bound sub-complex forms a tethering complex with the PM bound subcomplex, mediated vesicular docking. Subsequent fusion requires interactions between v-SNARE Snc1p/2p on vesicles with the syntaxins Sso1p/2p and t-SNARE Sec9p on the PM (Fig. 1.2). Sec6p regulates the interaction of the t-SNARE Sec9p with the syntaxins Sso1/2p by binding and repressing Sec9p function directly (Morgera et al., 2012). At the PM, Sec1p binds Sec6p, which releases Sec9p allowing it to bind Sso1p/2p and initiate SNARE-mediated fusion of the PM and vesicular membranes (Morgera et al., 2012). Sec1p also plays a role after SNARE complex assembly, suggesting it may have a role in vesicle fusion and/or SNARE interaction stabilization (Hashizume, Cheng, Hutton, Chiu, & Carr, 2009; Weber-Boyvat et al., 2016). After Sec9p/Sso1p complex formation, it can form a ternary complex with the v-SNARE Snc1p or Snc2p allowing for membrane fusion (Nicholson et al., 1998). Interestingly it has been shown that Sec4p also binds Sec9p during the fusion step, suggesting a role for Sec4p in regulating the last stages of exocytosis (Grosshans & Novick, 2008; Weber-Boyvat,

Aro, Chernov, Nyman, & Jäntti, 2011). The interaction between Sec4p and Sec9p is stabilized by the tomosyn proteins Sro7p and its homolog Sro77p (Grosshans & Novick, 2008; Hattendorf, Andreeva, Gangar, Brennwald, & Weis, 2007). After SNARE fusion has occurred the vesicle collapses into the PM resulting in membrane mixing and release of signaling factors out into the extracellular space.

As a final step of exocytosis, the exocyst complex is disassembled and released to the cytosol, except for Sec4p which remains attached to the PM via an N-terminal di-geranylgeranyl lipid modification (Garrett, Zahner, Cheney, & Novick, 1994). For the PM, the net result of exocytosis is an increase in proteins and lipids that affect membrane homeostasis and needs to be balanced by the removal of membrane material through endocytosis.

1.2.3. Endocytosis provides a vesicular transport pathway to remove bulk lipids and proteins from the PM

Endocytosis constitutes the major pathway for bulk protein and lipid retrieval from the PM and therefore plays an essential role in maintaining PM homeostasis. Endocytosis requires the sequential recruitment of proteins to the cytosolic leaflet of the PM. This recruitment results modifications to the cytoskeleton at the PM establishing the nascent endocytic sites. These modifications facilitate membrane internalization and vesicle fission. In yeast, endocytosis occurs at actin-rich sites on the cell cortex, known as actin patches (K. Kim et al., 2006) The establishment and maturation of actin patches is a highly regulated and coordinated process that can be divided into four phases (Figure 1.3): i) the early coat proteins assemble at the cell cortex (early coat phase), ii) the recruitment of late coat proteins and their regulatory proteins(late coat phase), iii) the late coat proteins help stimulate actin polymerization machinery resulting in actin polymerization and PM invagination (actin polymerization/invagination phase), and iv) the scission of the invaginated membrane (fission phase) (K. Kim et al., 2006; Skruzny et al., 2015). Intense research in yeast endocytosis over the last 15 years has resulted in a good understanding of the actin patch assembly and maturation processes on a molecular level.

Figure1.3. Temporal recruitment of proteins to actin patches results in membrane morphology modification, invagination and vesicle fission from the PM.

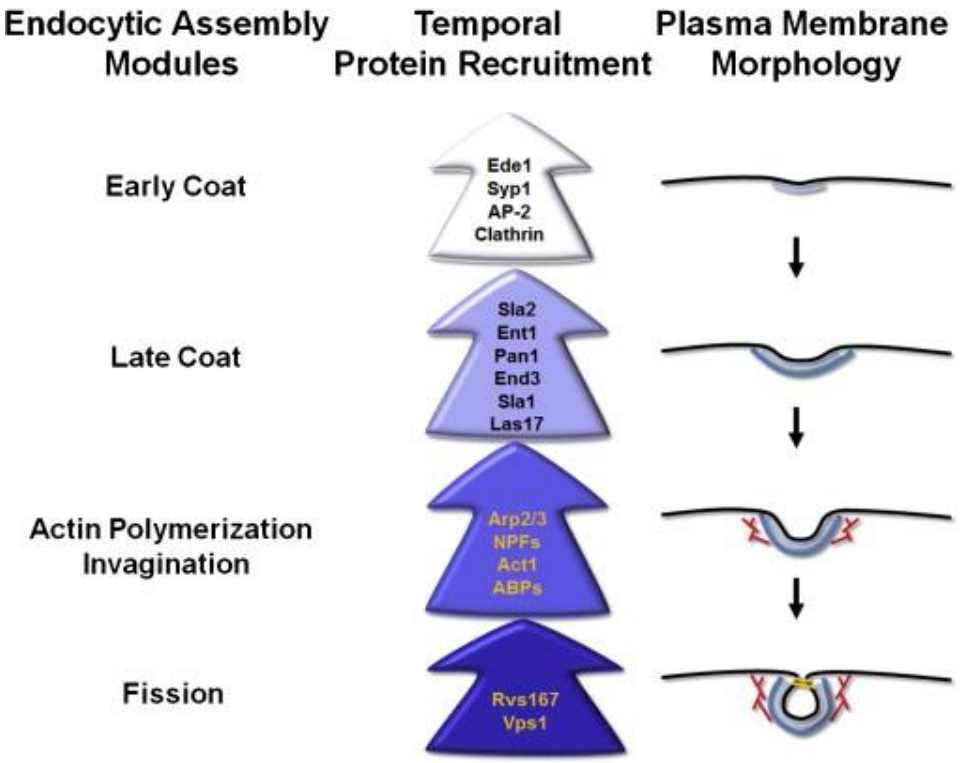

Diagram showing the temporal recruitment of actin patch components during each phase with a drawing showing the morphology of the plasma membrane during the respective stage. The blue shading in the diagram to the right indicates the coat, while red shows filamentous actin and orange indicate the amphiphysins Rvs161p and Rvs167p. This figure is adapted from (McDermott & Kim, 2015)

During the early coat phase of actin patch assembly, proteins are recruited to the PM. Here they act as scaffold proteins and help organize endocytic cargo, and early coat proteins into a complex that establishes the early actin patch. Early coat phase is initiated by the arrival of Ede1p and Syp1p, which are the yeast homologs of the metazoan Eps15 and FCHO1/2, respectively (Dores, Schnell, Maldonado-Baez, Wendland, & Hicke, 2010; Reider et al., 2009). PM Ede1p recruitment is believed to be mediated by ubiquitin-dependent binding of transmembrane proteins targeted for internalization (Boettner et al., 2009; Stimpson, Toret, Cheng, Pauly, & Drubin, 2009). However, studies do imply that Ede1p can initiate ubiquitin-independent endocytosis, however, the mechanism remains unclear (Aguilar, Watson, & Wendland, 2003). Syp1p binds Ede1p directly and interacts with the PM through its F-BAR domain which binds to

membranes with specific curvature (Aguilar et al., 2003; Reider et al., 2009). Upon their arrival, Ede1p and Syp1p stimulate the recruitment of clathrin by directly binding to its adaptor proteins Yap1801/2p and the adaptor complex AP-2 (Luo, Li, Yu, Kramer, & Cristea, 2010). Once recruited, clathrin forms a triskelion lattice on the PM surface (Pearse, 1975) which is believed to affect membrane curvature generating a clathrin-coated pit (figure 1.3) (Avinoam, Schorb, Beese, Briggs, & Kaksonen, 2015; Kukulski, Picco, Specht, Briggs, & Kaksonen, 2016). In mammals this clathrin pit serves as the scaffold for recruitment of additional protein complexes, however, the role of yeast adaptor proteins and clathrin during endocytosis remain controversial as clathrin or AP-2 knockout cells remain viable with only mild endocytic defects (Susheela Y. Carroll et al., 2009; Payne, Baker, Van Tuinen, & Schekman, 1988).

After actin patch assembly, it serves as a scaffold for the generation of an outer protein coat, which occurs during the late coat phase. The arrival of Sla2p, an endocytic adaptor to the actin patches initiates the late coat phase. This recruitment is mediated by the ANTH (AP180 N-Terminal Homology) domain of Sla2p and its physical interactions with clathrin and Ede1p (Gavin et al., 2002, 2006; Newpher & Lemmon, 2006; Wesp et al., 1997). After arriving, Sla2p interacts with the Epsin, Ent1p forming a $PI(4,5)P_2$-dependent ANTH/ENTH (Epsin N-Terminal Homology) domain dimer that initiates PM deformation.(Skruzny et al., 2012). The importance for Sla2p binding to $PI(4,5)P_2$ was underlined by the observation that deleting the ANTH domain in Sla2p causes depolarization of actin patch formation and reduced endocytosis, despite normal Sla2p localization (Sun, Kaksonen, Madden, Schekman, & Drubin, 2005). The Ent1p/Sla2p dimer serves as a scaffold that binds the actin cytoskeleton directly which stabilizes actin at actin patches. This binding is achieved through the Actin Cytoskeleton Binding (ACB) domain and Talin-HIP1/R/Sla2p Actin-Tethering C-terminal Homology (THATCH) domains of Ent1p and Sla2p respectively, attaching the actin patch directly to the actin cytoskeleton playing an important role in force generation during membrane invagination (Baggett, D'Aquino, & Wendland, 2003; Itoh et al., 2001; Skruzny et al., 2012; Yang, Ayscough, & Drubin, 1997). The interaction between the actin cytoskeleton and the actin patches promotes recruitment of the Pan1p/End3p/Sla1p heterotrimer, which generates an outer coat by binding to clathrin and the clathrin adaptor proteins. This suggests that Pan1p/End3p/Sla1p together with Sla2p/Ent1p may coordinate the assembly of actin

filaments with the maturing actin patch, prior to actin polymerization (Marko Kaksonen, Toret, & Drubin, 2006; Tang, Xu, & Cai, 2000). Studies indicate that Sla1p predominantly exists in a complex with Las17p, the yeast Wiskott–Aldrich Syndrome Protein (WASp) homolog. This results in Las17p inhibition upon actin patches arrival, suggesting that Las17p arrival is tightly linked to outer coat establishment (Feliciano & Di Pietro, 2012).

The actin polymerization/invagination phase is characterized by the activation of Las17p. Las17p is one of the best-characterized nucleation promoting factors (NPFs) that is recruited to actin patches and plays a direct role in stimulating the formation of filamentous actin (F-Actin). The activity of Las17p is tightly controlled through interactions with a number of SH3 containing proteins, including Sla1p, Pan1p, Bzz1p, and Myo3/5p. (Mirey, Soulard, Orange, Friant, & Winsor, 2005; A. A. Rodal, Manning, Goode, & Drubin, 2003; Spiess et al., 2013). The mechanism of how Las17p is released from inhibition remains unknown. In mammals, a major regulator of WASp activity is the Rho GTPase Cdc42, which regulates the actin machinery and endocytosis by controlling actin polymerization (Miki, Miura, & Takenawa, 1996; Rohatgi et al., 1999; Sharifai et al., 2014; Symons et al., 1996). However, since Las17p lacks a CRIB domain required for Cdc42p-Las17p interaction, Cdc42p can not be a regulator of Las17p in yeast, indicates that yeast must possess an alternative mode of activating Las17p and stimulating actin nucleation.

Once Las17p is activated, actin nucleation is initiated resulting in the generation of F-actin, which generates force on the PM, causing invagination. Activated Las17p binds the Arp2/3p complex using its VCA (Verprolin homology, Cofilin-like, Acidic) regions, resulting in conformational changes in the Arp2/3p complex which stimulates its activity resulting in actin nucleation (D'Agostino & Goode, 2005; A. a Rodal et al., 2005; Rohatgi et al., 1999; Wen & Rubenstein, 2005). Initial actin nucleation stimulates the recruitment and activation of more NPFs, including Abp1p, Myo3p, and Myo5p, which induces further rapid actin polymerization (Moseley & Goode, 2006; D. Wang, Sletto, Tenay, & Kim, 2011). It is speculated that the multiple NPFs provide a fail-safe mechanism for endocytosis as any of the NPFs individually are capable of stimulating actin nucleation, albeit less effectively than Las17p (D'Agostino & Goode, 2005). Membrane deformation stimulates the recruitment of BAR domain proteins, such as

Rvs161p and Rvs167p, which mediate distortion and stabilization of the membrane, establishing membrane curvature and ultimately aiding vesicle scission (M Kaksonen, Toret, & Drubin, 2005; Peter et al., 2004).The initial deformation of the membrane by the BAR proteins marks the entry into the fission phase (figure 1.3)

Once sufficient invagination of the PM has occurred, scission of the matured vesicle proceeds to release it into the cytosol. It is believed that the force provided by continuous actin polymerization and membrane bending by the N-BAR proteins, Rvs161 and Rvs167p, synergistically mediate the fission of the plasma membrane in yeast (Friesen et al., 2006; M Kaksonen et al., 2005; Kishimoto et al., 2011; Sivadon, Bauer, Aigle, & Crouzet, 1995). The mechanism remains controversial, but one prominent model is that Rvs161/167 heterodimers generate a contractile ring that narrows around the base of the membrane invagination ultimately leading to detachment of the endocytic vesicle. This is in stark contrast to mammalian endocytosis where fission is regulated by the membrane-binding GTPase, dynamin, which has been shown to regulate the fission process through direct binding (Ferguson & De Camilli, 2012; Loerke et al., 2009). The role of dynamin in yeast remains controversial as deletion of the yeast dynamic homolog, *VPS1*, only displayed mild endocytic defect (Burston et al., 2009). However, a recent study showed a functional cooperation of the yeast dynamin, Vps1p, with Rvs167p, suggesting a possible role for Vps1p in the endocytic scission process, albeit not an essential one (Smaczynska-de Rooij et al., 2010, 2012). Upon vesicle fission, the actin patch coat is disassembled in a synaptojanin dependent manner. In short, the synaptojanins, Inp51/52/53p, dephosphorylate PI(4,5)P_2, releasing all membrane bound coat components (C J Stefan, Audhya, & Emr, 2002; Zeng, Yu, & Cai, 2001). The turnover of PI(4,5)P_2 is also required for fission as loss of Inp51-53p results in stable membrane invaginations that protrude deep into the cell which never ultimately excise from the PM (C J Stefan et al., 2002). The disassembly of the Pan1p/End3p/Sla1p outer coat complex is mediated by the serine/threonine protein kinases Ark1p and Prk1p, along with the continuous disassembly of the inner coat (C J Stefan et al., 2002; Zeng et al., 2001). Upon coat removal, the endocytic vesicle is targeted and transported to the endosomal system.

Vesicular transport constitutes large amounts of membrane material being transported to and from the PM involving dramatic changes to PM homeostasis. To mediate smaller local changes in PM lipid composition, the cell can utilize lipid transport pathways independently of the vesicular pathways. These pathways are aptly named non-vesicular transport pathways.

1.2.4. Non-vesicular lipid transfer provides an alternative lipid transport mechanism to vesicular transport for moving lipids to-and-from the cell cortex

Non-vesicular lipid transport is a process where lipids are transported between intracellular organelles independently of vesicle formation, providing a rapid inter-organelle lipid exchange mechanism. The presence of non-vesicular lipid transport is well supported by evidence (Baumann et al., 2005); however, the exact molecular mechanisms of non-vesicular transport remain the subject of debate. Originally it was proposed that non-vesicular transport of lipids was mediated by soluble lipid transfer proteins (LTPs) that acted like lipid ferries. In this model, LTPs bind lipids at one membrane, thereby shielding the lipids from the cytosol as they transfer them to their destination. While several protein families, including the STARD4 and oxysterol related protein (ORP) families, have been shown to be capable binding lipids and transferring them between membranes exist *in vitro*, the molecular mechanism of their function and *in vivo* relevance remain obscure (Alpy & Tomasetto, 2014; Lev, 2010; Weber-Boyvat, Zhong, Yan, & Olkkonen, 2013).

It has been hypothesized that by shortening the distance of transfer, membrane contact sites act as hot-spots for non-vesicular transport (Kvam & Goldfarb, 2004; T. Levine, 2004; Loewen, Roy, & Levine, 2003; Schulz et al., 2009; Christopher J. Stefan et al., 2011). Membrane contact sites are defined as intracellular regions where two distinct organelle membranes come into close proximity (10-50nm) of each other (West, Zurek, Hoenger, & Voeltz, 2011). These contact regions are stabilized by contact site-specific tethering proteins that span the gap between the opposing membranes and allow for lipid exchange (Kornmann et al., 2009; Manford, Stefan, Yuan, MacGurn, &

Emr, 2012). While the exact mechanism of lipid transfer remains unclear several hypothetical models have been proposed (Figure 1.4). These models can be sub-divided into two fundamentally different models: i) passive lipid transfer which occurs independently of proteins and ii) facilitated transfer which is mediated by proteins (Quon & Beh, 2015). However, passive lipid transfer can not be efficient since the energy required to expel most lipids from the membrane into the aqueous cytosol is too high to maintain lipid transfer rates observed *in vivo*. (Ferrell, Lee, & Huestis, 1985; Georgiev et al., 2011). An alternative model suggests that two adjacent membranes can physically associate with each other creating stabilized hemifusions. These hemifusion are stretches where two membranes partially fuse without mixing organelle content, allowing for membrane exchange to occur through membrane mixing (figure 1.4). A hemifusion could arise both through passive or facilitated means, where SNARE proteins could interact to stabilize the hemifused membranes (Petkovic et al., 2014; Prinz, 2010). While this model could be fast enough to work, it has never been experimentally observed, making it unlikely to be physiologically relevant (West et al., 2011). Facilitated non-vesicular lipid transfer models are hypothesized to rely on LTPs to transfer lipids between the two associated membranes and/or protein tunnels which generate bridges between the adjacent membranes allowing for rapid lipid transfer (T. Levine, 2004; Quon & Beh, 2015; Schauder et al., 2014). However, structural analysis of the potential lipid tunnel proteins suggests that they act as lipid transfer proteins *in vivo* questioning if the lipid tunnel mechanism is functionally viable (AhYoung et al., 2015; Jeong, Park, & Lee, 2016; Schauder et al., 2014). Taken together, this data suggests that hypothetical facilitated lipid transfer at membrane contact sites, most likely occurs through LTPs.

Figure1.4. Proposed models of non-vesicular lipid transfer between the ER and the PM.

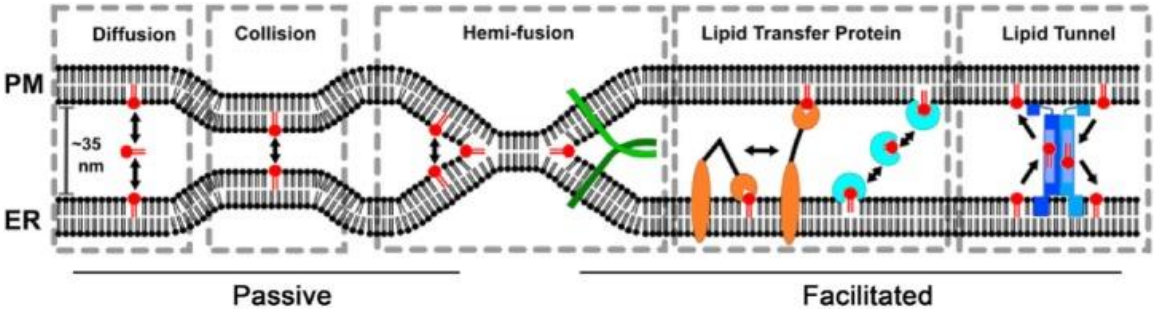

Proposed models for non-vesicular lipid transport between the ER and PM at membrane contact sites. Lipids (red) are proposed to be transferred between the PM and the ER by one or more of these mechanisms. Diffusion involves the spontaneous passive transfer of lipids by overcoming a large energy barrier to expel lipids into the cytosol allowing for their diffusion to their destination. Collisions between the two membranes may allow for lipid transfer as they transiently interact. Hemi-fusion is a stabilized version of the collision model where interaction between the membranes persists. This interaction may be supported by proteins (green) acting as SNARE-like proteins. In facilitated transport, it is proposed that proteins mediate lipid transfer, between membranes, either as lipid transfer proteins (LTPs) or by generating hydrophobic tunnels (blue) allowing for rapid passage of lipids. This figure originates in (Quon & Beh, 2015)

Since the models for non-vesicular transfer are not mutually exclusive, it remains important to keep them in mind when investigating potential mechanisms for transport pathway integration. To gain a better understanding of how non-vesicular transport plays a role in maintaining PM homeostasis, one needs to investigate the lipids transferred at the PM and how this transport may be mediated. In yeast, the association between the PM and ER is extensive, with ~45% of internal PM being covered with ER membrane patches. Here the distance between the membranes come within membrane contact sites distances (West et al., 2011), indicating that PM-ER membrane contact sites are important for cellular function. The contact between the PM and cortical ER has been shown to be mediated the yeast tricalbins, Tcb1p–Tcb3p, members of the E-Syt/SMP family proteins (Toulmay & Prinz, 2012) and Ist2p and the VAP orthologs Scs2p/Scs22p (figure 1.5) (Manford et al., 2012). While it has been speculated that these six proteins form a single large complex, studies indicate that there may be several distinct PM-ER tethering complexes composed of different combinations of these proteins (Babu et al., 2012; Creutz, Snyder, & Schulz, 2004; Manford et al., 2012; Tarassov et al., 2008). Association between the PM and the ER is achieved by creating a protein bridge between the membranes by the ER embedded tether proteins binding to PI(4,5)P2 in the PM (figure 1.5) (Fischer, Temmerman, Ercan, Nickel, & Seedorf, 2009; Kagiwada & Hashimoto, 2007; Schulz & Creutz, 2004) The affinity of Tcb1p-3p towards PI(4,5)P2 is shared by their mammalian homologs the extended synaptotagmins (E-syts) (Ercan et al., 2009), indicating that PIPs play an important role in establishing ER-PM contact sites (Maléth, Choi, Muallem, & Ahuja, 2014). Regulation of local PIP environment may be stimulated by the activity of the VAP ortholog Scs2p. Scs2p serves as the central organizer of tethering complexes as it makes numerous protein-protein interactions with other tether proteins, along with proteins regulating PIP metabolism. Among these PIP

regulating proteins is the PI(4)P phosphatase Sac1p and several putative non-vesicular lipid transport proteins (Gavin et al., 2002; Kagiwada & Hashimoto, 2007; Manford et al., 2012; Riekhof et al., 2014; Tavassoli et al., 2013). Simultaneous deletion of *TCB1-3*, *SCS2/22* and, *ICE2* resulted in substantial reduction in PM-ER association, however, some contact between the ER and PM remained, indicating that more PM-ER tether proteins may exist (Manford et al., 2012). Further research will be needed to fully understand the importance of PM-ER membrane contact sites and how these sites are implicated in regulating PM homeostasis

Figure 1.5 Cartoon of the proposed PM-ER tether in yeast.

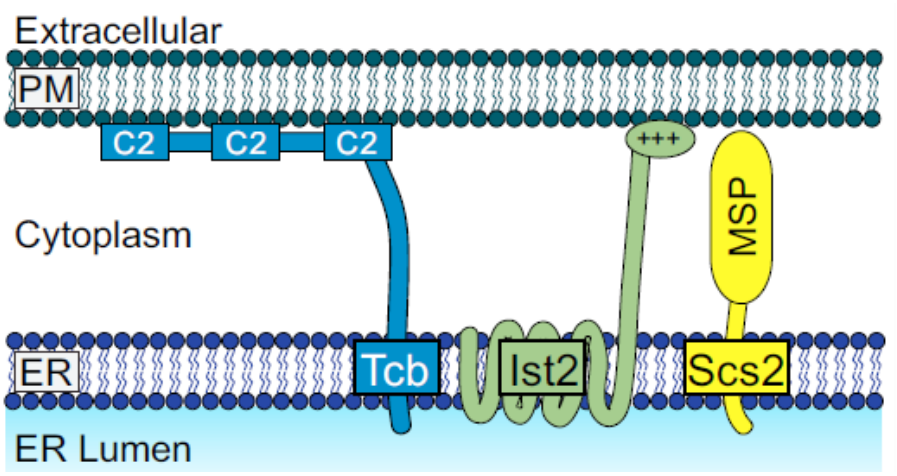

The ER membrane bound tether proteins create a protein bridge between the PM and ER by binding to PI(4,5)P_2 in the PM. This binding is mediated by the C2 domains of the tricalbins (Tcb1p-3p) and via charge interactions with the C-terminal of Ist2p. The major sperm protein domain of Scs2p is proposed to interact with negatively charged lipids in the PM. This figure is adapted from (Manford et al., 2012)

While the exact role of membrane contact in maintaining PM homeostasis remains unclear, it has been established that some mechanism of non-vesicular transport mediates the transport of lipids to-and-from the PM. Particularly non-vesicular transport of sterols has been well studied.

1.2.5. Sterols are transported to the PM by non-vesicular transfer forming PM microdomain lipid rafts with sphingolipids.

Sterols are synthesized in the ER and subsequently transported to the PM via a non-vesicular transport mechanism which concentrates sterols in the PM. Approximately 40% of total PM lipids sterols in yeast, which is achieved by sequestering them into densely packed lipid/protein microstructures called lipid rafts, which primarily consist of sphingolipids and sterols (Drin, von Filseck, & Čopič, 2016). Once sterols are incorporated into lipid rafts they become unavailable for retrograde transport, effectively making the PM act as a sterol sink (Mesmin & Maxfield, 2009). Though the dynamics of non-vesicular transport are well understood, the mechanism remains shrouded in mystery.

It has been well established that in the absence of vesicular transfer, sterols are still capable of bi-directional transfer between the PM and ER (Baumann et al., 2005). Since passive transfer of sterols would be highly energetically unfavorable, research has focused on identifying sterol transfer proteins (STPs) involved in ER to PM sterol transfer (Lev, 2012). Particularly two protein families have been strongly implicated as STPs in yeast and metazoan systems. These families, the steroidogenic acute regulatory protein (StAR)-related domain lipid transfer (START) protein and the oxysterol-binding protein (OSBP)-related proteins (ORPs) families, have both been implicated as STPs, however the molecular mechanism of their function remains unclear (Christopher T Beh, McMaster, Kozminski, & Menon, 2012; Clark, 2012; Lev, 2010).

The START protein family has been shown to bind and transfer sterols *in vitro* and is characterized by a conserved 210-residue hydrophobic lipid binding pocket (Alpy & Tomasetto, 2005; Romanowski, Soccio, Breslow, & Burley, 2002; Thorsell et al., 2011; Tsujishita & Hurley, 2000). While many of the StART domain containing proteins have been shown to bind sterols, most localize away from the PM, making it unlikely that they are directly involved in non-vesicular sterol transport at the PM. The two most likely candidates for StART proteins directly involved in non-vesicular transport to and from the PM are STARD4 and STARD5 (Romanowski et al., 2002). They are members of the STARD4 sub-group which consist of STARD4, STARD5, and STARD6, and contain no

targeting sequences which allows them to operate as cytosolic LTPs (Alpy & Tomasetto, 2014; Soccio et al., 2002). Both STARD4 and STARD5 have been shown to bind sterols and oxysterols, with high affinity, making it possible that STARD4 and STARD5 are involved in regulating oxysterol levels throughout the cell (Rodriguez-Agudo et al., 2005; Soccio et al., 2002) Both proteins localize to membrane contact sites throughout the cell (Mesmin et al., 2011; Soccio et al., 2002). However, STARD5 was enriched at the ER-mitochondria contact sites and was shown to be further enriched during ER stress, indicating that STARD5 in likely not involved in PM sterol transfer (Rodriguez-Agudo et al., 2012). While the exact mechanism remains unclear, a recent study did implicate STARD4 in directed cholesterol transport to the PM in mouse hepatocytes (Soffientini, Dolan, & Graham, 2015). However, others have failed to recapitulate these results in other cell types (Riegelhaupt, Waase, Garbarino, Cruz, & Breslow, 2010). Recently several StART-like proteins may have been identified in yeast (Gatta et al., 2015). Two of the identified proteins, Ysp2p and Lam4p, contained two StART-like domains and bound to sterols *in vitro.* Further analysis indicated that they localize at PM-ER membrane contact sites, indicating that Ysp2p and Lam4p may be involved in non-vesicular sterol transfer between the ER and PM. However, deletions of *YSP2* or *LAM4* resulted in only minor defects in retrograde sterol transfer (Gatta et al., 2015). While one cannot exclude that StAR-like proteins act redundantly with another non-vesicular sterol transfer protein, it does show that they do not constitute the only mechanism for sterol transfer, if they act as sterol transfer proteins at all. Together this data raises the question if StART and StART like proteins are involved in non-vesicular sterol trafficking. While they do bind sterols, no evidence for *in vivo* sterol transfer activity has been proposed. It is possible that multiple mechanisms for non-vesicular sterol transfer exist, which would mask the contribution of StAR-like proteins in single knockout studies. Another possibility is that sterol binding regulates the activities of the StAR-like proteins rather than serve as their cargo. More research is needed to establish their role in PM sterol homeostasis.

Another protein family that has been implicated in non-vesicular sterol transport is the highly conserved ORP family. Yeast contains seven ORPs know as the Oxysterol

binding protein homologs (Oshs). The yeast Oshs were first fully characterized as a protein family in 2001 (Christopher T. Beh, Cool, Phillips, & Rine, 2001). The Osh protein family can be subdivided into two classes: short Oshs (Osh4p-Osh7p) which consist of the conserved lipid binding ORP Related Domain (ORD), and long Oshs (Osh1p-Osh3p) which also contain variable N-terminal extensions in addition to the ORD (Figure 1.6) (Christopher T Beh et al., 2012; Lehto & Olkkonen, 2003).

Figure1.6. Osh protein structure and crystal structure of Osh4p in lipid-bound states.

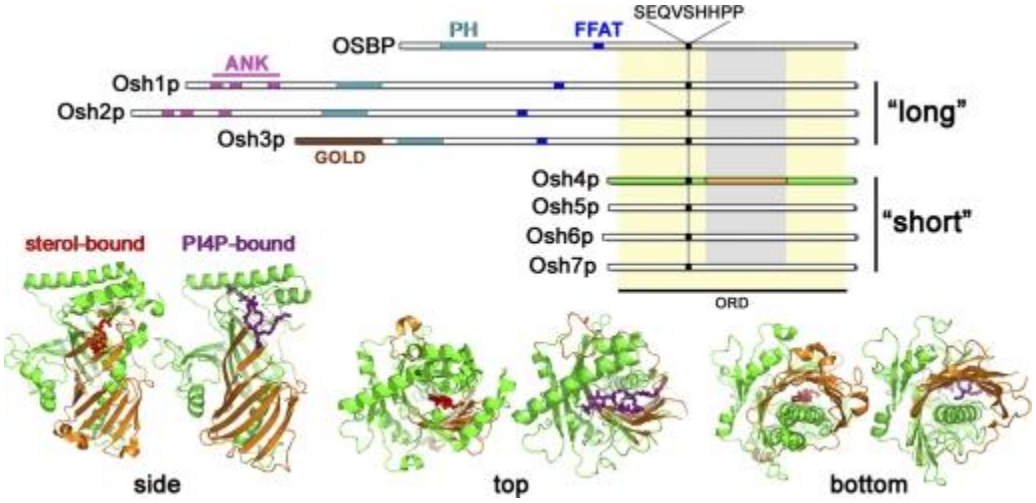

Schematic of the domains of mammalian OSBP compared to all yeast Osh proteins (top). ORPs are defined by the ORD domain (yellow highlight). Long Oshs (Osh1-3p) contain N-terminal protein-binding domains including an FFAT motif, ankyrin repeats (ANK), or a Golgi dynamics (GOLD) domains. Long Osh proteins also contain a PI(4)P-binding domain (PH). The short Oshs contain a conserved surface region (orange) that can interact with anionic lipids, such as $PI(4,5)P_2$. The corresponding sterol-bound (red) and PI(4)P-bound (purple) crystal structures Osh4p show the relative positions of these domains on the folded protein (bottom). This figure originates from (Christopher T Beh et al., 2012)

Depleting cells from Osh protein function showed that Oshs share at least one essential function as it caused cell lethality (Christopher T. Beh et al., 2001). Analysis of the Osh depleted cells revealed morphological changes indicative of lipid homeostasis and vesicular trafficking defects (Christopher T Beh & Rine, 2004). A role for Osh proteins in maintain lipid homeostasis is supported by the discovery that the ORD of Osh4p/Kes1p bound sterols with high affinity and that Osh4p was able to transfer sterols *in vitro* (Im, Raychaudhuri, Prinz, & Hurley, 2005). Combined with the finding that OSBP binds sterols it was proposed that ORPs were soluble STPs (Im et al., 2005; Kandutsch

& Shown, 1981). Analysis of the most abundant Osh, Osh4p, showed that it localizes to the Golgi in a PI(4)P-dependent manner (Fang et al., 1996). This observation combined with the discovery that over-expression of *OSH4* bypasses the requirement of *SEC14*, which encodes an essential PIPT, implicates Osh4p in PI(4)P regulation (Xinmin Li et al., 2002). Based on these findings it was suggested that Osh proteins act as PI(4)P/Sterol exchange proteins (Fang et al., 1996; Xinmin Li et al., 2002). Analysis of the ORD of Osh4p showed that it binds PI(4)P and sterols with the same binding pocket in a mutually exclusive manner. This suggests that Osh4p, and Oshs in general, may act as PI(4)P/sterol shuttles between membranes (de Saint-Jean et al., 2011; Mesmin, Antonny, & Drin, 2013). However, several studies have questioned this model. If the conserved function of Oshs is to transport sterols, then it would be expected that depleting a cell from Oshs would have dramatic effects on PM sterol levels, however, no such effect was observed (Georgiev et al., 2011). While deletion of *OSH4* had no effect on sterol levels it did lead to an increase in cellular PI(4)P levels, indicating that Oshs could function as regulators of PI(4)P levels (Gregory D Fairn, Curwin, Stefan, & McMaster, 2007). The facts that ORDs can bind multiple lipids and that PI(4)P-binding is predicted to be conserved amongst ORPs (J. Tong, Yang, Yang, Eom, & Im, 2013) has lead to the hypothesis that ORPs transfer lipids at membrane contact sites (Chung et al., 2015; Kvam & Goldfarb, 2004; T. P. Levine & Munro, 2001; Loewen et al., 2003; Schulz et al., 2009; Christopher J. Stefan et al., 2011). The concept of 'dual targeting' describes the ability of ORPs to target two distinct membranes by utilizing specific domains for membrane and protein association localized in the N-terminus of many ORPs allowing for the ORPs to translocate between membranes (Christopher T Beh et al., 2012; T. P. Levine & Munro, 2001). An alternative model is that ORPs regulate the activity of other proteins in response to PI(4)P-binding, at membrane contact sites (Manford et al., 2012; Christopher J. Stefan et al., 2011). These studies implicate the Oshs/ORPs as direct regulators of PI(4)P levels at membrane contact sites, however, they do not exclude that ORPs affect sterol transfer at membrane contact sites.

While the mechanism of non-vesicular transport of sterols remain controversial, increasing evidence is showing that non-vesicular transport mechanisms are not limited to sterol transfer. Recent years have provided growing amounts of evidence that

phospholipid homeostasis at the PM is dependent on non-vesicular transport in both yeast and mammalian systems.

1.2.6. Phosphatidylserine concentration gradient between the PM and ER is maintained by non-vesicular trafficking

The phospholipids consist of four primary lipid species: i) phosphatidylcholine (PC), ii) phosphatidylethanolamine (PE), iii) phosphatidylserine (PS) and phosphatidylinositol (PI). All of which play an important role in membrane structure, function and identity. Due to their multiple phosphorylation states, PIPs are generally considered their own class of phospholipid. Like sterols, PS is synthesized in the ER and subsequently transported against its concentration gradient to the PM by non-vesicular transport (Chung et al., 2015; Drin et al., 2016; Leventis & Grinstein, 2010; Maeda et al., 2013; Moser von Filseck et al., 2015).

Figure 1.7. Proposed mechanism for PS and PI(4)P exchange at PM-ER membrane contact sites in yeast and mammals.

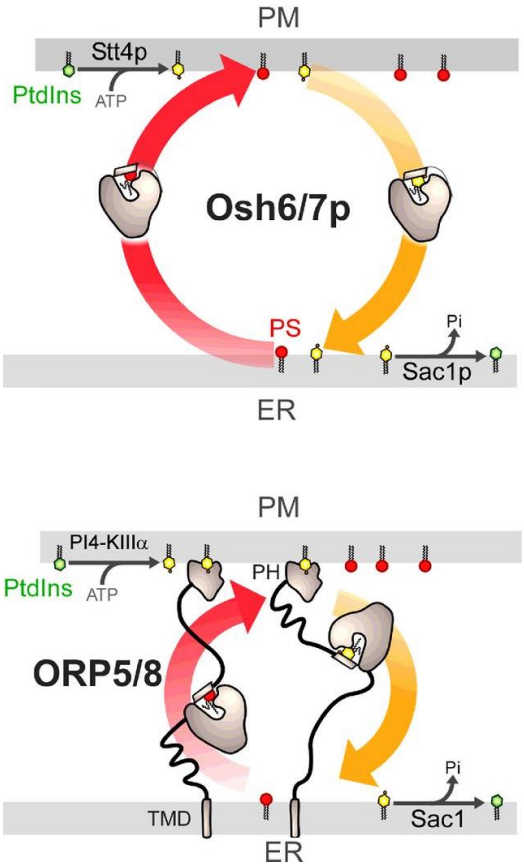

In yeast (top), PS (red lipids) is synthesized in the ER where Osh6/Osh7p subsequently transport PS from the ER to the PM, in exchange for PI(4)P (yellow lipids) which is transported back to the ER. The PI-4 kinase Stt4p ensure the ATP-dependent phosphorylation of Phosphoinositide (Ptdins, green lipid) into PI(4)P occurs locally in the PM. At the ER, Sac1p hydrolyses PI(4)P into PtdIns to generate a local PI(4)P concentration gradient, allowing for vectorial transfer of PS against its concentration gradient. In mammals (bottom) a similar mechanism allows for ORP5/8 to transport PS from the ER to the PM. ORP5/8 function as membrane tethering proteins as they are imbedded into the ER by trans membrane domains and interact with PI(4)P in the PM by PH domains. This figure is adapted from (Drin et al., 2016)

In yeast, a recent study showed that the yeast ORPs, Osh6p and Osh7p, mediated non-vesicular PS transfer at PM-ER membrane contact sites (Figure 1.7) (Maeda et al., 2013). Further studies have shown that Osh6/7p binds PI(4)P and functions as a PS/ PI(4)P exchanger *in vitro* (Moser von Filseck et al., 2015). In this model, Osh6/7p functions as a bi-directional lipid transporter for PS and PI(4)P. Osh6p can bind PS in the ER and transport it against is concentration gradient to the PM where

PS is exchanged for PI(4)P. PI(4)P is then transferred along its concentration gradient to the ER where it is rapidly dephosphorylated to PI by the ER-resident PI(4)P phosphatase Sac1p. This model suggests that the movement of PS against its concentration gradient is driven by PI(4)P translocation along its concentration gradient and the rapid dephosphorylation of PI(4)P by Sac1 constantly maintains the unequal distribution of the later. (Figure 1.5) (Maeda et al., 2013; Moser von Filseck et al., 2015). Since this model relies on the PM bound phosphoinositol-4 kinase, Stt4p, and the ER-bound PI(4)P phosphatase, Sac1p, to maintain a local PI(4)P concentration gradient between the ER and PM, one would expect that deletion of either *SAC1* or *STT4* would result in PS distribution defects. A similar PI(4)P /PS exchange model has been proposed in mammalian cells where ORP5 and ORP8 have been implicated in ER to PM PS transfer. Unlike Osh6/7p, which are cytosolic, ORP5 and ORP8 are imbedded into the ER by transmembrane domains and make physical contact with the PM by binding PI(4)P through pleckstrin homology (PH) domains (Figure 1.7) (Chung et al., 2015). However, an alternate explanation for PS transfer defects observed upon PI(4)P depletion is that ORP5/8 PM-ER contact dissociates upon loss of PI(4)P, thus stopping PS transfer.

While advances have been made in the understanding of non-vesicular lipid transport, much work is still required to fully understand the mechanisms involved. The current models favor that non-vesicular transport proteins are regulated by local PI(4)P concentration gradients between membranes. Therefore, it is possible to regulate PS transfer by modifying the local PI(4)P gradients giving tight regulatory control over PS transfer. If this is true then regulating local PIP levels might regulate multiple non-vesicular transport pathways simultaneously, making them mechanistically integrated with each other. However, more research is needed to establish if this is true.

1.3. Mechanistic integration of membrane transport pathways is required for PM homeostasis

Cellular membrane trafficking involves large fluxes in lipid and protein composition of biological membranes which requires communication between transport pathways to maintain membrane homeostasis. Particularly, vesicular trafficking involves major changes in membrane composition making it paramount for cell viability that endocytosis and exocytosis are carefully balanced at the PM. Cells with high secretion rates, such as neurons, an integrated model called compensatory endocytosis has been demonstrated. What remains unknown is the exact mechanism of integration and if similar mechanisms exist in general cell types. Furthermore, a balance between vesicular and non-vesicular transport also needs to be maintained to control PM homeostasis, however, integration of vesicular and non-vesicular remains poorly understood.

1.3.1. Integrating exocytosis with endocytosis by compensatory endocytosis

Compensatory endocytosis is a mechanistic link between endocytosis and exocytosis, meaning that an exocytic event directly stimulates an endocytic response. Compensatory endocytosis is best understood in specialized cells that display a high frequency of exocytosis; like neuronal synapses and maturing Xenopus oocytes (Gauthier-Kemper, Kahms, & Klingauf, 2015; Rizzoli & Jahn, 2007; Anna M. Sokac & Bement, 2006; Stevens & Williams, 2000). The mechanisms whereby compensatory endocytosis in achieved varies greatly from cell type to cell type. In Xenopus oocytes, membrane fusion between a specialized exocytic vesicle called a cortical granule, and the PM results in F-actin coating and stabilization of a partially fused vesicle, inhibiting full collapse into the PM. This stabilization allows for the granules to persist in a semi-fused state for up to several minutes (Anna M. Sokac & Bement, 2006; Anna Marie Sokac, Co, Taunton, & Bement, 2003). In synapses, turnover of exocytic vesicles is extremely fast allowing for constant secretion during nerve impulses. Therefore, the mechanism of membrane retrieval must be extremely tightly regulated to compensate for the large volume of material delivered to the PM. Two main models have been

presented for synaptic compensatory endocytosis: i) kiss-and-run exocytosis, where vesicles only make transient interactions with the PM (Alés et al., 1999; Stevens & Williams, 2000), and ii) the full collapse model, where exocytic vesicles fully fuse with the PM stimulating endocytosis by mixing of the vesicular membrane with the PM (Takei, Mundigl, Daniell, & De Camilli, 1996; Torri-Tarelli, Haimann, & Ceccarelli, 1987). To determine if a mechanism for generalized compensatory endocytosis exists, one first needs to understand the mechanisms of these specialized events.

1.3.2. Compensatory endocytosis in Xenopus is mediated by stabilizing exocytic vesicles on the PM with an actin coat during Kiss-and-coat

In Xenopus oocytes, exocytosis is linked to endocytosis by an actin-dependent stabilization and modification of a semi-fused secretory vesicle called Kiss-and-coat compensatory endocytosis. During fertilization, cortical granules fuse with the PM and releases factors into the extracellular matrix to avoid polyspermy (M. Liu, 2011). In Xenopus eggs, live cell imaging revealed that cortical granules become surrounded by F-actin upon fusion with the PM, stabilizing the granules in a semi-fused state (Figure 1.8) (Anna Marie Sokac et al., 2003). During this state, the granule lipids and proteins are modified before it is retrieved into the cell surface (Bement, Benink, Mandato, & Swelstad, 2000; Anna M. Sokac & Bement, 2006). Similar F-actin stabilized cortical granules have been observed in other oocytes studied, including zebrafish and sea urchins, indicating that kiss-and-coat like mechanisms may be common during oocyte maturation (Becker & Hart, 1999). Disruption of F-actin formation in Xenopus oocytes result in the full collapse of the vesicles into the PM, showing the importance for the F-actin coat for vesicle stabilization (Anna Marie Sokac et al., 2003). A similar F-actin-mediated mechanism for vesicle maturation and retrieval has been described in pancreatic acini cells upon zymogen granule fusion with the PM (T Nemoto et al., 2001; Tomomi Nemoto, Kojima, Oshima, Bito, & Kasai, 2004), indicating that F-actin stabilization may be one general mechanism for specialized vesicle maturation. After stabilization, membrane and protein components are modified in the cortical granule, before the F-actin coat is dissolved and the vesicle is retracted through the endosomal pathway, allowing for material exchange before endocytosis (Bement et al., 2000).

Figure1.8. Membrane mixing induces F-actin-dependent stabilization of cortical granules during kiss-and-coat compensatory endocytosis.

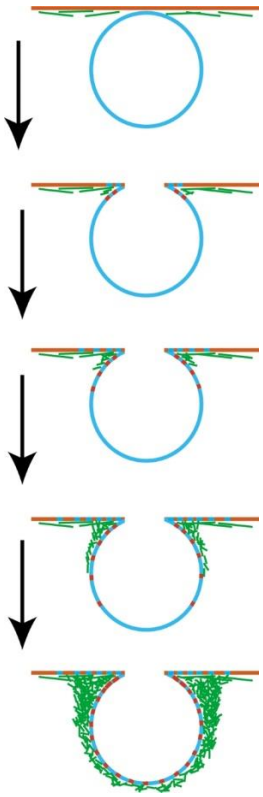

Cartoon showing the proposed “compartment-mixing” model. After fusion of the cortical granule (blue) with the PM (orange), mixing between the two compartments induce actin F-actin formation. This induction results in accumulation of F-actin fibers (green) which ultimately completely enclose the vesicle at the PM, stabilizing it in a hemi-fused conformation, allowing for subsequent membrane modifications. This figure originates from (Anna M. Sokac & Bement, 2006).

Stabilization of the cortical granule at the PM is important for proper PM maturation of the Xenopus oocyte (Bement et al., 2000), however, identification of proteins or factors regulating both processes directly is needed to classify it as a mechanistic link between endocytosis and exocytosis. One model stated that fusion induced increased local intracellular calcium levels which were responsible for activating F-actin formation and vesicle coating (Kline & Nuccitelli, 1985). However, analysis of the timing of F-actin polymerization did not show any correlation with intracellular calcium levels, making it unlikely that changes in calcium levels stimulate F-actin coating

(Tomomi Nemoto et al., 2004; Anna M. Sokac & Bement, 2006). Further analysis of the timing between vesicle fusion to the PM and F-actin polymerization perfectly correlated indicating that membrane mixing between the cortical granule and the PM stimulates F-actin formation (Figure 1.6) (H.-Y. E. Yu & Bement, 2007). While the exact mechanism of how membrane mixing results in F-actin formation remains unknown, several observations have given clues as to how regulation may occur. Upon vesicle fusion with the PM, $PI(4,5)P_2$ from the PM diffuses into the cortical granule membranes, which generates a local $PI(4,5)P_2$ gradient between the PM and the vesicle. It is believed that this gradient stimulates F-actin formation by promoting actin assembly by recruiting and activating N-WASp–Arp2/3 actin nucleation (Insall & Machesky, 2004). The notion that mixing of the two membranes is stimulating F-actin formation is supported by the finding that the diacylglycerol (DAG) analog, phorbol 12-myristate 13-acetate, promotes actin assembly on vesicles in Xenopus eggs *in vivo* and *in vitro* (Taunton et al., 2000). Further studies showed that F-actin formation was dependent on N-WASp and Cdc42 function, indicating that membrane mixing stimulates recruitment and activation of N-WASp and Cdc42, which activates F-actin stabilization (Insall & Machesky, 2004; Anna Marie Sokac et al., 2003; Taunton et al., 2000). The findings that lipid mixing triggers vesicle stabilization and compensatory endocytosis highlights the importance of membrane mixing when controlling cellular transport events. Does membrane mixing play any role in other types of compensatory endocytosis?

1.3.3. Maintenance of constant cell volume at synapses active zones require rapid compensatory endocytosis

During nerve impulses, a large number of synaptic vesicles carrying neurotransmitters fuse with the PM to release their contents into the synapse allowing for nerve signal transduction. To avoid PM expansion at active zones, where synaptic vesicle fusion occurs, a rapid mechanism for membrane retrieval must exist (Cremona & De Camilli, 1997; Stevens & Williams, 2000). Based on the speed required for efficient neuronal signal transduction, it was suggested that synaptic vesicles only made transient interactions with the PM and were retracted back into the cell before fully fusing, thus

allowing the PM to stay unaffected (Figure 1.9 1) (Fesce, Grohovaz, Valtorta, & Meldolesi, 1994). This model was called kiss-and-run exocytosis and was long considered the most likely model. However, while the model is enticing in its simplicity and speed it remains unobserved *in vivo*. Recent results obtained by high-resolution cryo-electron microscopy (EM) after rapid high pressure freezing revealed an ultrafast endocytosis mechanism where the exocytic vesicles fully collapsed into the PM (Figure 1.9 2) (Watanabe et al., 2013). But if the kiss-and-run model does not hold up, then how do neuronal cells retrieve membrane material fast enough to maintain PM homeostasis?

Figure 1.9. Neuronal compensatory endocytosis: one mechanism, two models.

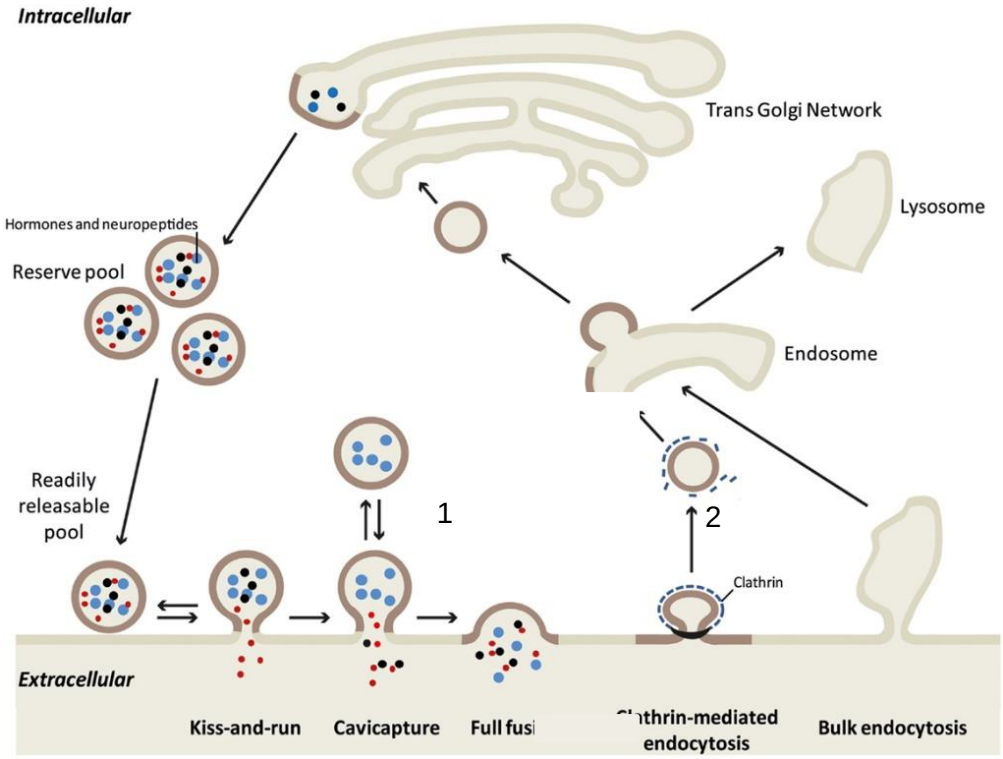

Neurotransmitters and/or hormones are packaged into secretory vesicles at the TGN. These vesicles can either be retained in the cytosol as a reserve pool or be targeted to the PM for neurotransmitter release (colored dots). After vesicle fusion with the PM, the synaptic vesicles can be retrieved by one of two potential mechanisms. 1) During “kiss-and-run” exocytosis synaptic vesicles make transient interactions with the PM, releasing their contents into the synapse and ultimately retrieved back into the cytosol. 2) During full fusion exocytosis, the membrane of the synaptic vesicle fully collapses into the plasma membrane, causing membrane mixing, which stimulates clathrin-mediated endocytosis. This figure is adapted from (Houy et al., 2013)

Based on EM studies clathrin-mediated endocytosis seems to be the major pathway for recycling synaptic vesicles from the PM (Takei et al., 1996). Therefore, exocytosis and endocytosis must be spatially separated but remain mechanistically integrated, meaning that exocytic events in the active zone must stimulate endocytosis outside of this zone (Figure 1.9 2). Since clathrin binding has been shown to be important for synaptic membrane recycling (Takei et al., 1996), but is unable to bind directly to the membrane of synaptic vesicles it must rely on adaptor proteins to recognize and bind the membrane destined for internalization (Maritzen, Podufall, & Haucke, 2010). How is such recognition possible? One possibility is that the lipids and proteins of the synaptic vesicle diffuse freely in the PM upon fusion, resulting in complete mixing. Since these proteins and lipids need to be reabsorbed through endocytosis sorting would be required before retrieval is possible (Fernández-Alfonso, Kwan, & Ryan, 2006). Since proteins and lipids are free to diffuse in this model assembly of endocytic vesicles will require either some degree of self-assembly of the endocytic sites or adaptor proteins can manage to sort the proteins and lipids that need internalizing. The best understood adaptor protein complex known to regulate clathrin-mediated endocytosis at synapses is AP-2 (Slepnev & De Camilli, 2000). However, knockdown or knockout of AP-2 subunits in neurons resulted in a minor reduction in synaptic vesicle retrieval, indicating that other adaptor proteins may be sufficient to compensate for the lack of AP-2 (S. H. Kim & Ryan, 2009; Willox & Royle, 2012). Stonin2 is the only adaptor protein that has been directly linked to retrieval of synaptic vesicles. It was shown to be involved in recycling of synaptotagmin, Syt1, from synaptic vesicles (Willox & Royle, 2012), however, a role as an adaptor for all synaptic vesicle retrieval remains uncertain. Furthermore, studies indicate that stonin2 function is dependent on AP-2, making it unlikely that it can function as an adaptor protein for compensatory endocytosis (Diril, Wienisch, Jung, Klingauf, & Haucke, 2006). Together this data makes it unlikely that the reassembling the synaptic vesicle upon diffusion is feasible. An alternative model states that the synaptic vesicle remains completely intact upon collapse into the PM. This would result in a raft-like structure that diffuses away from the active zone and stimulates endocytosis upon exit (Willig, Rizzoli, Westphal, Jahn, & Hell, 2006). This model was supported by early stimulated emission depletion (STED) confocal microscopy experiments that indicated that the components of the synaptic vesicle remained associated after fusion (Willig et al., 2006). However, subsequent studies have

questioned these findings and suggest that the vesicle at least partially dissociates post-fusion (Hua et al., 2013). One interesting discovery was that the synaptic endocytic sites were highly enriched in cholesterol and sphingolipids indicating that lipid rafts from the synaptic vesicle may play a role in regulating synaptic vesicle retrieval (Takamori et al., 2006). The fact that membrane mixing plays a crucial role in both types of compensatory endocytosis could imply that lipids, or lipid associated proteins may be the key for integrating endocytosis with endocytosis in non-specialized cells types.

1.3.4. Compensatory endocytosis might be a general mechanism for PM homeostasis maintenance in all metazoan cells.

While compensatory endocytosis is well-established in specialized cell types, the question remains if compensatory endocytosis is a general mechanism for maintaining PM homeostasis in all cells. Recent studies have shown that proteins involved in regulating exocytosis also regulate aspects of endocytosis in non-specialized cell types supporting a potential compensatory endocytosis mechanism in all cells. In 2010; a study showed that the small Rab GTPase, Rab3, which plays an essential role during exocytic vesicular fusion with the PM, is involved in recruiting the endocytic machinery to sites of endocytosis in *C.elegans* (Bai, Hu, Dittman, Pym, & Kaplan, 2010), indicating that proteins involved in exocytosis may play a role in regulating endocytosis. Further evidence for generalized compensatory endocytosis came in 2015 when Wang et al., showed that knocking down Rabin8, the mammalian homolog of the GEF Sec2p, dramatically reduced the efficiency of a transferrin endocytosis assay (J. Wang et al., 2015). Since Rabin8 is an essential regulator of exocytosis in all cells, this experiment strongly supports a potential mechanistic link between exocytosis and endocytosis in higher organisms. While some support might be given to potential mechanisms for compensatory endocytosis in all cells, direct evidence is still lacking. To gain more insight into how a general compensatory endocytosis mechanism may work one could look to yeast to see if a conserved mechanism may exist.

1.3.5. Preliminary evidence hints at the existence of compensatory endocytosis in yeast.

While compensatory endocytosis is yet to be established in yeast, circumstantial evidence does support a possible mechanism. In yeast, loss of endocytosis results in loss of cell polarity during cell division due to regulators of cell polarity, such as Cdc42p, diffusing away from the tip of the bud (Marco, Wedlich-Soldner, Li, Altschuler, & Wu, 2007). While such observations show that exocytosis and endocytosis are functionally linked it does not prove that exocytosis and endocytosis may be linked mechanistically. The first evidence for yeast compensatory endocytosis was presented by Howard Riezman in 1985. While performing a lucifer yellow uptake assay to identify novel endocytosis mutants it was discovered that a certain subset of proteins essential for exocytosis also displayed strong endocytic defects (Riezman, 1985). Specifically, he identified late SEC mutants essential for late steps in exocytosis (after the vesicle leaves the TGN) displayed severe lucifer yellow uptake defects, while early SEC mutants (essential for steps before vesicles leaving the TGN) displayed only mild or no defects on Lucifer yellow uptake. The distinct separation between early and late SEC mutants shows that a potential link between exocytosis and endocytosis may be found in the genes encoding the exocyst, Sec2p, and/or Sec4p. This discovery was supported by a recent high throughput assay using robot-based imaging and phenotype scoring. When assaying endocytic mutants, the study identified several of the exocyst components along with Sec2p as having strong endocytic defects (Carroll et al 2012). Together these studies strongly imply that yeast does have a compensatory endocytosis mechanism, albeit the details of what proteins and/or lipids that may be involved remain unknown.

1.4. Lipids regulate both vesicular and non-vesicular trafficking directly

If membrane transport pathways are integrated with each other to maintain PM homeostasis, then there must be lipids and/or proteins that act as direct regulators of both pathways considered to be integrated. To investigate this claim it would be helpful to look at potential lipid transport regulators independently of potential regulatory proteins. Lipids are often simply considered as structural membrane components, but

many lines of evidence have shown that lipids directly regulate transport to and from the PM. Particularly PIPs, lipid rafts, and phospholipids have been implicated as regulators of transport. Could any of these lipids link transport pathways mechanistically?

1.4.1. PIPs regulate both membrane structure and trafficking directly at the PM

PIPs are lipids that serve as structural lipids essential for giving distinct properties to all organelles. They have also been shown to regulate steps during both exocytosis and endocytosis at the PM, partially by binding the protein machinery to the PM, and partially by directly regulating protein activity (Albert & Gallwitz, 2000; Di Paolo & De Camilli, 2006; Faulhammer et al., 2007; Finger, Hughes, & Novick, 1998; Höning et al., 2005; Y. Liu & Bankaitis, 2010; Mizuno-Yamasaki et al., 2010; Santiago-Tirado et al., 2011; C J Stefan et al., 2002). PIPs are special amongst lipids because their inositol head group that can be phosphorylated at multiple locations which can give the lipid special characteristics depending on phosphorylate position (Figure 1.10) (Di Paolo & De Camilli, 2006). Due to this specificity, different PIP species are spatially restricted to specific organelle membranes (Di Paolo & De Camilli, 2006) with many phosphatases and kinases dedicated to controlling the correct PIP composition of every cellular membrane (Figure 1.10) (Y. Liu & Bankaitis, 2010). This specificity allows PIPs to target proteins to membranes via lipid binding domains that recognize PIP species. These lipid binding domains include the ANTH and ENTH domains that are thought to specifically bind $PI4,5P_2$ (Itoh et al., 2001; Sun et al., 2005) and pleckstrin homology domains that bind PI(4)P (Roy & Levine, 2004). PI is the precursor to PIPs and is synthesized in the ER (Kumano & Nikawa, 1995). PI can subsequently be transported to other membranes by PI specific transporters known as PIP-specific lipid transfer proteins (PITPs), which play critical roles in cell signaling by regulating PIP levels of membranes either through PI transport (Cockcroft, 2001; X Li et al., 2000; Phillips et al., 1999), or by controlling PI(4)P levels by regulating Pik1p activity in the Golgi (Strahl, Hama, DeWald, & Thorner, 2005). Studies have shown that PI(4)P is mostly restricted to the ER, Golgi, and exocytic vesicle membranes, where it constitutes the most abundant PIPspecies. (Di Paolo & De Camilli, 2006). However, studies utilizing using immunocytochemical assays and fluorescent proteins fused to PI(4)P-specific PH domains indicate that pools of PI(4)P

are present in the PM across species (Hammond, Schiavo, & Irvine, 2009; Roy & Levine, 2004). These findings remain controversial as maintaining fidelity of lipid binding domains when excised out of their nascent proteins remains an issue, making it unclear how much PI(4)P resides in the PM.

Figure 1.10. Schematic of the primary PIP species at the yeast PM and the proteins regulating their levels

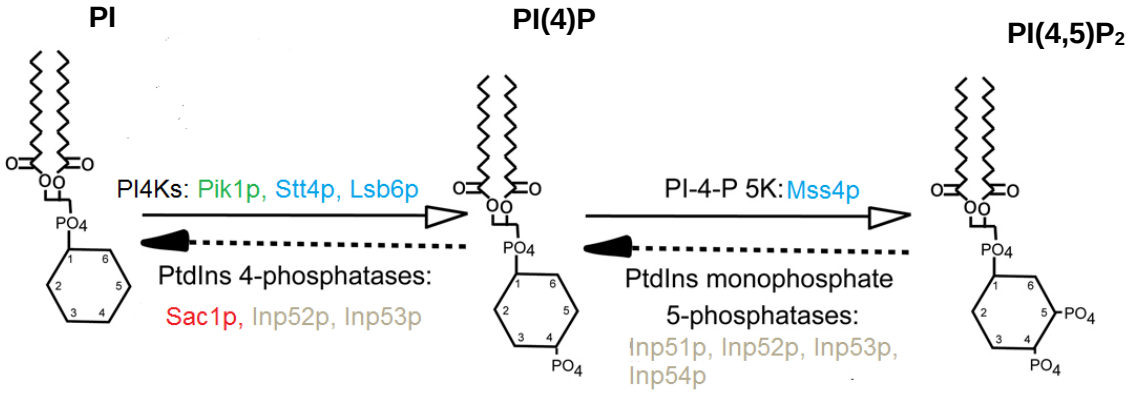

PI (left) can be phosphorylated at the R-4 position generating PI(4)P (middle) by the PI4Ks Pik1p, Stt4p, and Lsb6p. PI(4)P can be further phosphorylated on the R-5 position to $PI(4,5)P_2$ (right) by Mss4p. Inp51-54p can dephosphorylate $PI(4,5)P_2$ to PI(4)P, which can be converted into PI by Sac1p, Inp52, and Inp53p. Colors indicate the cellular location of the kinases and phosphatases. Blue = PM, Red = ER, Green = Golgi and Tan = cytosolic. This figure is adapted from (Y. Liu & Bankaitis, 2010)

While the amount of PI(4)P in the PM may be controversial, it is well established that $PI(4,5)P_2$ is the most abundant PM PIP (Santiago-Tirado & Bretscher, 2011). In all species tested where it is mostly restricted to the inner leaflet of the PM, where it is accessible for interactions with proteins (T. Balla, Szentpetery, & Kim, 2009; Van Leeuwen, Vermeer, Gadella, & Munnik, 2007; Watt, Kular, Fleming, Downes, & Lucocq, 2002). While $PI(4,5)P_2$ levels are relatively uniform across the PM, the existence of $PI(4,5)P_2$-rich microdomains within the PM have been established experimentally in mammalian cells. The exact nature of these domains remains controversial since some studies indicate that $PI(4,5)P_2$ domains associate with lipid rafts within the PM while others indicate that $PI(4,5)P_2$ is sequestered directly by proteins generating $PI(4,5)P_2$ reservoirs known as ‘‘pipmodulins’’ (Laux et al., 2000; McLaughlin & Murray, 2005). Considering 50% of $PI(4,5)P_2$ is associated with microdomains, this indicates that compartmentalization of $PI(4,5)P_2$ plays a role in optimizing the functional role of

$PI(4,5)P_2$(Johnson & Rodgers, 2008; Pike & Miller, 1998). This hypothesis may explain the role of $PI(4,5)P_2$ during endocytosis, where $PI(4,5)P_2$ is required for actin patch and cytoskeleton organization in yeast. but the existence of $PI(4,5)P_2$ enriched domains in yeast has yet to be established.

Maintenance of the balance between PIP synthesis and degradation is essential for cell viability and therefore is tightly controlled so distinct pools of PIPs can be maintained (Di Paolo & De Camilli, 2006; Krauss & Haucke, 2007; Y. Liu & Bankaitis, 2010). The PIP pool in the PM is affected by PIPs arriving on exocytic vesicles, PIP kinases and phosphatases acting directly on the PM and the removal of PIPs by endocytosis. The major species of PIPs in exocytic vesicles are PI and PI(4)P (Santiago-Tirado & Bretscher, 2011). PI(4)P is generated in the Golgi by the phosphatidylinositol 4-kinase PI4K, which phosphorylates PI at the R4-position of the inositol ring. (Flanagan et al., 1993; Strahl et al., 2005). At the PM, PI phosphorylated by the PM resident phosphatidylinositol 4-kinase (PI4K) Stt4p to generate more PI(4)P (Anjon Audhya & Emr, 2002) and PI(4)P can then be phosphorylated by the phosphatidylinositol 5-kinases (PI5K), Mss4p to generate $PI(4,5)P_2$ (A. Balla & Balla, 2006; Desrivières, Cooke, Parker, & Hall, 1998; Homma et al., 1998). In addition to Stt4p, which is expressed throughout the PM, yeast has another specialized PI4K, Lsb6p, which plays a specific role during endocytosis where it binds Las17p and modifies the PM at actin patches (Han, Audhya, Markley, Emr, & Carman, 2002). Since the balance of PI to PI(4)P to $PI4,5P_2$ is essential for PM function a number of PIP phosphatases act on the PM to help maintain this dynamic balance. In yeast, the best understood PI(4)P phosphatase is ER resident phosphatidylinositol 4-phosphatase Sac1p, which removes the R4 phosphate of PI(4)P resulting in PI (A. E. Cleves et al., 1989; Stolz, Huynh, Thorner, & York, 1998). Sac1p is believed to play a role in generating PI in the ER membrane and during exocytic vesicle formation but has also been shown to act in trans on PM PI(4)P pools at PM-ER membrane contact sites (Schorr, Then, Tahirovic, Hug, & Mayinger, 2001; Christopher J. Stefan et al., 2011; Tahirovic, Schorr, & Mayinger, 2005). While PIP kinases are very substrate specific, PIP phosphatases are considered to have broader substrate specificities, since some can act upon more than one substrate (Y. Liu & Bankaitis, 2010). Amongst the promiscuous phosphatases at the PM are the Sac1p-familiy phosphatases: Inp51p, Inp52p, Inp53 and Inp54p generally convert $PI(4,5)P_2$ into PI(4)P

by their 5-phosphatase activity, however, these phosphatases can further dephosphorylate their substrate to PI (Stolz, Huynh, et al., 1998; Stolz, Kuo, Longchamps, Sekhon, & York, 1998; Strahl & Thorner, 2007; Wiradjaja et al., 2001). The mechanism of How dephosphorylation is regulated remains poorly understood. While Sac1p plays a general role in global PI(4)P levels, Inp51-54p play more specific roles in vesicular trafficking, particularly in late stages of endocytosis (C J Stefan et al., 2002; Tahirovic et al., 2005). Sac1p function has also been implicated in vesicular transport as a deletion of *SAC1* results in increased PI(4)P levels and misregulation vesicular transport when deleted together with *INP54* (Wiradjaja et al., 2007). The tight control of PIP composition of the PM allows for specific regulation of local membrane properties and local membrane trafficking by regulating local protein function. How is this PIP-dependent protein regulation achieved?

Over the last decades, it has become increasingly clear that PI(4)P and PI(4,5)P_2 can serve as signaling molecules by interacting with effector proteins during membrane transport. This regulatory power is likely a consequence of PIPs recruiting regulatory proteins to specific membrane locations, where the proteins exert their functions directly or colocalized with signaling partners to regulate cellular transport (Garrenton, Stefan, McMurray, Emr, & Thorner, 2010). One example of this is PIP-dependent recruitment and activations of multiple Rab GTPases in vesicular transport. Here PIPs regulate vesicular transport by recruiting distinct GTPases through successive membrane compartments as vesicles mature or undergo multiple membrane fusion and fission events as vesicles pass through multiple organelles (Jean & Kiger, 2012; Rink, Ghigo, Kalaidzidis, & Zerial, 2005). This kind of mechanism has been described in yeast where a Rab GTPase switch is required for trafficking through the late Golgi. This switch is ensured by the coordinated inactivation of Ypt1p and activation of Sec4p. This is mediated by a PI(4)P-dependent recruitment of Ypt31/32p, which inactivates Ypt1p and subsequently recruits Sec2p. Sec2p and Ypt31/32p then recruits and activates Sec4p, completing the Rab GTPase swap (Figure 1.11) (Ortiz et al., 2002; Rivera-Molina & Novick, 2009). A similar Rab regulatory cascade occurs during early-to-late endosomal maturation, which is regulated by Rab5-mediated recruitment of a Mon1–Ccz1 complex. This functions as a Rab7 GEF which stimulates Rab7 in a PI(3,5)P_2 dependent manner (Nordmann et al., 2010; Rink et al., 2005). Another example of PIP regulated trafficking

events can be seen during endocytosis when PIPs spatially restrict proteins during actin patch maturation where multiple proteins including, Syp1p, Sla2p, and Ent1/2p make direct contact with the PM through PIP-binding domains (Itoh et al., 2001; Sun et al., 2005). The importance of PIPs during endocytosis is further highlighted by the fact that turnover of $PI(4,5)P_2$ is required to complete vesicle scission (C J Stefan et al., 2002). This data clearly show that PIP composition of the PM plays an essential role in regulating vesicular transport and combined with the hypothesis that PI(4)P concentration gradients between the ER and the PM is the main driving force for non-vesicular trafficking (Chung et al., 2015; Mesmin, Bigay, et al., 2013), make PIPs good candidates for lipids that can integrate transport pathways.

Figure 1.11 Schematic model for the Ypt31/32p Rab GTPase cascade regulating vesicle transport in yeast

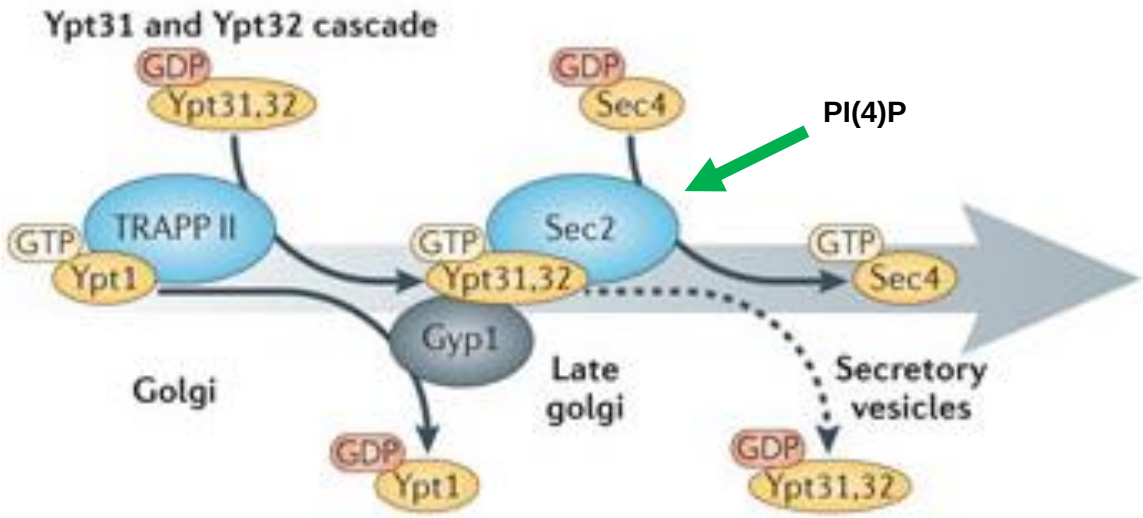

A conceptual diagram of the Ypt31/32p Rab cascade during yeast exocytosis. Upon arrival at the Golgi, vesicle maturation occurs with inactivation of the early Golgi-associated Ypt1p by its GAP Gyp1, that is recruited at the late Golgi by Ypt31/32p Ypt32. GTP-bound Ypt31/32p also recruit Sec2p in a PI(4)P-dependent manner. Sec2p, in turn, activates Sec4p to drive exocytosis. In this way, Ypt31/32p regulates a Rab GTPase cascade resulting in coordination between Ypt1p inactivation with Sec4p activation. This figure is adapted from (Jean & Kiger, 2012)

1.4.2. Sterols and sphingolipids generate lipid rafts in the PM that affect membrane structure and regulate lipid trafficking events

Lipid rafts are PM domains enriched in ergosterol (yeast equivalent of cholesterol) and sphingolipids have been implicated in regulation of PM physical structure and endocytosis directly. Lipid rafts are characterized by being non-extractable with non-ionic detergents and are thought to play a role in regulating membrane fluidity and membrane organization by preferentially interacting with transmembrane proteins and proteins containing saturated lipid modifications, like GPI anchors and myristylation modifications (Figure 1.12) (Levental, Lingwood, Grzybek, Coskun, & Simons, 2010). Lipid rafts remain a subject of much debate and particularly the molecular mechanisms for their formations is a matter of controversy since multiple factors, like membrane lipid composition, protein interactions and cellular physiological conditions, such as temperature, pH, and salinity, all contribute to raft formation (Bagatolli, Ipsen, Simonsen, & Mouritsen, 2010; Deleu, Crowet, Nasir, & Lins, 2014). However, there is a consensus that the high abundance of sterols and complex sphingolipids in the PM (30-40% sterols and 10-20% sphingolipids) are required for generating ordered lipid domains required for raft formation since depleting one or the other results in raft breakdown (Goñi & Alonso, 2009; London, 2002; Stott et al., 2008). This implies that a steady source of sterol and sphingolipid transport to the PM is needed to maintain potential lipid rafts in yeast, but how this transport is regulated and the role sterols or sphingolipids play in its regulation remains unknown.

Figure1.12. Model of lipid raft structures in the yeast PM.

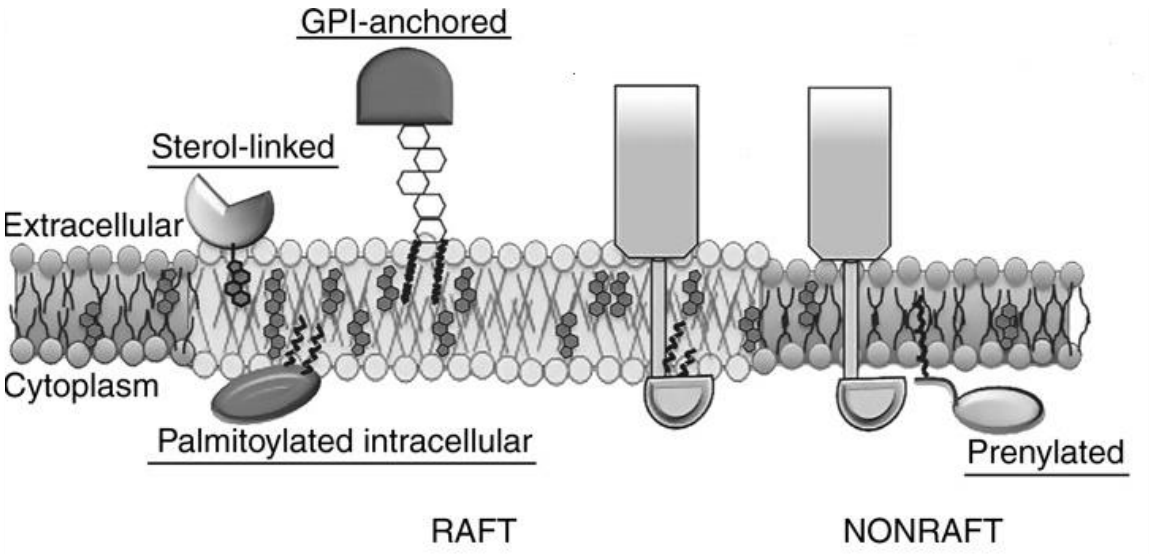

The ordered lipid organization of lipid rafts allow for lipid-modified proteins associate with rafts. Various lipid anchors play important roles in protein trafficking, membrane partitioning, and proper function, likely mediated by their affinity for lipid rafts. The general hypothesis is that protein modification and anchoring by saturated fatty acids and sterols target proteins to the more ordered lipid environment of lipid rafts, whereas unsaturated and branched hydrocarbon chains favor association with more disorganized nonraft membranes. Adopted from (Simons & Sampaio, 2011)

Both sterols and sphingolipids are synthesized in the ER and subsequently transported to the Golgi where rafts are formed prior to their transport to the PM. In the Golgi, rafts may play a role in sorting proteins and lipids into vesicles, which promotes interactions with saturated lipids and proteins with lipid modifications because of their ordered lipid structure (Figure 1.12). Lipid analysis has shown that exocytic vesicles were highly enriched in sterols and sphingolipids and cells depleted of sterol and sphingolipid impaired vesicle exit from the TGN, showing that lipid rafts are important for TGN vesicle biogenesis (Klemm et al., 2009; Proszynski et al., 2005). Structural lipid modifications drive vesicle biogenesis in the TGN during exocytosis. Apart from the structural changes in membrane organization that initiates vesicle budding, specific lipids are also sorted as cargo into nascent vesicles. Complex sphingolipids and ergosterol are enriched in secretory vesicles compared to the Golgi membrane from whence they came (Klemm et al., 2009; Proszynski et al., 2005; Surma, Klose, Klemm, Ejsing, & Simons, 2011). The synthesis of the lipid components of these microdomains appears to be

integrated with vesicle formation at the Golgi in order to sort and concentrate specific membrane proteins (Fig. 1.12).

In budding yeast, the biosynthesis of sphingolipids is simple as compared to metazoans and only three “complex” species of inositol phosphate-containing sphingolipids are made (Dickson, Sumanasekera, & Lester, 2006). After its synthesis in the ER, ceramide passes to the Golgi where mannose and inositol phosphates are sequentially added to produce all complex sphingolipids (Dickson et al., 2006). PI serves as a precursor of inositol phosphate in the Golgi making the maintenance of PI pools extremely important for complex sphingolipid synthesis. In the Golgi, PI is generated by Pis1p (phosphatidyl inositol synthase 1), which couples a phosphatidyl moiety from CDP-DAG (CDP-diacylglycerol) to inositol (Leber, Hrastnik, & Daum, 1995), and by Sac1p-mediated dephosphorylation of PI(4)P (Hama et al., 1999). For the latter, inositol phosphate-containing sphingolipids are generated at the expense of PI(4)P used in DAG production (Fig. 1.2). Presumably, the natural affinity between sterols and sphingolipids spontaneously leads to membrane microdomain formation. The coordinated regulation of PI and sphingolipid metabolism, therefore, appears to be important for integrating membrane sorting with vesicle formation.

The generation of sterol/sphingolipid microdomains in the Golgi membrane promotes the exocytosis of several well-defined PM transporters as well as glycosylphosphatidylinositol (GPI)-anchored proteins like Gas1p. Unlike other membrane proteins transported to the cell cortex, mutations that perturb ergosterol or sphingolipid metabolism disrupt the trafficking and distribution of the H^+-ATPase Pma1p, the Tat2p tryptophan permease, the arginine permease Can1p, the Gap1p general amino acid permease, and the uracil permease Fur4p (Bagnat, Chang, & Simons, 2001; Fröhlich et al., 2009; Lauwers & André, 2006; Surma et al., 2011; Umebayashi & Nakano, 2003). Gas1p and Pma1p are sorted into membrane microdomains in the ER before reaching the Golgi (Bagnat, Keränen, Shevchenko, Shevchenko, & Simons, 2000; Lee, Hamamoto, & Schekman, 2002; Markham et al., 2011). but the other transporters are concentrated into DRMs within the Golgi membrane (Bagnat et al., 2000; Hearn, Lester, & Dickson, 2003; Malinska, Malinska, Operakova, & Tanner, 2003; Umebayashi & Nakano, 2003). The original site of sorting into DRMs roughly correlates with the lateral

segregation of these proteins within different membrane domains once at the PM. In *S. cerevisiae*, the PM is compartmentalized into at least three different microdomains (Malinsky, Opekarová, & Tanner, 2010). Eisosomes or MCC (membrane compartment of Can1p) domains are stable and relatively immobile 300 nm-sized patches on the PM containing Can1p, Fur4p, and Tat2p (Fröhlich et al., 2009; Malinsky et al., 2010; Walther, Brickner, Aguilar, Bernales, & Walter, 2006). MCP (membrane compartment occupied by Pma1p) domains contain Pma1p and represent PM regions containing readily diffusible proteins that are excluded from the MCC (Malinsky et al., 2010). The third membrane domain, MCT (membrane compartment containing TORC2), consists of punctate patches containing the TORC2 complex that regulates the actin cytoskeleton and ceramide synthesis (Berchtold & C.Walther, 2009). Because the resident proteins are stably contained within these membrane domains, the lateral segregation of these proteins at the PM appears to be predetermined at the ER or the Golgi, depending on where the membrane domain originally formed.

In addition to promoting vesicle biogenesis, it has been proposed that lipid rafts promote vesicle instability once the vesicle reaches a terminal size promoting scission from the Golgi. This suggests that lipid rafts may also affect final steps of exocytic vesicle biogenesis (Lipowsky, 1993; Muralidharan-Chari, Clancy, Sedgwick, & D'Souza-Schorey, 2010).

Upon arrival in the PM, the lipid rafts are believed to serve as organizational tools, creating domains enriched for sterols, sphingolipids, lipids with saturated acyl chains, and proteins with lipid modifications or transmembrane domains (Levental et al., 2010; Sengupta, Hammond, Holowka, & Baird, 2008). Interestingly, it has been found that mutations in *LCB1*, a component of serine palmitoyltransferase which regulates the rate-limiting step in ceramide synthesis, caused depletion of complex sphingolipids leading to reduced lipid raft formation. These mutations resulted in reduced internalization of alpha factor via endocytosis, indicating that lipid rafts play an important role in regulating endocytosis during mating (Munn & Riezman, 1994; Zanolari et al., 2000). This hypothesis is in agreement with enrichment of sphingolipids and cholesterol reportedly stimulating compensatory endocytic in synapses (Takamori et al., 2006). One potential reason for this discovery is that complex sphingolipids are required for efficient

recruitment of N-BAR proteins Rvs161p and Rvs167p during vesicle scission (Youn et al., 2010). These discoveries indicate that lipid rafts may act as regulators of endocytosis.

In addition to their implications in regulating vesicular transport, sterols are transported by an unknown non-vesicular transport mechanism (Drin et al., 2016; Henne, Liou, & Emr, 2015). Since the mechanism of non-vesicular sterol transport remains elusive it is impossible to predict how sterols may regulate the mechanism directly. The role of lipid rafts as direct transport regulators may be underappreciated, but the findings that they may play a role in controlling endocytosis, as a potential initiator of compensatory endocytosis and as a regulator of N-BAR proteins as in case of sphingolipids, will help the understanding of how lipid domains can help regulate transport events at the PM. This opens for another question. If local domains are important for regulation of transport events, what about trans-leaflet domains? Does leaflet asymmetry affect transport function?

1.4.3. Phospholipid asymmetry is essential for membrane function and may regulate transport at the PM

Phospholipids are distributed asymmetrically across the PM leaflet restricting PE and PS in the cytosolic leaflet and concentrating PC in the extracellular side (Figure 1.13). This asymmetry is essential for maintaining cell polarity because loss of PS asymmetry disrupts cell polarity (Gregory D Fairn, Hermansson, Somerharju, & Grinstein, 2011; Mioka, Fujimura-Kamada, & Tanaka, 2014). (Mioka et al., 2014; Xu, Baldridge, Chi, Burd, & Graham, 2013). PS asymmetry is initially established in the Golgi. With these observations, along with the fact that PS is transported to the PM through both non-vesicular and vesicular trafficking, PS could be a regulator of both vesicular and non-vesicular pathways (Moser von Filseck et al., 2015). However, there is no evidence to support that PS directly regulates the protein machinery involved in vesicular trafficking. Rather PS acts as an essential building block of vesicles, due to its physical properties. Furthermore, the mechanism of non-vesicular PS transport remains poorly defined making it impossible to argue for a regulatory role for PS.

Figure1.13. Phospholipid distribution of the PM

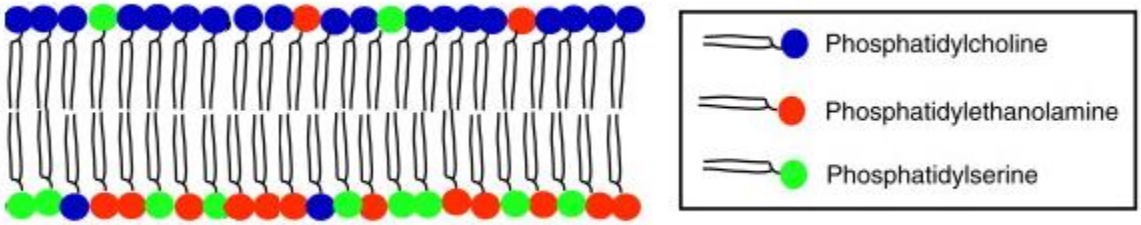

The negatively charged phosphatidylserine and phosphatidylethanolamine are restricted to the cytosolic leaflet of the PM while the neutral phosphatidylcholine is restricted to the extracellular side of the PM. This figure is adapted from (Tuck, 2011)

While PC has been suggested to regulate vesicle biogenesis at the TGN (Bankaitis et al., 1990), more recent studies indicate that DAG rather than PC itself is what regulates vesicle biogenesis, (Kearns et al., 1997), as for PE, no regulatory role has been attributed to it during vesicular trafficking. Furthermore, no non-vesicular transport pathways to and from the PM have been suggested for PC or PE, making it highly unlikely that they can function in integrating different transport pathways.

Lipids play a major regulatory role during both vesicular and non-vesicular trafficking in a multitude of ways. While PIPs rely on their phosphorylation state to modify responses, structural components like lipid rafts and PS alter transport pathways by modifying the physical properties of the membranes themselves. However, this still leaves one to question how lipid binding proteins affect transfer processes and what makes these proteins special.

1.5. Lipid-binding proteins directly regulate vesicular and non-vesicular trafficking

Since all transport pathways, both vesicular and non-vesicular, are regulated by lipid binding or lipid interacting proteins it positions these proteins perfectly for regulating

multiple pathways at once, and integrating them together. While many lipid binding proteins have been discovered, new knowledge has given us a better understanding of how individual proteins can regulate PM homeostasis by being involved in many transport events at once, and potentially integrating them. In yeast, the Osh protein family, Sec14p, and Arv1p are some of the proteins that have been studied as regulators of lipid transport to and from the PM, based on their lipid binding ability. The question is, are these bona fide transport pathway integrators?

1.5.1. ORPs are putative non-vesicular transport proteins implicated as regulators of vesicular transport

The ORPs have been implicated in non-vesicular transport of PI(4)P, sterols and PS at membrane contact sites (Chung et al., 2015; de Saint-Jean et al., 2011; Christopher J. Stefan et al., 2011). In addition to a role as regulators of non-vesicular lipid transporters ORPs have been linked to vesicular trafficking since OSBP, ORP3 and ORP1L binds to the small GTPases, Arf1, R-Ras and Rab7 respectively during vesicular transport (Johansson, Lehto, Tanhuanpa, Cover, & Olkkonen, 2005; Mesmin, Bigay, et al., 2013; Weber-Boyvat et al., 2015) Furthermore, yeast *OSH4* (also known as *KES1*) has been suggested to play a specific role in polarized exocytosis (Alfaro et al., 2011; Christopher T. Beh et al., 2001; Keith G. Kozminski, Alfaro, Dighe, & Beh, 2006; Ling, Hayano, & Novick, 2014). Osh4p has been proposed to affect exocytosis at numerous levels. Based on mutational analysis along with genetic evidence it has been suggested that PI(4)P - bound Osh4p is an upstream activator of Sac1p, but Osh4p is inhibited when in the sterol-bound form (Alfaro et al., 2011; Johansen et al., 2012; Christopher J. Stefan et al., 2011). In the negative feedback model, Osh4p promotes Sac1p dephosphorylation of PI(4)P to produce PI pools in the Golgi thus stimulating complex sphingolipid synthesis. Within the Golgi membrane, newly synthesized sphingolipids concentrate with sterols, which might trigger the inhibitory exchange wherein a sterol replaces PI(4)P for Osh4p binding. As a result, Sac1p activity is reduced and PI(4)P levels in the Golgi increase, which is an initiating event for vesicle formation. Vesicle biogenesis is thereby delayed until sphingolipid/sterol microdomains can be generated for cargo sorting. This model is supported by multiple lines of evidence: (i) complex sphingolipid levels are reduced in *osh4*Δ cells (LeBlanc et al., 2013); (ii) similar to that

observed in *sac1*Δ cells, the deletion of *OSH4* also causes missorting of proteins associated with sterol/sphingolipid membrane domains (LeBlanc et al., 2013; Proszynski et al., 2005); (iii) like *sac1*Δ, the deletion of *OSH4* restores PI(4)P levels in cells with conditional *PIK1* or *SEC14* mutations (Gregory D Fairn et al., 2007; Xinmin Li et al., 2002); (iv) the deletion of either *OSH4* or *SAC1* bypasses the essential requirement for *SEC14*, because increases in Golgi PI(4)P levels might induce vesicle biogenesis with associated decreases in PC or increased levels of DAG and/or sphingolipids (Fang et al., 1996). Thus, PI(4)P turn-over during vesicle biogenesis is in part controlled by Osh4p and its downstream effector Sac1p.

Osh proteins and Sac1p are also implicated in PI(4)P turnover later in vesicle transport well after post-Golgi vesicle formation (Christopher T Beh et al., 2012; Ling et al., 2014). Despite its importance in regulating vesicle budding from the Golgi, Osh4p is not required for vesicle biogenesis. Rather, all proteins of the Osh family must be inactivated to inhibit polarized transport, and the block is manifested only when vesicles dock with the PM but not earlier in exocytosis (Alfaro et al., 2011; Keith G. Kozminski et al., 2006). Because PI(4)P turn-over in vesicles regulates Rab GTPase interactions with both Myo2p and exocyst complex subunits, and Osh4p travels along with exocytic vesicles to the cell cortex, it is proposed that Osh proteins might regulate PI(4)P sequestration and/or dephosphorylation events even after vesicle release from the Golgi. PI(4)P sequestration is important for recruitment of the exocyst complex to the vesicle and recent evidence suggests that Osh4p may play a role in regulating exocyst complex assembly (Ling et al., 2014; Mizuno-Yamasaki et al., 2010). However, more evidence is needed to fully establish how Osh4p may act as a regulator of the exocyst complex during early vesicle transport. On the other hand, multiple findings support a proposed role for Osh proteins during vesicle docking: (i) Osh proteins associate *in vivo* with exocyst complex subunits and their GTPase regulators (but not Myo2p); (ii) genetic interactions reveal functional interactions between Osh proteins and the exocyst complex; (iii) Osh proteins are required for Cdc42p and Rho1p polarized localization at the PM; (iv) Sec4p association with exocytic vesicles is not Osh-dependent, but the docking of Sec4p-containing vesicles with the PM is Osh-dependent; (v) both *OSH4* and *SAC1* overexpression cause severe growth defects in conditional *MYO2* mutants,

potentially due to reductions in PI(4)P levels (Alfaro et al., 2011; Keith G. Kozminski et al., 2006; Santiago-Tirado et al., 2011).

Given that ORPs play important roles in regulating both vesicular and non-vesicular transport processes, it is an intriguing possibility that these proteins may act as a mechanistic link between multiple transport pathways to ensure PM homeostasis. However, since the mechanism for ORP function is still poorly understood, more research will have to be conducted to validate such proposals.

1.5.2. Sec14p: Proposed lipid transfer protein that regulates TGN vesicle biogenesis by regulating membrane lipid composition

Sec14p is an essential PI-PC transporter, shown to be required for vesicular transport from the TGN (Bankaitis et al., 1990, 1989). Sec14p is classified as a PI transfer protein (PITP) based on its ability to bind PI and PC and transfer them between liposomal membranes in vitro (Bankaitis et al., 1990). However, although PI and PC-binding contributes to Sec14p function, data suggests that lipid transfer activity may be irrelevant in vivo. Rather, Sec14p acts as a sensor of membrane phospholipid composition in turn regulating PC and PI metabolic pathways to modify the lipid environment, promoting vesicle biogenesis (Ile, Schaaf, & Bankaitis, 2006). The importance for Sec14p in regulating PI metabolism *in vivo* is highlighted by the finding that depletion of Sec14p function results in 50% loss of cellular PI(4)P and depletion of Golgi PI(4)P pools (Gregory D Fairn et al., 2007). Furthermore depleting cells of Sec14p function stimulated PC synthesis and Spo14p (PC-phospholipase D) dependent PC turnover, while PC turnover by Nte1p, a PC-phospholipase B, was reduced (Fernández-Murray & McMaster, 2005; Henneberry et al., 2001; Sreenivas et al., 1998). While it is well understood that Sec14p regulates PI and PC metabolism the molecular mechanism remains elusive. Furthermore, Sec14p's role in regulating PI and PC metabolism is highlighted by the finding the modulating other proteins affecting PI and PC metabolite levels was able to rescue or exacerbate the phenotypes associated with loss of Sec14p function (Ann E. Cleves et al., 1991; Gregory D Fairn et al., 2007; Fernández-Murray & McMaster, 2005; Xinmin Li et al., 2002; Schaaf et al., 2008; Sreenivas et al., 1998; Xie

et al., 1998; Xie, Fang, & Bankaitis, 2001). Particularly deleting either Sac1p or Osh4p in a temperature sensitive *SEC14* allele restored cell viability to almost normal, highlighting the importance of PI(4)P metabolism for Sec14p function (G. D. Fairn & McMaster, 2008; Fang et al., 1996; Rivas et al., 1999). These studies indicate that while being important for vesicle biogenesis, Sec14p is a regulator of local lipid metabolism, not a direct regulator of vesicular transport *per se*, making it unlikely to be a good candidate for a protein involved in directly regulating multiple transport pathways.

1.5.3. Integral ER membrane protein Arv1p is proposed to mediate ER to PM sterol transfer

Arv1p is an ER protein that has been implicated in direct sterol transfer, while evidence suggests that sterol transfer may be a secondary effect of Arv1p function in ER morphology maintenance. Arv1p has been implicated in regulating sterol homeostasis in yeast as well as in mammalian systems (Lagor et al., 2015; Swain et al., 2002; Tinkelenberg et al., 2000; F. Tong et al., 2010). Based on the observation that deletion of *ARV1* resulted in altered cellular sterol distribution Arv1p was hypothesized to function as an ER-PM non-vesicular sterol transporter (Tinkelenberg et al., 2000). However, other studies have pointed to a role for Arv1p in regulating GPI lipid anchors at the ER (Kajiwara et al., 2008). Since GPI anchors are a component of lipid rafts it is possible that reduced GPI anchor production leads to the scrambling of lipid rafts, which in turn causes sterol redistribution. With very little known about Arv1p and its function, it is impossible to make a claim for it as an integrator of transport pathways as more research is needed.

1.6. Potential transport integrators. What does it take for lipids or proteins to be considered transport integrators?

Lipids and lipid-regulated/binding proteins play key roles in regulating individual transport pathways, however, the ability of these lipids and proteins to integrate different transport events remain largely unknown. If they are to be considered as transport integrators at the PM, then both lipids and proteins must fulfill important criteria. 1) They

must be at the right localization at the right time to be involved in multiple pathways. 2) They must be functionally required for multiple transport processes to occur normally and 3) They must directly bind and regulate the function of known transport regulating proteins during the transport process. Given what we know about the lipids and proteins involved in regulating PM homeostasis, which would be the most likely integrators of multiple transport events?

1.6.1. PIPs and lipid rafts regulate multiple transport pathways but are they transport integrators?

When considering all lipid species, the most likely to integrate multiple pathways are the PIPs. They have been shown to directly regulate the function of proteins important for both endocytosis and exocytosis (Mizuno-Yamasaki et al., 2010; Santiago-Tirado et al., 2011; C J Stefan et al., 2002), and have been implicated in regulation of non-vesicular lipid transport (Moser von Filseck et al., 2015) making them a potential integrator of multiple pathways. However, their rapid interconversion makes it difficult to identify individual species as key regulators of a specific point of a transport pathway. Rather it is the constant modifications of PIP species and local PIP concentration gradients that are driving membrane transport. This fact makes it hard to classify an individual PIP species as a transport integrator, but considering the entire PIP lipid class as directors of membrane traffic would seem more appropriate.

A similar argument can be made about lipid rafts as their presence is required during vesicle biogenesis at the TGN and as regulators of endocytosis (Lipowsky, 1993; Muralidharan-Chari et al., 2010; Youn et al., 2010). However, the exact mechanisms whereby lipid rafts regulate these transport pathways remain unclear. Furthermore, lipid rafts serve as structural elements that attract proteins due to their physical properties, thus implying that rafts may act as beacons for raft-associated proteins (Bagatolli et al., 2010). If transport regulation is achieved through the raft-associated proteins rather than the lipid rafts themselves, then transport phenotypes would arise upon lipid raft formation defects without lipid rafts acting as direct regulators of the process *per se*. These considerations make it hard to consider lipid rafts as integrators of transport, but rather as structural elements required for optimal cellular transport.

1.6.2. Lipid binding proteins and small Rab GTPase cascades integrate vesicular trafficking?

In yeast, the most promising candidates for lipid binding proteins that could integrate transport processes are the Osh proteins. While the exact molecular mechanisms remain unknown, Oshs have been implicated as direct regulators of non-vesicular transport at membrane contact sites (Manford et al., 2012; Schulz et al., 2009; Christopher J. Stefan et al., 2011). Furthermore, Osh4p has been shown to be an important regulator of PI(4)P levels during vesicle biogenesis at the TGN and the Osh proteins as a family are important for vesicular trafficking (Christopher T Beh & Rine, 2004; Gregory D Fairn et al., 2007; Fang et al., 1996; Xinmin Li et al., 2002). Interestingly, studies showed distinct genetic interactions with Osh4p and Cdc42p, indicating that Osh4p may play a direct role at the bud tip during polarized exocytosis (Keith G. Kozminski et al., 2006), supporting the idea that Osh4p may integrate vesicular and non-vesicular transport. However, more evidence is needed to establish such a mechanism.

Arv1p is another putative sterol transporting protein that may act as a regulator of multiple transport pathways (Gallo-Ebert et al., 2012; Tinkelenberg et al., 2000). However, our knowledge of this protein remains very limited and one would have to definitively answer the question if Arv1p is a regulator of sterol homeostasis at the PM, before further investigations can take place.

A final class of proteins that needs to be included when discussing potential integrators of transport pathways are the small Rab GTPases. Maintaining balance between vesicular transport pathways necessitates that they are integrated to regulate incoming vesicles with outgoing. One recent hypothesis states transition between vesicular transport events is regulated by an exchange of small Rab GTPases that regulate the individual transport steps (Lipatova, Hain, Nazarko, & Segev, 2015; Rivera-Molina & Novick, 2009). Small Rab GTPases lipidated proteins known to regulate motor proteins, targeting complexes and SNARE binding during vesicular trafficking events (Hutagalung & Novick, 2011), thus acting as central regulators of vesicular transport. In yeast, small GTPases have been shown to regulate vesicular trafficking, with the exception of endocytosis where no Rab GTPase has been identified to date (Lipatova et

al., 2015; Park & Bi, 2007). The activity of Rab GTPases is regulated by its GTP-bound state and by covalent lipid modifications (Wennerberg, Rossman, & Der, 2005). Most Rab GTPases are prenylated at their C-terminal ends with two geranylgeranyl groups by the cytoplasmic geranylgeranyl transferase (GGTase) II complex. This modification targets the Rab GTPases to membranes and plays a role in regulating their activity and plays an important role in regulating Sec4p and Ypt31/32p activities. Several proteins that recognize and bind to the di-geranylgeranyl modification determine the targeting of Sec4p and Ypt31p/32p to membranes. Mrs6p is a GGTase II complex chaperone that recognizes newly synthesized Rab GTPases for prenylation and then delivers them to membranes. As a Rab escort protein (REP), Mrs6p cannot retrieve Sec4p or other Rab GTPases after membrane delivery (Alory & Balch, 2003). In contrast, Gdi1p, the yeast Rab guanine-nucleotide dissociation inhibitor (GDI), removes Rab GTPases from membranes after they complete GTP hydrolysis. For example, Gdi1p extracts prenylated GDP-bound Sec4p from membranes for recycling back to re-initialize post-Golgi vesicle transport (Garrett et al., 1994). Since Sec4p is the central regulator of exocytosis (Ortiz et al., 2002; Walch-Solimena, Collins, & Novick, 1997; Walworth, Brennwald, Kabcenell, Garrett, & Novick, 1992) and Sec4p remains associated with the PM after exocytosis is completed, it is possible that Sec4p could act as regulator of both transport pathways. Such a model is supported by the finding that late *SEC* mutants (including Sec4p) display endocytic defects (Riezman, 1985). If this model is true, then Sec4p would be the first direct mechanistic link between exocytosis and endocytosis in yeast, integrating the two processes.

Taken together, these considerations raise 3 testable questions that constitute the foundation of my Ph.D. thesis work that I aimed to answer. 1) Is Osh4p a direct regulator of polarized exocytosis? 2) Is Arv1p involved in non-vesicular sterol transfer between the PM and ER? 3) Is Sec4p a bona fide regulator of both exocytosis and endocytosis?

Chapter 2. The Sterol-Binding Protein Kes1/Osh4p is a Regulator of Polarized Exocytosis

Alfaro G, Johansen J, Dighe SA, Duamel G, Kozminski KG, Beh CT. Published in Traffic Nov 2011 Vol 12 :1521-36.

Oxysterol-binding protein (OSBP)-related protein Kes1/Osh4p is implicated in nonvesicular sterol transfer between membranes in *Saccharomyces cerevisiae*. However, we found that Osh4p associated with exocytic vesicles that move from the mother cell into the bud, where Osh4p facilitated vesicle docking by the exocyst tethering complex at sites of polarized growth on the plasma membrane. Osh4p formed complexes with the small GTPases Cdc42p, Rho1p, and Sec4p, and the exocyst complex subunit Sec6p, which was also required for Osh4p association with vesicles. Although Osh4p directly affected polarized exocytosis, its role in sterol trafficking was less clear. Contrary to what is predicted for a sterol-transfer protein, inhibition of sterol binding by the Osh4p Y97F mutation did not cause its inactivation. Rather, *OSH4*^{Y97F} is a gain-of-function mutation that causes dominant lethality. We propose that in response to sterol binding and release Osh4p promotes efficient exocytosis through the coordinate regulation of Sac1p, a phosphoinositide 4-phosphate (PI(4)P) phosphatase, and the exocyst complex. These results support a model in which Osh4p acts as a sterol-dependent regulator of polarized vesicle transport, as opposed to being a sterol-transfer protein.

As a principal component of the plasma membrane (PM), cholesterol is a key determinant of PM structure and function (Mesmin & Maxfield, 2009). Despite the overall importance of cholesterol to membrane organization, the mechanism for the intracellular trafficking of sterols between organelles is poorly understood. Apart from the exocytic vesicles that transport most proteins and phospholipids destined for the PM, a parallel "nonvesicular" pathway transfers cholesterol from its site of synthesis in the endoplasmic reticulum (ER) membrane to the PM, where sterols are concentrated (Baumann et al., 2005; Urbani & Simoni, 1990). An appealing model for nonvesicular sterol transport envisions that soluble lipid-transfer proteins ferry sterols through the cytoplasm to the PM, after their extraction from the cytoplasmic leaflets of intracellular membranes (Maxfield & Menon, 2006).

Oxysterol-binding protein-related proteins (ORPs) represent perhaps the most promising candidates for sterol-transfer proteins. The 7 ORPs in *Saccharomyces cerevisiae*, encoded by the *OSH1-OSH7* genes, and the 19 human ORPs (encoded by 12 different ORP genes), bind sterols and many are implicated in sterol-dependent regulatory pathways (G. D. Fairn & McMaster, 2008; Olkkonen & Levine, 2004). *In vivo* and *in vitro* studies suggest that the yeast ORP Kes1/Osh4p (hereafter Osh4p) affects sterol transfer between the ER and PM (Christopher T Beh & Rine, 2004; Raychaudhuri, Im, Hurley, & Prinz, 2006). However, other investigations point to a role for Osh4p in post-Golgi vesicle transport (Gregory D Fairn et al., 2007; Fang et al., 1996; Keith G. Kozminski et al., 2006; Xinmin Li et al., 2002; Muthusamy et al., 2009). Deletion of *OSH4*, for example, bypasses the essential requirement for *SEC14*, which encodes a phosphatidylcholine/phosphatidylinositol (PC/PI) transfer protein required for vesicle budding from the Golgi (Fang et al., 1996). The deletion of *OSH4* by itself, however, does not block vesicle transport from the Golgi, though Osh4p and Golgi P4-ATPase lipid-flippases have mutually antagonistic functions that affect membrane biogenesis (Muthusamy et al., 2009). These findings raise further questions about how Osh proteins and their binding of sterols might affect both nonvesicular sterol trafficking and vesicle-mediated exocytosis.

Apart from Osh4p functions at the Golgi, the *OSH* gene family is collectively required for polarized exocytosis during the last steps of polarized transport (Keith G.

Kozminski et al., 2006). In budding yeast cells, the release of exocytic vesicles from the actomyosin cytoskeleton is coordinated with vesicle docking at the PM, specifically at the bud tip or mother-bud junction (Park & Bi, 2007). These dynamic events can be tracked by observing the motility of Sec4p (Boyd et al., 2004), a vesicle-anchored Rab GTPase that links exocytic vesicles to actin cables via the myosin motor Myo2p, which facilitates transport to specific docking sites in the bud (D. Pruyne & Bretscher, 2000; D. W. Pruyne, Schott, & Bretscher, 1998; Wagner, Bielli, Wacha, & Ragnini-Wilson, 2002). When temperature-sensitive *osh*Δ *osh4-1*^{ts} cells (*osh*Δ refers to the deletion of all *OSH* genes) are incubated at elevated temperatures, the entire, functionally redundant, *OSH* gene family is inactivated and GFP-Sec4p-marked vesicles transit into the bud but do not fuse with the PM (Keith G. Kozminski et al., 2006). This result is consistent with the observed buildup of polarized exocytic cargo within cells after *OSH* gene inactivation (Keith G. Kozminski et al., 2006) and suggests a defect in vesicle docking with the PM, as mediated by the exocyst complex. When a vesicle is closely juxtaposed to the PM, interactions between membrane- and vesicle-bound exocyst complex subunits result in vesicle docking, which actuates SNARE-mediated fusion with the PM (He & Guo, 2009). When vesicles are docked at the PM, the final assembled exocyst complex includes Sec3p and Exo70p, the Rho family GTPases Cdc42p and Rho1p (He et al., 2007; Zhang et al., 2008), and the six other subunits that are tethered to vesicles by an association with Sec4p (Novick et al., 2006). Several *OSH* family members, including *OSH4*, genetically interact with genes encoding exocyst complex subunits and their small GTPase regulators (Keith G. Kozminski et al., 2006). Thus, there are compelling indications of a link between Osh proteins and the exocyst complex.

In this study, we describe a direct role for Osh proteins in the regulation of exocytic vesicle docking at the PM during polarized transport. We found that Osh4p is attached to post-Golgi exocytic vesicles as they are released from the Golgi and are targeted to the PM in the growing bud. Once at the PM, Osh4p facilitates vesicle docking through physical interactions with the exocyst complex and its regulators. Structure/function analysis of mutant Osh4 proteins indicated that sterol binding is dispensable for at least some Osh4p functions, and these results present an alternative to current models positing that Osh4p acts solely as a sterol transfer protein for the nonvesicular transport of sterols. Instead, Osh4p appears to be both a lipid-dependent

regulator of the Sac1p PI(4)P phosphatase and of events involving vesicle docking at sites of polarized growth at the PM.

2.1. Results

2.1.1. Docking of exocytic vesicles is defective in cells lacking functional Osh proteins

The elimination of all Osh protein function results in the depolarized localization of both Rho1p and Cdc42p, and the aberrant accumulation of Sec4p-marked vesicles within yeast cell buds (Keith G. Kozminski et al., 2006). These defects are consistent with a block in vesicle/PM docking in which vesicle-bound exocyst complex subunits (Sec5p, Sec6p, Sec8p, Sec10p, Sec15p, Exo70p, Exo84p) fail to assemble with PM-bound exocyst subunits (Sec3p and Exo70p) at sites of polarized growth (Boyd et al., 2004). Other predicted defects resulting from such a failure include an accumulation of vesicle-associated exocyst complex subunits within buds, a reduction in the turnover of these subunits after vesicle docking, and the depolarized localization of undocked subunits.

To determine how *OSH* mutants affect exocyst complex assembly, the dynamic localization of Sec5p-3xGFP, GFP-Sec4p, and GFP-Exo70p particles was analyzed in detail in wild-type, *osh*Δ *OSH4*, and *osh*Δ *osh4-1*^{ts} cells cultured at 23˚C and then incubated at 37˚C for 4 h. In small-, medium-, and large-budded wild-type cells, these proteins are observed at sites of polarized membrane growth corresponding to the bud tip, around the bud cortex, and at the mother-bud junction, depending on cell-cycle stage (Boyd et al., 2004) (Figure 2.1A,C,E). In *osh*Δ *OSH4* cells, the localization of Sec5p-3xGFP, GFP-Sec4p, and GFP-Exo70p particles to these polarized sites was similar to wild type (Figure 2.1A,C,E). Thus, despite the deletion of six *OSH* genes, *OSH4* expression alone was sufficient for polarized exocytosis, presumably due to functional redundancy among *OSH* genes (Christopher T. Beh et al., 2001). In contrast, when *osh*Δ *osh4-1*^{ts} cells were incubated at 37˚C, we observed a 3-fold increase in

Sec5p-3xGFP aggregation within buds relative to wild type (n > 180 cells; p = 0.0003), similar to the reported aggregation in GFP-Sec4p-expressing cells (Keith G. Kozminski et al., 2006) (Figure 2.1C). Furthermore, if we quantified just discrete non-aggregated particles, in *osh*Δ *osh4-1*^{ts} cells incubated at 37˚C many were mislocalized from buds into mother cells as shown by the increased ratio of Sec5p-3xGFP and GFP-Sec4p particles in mother cells relative to buds (Figure 1A,C). Sec15p-3xGFP, another vesicle-associated exocyst complex subunit, was also mislocalized in *osh*Δ *osh4-1*^{ts} cells (data not shown). When cultured at 23˚C, no statistically significant differences were observed for the polarized localization of GFP-Sec4p, Sec5p-3xGFP, or Sec15p-3xGFP in *osh*Δ *osh4-1*^{ts} cells relative to *osh*Δ *OSH4* or wild-type cells (n > 40 cells for each strain and each marker; p > 0.05). For PM-associated exocyst complex subunits, the polarized localization of GFP-Sec3p was not affected in *osh*Δ *osh4-1*^{ts} cells (Keith G. Kozminski et al., 2006) and the defect in GFP-Exo70p polarized localization was moderate (2.5 fold) as compared to the 3.8-fold and 3.5-fold increases in mother/bud ratios for Sec4p and Sec5p, respectively (Figure 2.1E). Because Sec3p localization to the PM does not require vesicle transport, and Exo70p is only partially dependent on vesicle transport (Boyd et al., 2004; He et al., 2007), these results indicated that Osh protein inactivation mainly affects the localization of exocyst complex-associated proteins carried on exocytic vesicles, consistent with a vesicle-docking defect.

In Osh-deficient cells, the observed accumulation of vesicles in the mother cell might result either from defective vesicle movement into the bud or a return of vesicles back into the mother cell because of the failure of vesicles to attach and then fuse with the PM. Compared to wild-type cells, 89% of Sec5p-3xGFP and 79% of GFP-Sec4p particles were properly targeted into the bud in *osh*Δ *osh4-1*^{ts} cells at 37˚C, when tracked by wide-field video microscopy (n ≥ 20 vesicles). In these *osh*Δ *osh4-1*^{ts} cells, the small fraction (~10-20%) of particles that stay within the mother cell do not account for the large increase in the ratio of particles in the mother cell versus the bud. Thus, in Osh-deficient cells the backlog of undocked polarized exocytic vesicles resulted in both their accumulation within buds and their overflow back out into the mother cell.

To determine whether Osh proteins affected the lifespan/turn-over of exocyst complex proteins within the bud, wide-field video microscopy was used to monitor

individual particles at the PM. In comparison to wild-type and *osh*Δ *OSH4* cells, in *osh*Δ *osh4-1*^{ts} cells incubated at 37˚C we observed 1.9 to 3.4-fold increases in the lifespan of Sec5p-3xGFP, GFP-Sec4p, and GFP-Exo70p particles within the bud ($p < 0.001$), as timed immediately after particles first reached the cell cortex (Figure 2.1B,D,F). These findings suggested that without Osh proteins exocyst complex subunits do not dissociate from vesicles as a result of incomplete vesicle/PM docking, and the subunits, therefore, persist on these undocked vesicles.

Figure 2.1. Localization and lifespan of exocyst-associated subunits in cells lacking *OSH* gene function.

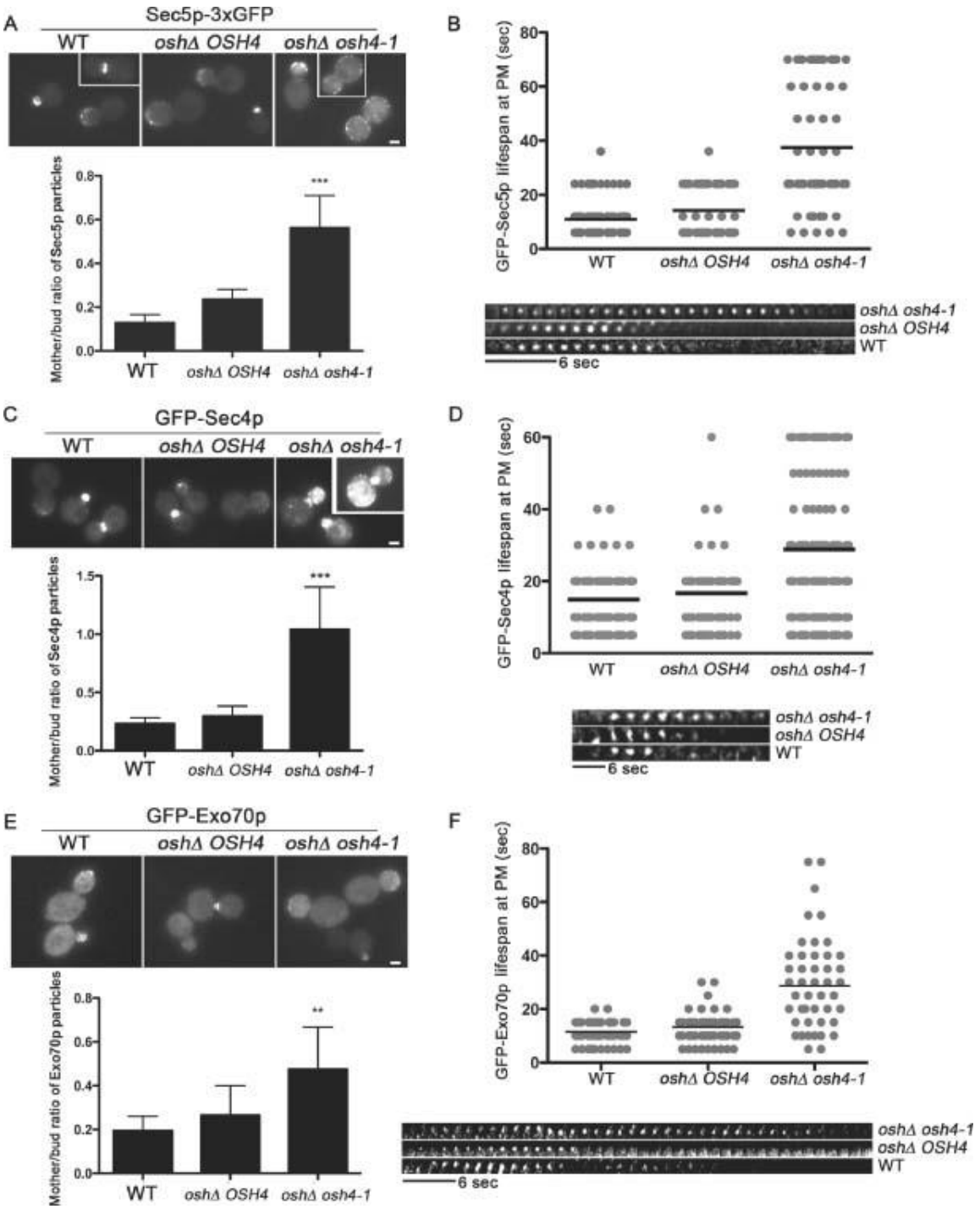

A and B) Sec5p-3xGFP, (C and D) GFP-Sec4p, and (E and F) GFP-Exo70p particles were tracked in log-phase wild-type (WT; SEY6210), *osh*Δ *OSH4* (CBY924), and *osh*Δ *osh4-1* cells (CBY926) cultured at 25˚C and then at 37˚C for 4 h. A and C and E) Representative cell images are shown and polarization defects are quantified in each corresponding histogram. Because discrete particles were difficult to resolve within small buds, only distinct, non-aggregated, particles in medium- and large-budded cells were counted (though this underestimates particle numbers within buds). The fraction of discrete particles in mother cells relative to those in buds is shown (1.0 indicates an even distribution between bud and mother cells, and indicates complete particle depolarization; $n \geq 181$ total particles counted in 20 – 48 cells for each strain). Single asterisk indicates $p < 0.05$, double indicates $p = 0.002$; triple asterisk indicates $p < 0.0001$. Scale bars = 2 µm. B and D and F) Scatterplots showing Sec5p-3xGFP, GFP-Sec4p, and GFP-Exo70p particle lifespans timed immediately after their appearance at the cell cortex, were plotted per 5 s intervals from 70 s, 60 s, and 80 s time-lapse videos, respectively ($n > 50$ particles). Below each graph, a time series from movies show representative particle lifespans at the PM. In all experiments, statistically, significant differences were evident between either *osh*Δ *osh4-1* and WT cells, or *osh*Δ *osh4-1* and *osh*Δ *OSH4* cells ($p < 0.0001$). Experiments were performed by G.A

2.1.2. Osh4p associates with vesicles targeted to sites of polarized growth

To address whether Osh proteins themselves associate with exocytic vesicles, we analyzed the localization of Osh4p fused to RFP (red fluorescent protein) or YFP (yellow fluorescent protein) using three-dimensional time-lapsed (4D) video confocal microscopy. Consistent with previous studies (Xinmin Li et al., 2002), Osh4p-YFP was observed in wild-type cells both throughout the cytoplasm and in association with a population of punctate structures co-localizing with the Golgi-marker Kex2p-CFP (cyan fluorescent protein) (Figure 2.2A). In addition, we found a population of small highly motile Osh4p-YFP particles that did not co-localize with Kex2p-CFP (Figure 2.2A). The dynamic behavior of these smaller particles suggested they correspond to exocytic vesicles. When the motile Osh4p-RFP particles were tracked by 4D confocal microscopy (Figure 2.2B,C), most co-localized with the post-Golgi vesicle marker GFP-Sec4p (D. H. Schott, Collins, & Bretscher, 2002). These Osh4p-RFP/GFP-Sec4p particles moved together into the bud (Figure 2.2C) and congregated at sites of polarized growth on the PM (Figure 2.1B, arrows). This result is also consistent with previous observations using electron microscopy in which an accumulation of vesicles was seen within buds of cells lacking functional Osh proteins (Christopher T Beh & Rine, 2004). These findings established that Osh4p associates with post-Golgi vesicles, providing further support for a role of Osh4p in polarized vesicular transport.

Figure 2.2. Osh4p resides on vesicles targeted to sites of polarized growth.

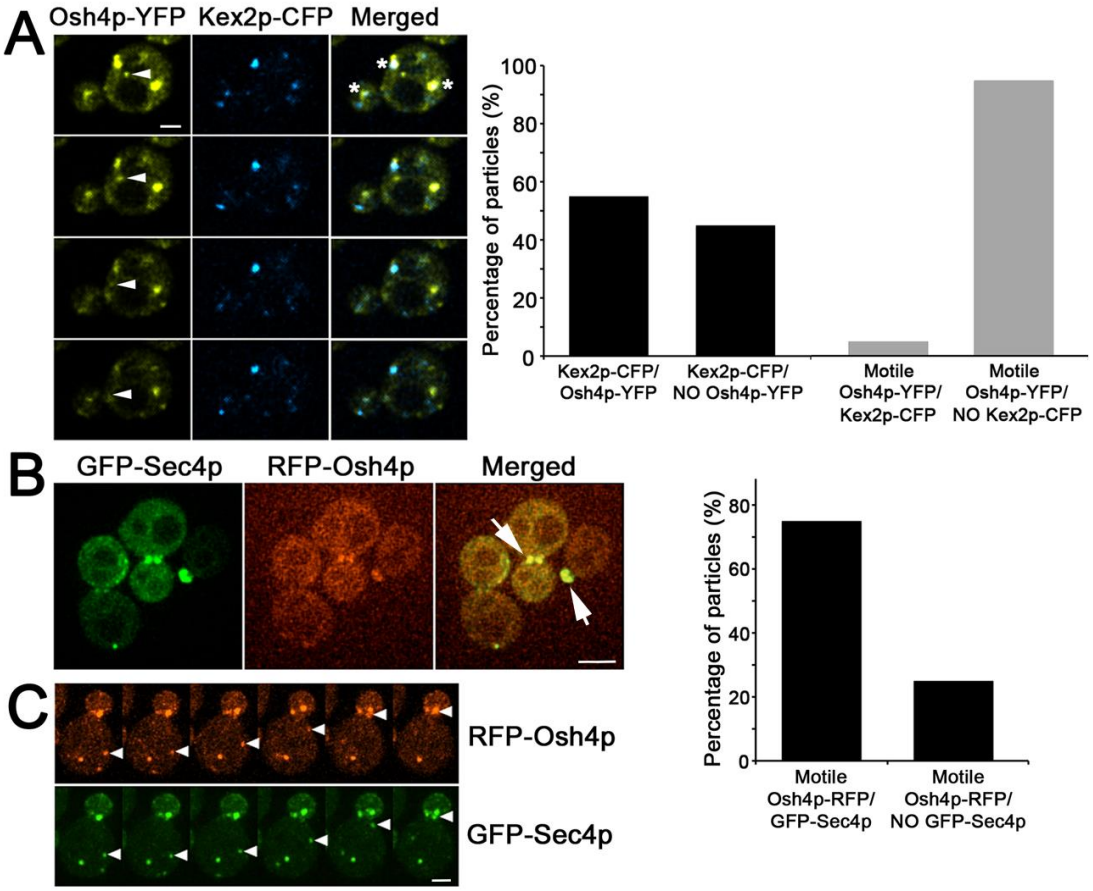

A) Osh4p-YFP co-localized with Kex2p-CFP Golgi on motile particles that transit into the bud. Wild-type cells (SEY6210) expressing Osh4p-YFP and Kex2p-CFP from integrated constructs were viewed by confocal microscopy. Each panel column (top to the bottom) represents images acquired at a single focal plane (1.6 s/frame). Arrowheads indicate an Osh4p-YFP motile particle moving from the mother cell towards the daughter bud. In merged images, Osh4p-YFP/Kex2p-CFP overlap is shown in white, and asterisks indicate Osh4p-YFP particles that co-localized with Kex2p-CFP for one or more frames. Scale bar = 2 μm. B) Osh4p-RFP and GFP-Sec4p visualized by confocal microscopy in log-phase wild-type cells (SEY6210) cultured at 30˚C. The merged image shows overlap between Osh4p-RFP and GFP-Sec4p localization at the bud tip and bud neck in small-budded and large-budded cells, respectively (arrows). Scale bar = 4 μm. Co-localization of motile Osh4p-RFP particles with GFP-Sec4p is quantified in the graph. Note that increased *SEC4* dosage enhanced Osh4p-RFP fluorescence at polarized sites over that observed in (A). C) Osh4p-RFP co-localized with GFP-Sec4p post-Golgi vesicles moving from the mother cell into the bud (arrowheads). Each frame was acquired at 2.6 s intervals (0.6 s delay between Osh4p-RFP/GFP-Sec4p image acquisitions), and vesicles were tracked in one focal plane. Scale bar = 2 μm. Experiments were conducted by G.A

2.1.3. Osh4p association with polarized exocytic vesicles is SEC6-dependent

To test whether Osh4p association with vesicles was dependent on the exocyst complex, the association of Osh4p with exocytic vesicles was analyzed following the disruption of exocyst complex assembly. At 37˚C, the *sec6-4*^{ts} mutation causes Sec6p destabilization and disrupts exocyst complex assembly (Songer & Munson, 2009), which results in the accumulation of Sec4p-marked exocytic vesicles within the bud (Walch-Solimena et al., 1997). Using *sec6-4*^{ts} cells (TerBush & Novick, 1995) expressing Osh4p-YFP, we tested if the disruption of the exocyst complex affected Osh4p localization on vesicles or at sites of polarized growth at the PM. Consistent with the data above (Figure 2.2B), in wild-type and *sec6-4*^{ts} cells cultured at 25˚C, Osh4p-YFP was observed on motile particles/vesicles targeted to sites of polarized growth. Osh4p-YFP was also observed on immotile particles that co-localized with the Golgi marker Sec7p-dsRED (Losev et al., 2006) (Figure 2.3). After incubating *sec6-4*^{ts} cells at 37˚C, the motile population of Osh4p-YFP particles decreased 8.7-fold relative to that observed in wild-type cells at 37˚C. Conversely, the population of immotile particles in these cells containing both Osh4p-YFP and Sec7p-dsRED increased 1.5-fold relative to wild type (Figure 2.3). Thus, Osh4p-YFP association with the Golgi was largely unaffected in *sec6-4*^{ts} cells at 37˚C, despite the increased size of Golgi as visualized with the Sec7p-dsRED marker (Figure 2.3). Consistent with these results, we found that Osh4p co-fractionates with membrane fractions containing exocytic vesicles, and this co-fractionation was also *SEC6* dependent. Using extracts of yeast grown at 25˚C, Osh4p co-fractionated with markers of polarized exocytic vesicles (i.e. Sec4p) on 18-34% Nycodenz-sorbitol buoyant density gradients (Figure 2.1S). When membrane extracts derived from *sec6-4*^{ts} cells incubated at 37˚C for 1.5 hr were centrifuged in an 18-34% Nycodenz-sorbitol buoyant density gradient, Osh4p no longer co-fractionated with markers of polarized exocytic vesicles (i.e. Sec4p and Bgl2p) (Figure 2.1S). Altogether, these results suggested that the recruitment or maintenance of Osh4p on exocytic vesicles is affected by *SEC6* and the integrity of the exocyst complex, whereas Osh4p association with the Golgi is *SEC6* independent.

Figure 2.3. Osh4p-YFP localization on motile (vesicle) particles was disrupted in *sec6-4*^{ts} cells.

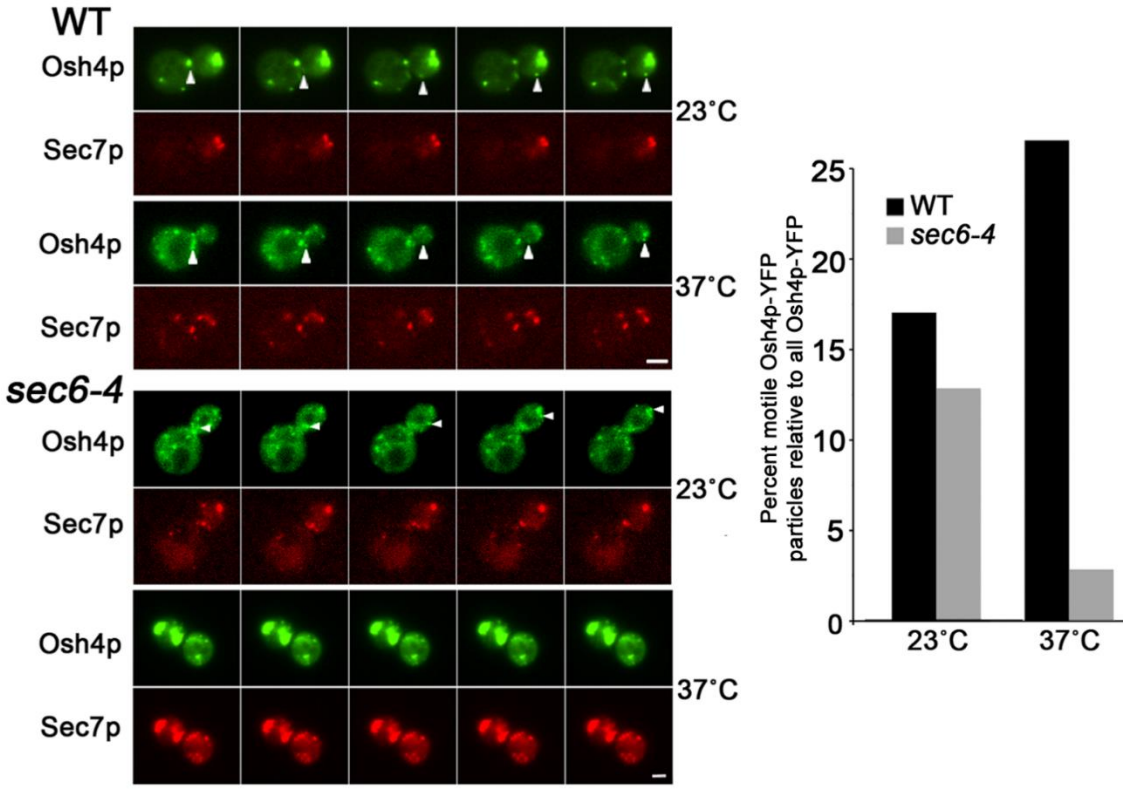

Images of log-phased wild-type (WT; BY4741) and *sec6-4* cells (CBY4712) transformed with plasmids expressing Osh4p-YFP (pCB876) and Sec7p-dsRED (pLC1329), cultured at 23˚C or shifted to 37˚C for 2 h. When either strain was cultured at 23˚C, Osh4p-YFP was detected on immotile particles that co-localized with the Golgi marker Sec7p-dsRED. Osh4p-YFP was also observed on motile Sec7p-dsRED-independent vesicles (arrowheads) that moved from the mother cell into the bud. Scale bars = 2 μm. In the histogram, the relative proportions of motile Osh4p-YFP vesicles relative to all Osh4p-YFP were quantified; motile Osh4p-YFP particles did not co-localize with Sec7p-dsRED and moved for 3 consecutive frames (3 s each) in a polarized direction toward the bud. For all cells, $n \geq 162$ particles counted. Experiments were conducted by G.A

2.1.4. Osh4p forms complexes with exocyst-associated proteins

Osh4p and Sec4p co-localization and co-fractionation, and genetic interactions between *OSH4* and exocyst complex regulators (Keith G. Kozminski et al., 2006), suggested that Osh4p physically interacts with proteins required for vesicle docking. We first tested whether Osh4p interacts *in vivo* with the small GTPases required for exocyst complex formation. We found by tandem affinity purification (TAP) that the small

GTPases Cdc42p and Rho1p co-purified with TAP-tagged Osh4p from detergent-treated yeast extracts, but not with TAP-tagged Tdh1p (glyceraldehyde-3-phosphate dehydrogenase [GAPDH]), which is not involved in cell polarization (Figure 2.4A). Non-ionic detergent was added to all extracts (unless otherwise indicated) to ensure membrane disruption and solubilization of membrane-associated proteins. These results were also confirmed by co-immunoprecipitation (coIP). An anti-Osh4p antibody immunoprecipitated endogenous Osh4p and co-precipitated endogenous Rho1p, whereas an anti-HA antibody precipitated Osh4p-2xHA and co-precipitated endogenously expressed Cdc42p (Figure 2.4B). Therefore, we also tested whether Osh4p might co-purify with Sec4p, the GTPase that binds exocyst subunits to the vesicle membrane (Boyd et al., 2004). Using TAP, we found that GFP-Sec4p co-purified with Osh4p-TAP from detergent-treated yeast extracts, but not with the Tdh1p-TAP control (Figure 2.4C). As confirmation of this result, an antibody that immunoprecipitated endogenous Osh4p also co-precipitated Sec4p (Figure 2.4D). Independent from the exocyst complex, Sec4p associates with the type V myosin Myo2p (TerBush & Novick, 1995). However, in TAP experiments Osh4p did not co-purify with Myo2p (data not shown). Again, this result indicated that Osh4p specifically co-precipitates exocyst complex subunits and does not interact with other Sec4p-associated complexes – even those affecting related but separate aspects of vesicle transport.

Given that Osh4p co-purified with vesicle- and PM-associated GTPases that regulate the exocyst complex, we also tested if Osh4p physically associates with Sec6p, the exocyst subunit that stabilizes the assembled exocyst complex at sites of secretion (Songer & Munson, 2009). By TAP, Osh4p-2xHA co-purified from detergent-solubilized yeast extracts with Sec6p-TAP, but not Tdh1p-TAP (Figure 2.4E). Similarly, an anti-GFP antibody that precipitated Sec6p-GFP also co-precipitated Osh4p-2xHA (Figure 2.4F). Using the same extracts and conditions, we also found that lipid-modified Ras2p did not co-precipitate with Osh4p-2xHA, indicating that Osh4p does not have a general affinity for prenylated small GTPases (Figure 2.4F). We also found that the exocyst subunit Sec8p-Myc coIPed with Osh4p-2xHA (data not shown). Finally, we tested whether Osh4p interactions were affected by *sec6-4*^{ts}, a mutation that reduces the association of some, but not all, exocyst complex associations (Songer & Munson, 2009; TerBush & Novick, 1995). In coIPs from extracts isolated after *sec6-4*^{ts} cells were incubated at

37˚C, there was a 2.2-fold reduction in the amount of Osh4p-2xHA that co-purified with native Rho1p relative to coIPs from wild-type extracts (Figure 2.4G). In similar coIP experiments from *sec6-4*^{ts} and wild-type cell extracts, the relative amount of Osh4p-2xHA that co-precipitated with native Sec4p was equivalent (data not shown). Altogether, these experiments strongly suggested that Osh4p forms a functional complex *in vivo* with the assembled exocyst complex, and this association is affected in part by *SEC6*.

Figure 2.4. Osh4p interacts with exocyst complex-associated proteins.

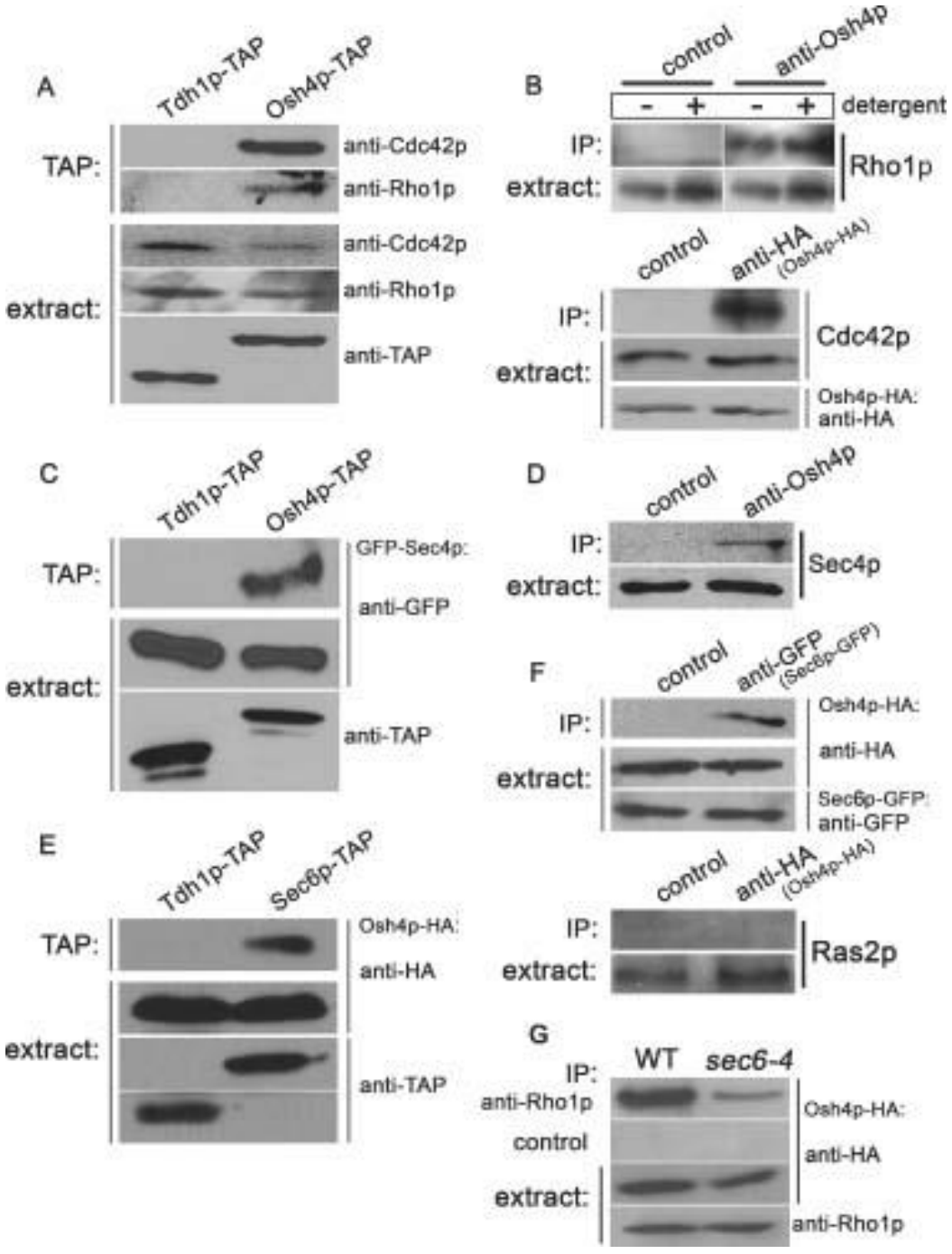

Immunoblots of (A) Cdc42p and Rho1p, and (C) GFP-Sec4p, before (extract) and after TAP from wild-type cells (BY4741) expressing TAP-tagged Osh4p and Tdh1p. Osh4p-TAP and Tdh1p-TAP were expressed from integrated constructs from their endogenous promoters and were detected with an anti-TAP antibody. Anti-Cdc42p and anti-Rho1p antibodies specifically recognized the endogenous wild-type proteins, whereas an anti-GFP antibody detected GFP-Sec4p. Crude extract samples corresponded to 1.5% of input extract used per TAP experiment. B) Immunoblots of co-precipitated Cdc42p after Osh4p-2xHA IP with an anti-HA antibody, and co-precipitated Rho1p after IP of endogenous Osh4p with an anti-Osh4p polyclonal serum. Mouse IgG-agarose and rabbit IgG-agarose were negative controls for Cdc42p and Rho1p precipitation, respectively. Rho1p co-precipitated with native Osh4p after IP in the absence or presence of 1% Triton X-100. D) As detected with an anti-Sec4p polyclonal antibody, native Sec4p co-precipitated with native Osh4p after IP with an anti-Osh4p polyclonal serum and Sec4p did not precipitate with the rabbit IgG-agarose control. E) Osh4p-2xHA co-precipitated with Sec6p-TAP from cell extracts after TAP, but Osh4p-2xHA did not precipitate with the Tdh1p-TAP negative control. F) Osh4p-2xHA co-precipitated with Sec6p-GFP after IP with the anti-GFP antibody, whereas Osh4p-2xHA was not detected upon precipitation with rabbit IgG-agarose (upper panels). From the same cell extracts, Ras2p did not co-precipitate with Osh4p-2xHA after IP with the anti-HA antibody (lower panels). G) Relative to the wild-type control, in extracts prepared from *sec6-4*^{ts} cells incubated at 37˚C for 90 min 2.2-fold less Osh4p-2xHA co-precipitated with native Rho1p using an anti-Rho1p antibody (averaged from triplicate independent trials). Experiments were performed by G.A

2.1.5. The Osh4(Y97F)p sterol-binding mutant increases Osh4p activity causing lethality

Sterol binding is clearly an important determinant of ORP localization and presumably for the role ORPs play in the nonvesicular transfer of sterols between membranes (Christopher T. Beh et al., 2009). To determine how sterol binding affects Osh4p activities with respect to *SEC14* or the essential overlapping function of all *OSH* genes, we analyzed two previously engineered mutations, Osh4(L111D)p and Osh4(Y97F)p (Im et al., 2005) (Figure 2.5A). These mutations were designed to prevent Osh4p association with sterols (Im et al., 2005). As previously reported (Im et al., 2005), neither of these *OSH4* mutations rescued *osh*Δ *osh4-1*^{ts} growth defects nor reversed the *osh4*Δ bypass suppression of *sec14-3*^{ts} at elevated temperatures (Figure 2.5B). Consistent with a loss-of-function mutation, Osh4(L111D)p expression also had little impact on growth when expressed in wild-type cells (Figure 2.5B). At first glance, these results suggested that sterol binding is generally required for Osh4p function. However, we extended this analysis and discovered that the Y97F substitution had quite different effects. We verified that Osh4(Y97F)p does not bind sterols *in vitro* ((Im et al., 2005); data not shown), but our *in vivo* data indicated that the Y97F substitution was not a loss-of-function mutation that inactivates the Osh4 protein. When methionine was absent from the medium, the induction of P^{MET3}-*OSH4*^{Y97F} expression was lethal in *sec14-3*^{ts} and

*osh4*Δ *sec14-3*^{ts} cells even at 25˚C, a temperature at which these cells otherwise grow (Figure 2.5B). Expression of Osh4(Y97F)p was also lethal in *osh*Δ *osh4-1*^{ts} cells at 25˚C, which is also a temperature at which these cells are viable (Figure 2.5B). Even more surprising, the expression of P^{MET3}-*OSH4*^{Y97F} at equivalent levels to endogenous *OSH4* expression caused dominant lethality in all wild-type strains tested, regardless of genotype, genetic background, or temperature and/or growth medium (Figure 2.5B and Figure 2.2S; data not shown). Thus, a higher total level of Osh4 protein, or genotypic differences between strain backgrounds, was not the cause of *OSH4*^{Y97F} lethality. In short, in contrast to the Osh4(L111D)p loss-of-function mutant, Osh4(Y97F)p cannot bind sterols and is a dominant mutant protein.

A possible mechanism for how *OSH4*^{Y97F} affects cell growth is simply by interfering with the formation of a presumptive sterol-transport complex, acting as a dominant-negative (antimorphic) mutation (as defined by Müller (Muller, 1932)). Operationally, it is predicted that such a mutation is suppressed by increased wild-type gene dosage (Wilkie, 1994). In contrast, a dominant mutation that has acquired a completely new function (neomorph) is unaffected by increased wild-type gene dosage, whereas a dominant mutation increasing gene function (hypermorph) exhibits worsened phenotypic defects (Muller, 1932; Wilkie, 1994). Examples of the latter include gain-of-function mutations in cell signaling genes such as transforming alleles of ras (Beitel, Clark, & Horvitz, 1990). To test how the dominant Y97F mutation affects *OSH4* function, we transformed P^{MET3}-*OSH4*^{Y97F} cells with a low-copy plasmid thereby increasing wild-type *OSH4* dosage (stable transformants containing both P^{MET3}-*OSH4*^{Y97F} and a multicopy *OSH4* plasmid were inviable, regardless of culture condition). At moderate (20 mg/L [+ Met]) and high methionine (100 mg/mL [++ Met]) concentrations, the P^{MET3}-*OSH4*^{Y97F} construct was repressed, permitting cell growth (Figure 2.5C). In cells containing both P^{MET3}-*OSH4*^{Y97F} and wild-type *OSH4* plasmids, no growth was observed except at the highest levels of *OSH4*^{Y97F} repression (++ Met) (Figure 2.5C). Because increased *OSH4* dosage worsened P^{MET3}-*OSH4*^{Y97F} defects, the Y97F substitution functions as a hypermorphic mutation that increases Osh4p activity. In addition, P^{MET3}-*OSH4*^{Y97F} expression was still lethal in *osh4*Δ cells (Figure 2.2S), which also indicated that *OSH4*^{Y97F} is not a dominant-interfering mutation that counteracts wild-type Osh4p

function. Together these findings suggested that despite its inability to bind sterols, the Osh4(Y97F)p mutation did not abolish Osh4p function, but rather amplified it.

Figure 2.5. Osh4(Y97F)p is constitutively active and dominant-lethal.

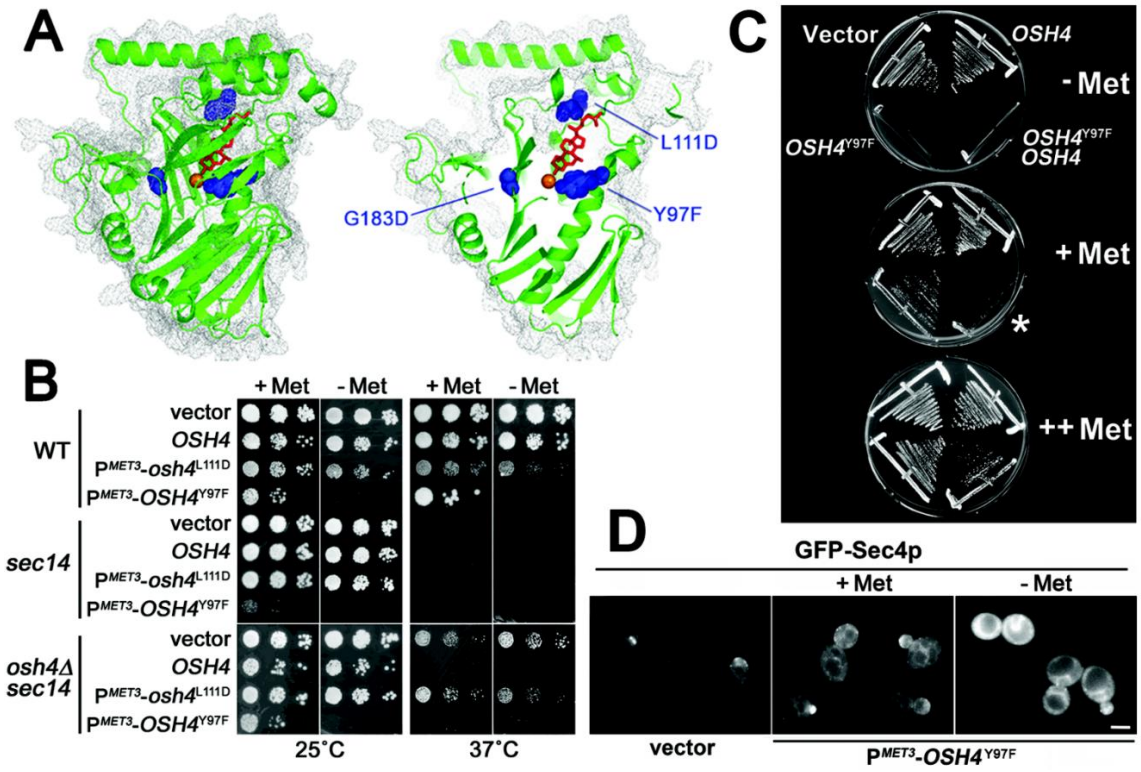

A) The full-length Osh4p structure (left) and the cut-away view (right) with bound sterol in red, hydrogen-bonded water in orange, and space-filling representations of mutated residues in blue. The G183D substitution corresponds to the temperature-sensitive *osh4-1*^{ts} mutation (Christopher T Beh & Rine, 2004)(7). L111D is a missense mutation at the entrance to the sterol-binding cavity and disrupts membrane association (Im et al., 2005)(30). The Y97F substitution disrupts sterol ligand binding within the protein core (Im et al., 2005)(30). B) Ten-fold serial dilutions of cells grown from equivalent culture densities spotted onto selective media without (- Met) or with 20 mg/L methionine (+ Met), which represses the *MET3* promoter (P^{MET3}). Wild-type (WT; SEY6210), *sec14-1*^{ts} (CTY1-1A), and *osh4*Δ *sec14-1*^{ts} (CBY844) cells were transformed with the vector control (YEplac195) or *OSH4* (pCB241), P^{MET3}-*osh4*^{L111D} (p426MET-OSH4L111D), P^{MET3}-*OSH4*^{Y97F} (p426MET-OSH4Y97F) multicopy plasmids. C) Wild-type cells (WT; SEY6210) transformed with a P^{MET3}-*OSH4*^{Y97F} high-copy plasmid (p426MET-OSH4Y97F), a low-copy wild-type *OSH4* plasmid (pCB254), or both, were streaked onto solid media containing increasing methionine concentrations at the same positions shown in the top plate. In the absence of methionine (- Met), P^{MET3}-*OSH4*^{Y97F} was expressed and cell growth was inhibited. With 20 mg/L methionine (+ Met), limited P^{MET3}-*OSH4*^{Y97F} repression permitted growth but cells containing both P^{MET3}-*OSH4*^{Y97F} and wild-type *OSH4* plasmid did not grow (asterisk). The latter strain grew poorly even on 100 mg/L methionine medium (++ Met). Cells transformed with the wild-type *OSH4* plasmid grew as well as those with the vector (YEplac195). D) In diploid cells expressing P^{MET3}-*OSH4*^{Y97F} grown at 30˚C, GFP-Sec4p localization was cytoplasmic and absent from motile vesicles. Viable wild-type haploid cells that contained both GFP-*SEC4* and P^{MET3}-*OSH4*^{Y97F} plasmid constructs could not be isolated. Scale bar = 4 µm. Panel A was prepared by C.B and experiments were conducted by G.A

To determine whether Osh4(Y97F)p caused specific defects in polarized exocytosis, we analyzed PM docking of GFP-Sec4p-marked exocytic vesicles in cells expressing P^{MET3}-*OSH4*^{Y97F}. After induction of P^{MET3}-*OSH4*^{Y97F} expression, GFP-Sec4p distribution was depolarized and diffuse, and no longer detected on any particles, let alone on vesicles transiting into the bud (Figure 2.5D; -Met). The induced *OSH4*^{Y97F} construct was also lethal in conditional *CDC42*, *RHO1*, and all exocyst complex mutants tested (data not shown). Together these findings suggested the increased activity of the *OSH4*^{Y97F} mutant disrupted Sec4p-mediated polarized vesicular transport, which resulted in the observed growth defect.

The dominant-lethal *OSH4*^{Y97F} mutation involves the substitution of a conserved tyrosine found in all Osh proteins and likely in all other ORPs regardless of species (Figure 2.6A). To determine whether the same residue substitution in the context of another Osh protein also confers dominant-lethality, we generated an inducible *OSH2* allele with a substitution analogous to Y97F in Osh4p (Figure 2.6A). In contrast to *OSH4*^{Y97F}, P^{MET3}-*OSH2*^{Y963F} expression in wild-type yeast did not cause any growth defects (Figure 2.6B). Moreover, the P^{MET3}-*OSH2*^{Y963F} construct was able to suppress the growth defects of *osh*Δ *osh4-1*^{ts} (Figure 2.6B), indicating P^{MET3}-*OSH2*^{Y963F}

was both expressed and functional. These experiments indicated that the *OSH4*^{Y97F} dominant growth defect was specific to that mutation in Osh4p, and the corresponding mutation in other ORPs might not have the same effect.

Figure 2.6. *OSH2*^{Y963F} is not dominant-lethal.

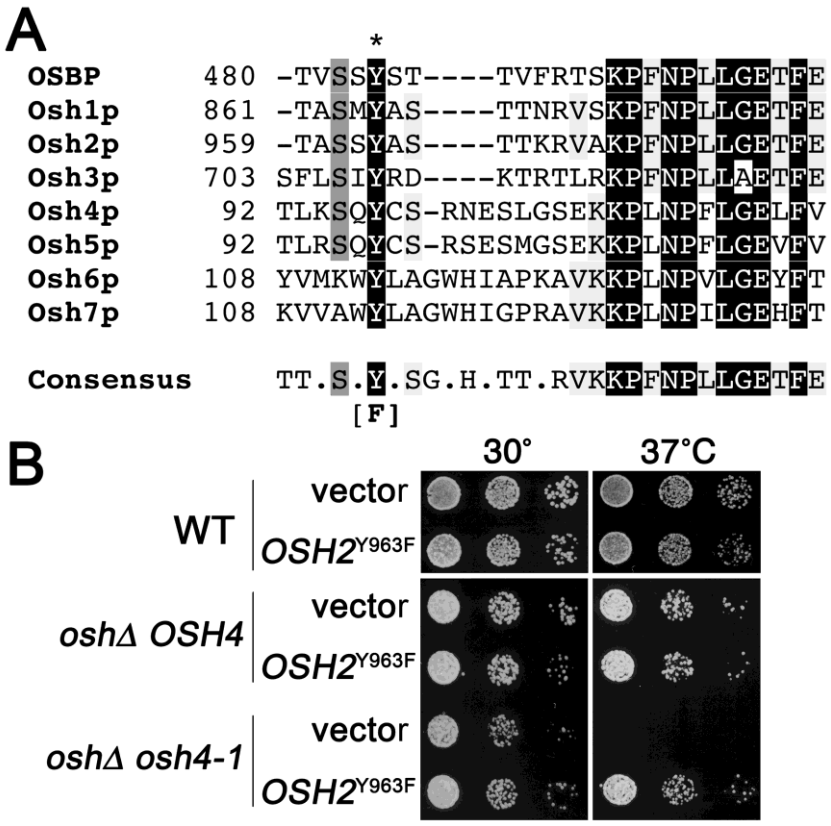

A) Sequence alignments of Osh1p-7p and human OSBP in regions including and adjacent to conserved tyrosines (asterisk) corresponding to Osh4p tyrosine (Y) 97, substituted for phenylalanine (F) in Osh4(Y97F)p. Solid boxes indicate amino acid identity and shaded boxes denote residue similarities. B) Equivalent culture dilutions were spotted onto solid selective medium without methionine and cultured at the temperatures indicated. P^{MET3}-*OSH2*^{Y963F} (pCB851) expression had no effect on growth in either *oshΔ OSH4* cells (CBY924) or wild-type cells (SEY6210). Compared to the control (pRS426), *OSH2*^{Y963F} rescued *oshΔ osh4-1* cells (CBY926) growth defects. Panel A was prepared by C.B while experiment was conducted by J.J

2.1.6. The dependence of Sec4p and Osh4p localization on sterols

The polarized exocytosis defect in *osh*Δ *osh4-1* cells only affects the last steps of vesicle docking at the PM. If this defect was an indirect consequence of either diminished sterol trafficking to the PM or a general disruption in sterol homeostasis, then reduced cellular sterol concentrations would also be predicted to cause similar vesicle docking defects. First, to test whether sterol levels influence polarized exocytosis, the localization of GFP-Sec4p-marked vesicles was examined by fluorescence microscopy in *erg9*Δ P^{MET3}-*ERG9* cells. In these mutant cells, sterols are depleted upon methionine addition to the medium, which represses expression of Erg9p/squalene synthase (Christopher T Beh & Rine, 2004). Erg9p is the first enzyme in the isoprenoid biosynthetic pathway specifically required for sterol production and it acts after the enzymatic steps that produce prenyl lipids such as those covalently attached to small GTPases (Sturley, 2000). For this reason, repression of *ERG9* expression was used to deplete sterols because it would not directly impact the synthesis of the non-sterol isoprenoid precursors needed for other cellular processes, including the lipid modification of Sec4p. As shown in Figure 2.7A, GFP-Sec4p fluorescence in the cytoplasm markedly increased in cells following Erg9p repression (Erg9p "off"). In these sterol-depleted cells, any remaining cortical GFP-Sec4p was not concentrated at sites of polarized growth. A minor amount of GFP-Sec4p perinuclear membrane fluorescence was detected in 33% of cells before Erg9p repression (n = 76 cells) and in 91% of cells after Erg9p repression (n = 108 cells). These results were in stark contrast to those observed in cells lacking Osh proteins, in which polarized exocytosis was defective but GFP-Sec4p still entered the bud and accumulated on exocytic vesicles (Keith G. Kozminski et al., 2006). The differences in GFP-Sec4p distribution between *OSH* mutant cells and sterol-depleted cells suggested the role of Osh proteins in polarized exocytosis is not caused by gross changes in sterol homeostasis.

The localization of the canonical mammalian OSBP is affected by oxysterol-binding (Ridgway, Dawson, Ho, Brown, & Goldstein, 1992), and models for ORP translocation between membranes involve a sterol-binding and release cycle (Im et al., 2005). We tested whether sterol levels also influence Osh4p localization. As previously shown (Figure 2.1A), in wild-type cells Osh4p-YFP resides in the cytoplasm, the Golgi,

and on exocytic vesicles targeted to sites of polarized growth. In sterol-depleted *erg9*Δ P^{MET3}-*ERG9* cells, however, less Osh4p-YFP was associated with motile particles (vesicles) and Osh4p-YFP was largely redistributed into the cytoplasm and to immotile particles (Figure 2.7B). These findings indicated that sterols influence Osh4p association with vesicles.

Figure 2.7. GFP-Sec4p and Osh4p-YFP mislocalization after sterol depletion.

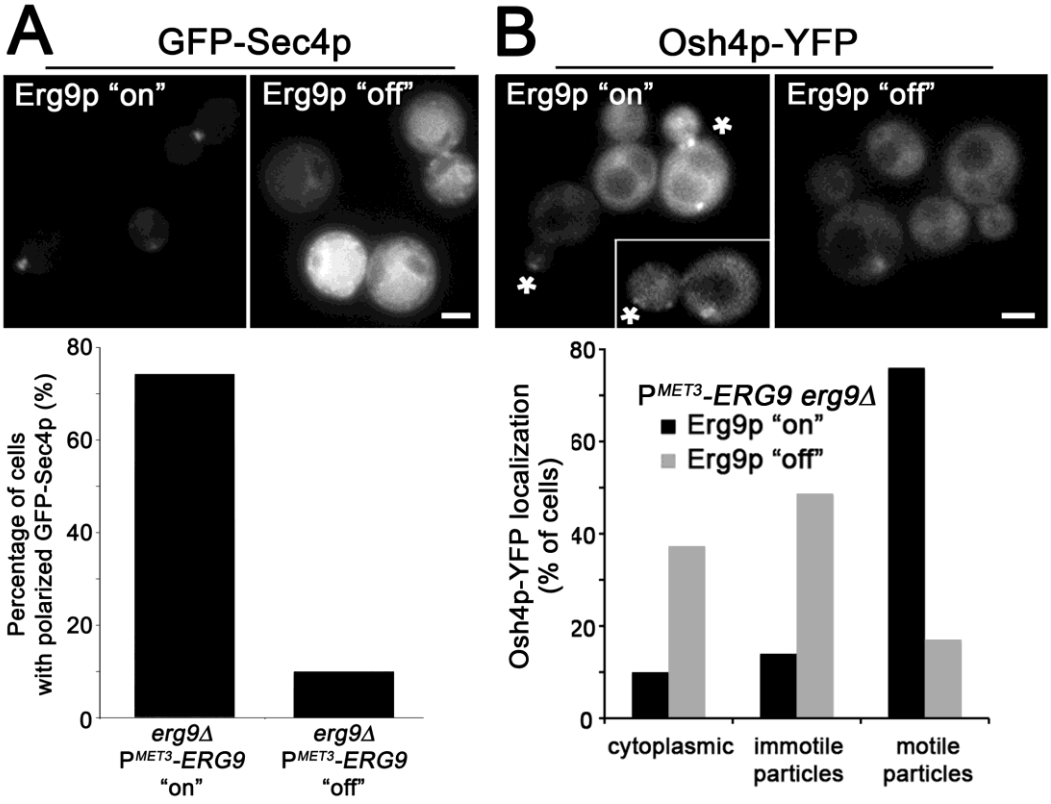

GFP-Sec4p (A) and Osh4p-YFP (B) localization were visualized in log-phase *erg9*Δ P^{MET3}-*ERG9* cells (CBY745) grown at 30˚C. A) In sterol-depleted cells (Erg9p "off") versus sterol-producing cells (Erg9p "on"), GFP-Sec4p localization on vesicles and sites of polarization was reduced, as shown in the cell images and quantified in the histogram. B) In sterol-containing cells (Erg9p "on") Osh4p-YFP was observed in the cytoplasm, at sites of polarized growth (indicated by asterisks), and motile and immotile particles. Following sterol depletion (Erg9p "off"), Osh4p-YFP on motile vesicles was reduced and cytoplasmic fluorescence increased, as quantified in the histogram. Images represent equal exposures. Scale bars = 2 µm. Experiments were conducted by G.A

2.1.7. Sterols affect OSH4 regulation of SAC1 lipid signaling

In addition to binding sterols, Osh4p associates with PI lipids and several findings suggest that Osh proteins regulate Sac1p, a PI(4)P phosphatase (Curwin, Fairn, & McMaster, 2009; LeBlanc & McMaster, 2010; Xinmin Li et al., 2002). High-level *OSH4* expression from a galactose-inducible promoter (P^{GAL}) results in reductions of PI(4)P and PI3P levels (LeBlanc & McMaster, 2010). Many of the same reported cellular defects in *osh*Δ *osh4-1* cells (Christopher T Beh & Rine, 2004) are also observed in *sac1*Δ cells (Foti, Audhya, & Emr, 2001; Novick, Osmond, & Botstein, 1989; Tahirovic et al., 2005). To determine if *OSH4* affects *SAC1* regulation in vivo, we tested the functional relationship of *OSH4* and *SAC1* by epistasis analysis.

If *OSH4* is an upstream regulator of *SAC1*, and if $OSH4^{Y97F}$ dominant lethality is manifested through *SAC1*, then deletion of *SAC1* is predicted to suppress growth defects caused by either high-level *OSH4* expression or expression of the dominant activated allele. In wild-type cells, P^{GAL}-*OSH4* induction on galactose medium resulted in a significant growth defect, relative to growth on glucose medium in which P^{GAL}-*OSH4* expression was repressed (Figure 2.8A) (LeBlanc & McMaster, 2010). In contrast, the growth defect caused by P^{GAL}-*OSH4* overexpression is suppressed in *sac1*Δ cells cultured with galactose. This result is consistent with *OSH4* being an upstream regulator of *SAC1*, though both genes still might operate in parallel pathways. If *OSH* genes only function to induce *SAC1* and downstream effectors, then increasing *SAC1* expression might remove the cellular requirement for *OSH* genes. On galactose medium, the induction of P^{GAL}-*SAC1* caused a modest growth defect in wild-type, *osh*Δ *OSH4*, and *osh*Δ *osh4-1*^{ts} cells (Figure 2.8B). More to the point, P^{GAL}-*SAC1* did not suppress the growth defect of *osh*Δ *osh4-1*^{ts} cells, regardless of temperature. This finding indicates that *OSH4* and other *OSH* genes are not just upstream activators of *SAC1*, but *OSH* genes might have additional regulatory effects that are downstream or independent of *SAC1*. It is important to note that *sac1*Δ cells grow poorly in media containing non-fermentable carbon sources or galactose (Dudley, Janse, Tanay, Shamir, & Church, 2005) and, relative to the vector control, the expression of P^{GAL}-*OSH4* partially suppresses the *sac1*Δ growth defect on galactose medium (Figure 2.8A). This

observation again supports the conclusion that *OSH* genes have effects downstream of *SAC1*, in addition to their upstream role.

To test whether the Osh4(Y97F)p sterol-binding mutation affects *SAC1* signaling and/or other functions during polarized exocytosis, the growth of *sac1*Δ cells was analyzed in response to *OSH4*^{Y97F} expression (Figure 2.8C). As previously determined, in wild-type cells cultured in the absence of methionine the induction of P^{MET3}-*OSH4*^{Y97F} expression was lethal. In contrast, the deletion of *SAC1* suppressed P^{MET3}-*OSH4*^{Y97F} dominant lethality and *sac1*Δ cells expressing *OSH4*^{Y97F} were viable. These results again point to *OSH4* as an upstream activator of *SAC1*. However, a clear growth defect was still evident in *sac1*Δ cells expressing *OSH4*^{Y97F} (as compared to the vector alone control) (Figure 2.8B) indicating that the *OSH4*^{Y97F} allele also impacts growth through another pathway independent of *SAC1* (e.g. exocyst complex assembly).

Sac1p dephosphorylates PI(4)P, which is generated *in vivo* by the Pik1p and Stt4p PI(4)P kinases (Foti et al., 2001; Schorr et al., 2001). Similar to *sac1*Δ, the deletion of *OSH4* suppresses the growth defects of *pik1*^{ts} cells and Osh4p directly binds PI(4)P (Gregory D Fairn et al., 2007; Faulhammer et al., 2007; LeBlanc & McMaster, 2010; Xinmin Li et al., 2002). Given the antagonistic relationship between the PI(4)P kinases and the Sac1p PI(4)P phosphatase, we predicted that constitutive activation of *SAC1* by the *OSH4*^{Y97F} mutation might negatively affect Pik1p and/or Stt4p function. As shown in Figure 2.8D, under conditions where the P^{MET3}-*OSH4*^{Y97F} is repressed, even the small residual expression of *OSH4*^{Y97F} was enough to severely inhibit the growth of *pik1-101*^{ts} cells and, to a minor degree, *stt4-4*^{ts} cells. Because Pik1p resides in the Golgi, and Stt4p localizes and affects PM PI(4)P levels, these results suggested that Osh4p primarily affects Pik1p function at the Golgi.

Figure 2.8. *SAC1* deletion suppresses growth defects caused by increased *OSH4* expression or by the *OSH4*^{Y97F} dominant activated allele.

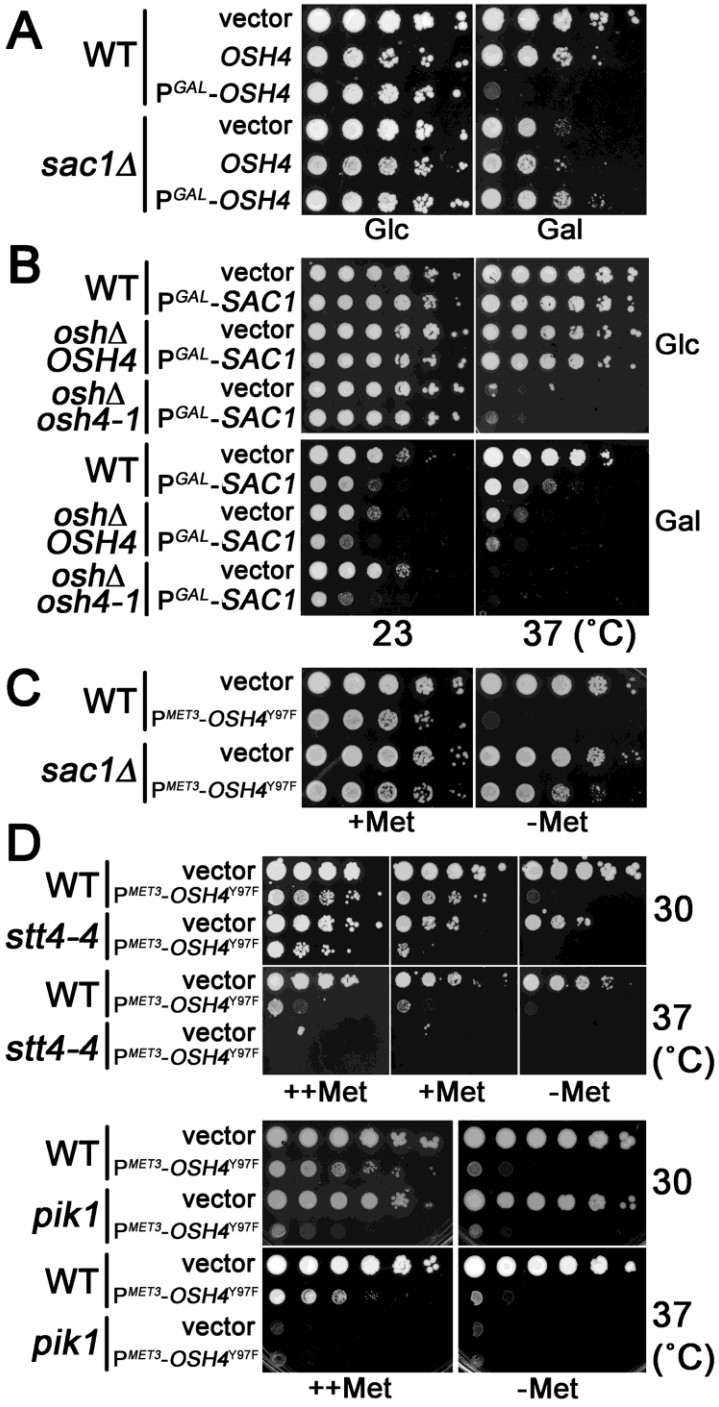

A) Ten-fold serial dilutions of cells grown from equivalent culture densities spotted onto solid selective media containing glucose (Glc) or galactose (Gal). Wild-type (WT; BY4741) and *sac1*Δ (CBY1730) cells were transformed with the vector control (YEplac195), a high-copy *OSH4* plasmid (pCB241), or a high-copy P^{GAL}-*OSH4* plasmid (pCB251). When induced in the presence of galactose, P^{GAL}-*OSH4* was deleterious to wild type but not *sac1*Δ cells. B) Ten-fold serial dilutions of WT (SEY6210), *osh*Δ *OSH4* (CBY924), and *osh*Δ *osh4-1* (CBY926) cells containing the vector control (pKT10-GAL-HA) or a plasmid expressing P^{GAL}-*SAC1* (pCB366) spotted on solid media containing either glucose (Glc) or galactose (Gal) and incubated at 23 versus 37˚C. C) Ten-fold serial dilutions of cells spotted onto selective media with 100 mg/L methionine (+ Met) or without methionine (- Met). Wild-type (WT; BY4742) and *sac1*Δ (CBY1730) cells were transformed with the vector control (pCB281) or a P^{MET3}-*OSH4*^{Y97F} high-copy plasmid (p426MET-OSH4Y97F). P^{MET3}-*OSH4*^{Y97F} expression was not lethal in *sac1*Δ cells. D) Serial dilutions of WT (SEY6210) and *stt4-4*^{ts} (AAY102) cells (upper panels), and WT (RSY255) and *pik1-101*^{ts} (NY2189) cells (lower panels), containing the vector or P^{MET3}-*OSH4*^{Y97F} plasmids spotted onto solid media containing 100 mg/L (++ Met), 20 mg/L (+ Met), or no methionine (- Met). Plates were cultured at the temperatures indicated. Experiments were conducted by G.A

2.2. Discussion

Previous work implicated the *OSH* gene family in the maintenance of Cdc42p-dependent cell polarization and polarized exocytosis (Keith G. Kozminski et al., 2006). In this study, we found that: (i) Osh4p is present on vesicles as they move from the mother cell to sites of polarized growth in the bud; (ii) in response to sterol binding Osh4p regulates the function of the Sac1p lipid phosphatase; (iii) Osh proteins interact *in vivo* with exocyst complex subunits and associated Rho- and Rab-family GTPases. In concert with the other Osh proteins, Osh4p facilitates exocyst complex interactions required for vesicle docking with the PM. Whereas Osh4p clearly affected polarized vesicular transport, the results did not support a direct role for Osh4p as a nonvesicular sterol-transfer protein. It stands to reason that without the capacity to bind sterols a sterol-transfer protein would be nonfunctional. Contrary to this prediction, however, an Osh4p mutant that blocked sterol binding had increased Osh4p activity. Although other studies have established that Osh proteins are in fact involved in sterol transfer (Christopher T Beh & Rine, 2004; Raychaudhuri et al., 2006), our results suggest a regulatory role for Osh4p. Consistent with this conclusion, *OSH4* acts as an upstream regulator of the *SAC1* PI(4)P phosphatase pathway, in addition to promoting vesicle docking. These results thus add to other studies implicating ORPs in cell signaling, such as the role of mammalian OSBP in extracellular signal-regulated kinase (ERK) regulation (P.-Y. Wang, Weng, & Anderson, 2005).

2.2.1. Osh4p is directly involved in exocyst-dependent vesicle docking

In the absence of all *OSH* function, GFP-Sec4p vesicles accumulate within the bud indicating a late defect in polarized exocytosis (Keith G. Kozminski et al., 2006). In these cells, vesicles and associated Sec4 protein were no longer localized at sites of polarized growth, even though the PM exocyst components Sec3p and Exo70p were properly polarized. A simple explanation for this result is that Osh proteins activate or stabilize vesicle docking at the PM by facilitating the interaction of exocyst subunits from each membrane. However, we cannot exclude the possibility that Osh proteins are required for exocyst complex disassembly, which is likely a precondition for membrane fusion. The fact that Osh4p co-precipitated *in vivo* with proteins associated with the fully assembled exocyst complex also supports the conclusion that Osh proteins promote final events in the docking and assembly of the entire exocyst complex.

In addition to its observation at the Golgi and in the cytoplasm (Xinmin Li et al., 2002), we detected Osh4p on moving exocytic vesicles and near sites of polarization on the PM. Our analysis showed that polarized exocytosis is a shared overlapping function of all Osh proteins, but we do not yet know if Osh proteins other than Osh4p also associate with exocytic vesicles. However, because almost all Osh proteins are free to diffuse through the cytoplasm, any Osh protein could encounter the exocyst complex if only by a stochastic mechanism. However, simple diffusion would presumably be less effective than directed transport on vesicles, which might explain why Osh4p is the most effective Osh protein at supporting vegetative growth (Christopher T. Beh et al., 2001). Regardless of the mechanism, Osh proteins other than Osh4p also co-precipitated with exocyst complex subunits from yeast extracts (data not shown). These findings again suggested that the interaction with the exocyst complex is a shared property of the Osh protein family.

At the Golgi complex, none of the *OSH* genes other than *OSH4* affects *SEC14*-dependent vesicle biogenesis (Christopher T Beh & Rine, 2004; Xinmin Li et al., 2002), and a recent report links Sec14p to the regulation of Bgl2p polarized

exocytosis(Curwin et al., 2009). As such, the genetic interaction between *OSH4* and *SEC14* might reflect a functional interaction at the trans-Golgi required for the biogenesis of Bgl2p-containing vesicles. Because the Sac1p PI(4)P phosphatase localizes to the ER and Golgi and appears to act downstream of Osh4p, the role of *OSH4* in *SAC1* signaling would also be likely to occur at the Golgi. In contrast, the functional interactions between Osh4p and Sec6p (or other exocyst complex-associated subunits) involve post-Golgi events during vesicle exocytosis. With a unique role at the Golgi and a role at the PM during exocyst complex docking, Osh4p appears to coordinate polarized exocytosis both at the beginning and end of polarized vesicle transport. Part of this coordination at the PM might also involve other Sac1p-domain-containing PI phosphatases, such as Inp51p, Inp52p, and/or Inp53p. If so, Osh4p might affect PI signaling a second time when it arrives at the PM to promote exocyst complex assembly.

2.2.2. The role of sterols in Osh4p regulation of vesicular and nonvesicular transport

In its sterol-free state, a sterol transfer protein is predicted to associate with the donor membrane where sterol binding triggers translocation of the protein with its bound lipid through the cytoplasm to the recipient membrane (Maxfield & Menon, 2006). Consistent with this model, the canonical mammalian OSBP translocates to the Golgi when bound to 25-hydroxycholesterol (Ridgway et al., 1992), though it is argued that cholesterol (not oxysterols) is the physiological ligand for ORPs (Im et al., 2005). Accordingly, if Osh proteins are sterol transfer proteins in yeast cells, then sterol depletion would cause the translocation of Osh proteins to donor membranes to acquire sterol cargo. Instead, we found that Osh4p mainly accumulated in the cytoplasm in response to sterol depletion (Figure 2.7B). This result represented another challenge to models that propose Osh4p as a soluble sterol transfer protein.

Although Sec4p localization was disrupted both in cells where all *OSH* genes were inactivated and in sterol-depleted cells, the pattern of Sec4p depolarization was completely different. In sterol-depleted cells, Sec4p was dispersed into the cytoplasm indicating that Sec4p was no longer associated with membranes. In contrast, *OSH*

inactivation did not affect Sec4p association with membranes, but rather Sec4p polarization along the PM was affected because of the block in exocytic vesicle docking. These differences in Sec4p localization suggested that the action of Osh proteins during vesicle docking is not an indirect effect of homeostatic changes in bulk sterol levels. On the basis of these findings, we propose that sterol binding primarily acts to regulate Osh4p signaling.

Our structure/function analysis of Osh4p indicated that its activity was dependent on membrane association, but not sterol binding *per se*. This conclusion was based on comparing the effects of *osh4*^{L111D} and *OSH4*^{Y97F} mutations on cell growth. The Osh4(L111D)p cannot associate with membranes irrespective of sterol binding (Im et al., 2005) and, as predicted if membrane association is required for Osh4p function, *osh4*^{L111D} was defective for all *OSH4* genetic interactions tested (Figure 2.5B; data not shown). In contrast, the Osh4(Y97F) protein was specifically engineered to abolish sterol binding (Im et al., 2005). Our *in vivo* functional tests indicated the Osh4(Y97F)p protein had increased function, as opposed to no activity. This conclusion was supported by the finding that *OSH4*^{Y97F} lethality was suppressed by the deletion of *SAC1*, which mimicked *sac1*Δ suppression of growth defects caused by *OSH4* overexpression. Osh4(Y97F)p expression also affected Sec4p distribution on vesicles, which is consistent with data that high-level Osh4p expression causes vesicular trafficking defects to the PM (LeBlanc & McMaster, 2010).

Because Osh4(Y97F)p exhibited increased function but cannot bind sterols, the most straightforward conclusion is that in the sterol-unbound form the wild-type Osh4 protein is activated. However, the Osh4(Y97F) protein might mimic wild-type Osh4p in a sterol-bound conformation and might bypass the requirement for sterols for its activation. Thus, it appears that sterols serve as regulatory ligands with respect to Osh4p activities during exocytosis.

2.2.3. A model for Osh4p activities during vesicle docking

OSH4 was originally designated *KES1* (*kre11-1* suppressor) because its deletion partially suppresses the resistance of *kre11-1* cells to the antifungal protein, K1 killer toxin (B. Jiang, Brown, Sheraton, Fortin, & Bussey, 1994). Kre11/Trs65p is a subunit of the TRAPPII complex, which is the guanine nucleotide exchange complex that activates the Rab GTPases Ypt31p and Ypt32p (S. Jones, Newman, Liu, & Segev, 2000). The genetic interaction between *KRE11*/*TRS65* and *OSH4* might be an indirect effect of PI(4)P regulation on Ypt32p inhibition of Sec4p function. During exocytosis, the decline in PI(4)P levels in vesicles signals the dissociation of Ypt32p from specific Sec4p activators, which releases them to bind Sec4p. The subsequent activation of Sec4p initiates the first steps in exocyst complex assembly (Mizuno-Yamasaki et al., 2010). We propose that Osh4p plays two roles in exocyst complex assembly: (i) by acting as an upstream regulator of Sac1p PI(4)P phosphatase activity, Osh4p affects the initial stages of exocyst complex assembly by promoting the decrease in PI(4)P on exocytic vesicles that releases Ypt32p from Sec4p activators; (ii) because Osh4p physically associates with exocyst complex subunits and their PM-associated regulators, and because Osh4p travels to the PM on vesicles that accumulate at the cell cortex in the absence of Osh proteins, Osh4p also affects exocyst complex assembly at the last steps of membrane docking at the PM. Consistent with this latter role, the deletion of *SAC1* did not completely suppress the growth defects caused by *OSH4* activation, indicating that *OSH4* has a secondary *SAC1*-independent function/s during polarized exocytosis.

The sterol-bound state of Osh4p affects the function of Sac1p and Pik1p, both of which reside at the Golgi. Thus, sterol pools in the Golgi and post-Golgi vesicles are determinants of Osh4p-dependent events that culminate in exocyst complex formation. Polarized exocytic vesicles contain elevated levels of ergosterol and sphingolipids relative to the Golgi membrane from which they came (Klemm et al., 2009). This finding suggests that sterols and sphingolipids are actively segregated from the Golgi membrane and enriched in polarized exocytic vesicles during their biogenesis. It is possible that Osh4p either directly participates or is recruited in response to sterol/sphingolipid sorting at the Golgi. In this scenario, the trigger for Osh4p activity with respect to Sac1p signaling can be traced back to the process of sorting and

concentrating sterols into nascent post-Golgi vesicles. This activity is in addition to the *SAC1*-independent Osh4p functions, all of which contribute to the net outcome of exocyst complex formation and vesicle docking at the PM.

Given the many functions ascribed to various ORPs, it is difficult to define a single conserved mechanism for the entire protein family. For instance, during late endocytic transport, the mammalian ORP1L mediates regulatory interactions between the small GTPase Rab7 and the dynactin complex (Johansson et al., 2007). As a close Rab7 homolog, yeast Sec4p plays a similar role in mediating interactions between myosin (Myo2p) and the exocyst complex. However, despite genetic interactions between *OSH4* and *MYO2* (Figure 2.3S), we were unable to co-precipitate Osh4p with Myo2p using TAP. Likewise, Osh4p was not detected in complexes with other molecular motors we tested (Smy1p, Kip2p, or Dyn2p). However, from such examples, a general model for ORP family function may be taking shape. Depending on their sterol-bound form, Osh4p and other ORPs may simply promote the rearrangement of regulatory protein interactions in coordination with the regulation of PI signaling, potentially by regulating different Sac1p-like lipid phosphatases (Christopher J. Stefan et al., 2011). This explanation is in accord with models proposing that ORPs facilitate sterol transfer via tethering complexes between closely apposed membranes (Schulz et al., 2009). In fact, the yeast ORP Osh1p interacts with a complex that forms a bona fide membrane contact site between the nuclear ER and the vacuole (Kvam & Goldfarb, 2004) and Osh3p mediates similar contact between the ER and the PM, which also involves Sac1p phosphatase activity (Christopher J. Stefan et al., 2011). Because the assembled exocyst complex is, in essence, a membrane contact site between exocytic vesicles and PM, the role of Osh proteins in polarized exocytosis might simply reflect a general function in promoting contact between adjoining intracellular membranes.

2.3. Materials and Methods

2.3.1. Strains, plasmids, microbial and genetic techniques

Standard methods were used for yeast strain constructions, plasmids, yeast genetic techniques and culture media (Amberg, Burke, & Strathern, 2005). Yeast strains and plasmids used in this study are listed in Supplemental Table S1 and S2, respectively. For Erg9p transcriptional repression in *erg9*Δ P^{MET3}-*ERG9* cells (CBY745), cells were cultured for 9 hrs in synthetic medium containing 100 mg/L methionine (Christopher T Beh & Rine, 2004). The method for generating Bgl2p antiserum, and test of antibody specificity, are also provided in Supplemental Materials. Descriptions of plasmid constructions are provided below; all protein fusions described were functional as proven by mutant rescue.

To construct pCB684, *OSH4* and its upstream promoter region was amplified from S288C genomic DNA using primers CBP358 (GGGGGATCCTCACAATCACTCGCGTCTAATCTC) and CBP359 (GGTAACTTAAGAGCGTAATCTGGAACATCGTATGGGTAAAGAGCGTAATCTGGAACATCGTATGGGTACAAAACAATTTCCTTTTCTTCG). The resulting *OSH4*-2xHA product was cloned into pGEM T-Easy (Promega Corp., Madison, WI) from which a *Bam*HI/*Kpn*I *OSH4*-2xHA fragment was isolated and subcloned into the same sites of pKT10-GAL-HA, generating pCB684. To construct pCB794, *EXO70* was amplified from S288C genomic DNA using primers CBP445 (GGGGTCGACCTATCTCACTAATTGGTTAAGAACAGTAG) and CBP447 (GGGGGATCCATGCCCGCTGAAATTGACAT). The resulting *EXO70* PCR product was cloned into CloneJET (Fermentas UAB, Lithuania) from which the *Bam*HI/*Sal*I *EXO70* fragment was subcloned into the same sites in pAGX2. The resulting plasmid, pCB794, fuses *EXO70* in-frame downstream of the coding sequences of eGFP. *OSH4*-YFP, *OSH4*-RFP, and *KEX2*-CFP fusions were generated as previously described (Longtine et al., 1998). To construct pCB866, an *OSH4-YFP:HIS3* fragment was amplified from CBY4457 genomic DNA using primers CBP516 (GTCGACCGTCTAATCTCAACGGAAGCAT) and CBP517 (GGCTCCTGATTCATTAACGTGAGGATGG). The resulting PCR product was digested

with *Sac*I and subcloned into the *Sac*I site in YEplac195, generating pCB866. pCB876 was constructed by re-closing pCB866 after excising a 740 bp *Stu*I/*Zra*I fragment that included part of the *URA3* gene. The missense mutation in *OSH2*(Y963F) was generated by site-direct mutagenesis using the Quick Change Lightning system as described by the manufacturer (Stratagene, La Jolla, CA). The primers used for the designed mutagenesis were CBP514 (CGGCATTTACCGCATCTTCATTCGCATCTACTACA) and CBP515 (TGTAGTAGATGCGAATGAAGATGCGGTAAATGCCG). The *OSH2*(Y963F) missense mutation was confirmed by sequencing. In the final plasmid construct (pCB851), *OSH2*(Y963F) expression was under the control of the *MET3* promoter. To generate the P^{GAL1}-*SAC1* expression construct pCB366, *SAC1* was amplified with KpnI and SalI sites at its ends and was inserted into the KpnI/XhoI sites of pKT10-GAL-HA.

2.3.2. Fluorescence microscopy and live cell imaging

Wide-field fluorescence imaging was performed as described previously (Keith G. Kozminski et al., 2006)(11). Confocal images were acquired using a Zeiss Axio Observer.Z1 microscope (Carl Zeiss International, Oberkochen, Germany) equipped with a CSU-10 Nipkow spinning disc (Yokogawa Electronic Corp., Tokyo, Japan). Z-stacks were acquired using an Improvision Piezo Focus Drive. Images were acquired using a Zeiss 100 X 1.4 N.A. Plan-Apochromat oil immersion lens and a Hamamatsu EM-CCD C9100-13 camera (Hamamatsu Photonics, Hamamatsu-city, Japan) mounted on a 1.5 X C-mount, using Volocity software (Improvision Inc., Lexington, MA, USA) for digital analysis. GFP and RFP fluorophores were excited with a 491nm and 561nm lasers respectively; emitted light was filtered with GFP ET520/40M or RFP ET593/40M emission filters (Chroma Technology Corp., Rockingham, VT). For each experiment, images were acquired with equivalent exposures and laser power. Bleed-through between fluorescence channels was not detected under the conditions used for image acquisition. To assess *p*-value statistical significance, one-way analysis of variance at a 99.99% confidence limit and subsequent Tukey's multiple comparison tests were used for scatterplot and analysis of Sec4p, Sec5p, and Exo70p polarization data. A two-tail t-test at a 95% confidence limit was used for bud-to-mother ratios of polarization, and a two-tail Fisher's exact test set at a 95% confidence interval was used for Sec5p-3xGFP

aggregation within buds. The statistical significance of all data compiled in histograms was determined at a 95% confidence interval.

2.3.3. Analyses of yeast *in vivo* protein-protein interactions

To isolate *in vivo* complexes associated with TAP-tagged proteins, TAP was performed with modifications as previously described (Roberts et al., 2006). Log-phase (1.0 OD_{600} unit/mL) yeast cells were washed in PBS and frozen in liquid nitrogen. Thawed pellets were resuspended in TAP-B1 buffer (Roberts et al., 2006) plus 0.15% NP-40 and extracts were prepared by disruption using acid-washed glass beads. Extracts were incubated for 4 hr with IgG Sepharose (GE Healthcare Bio-Sciences Corp., Piscataway, NJ) at 4˚C, washed once in TAP-B1 buffer plus 0.15% NP-40, and three times in TAP-B2 buffer (Roberts et al., 2006). For the first step in TAP isolation, purified complexes associated with TAP-tagged proteins were released from the IgG Sepharose beads after an overnight incubation in 1 mL TAP-B2 buffer with 0.1 U AcTEV Protease (Invitrogen, Carlsbad, CA) at 4˚C, and beads were pelleted by centrifugation and removed. The supernatant was retained and then incubated with calmodulin-affinity resin (Stratagene, La Jolla, CA) for 4 hr at 4˚C. The resin was washed three times in TAP-B2 buffer, and the TAP-purified proteins were separated by SDS-PAGE and detected on immunoblots.

Cdc42p, Sec6p-GFP, and Osh4p-2xHA were expressed in yeast and coIPed from cellular extracts derived from log-phase yeast cells as described by Zajac et al. (Zajac, Sun, Zhang, & Guo, 2005) with modifications; protein complexes were isolated by overnight incubation with antibodies at 4˚C, and protein G- and IgG-coupled beads were incubated at 4˚C for 5 hrs. A rabbit anti-GFP polyclonal antibody (Cell Signaling Technologies, Danvers, MA) was used to precipitate Sec6p-GFP, and a mouse anti-HA monoclonal antibody (Millipore, Billerica, MA) was used to precipitate Osh4p-2xHA. Complexes were isolated using protein G Dynabeads (Invitrogen, Carlsbad, CA). As a control for nonspecific protein precipitation, cell extracts were incubated with species-specific IgG agarose (Santa Cruz Biotechnology, Santa Cruz, CA).

CoIPs with endogenous Rho1p, Sec4p, and Osh4p were conducted as described above, except cell extracts were prepared in bead buffer (50 mM Tris-HCl pH 7.4, 100 mM NaCl, 2 mM EDTA, protease inhibitor cocktail) that was diluted 1:4 with dilution buffer (60 mM Tris-HCl pH 7.4, 190 mM NaCl, 6 mM EDTA, protease inhibitor cocktail). Detergent-treated cell pellets were resuspended in bead buffer containing 1% SDS and diluted 1:4 in dilution buffer containing 1.25% Triton X-100. Rho1p was precipitated using a rabbit anti-Rho1p polyclonal antibody, and Sec4p was precipitated with a goat anti-Sec4p polyclonal antibody. The precipitated proteins in these coIP experiments were detected as described in Zajac et al. (Zajac et al., 2005).

Sec6p-GFP and Osh4p-2xHA were expressed in yeast and coIPed from cellular extracts derived from log-phase yeast cells (1.0 OD_{600} units/mL) cultured in synthetic medium. Cell pellets were washed with cold PBS and frozen in liquid nitrogen. To prepare extracts for coIP, thawed cells were resuspended in lysis buffer and disrupted as described by Zajac et al. (Zajac et al., 2005). Cell extracts were incubated for 5 hrs at 4˚C with rabbit IgG agarose (Santa Cruz Biotechnology, Santa Cruz, CA), which was then pelleted by centrifugation. The IgG-conjugated agarose was washed three times in lysis buffer and retained as the control for nonspecific protein precipitation. The extract supernatant was incubated overnight at 4˚C with a rabbit anti-GFP polyclonal antibody (Cell Signaling Technologies, Danvers, MA) and isolated using Protein G Dynabeads (Invitrogen, Carlsbad, CA). After washing three times in lysis buffer, the beads were resuspended in SDS-loading buffer and released proteins were separated and analyzed on immunoblots. Sec6p-GFP was detected on immunoblots using 1:1000 titer of rabbit anti-GFP polyclonal antibody (Cell Signaling Technologies, Danvers, MA) and a 1:5000 titer HRP-conjugated anti-rabbit light chain-specific secondary antibody (Jackson Immunoresearch Laboratories, West Grove, PA). Osh4p-2xHA was detected on immunoblots using a 1:1000 titer of a mouse anti-HA monoclonal antibody (Millipore, Billerica, MA). Cdc42p and Osh4p-2xHA coIPs were as described above except extracts were pre-incubated with mouse IgG agarose (Santa Cruz Biotechnology, Santa Cruz, CA), and a mouse anti-HA monoclonal antibody (Millipore, Billerica, MA) was used to precipitate Osh4p-2xHA. Endogenous Cdc42p was detected on immunoblots using a 1:1000 titer of an affinity-purified rabbit anti-Cdc42p polyclonal antibody.

Endogenous Rho1p and Osh4p coIPs were also conducted as described above except cell pellets were resuspended in bead buffer (50 mM Tris-HCl pH 7.4, 100 mM NaCl, 2 mM EDTA, protease inhibitor cocktail) and the extract was diluted 1:4 with dilution buffer (60 mM Tris-HCl pH 7.4, 190 mM NaCl, 6 mM EDTA, protease inhibitor cocktail). Detergent-treated cell pellets were resuspended in bead buffer containing 1% SDS and diluted 1:4 in dilution buffer containing 1.25% Triton X-100. All extracts were pre-incubated with rabbit IgG agarose before an overnight incubation at 4˚C with a rabbit anti-Rho1p polyclonal antibody. After coIP, Rho1p was detected on immunoblots using a 1:1000 titre of the rabbit anti-Rho1p polyclonal antibody, whereas Osh4p was detected on immunoblots using a 1:750 titre of a rabbit anti-Osh4p polyclonal antibody (a gift from Dr. V. Bankaitis, UNC, Chapel Hill, NC) with the HRP-conjugated anti-rabbit light chain-specific secondary antibody. Rho1p and Osh4p-2xHA coIPs from *sec6-4* and wild-type cell extracts were performed as above except the precipitated proteins were detected on immunoblots using Millipore Snap ID (Millipore, Billerica, MA) with a 1:400 titre of Thermo clean blot HRP (Thermo Pierce, Rockford, IL) that was used to eliminate non-specific IgG cross-reactivity.

The coIP of endogenous Sec4p and Osh4p was also described as above, in which cell pellets were resuspended in bead buffer containing 1% SDS and cell extracts were diluted 1:4 with dilution buffer containing 1.25% Triton X-100. The extract was incubated for 5 h at 4˚C with goat IgG agarose (Santa Cruz Biotechnology, Santa Cruz, CA) and Sec4p was precipitated with a goat anti-Sec4p polyclonal antibody (Santa Cruz Biotechnology, Santa Cruz, CA). Sec4p and anti-Sec4p antibodies were isolated using Protein G Dynabeads (Invitrogen, Carlsbad, CA). The precipitated proteins were separated by SDS-PAGE and detected on immunoblots as previously outlined.

2.4. Acknowledgments

We thank Vytas Bankaitis, Charlie Boone, Patrick Brennwald, Anthony Bretscher, Elizabeth Conibear, Anthony Frankfurter, and James Hurley for antibodies, strains, and plasmids. We gratefully acknowledge Edina Harsay (U. of Kansas) for advice and

contributions to the production of the anti-Bgl2p antibody. Many thanks to Nick Harden, Nancy Hawkins, Michel Leroux for comments, and Will Prinz and Anant Menon for helpful discussions. This work was supported by a Natural Science and Engineering Research Council of Canada (NSERC) grant and by Canadian Foundation for Innovation and British Columbia Knowledge and Development Fund equipment grants. G.A. holds NSERC and Michael Smith Foundation for Health Research studentship awards. K.G.K. was funded by National Science Foundation grant 0723342.

2.5. Supporting Information

Table 2.1S. *S. cerevisiae* strains used

Strain	Genotype	Source
AAY102	SEY6210 *stt4Δ::HIS3* [*stt4-4 CEN LEU2*]	Audhya et al.(A. Audhya, Foti, & Emr, 2000) (57)
ABY531	*MAT*α *ura3-52 his3Δ200 lys2-801 leu2-3,112 MYO2::HIS3*	Schott et al.(D. Schott, Ho, Pruyne, & Bretscher, 1999) (58)
ABY534	MAT*α* ura3-52 his3Δ200 lys2-801 leu2-3,112 myo2-14::HIS3	Schott et al.(D. Schott et al., 1999) (58)
ABY536	MAT*α* ura3-52 his3Δ200 lys2-801 leu2-3,112 myo2-16::HIS3	Schott et al.(D. Schott et al., 1999) (58)
BY4741	MAT*a* his3Δ1 leu2Δ0 met15Δ0 ura3Δ0	(Winzeler et al., 1999)
BY4742	MAT*α* his3Δ1 leu2Δ0 lys2Δ0 ura3Δ0	(Winzeler et al., 1999)
CBY33	*MAT*α *ura3-52 his3Δ200 lys2-801am leu2-3,112 trp1Δ901 suc2Δ9 osh4Δ::HIS3*	
CBY745	*MAT*α *ura3Δ0 leu2Δ0 lys2Δ0 erg9Δ::kan-MX4 HIS3::*P^{MET3}*-ERG9*	Beh & Rine(Christopher T Beh & Rine, 2004) (7)
CBY844	*MAT*α *ura3-52 his3Δ200 lys2-801 leu2-3,112 sec14-1 osh4Δ::HIS3*	
CBY924	SEY6210 *osh1Δ::kanMX4 osh2Δ::kanMX4 osh3Δ::LYS2 osh4Δ::HIS3 osh5Δ::LEU2 osh6Δ::LEU2 osh7Δ::HIS3* [pCB254]	Beh & Rine (Christopher T Beh & Rine, 2004)(7)
CBY926	SEY6210 *osh1Δ::kanMX4 osh2Δ::kanMX4 osh3Δ::LYS2 osh4Δ::HIS3 osh5Δ::LEU2 osh6Δ::LEU2 osh7Δ::HIS3* [pCB255]	Beh & Rine (Christopher T Beh & Rine, 2004)(7)
CBY1730	BY4742 *sac1Δ::kan-MX4*	(Winzeler et al., 1999)
CBY3098	*MAT*a *his3Δ1 leu2Δ0 lys2Δ0 ura3Δ0 SEC6-GFP*:*HIS3*	Invitrogen
CBY3626	*MAT*a *his3Δ1 leu2Δ0 lys2Δ0 ura3Δ0 OSH4*-TAP:*HIS3*	Open Biosystems
CBY3823	*MAT*a *his3Δ1 leu2Δ0 lys2Δ0 ura3Δ0 TDH1*-TAP:*HIS3*	Open Biosystems

CBY4007	*MAT*α *ura3-52 his3Δ200 lys2-801am leu2-3,112 trp1Δ901 suc2Δ9 OSH4-mRFP:HIS3*	
CBY4457	*MAT*α *ura3-52 his3Δ200 lys2-801am leu2-3,112 trp1Δ901 suc2Δ9 OSH4-YFP:HIS3*	
CBY4462	CBY4457 *KEX2-CFP:TRP1*	
CBY4491	*MAT*a *his3Δ1 leu2Δ0 lys2Δ0 ura3Δ0 SEC6*-TAP:*HIS3*	Open Biosystems
CBY4712	*MAT*a *his3Δ1 leu2Δ0 lys2Δ0 ura3Δ0 sec6-4:KAN-MX4*	C. Boone, University of Toronto
CTY1-1A	*MAT*α *ura3-52 his3Δ200 lys2-801 leu2-3,112 sec14-1*	(Bankaitis et al., 1989)
DDY1300	*MAT*a *ura3-52 leu2-3,112 his3Δ200 lys2-801 CDC42:LEU2*	(K G Kozminski, Chen, Rodal, & Drubin, 2000)
DDY1304	*MAT*a *ura3-52 leu2-3,112 his3Δ200 lys2-801 cdc42-101:LEU2*	(K G Kozminski et al., 2000)
DDY1326	*MAT*a *ura3-52 leu2-3,112 his3Δ200 lys2-801 cdc42-118:LEU2*	(K G Kozminski et al., 2000)
DDY1344	*MAT*a *ura3-52 leu2-3,112 his3Δ200 lys2-801 cdc42-129:LEU2*	(K G Kozminski et al., 2000)
HAB821	SEY6210 *kes1/osh4Δ::HIS3*	(B. Jiang et al., 1994)
HAB835	SEY6210 *swh1/osh1Δ::URA3*	(B. Jiang et al., 1994)
KKY37	*MAT*a *rho1-104^{ts} leu2-3, 112 ura3-52 lys2-801am*	(Keith G. Kozminski et al., 2003)
NY17	*MAT*a *sec6-4^{ts} ura3-52*	(Novick, Field, & Schekman, 1980)
NY2189	*MAT*a *leu2-3,112 ura3-52 pik1-101*^{ts}	(Walch-Solimena & Novick, 1999)
RSY255	*MAT*α *ura3-52 leu2-3,112*	(Novick & Schekman, 1979)
SEY2102	*MAT*α *his4-519 leu2-3,112 ura3-52 bgl2::URA3*	(Klebl & Tanner, 1989)
SEY6210	*MAT*α *ura3-52 his3Δ200 lys2-801am leu2-3,112 trp1Δ901 suc2Δ9*	(J. S. Robinson, Klionsky, Banta, & Emr, 1988)

Unless otherwise referenced, all strains were created as part of this study.

Table 2.2S. Plasmids used

Plasmid	Description	Source
p426MET-OSH4L111D	P*MET3*-*osh4*^{L111D} 2µ *URA3*	(Im et al., 2005)
p426MET-OSH4Y97F	P*MET3*-*OSH4*^{Y97F} 2µ *URA3*	(Im et al., 2005)
pAGX2	P*ACT1*-GFP *CEN URA3*	(Ozaki-Kuroda et al., 2001)
pCB239	*OSH2* 2µ *URA3*	(Keith G. Kozminski et al., 2006)
pCB241	*OSH4* 2µ *URA3*	(Keith G. Kozminski et al., 2006)
pCB251	*P*^{GAL}-OSH4 *2µ* URA3	
pCB254	OSH4 CEN TRP1	(Christopher T Beh & Rine, 2004)
pCB255	*osh4-1*^{ts} *CEN TRP1*	(Christopher T Beh & Rine, 2004)
pCB366	P*GAL*-*SAC1* 2µ *URA3*	
pCB684	*OSH4*-2xHA 2µ *URA3*	
pCB794	P*ACT1*-GFP-*EXO70 CEN URA3*	
pCB851	P*MET3*-*OSH2*^{Y936F} 2µ *URA3*	
pCB866	*OSH4*-YFP:*HIS3*-MX 2µ *URA3*	
pCB876	*OSH4*-YFP:*HIS3*-MX 2µ	
pEH138	MBP-*BGL2*	E. Harsay, University of Kansas
pKT10-GAL-HA	P*GAL*-HA 2µ *URA3*	(Misu et al., 2003)
pLC1329	*SEC7*-dsRED *CEN URA3*	E. Connibear, University of BC
pPG5-SEC5-3xGFP	*SEC5*-3xGFP *URA3*	(Boyd et al., 2004)
pPG5-SEC15-3xGFP	*SEC15*-3xGFP *URA3*	(Boyd et al., 2004)
pRC2098	GFP-*SEC4 CEN URA3*	(Calero et al., 2003)
pRS426	2µ *URA3*	(Sikorski & Hieter, 1989)
YEplac195	2µ *URA3*	(Gietz & Akio, 1988)

Unless otherwise referenced, all plasmids were created as part of this study.

2.5.1. Supplemental Figures

Figure 2.1S. Osh4p co-fractionates with markers of polarized exocytic vesicles in *sec6-4* cells

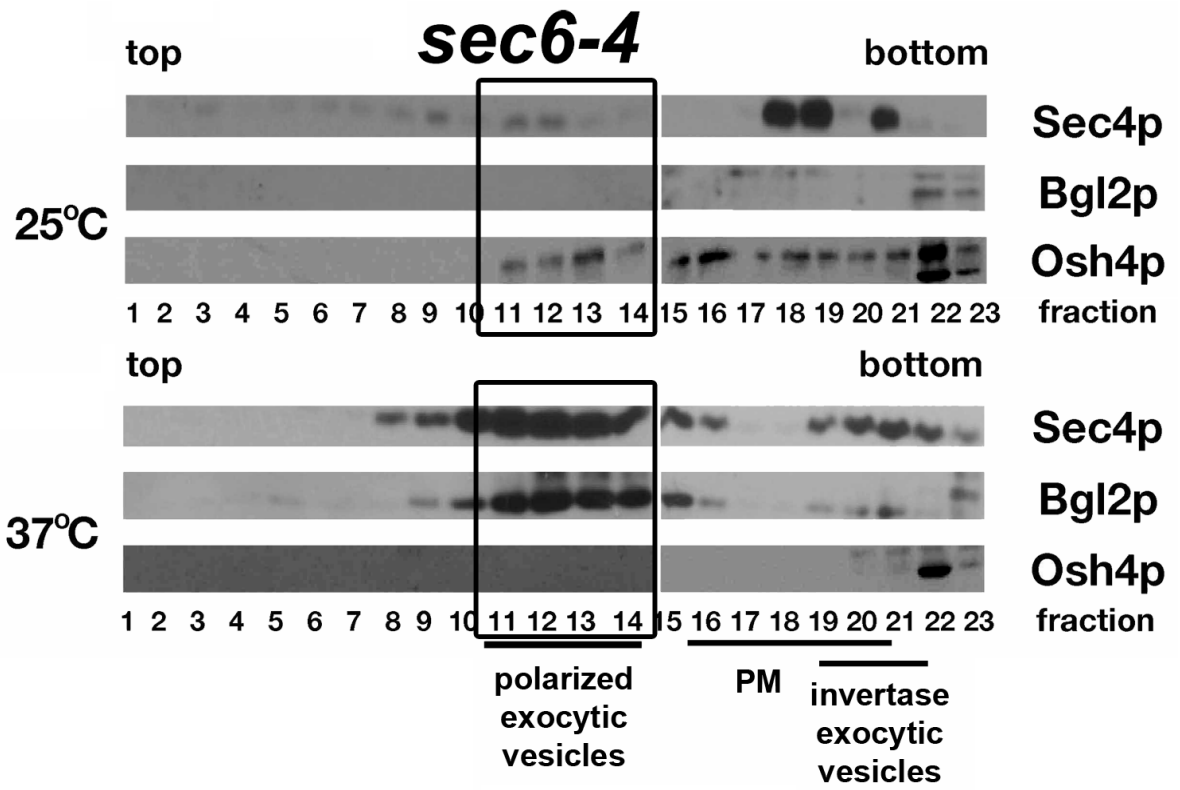

Immunoblots of 100,000 g pellets of fractions collected from top (fraction 1) to bottom (fraction 23) of an 18-34% Nycodenz-sorbitol buoyant density gradient loaded with extracts prepared from equivalent $O.D._{600}$ units of *sec6-4*^{ts} (NY17) cells cultured at 25 or 37˚C for 90 min. Equivalent fraction volumes were loaded in each lane for each set of blots and probed with the same antibody titer. Gradient densities corresponding to Bgl2p (polarized exocytic vesicles), invertase activity (invertase vesicles), and PM fractions are indicated. Experiment was conducted by D.S

.

S. cerevisiae contains two populations of exocytic vesicles with distinct, defined densities (Harsay & Bretscher, 1995), one containing Blg2p (β-glucanase) involved in polarized growth, the other involved in invertase secretion and marked by that enzymatic activity. The Rab GTPase Sec4p marks both vesicle populations and is also associated with the PM. These markers are not easily detected in internal membrane fractions (especially Bgl2p, which is normally secreted to the cell wall) unless exocytosis is

blocked (e.g. *sec6-4*^{ts} at 37˚C). At 37˚C, *sec6-4*^{ts} cells accumulate significant numbers of both Sec4p/Bgl2p-marked and Sec4p/invertase-marked vesicles. The black rectangles in the figure denote gradient fractions that correspond to the known density of Sec4p/Bgl2p-marked exocytic vesicles, which accumulate significantly upon shift from 25 to 37˚C. Osh4p co-fractionated with both exocytic vesicle populations when cells were grown at 25˚C, but not at 37˚C, when the presence of Osh4p on gradients was not observed or significantly diminished. The anti-Osh4p antibody detects two bands, which might indicate a post-translationally modified isoform.

To prepare whole cell extracts, *sec6-4*^{ts} (NY17) cells were grown in 200 mL of rich medium (YPD, 2% glucose) at 25°C to mid-log-phase and harvested by centrifugation. Cells were resuspended in YPD (5% glucose), and grown an additional hour at 25°C. This starting culture was split equally and processed in parallel, except one of the split cultures was first incubated at 37°C for 15 min. Thereafter, this sample was always incubated at 37˚C in pre-warmed media whereas the other was always incubated at 25˚C. Cells from both cultures were harvested and washed with sterile water. After the wash, cell pellets were resuspended in 100 mL of YPD (0.1% glucose) and incubated for 90 min. 34 optical density (OD_{600}) units of cells from each culture were harvested, washed once with Tris-EDTA (TE) Buffer (50 mM Tris-Cl, 1 mM EDTA, pH 7.5) and gently resuspended in ice-cold 10 mM NaN_3/10 mM KF prior to a 10 min incubation on ice; all samples were subsequently kept at 4°C. After centrifugation, cell pellets were washed with two volumes of cold water and resuspended in 1 mL TE Buffer containing a protease inhibitor cocktail (1 mM PMSF and 0.5 µg/mL each of leupeptin, aprotinin, pepstatin A, chymostatin, and antipain). Cells from each sample were lysed by glass bead disruption. Unbroken cells were pelleted at 1500 rpm for 5 min in a microcentrifuge, and the supernatants were collected.

To separate membranes and membrane compartments by buoyant density centrifugation, a mixture of 0.74 mL of extract supernatant, 1.13 mL 60% Nycodenz (Accurate Chemicals, Westbury, NY), and 0.13 mL 0.8 M D-sorbitol in TE Buffer was overlayed with 2 mL 30%, 3 mL 26%, 2 mL 22%, 1.5 mL 20%, and 1 mL 18% Nycodenz in 0.8 M D-sorbitol in TE Buffer. Density gradients were centrifuged at 4°C in a Beckman SW41 rotor at 30,000 rpm for 18 hr (to equilibrium). 0.5 mL fractions were collected from

top to bottom of the tube. To concentrate cellular membranes, each density gradient fraction was diluted 10-fold in TE Buffer and centrifuged at 100,000 g (TLA100.1 rotor) for 1 hr at 4°C. After centrifugation, the supernatant was discarded and samples were heated at 70°C in SDS sample buffer for 10 min before storage at -20°C. Polypeptides recovered from each fraction were separated by SDS-PAGE and then detected by immunoblot after incubation with secondary antibodies as described in Kozminski et al. (Keith G. Kozminski et al., 2006). Blots were probed with the following antibodies at the indicated dilutions, rabbit anti-Osh4p (1:1000) (Fang et al., 1996)(9), rabbit anti-Bgl2p (1:7500; this study), mouse anti-Sec4p (1:10,000; mAb1.2.3, a gift from Patrick Brennwald, UNC-Chapel Hill). Fraction densities were measured relative to the refractive index of equivalent fractions from a no extract gradient run in parallel. Values were plotted relative to a standard curve of Nycodenz-sorbitol concentration versus refractive index.

Figure 2.2S. P^{MET3}-*OSH4*^{Y97F} expression from a low-copy (*CEN*) plasmid produced Osh4(Y97F)p at comparable levels to endogenous Osh4p.

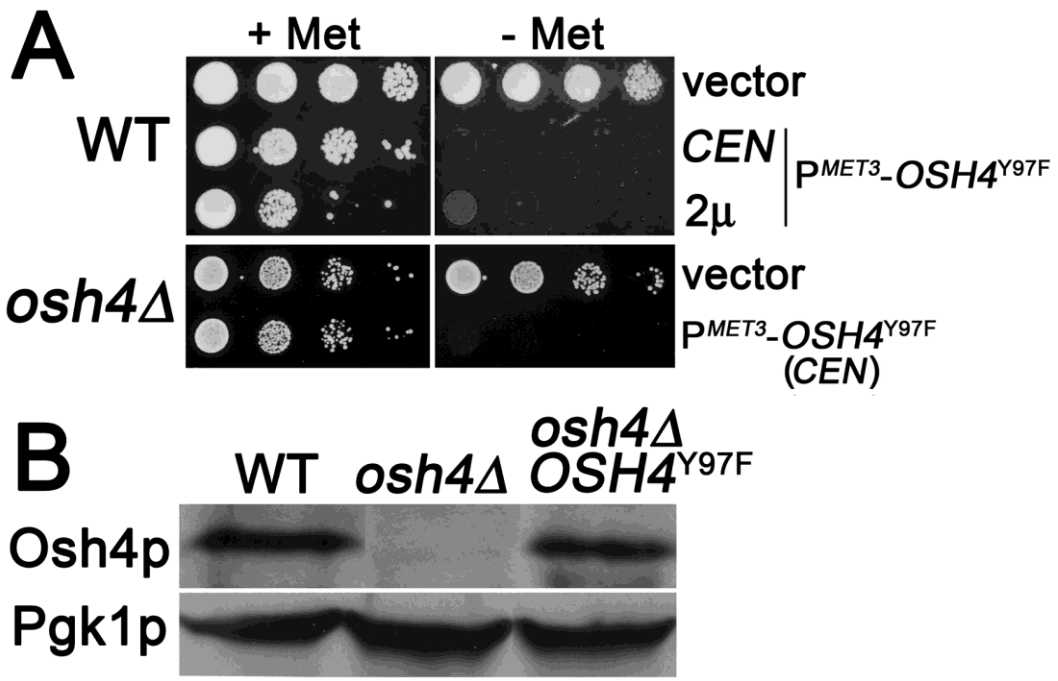

A) Ten-fold serial culture dilutions (left to right) of wild-type (WT; SEY6210) and *osh4*Δ (HAB821) transformants were spotted onto selective synthetic medium containing either 20 mg/L (+ Met) or no (- Met) methionine and incubated at 30˚C. Wild-type cells transformed with either *CEN*- or multicopy 2µ-based plasmids containing P^{MET3}-*OSH4*^{Y97F} (pCB743 and p426MET-OSH4Y97F, respectively) were inviable when *OSH4*^{Y97F} expression was induced (- Met), as compared to a vector control (pRS426). Expression of P^{MET3}-*OSH4*^{Y97F} on a low-copy *CEN*-based plasmid (pCB743) was also lethal in *osh4*Δ cells as compared to *osh4*Δ cells transformed with the vector control (pRS426). B) After overnight growth in medium lacking methionine, cellular extracts were isolated from log-phase wild-type cells (WT; SEY6210), *osh4*Δ cells (HAB821), and *osh4*Δ cells that were transformed with the *CEN* plasmid containing P^{MET3}-*OSH4*^{Y97F} (pCB743). Extract proteins were separated by SDS-PAGE, after which Osh4p and Pgk1p (a loading control) were detected on separate immunoblots using anti-Osh4p and anti-Pgk1p antisera. The level of Osh4(Y97F)p was equivalent or slightly less than the endogenous level of Osh4p expressed in wild-type cells. Experiments were conducted by G.A

Figure 2.3S. Increased dosage of *OSH4* exacerbated growth defects of conditional *MYO2* mutants.

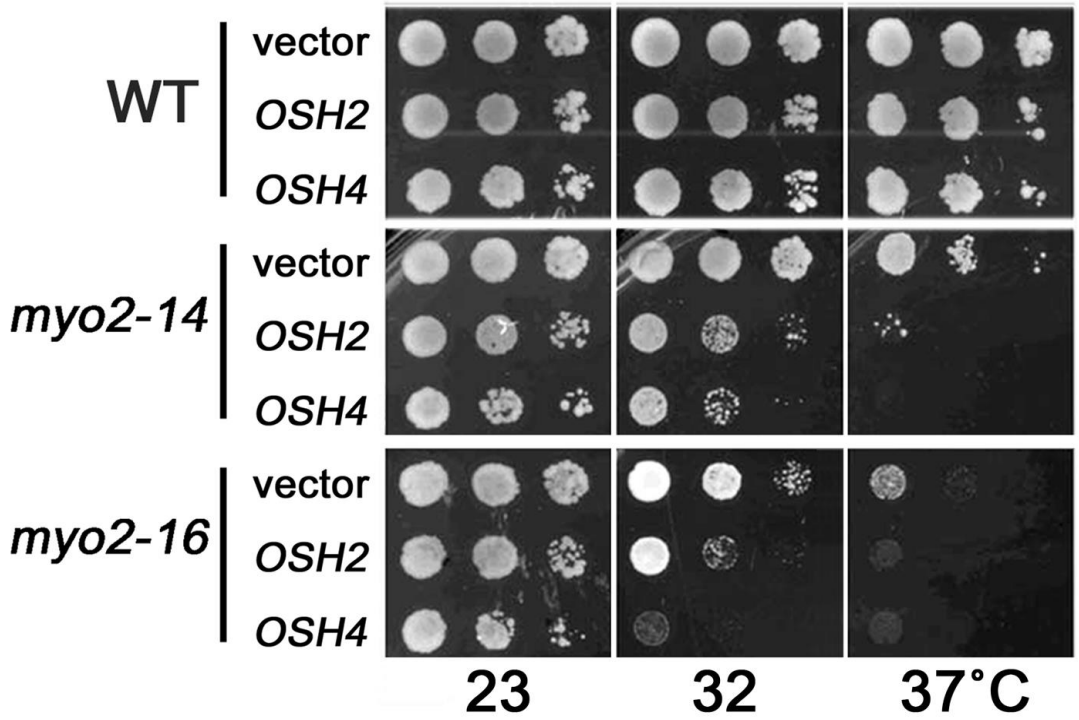

10-fold serial culture dilutions were spotted onto selective synthetic medium to compare growth of wild-type (WT; ABY531), myo2-14ts (ABY534), and myo2-16ts (ABY536) cells transformed with multicopy plasmids containing OSH2 (pCB239), OSH4 (pCB241), or the vector alone control (pRS426). Transformed strains were incubated at 23˚C (permissive growth temperature for myo2ts), 32°C (semi-permissive growth temperature), and 37˚C (restrictive growth temperature). Multicopy OSH4 caused growth defects at 32 and 37˚C when expressed in myo2-14ts and -16ts cells, whereas multicopy OSH2 had a significant but lesser effect. Experiments were conducted by G.A

Figure 2.4S. Anti-Bgl2p antibody production.

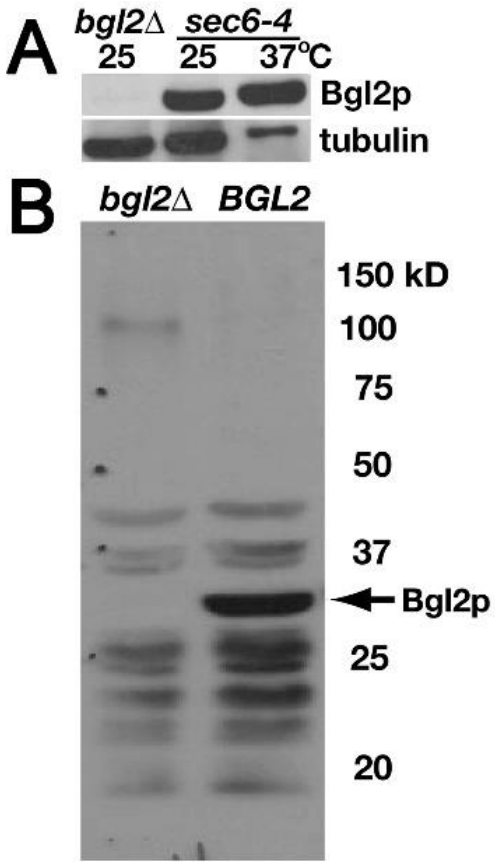

A) From whole-cell extracts the anti-Bgl2p serum specifically recognized Bgl2p as shown by its accumulation in extracts from *sec6-4* cells cultured at 37˚C versus 25˚C (as previously reported (Harsay & Bretscher, 1995)[73]) and its absence in *bgl2*Δ cell extracts. Bgl2p levels are shown relative to the tubulin internal control, which was detected with monoclonal antibody AA2 [gift of A. Frankfurter, U. of Virginia]). B) Anti-Bgl2p immunoblot showing all detectable bands in whole-cell extracts (including periplasmic proteins) from *BGL2*-expressing cells versus *bgl2*Δ cells. The Bgl2p band detected migrated at the predicted molecular weight of 34 kDa. Experiments were conducted by D.S

To produce a Bgl2p antiserum, a Maltose Binding Protein (MBP)-Bgl2p fusion protein was expressed in *E. coli* BL21(DE3) from pEH138 after induction with IPTG, and the fusion protein was purified on amylose resin (New England Biolabs, Ipswich, MA). The protocol for raising rabbit polyclonal antibodies against an MBP fusion protein was followed as previously described (Dighe & Kozminski, 2008). Immunizations and bleeds were performed by Convance Research Products, Inc. (Denver, PA). The specificity of the anti-Bgl2p serum was affirmed by the absence of detectable Bgl2p in a *bgl2*Δ strain.

Chapter 3. PM and ER membrane organization is affected by Arv1 but intracellular sterol transport is not

Georgiev* AG, Johansen* J, Ramanathan VD, Sere YY, Beh CT, Menon AK. Published in Traffic 2013 Vol 14:912-21 * = authors have contributed equally to this work

The pan-eukaryotic endoplasmic reticulum (ER) membrane protein Arv1 has been suggested to play a role in intracellular sterol transport. We tested this proposal by comparing sterol traffic in wild-type and Arv1-deficient *Saccharomyces cerevisiae.* We used fluorescence microscopy to track the retrograde movement of exogenously supplied dehydroergosterol (DHE) from the plasma membrane (PM) to the ER and lipid droplets and high-performance liquid chromatography to quantify, in parallel, the transport-coupled formation of DHE esters. Metabolic labeling and subcellular fractionation were used to assay anterograde transport of ergosterol from the ER to the PM. We report that sterol transport between the ER and PM is unaffected by Arv1 deficiency. Instead, our results indicate differences in ER morphology and the organization of the PM lipid bilayer between wild-type and *arv1*Δ cells suggesting a distinct role for Arv1 in membrane homeostasis. In *arv1*Δ cells, specific defects affecting single C-terminal transmembrane domain proteins suggest that Arv1 might regulate membrane insertion of tail-anchored proteins involved in membrane homeostasis.

Sterols are highly enriched in the plasma membrane (PM) of eukaryotic cells (Maxfield & Menon, 2006; Maxfield & van Meer, 2010). For example, ~70% of total cellular ergosterol is found in the PM of the budding yeast *Saccharomyces cerevisiae*, comprising ~40 mole percent of PM lipids (Sullivan, Ohvo-Rekilä, Baumann, Beh, & Menon, 2006). Ergosterol is synthesized in the endoplasmic reticulum (ER) and transported to the PM primarily by an ATP-requiring, non-vesicular mechanism (Jacquier

& Schneiter, 2012; Maxfield & Menon, 2006; Sullivan et al., 2006). Retrograde transport also occurs, because exogenously supplied sterols move from the PM to the ER, where they are esterified by the sterol acyltransferase enzymes Are1 and Are2 for encapsulation in lipid droplets (LDs)(Jacquier & Schneiter, 2012). As sterols are largely insoluble in water, they must be shielded from the aqueous environment for transport to occur efficiently. In analogy with other lipid transport processes, sterol transfer might require a cytoplasmic lipid transport protein, similar to the ceramide transport protein (CERT)(Hanada, Kumagai, Tomishige, & Yamaji, 2009) and the steroidogenic acute regulatory protein (StAR)(Alpy & Tomasetto, 2005; Mesmin et al., 2011). Oxysterol binding protein homologs (termed Osh proteins in yeast) are cytoplasmic, sterol-binding proteins that could function as ergosterol transporters(Raychaudhuri et al., 2006). We recently eliminated these proteins from consideration by showing that sterol transport between the ER and PM is unaffected in yeast cells lacking functional Osh proteins(Christopher T Beh et al., 2012; Georgiev et al., 2011). Thus the mechanism of intracellular sterol transport remains enigmatic.

The ER membrane protein Arv1(Tinkelenberg et al., 2000; Villasmil & Nickels, 2011) (Fig. 3.1A) has been proposed to be a key element of the sterol homeostatic machinery in all eukaryotic cells, with an unspecified role in sterol transport between the ER and PM. Arv1 was originally discovered through its essential function in maintaining the viability of *S. cerevisiae* cells that lack Are1 and Are2. It was subsequently discovered that in the absence of Arv1, yeast cells upregulate the unfolded protein response (Copic et al., 2009; Shechtman et al., 2011) and display a variety of lipid-related phenotypes. These include altered intracellular sterol distribution (Christopher T Beh & Rine, 2004; Tinkelenberg et al., 2000), sphingolipid metabolism (Swain et al., 2002), GPI-protein biosynthesis (Kajiwara et al., 2008) and PI(4,5)P_2 polarization in response to pheromone treatment (Villasmil, Ansbach, & Nickels, 2011). It has been suggested that defective sterol transport in *arv1*Δ cells gives rise to these pleiotropic 'lipid phenotypes', leading eventually to induction of the unfolded protein response (Shechtman et al., 2011). Here we examine the proposal that Arv1 is involved in sterol transport between the ER and PM. Our data indicate that whereas sterols traffic normally in *arv1*Δ cells, Arv1 deficiency results in dramatic changes in the organization of the PM lipid bilayer and in ER morphology.

3.1. Results and Discussion

3.1.1. Arv1 is localized to the cortical ER

To determine the sub-cellular localization of Arv1 in budding yeast we expressed GFP-Arv1 (previously shown to be functional (Copic et al., 2009) on a high-copy plasmid under the control of its own promoter. Fluorescence microscopy revealed a perinuclear and cortical fluorescence pattern (Fig. 1B) as previously reported (Copic et al., 2009; Swain et al., 2002), consistent with localization of the protein at the nuclear and cortical ER, respectively. As Arv1 over-expression might result in its accumulation at sites where it is not normally found (Copic et al., 2009), we expressed GFP-Arv1 at physiological levels under control of its own promoter on a low-copy-number plasmid. Using long exposure times and reiterative image deconvolution, we could detect GFP-Arv1 even when expressed at these low levels. Under these conditions, the perinuclear fluorescence observed with over-expressed GFP-Arv1 was not seen but only cortical fluorescence remained (Fig. 3.1C). Whereas perinuclear fluorescence was seen in >80% of cells with over-expressed GFP-Arv1, it could be detected in fewer than 5% of cells in which GFP-Arv1 was expressed at low levels (bar chart, Fig. 3.1D). Over-expressed GFP-Arv1 always co-localized with the nuclear and cortical ER marker RFP-ER (RFP fused to the transmembrane domain of Scs2) (Fig. 3.1E); we were unable to perform similar co-localization analyses with GFP-Arv1 expressed at low levels on account of low signal intensity. Nevertheless, our data suggest that Arv1 is normally restricted to the cell periphery in a distribution consistent with cortical ER.

Figure 3.1. Arv1 – membrane topology and subcellular localization.

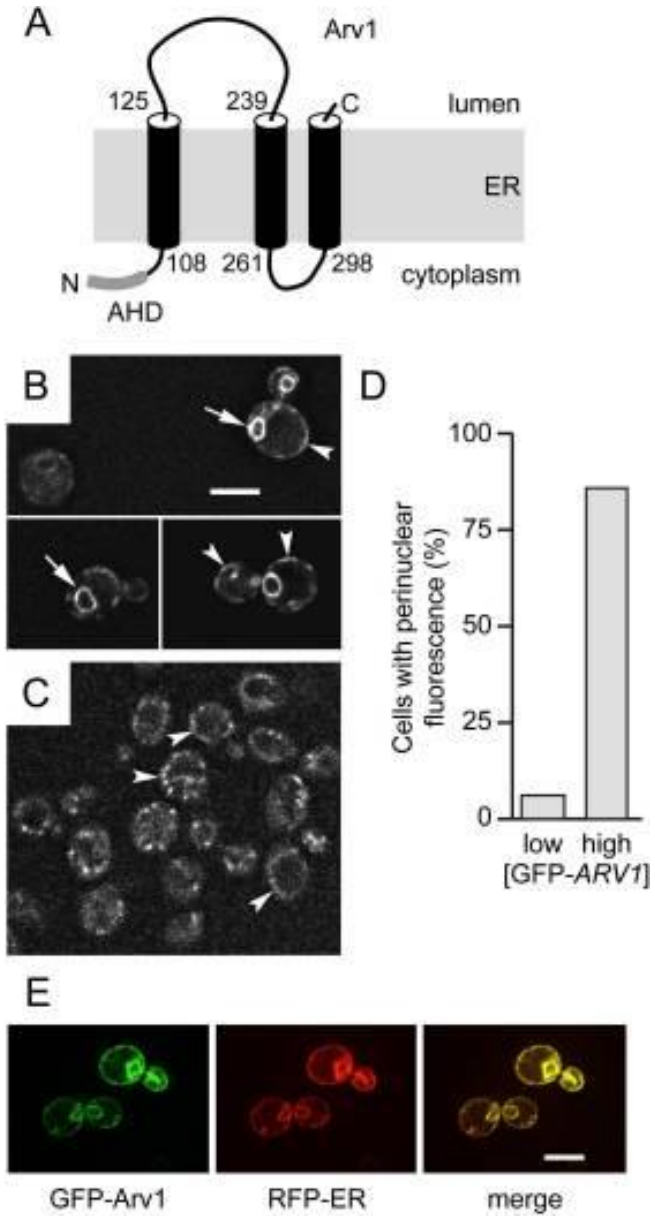

A Experimentally determined membrane topology of Arv1 (Villasmil & Nickels, 2011) (12). *S. cerevisiae* Arv1 is a 321 amino acid protein. The Arv1 homology domain (AHD; amino acids 2-63 of yeast Arv1) is indicated as a thick gray line. **B** Perinuclear localization of over-expressed GFP-Arv1. Deconvolved widefield fluorescence microscopy of GFP-Arv1 expressed from a high-copy 2μ plasmid (pCB1033) in wild-type cells (BY4741) in which cortical (arrowheads) and perinuclear ER (arrows) localization was detected. **C** Perinuclear fluorescence was largely absent in wild-type cells expressing GFP-Arv1 from a low-copy plasmid (pCB1031). **D** Quantification of GFP-Arv1 perinuclear localization in wild-type cells expressing GFP-Arv1 from "low" (CEN) or "high" (2μ) copy-number plasmids (N = 100 cells). **E** Wt cells co-expressing both GFP-Arv1 from a high-copy plasmid and the ER marker RFP-ER (pCB1024) visualized by confocal fluorescence microscopy. Scale bar, 5 μm. Panel A was made by A.M. Experiments were conducted by J.J

3.1.2. Characterization of S. cerevisiae arv1∆ cells

We examined key characteristics of *arv1*∆ cells as a prelude to studies of intracellular sterol transport in these cells. We confirmed that *arv1*∆ cells have a temperature-sensitive growth phenotype (Fig. 2A) and established that they grow slowly when incubated under hypoxic conditions in media containing ergosterol and fatty acids (Fig. 3.2B). It has been suggested (Tinkelenberg et al., 2000) that the slow growth of *arv1*∆ cells under hypoxic conditions may be due to a reduced ability to incorporate sterols from the growth medium into the plasma membrane (PM). However, our experiments reveal that the fluorescent sterol DHE (Fig. 3.3A) is incorporated into the PM of *arv1*∆ cells to an extent similar to that seen in wild-type cells (Fig. 3.3B, left panels), indicating that the hypoxic growth phenotype of *arv1*∆ cells may require a more complex explanation.

Figure 3.2. Characterization of *arv1*Δ cells

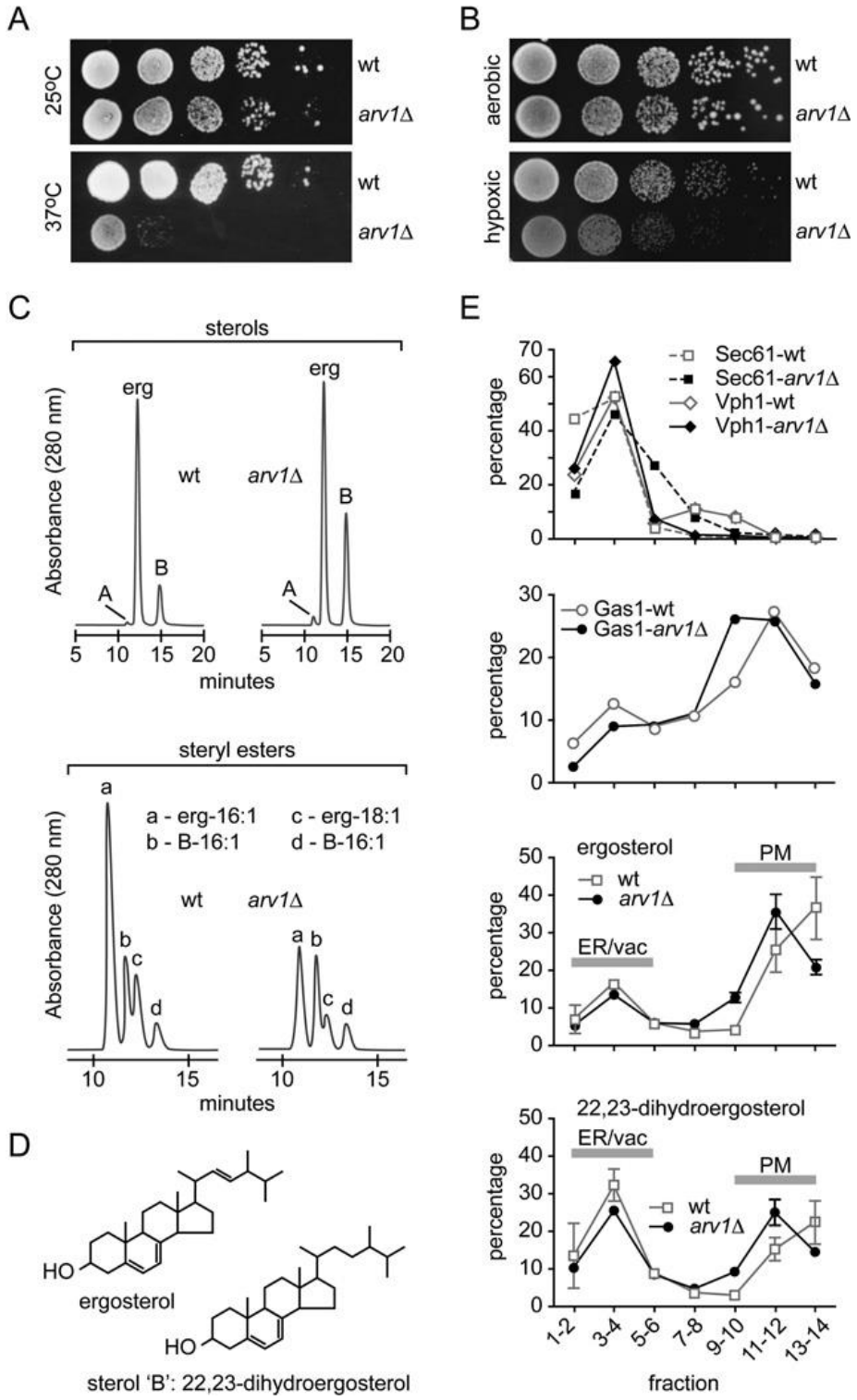

A 10-fold serial dilutions of wild-type (wt) and *arv1*Δ yeast cultures growing in YPD were placed on YPD plates and incubated for two days at 25°C or 37°C.**B** Serial dilutions of wt and *arv1*Δ cultures were placed on YPD plates containing 20 mM ergosterol, 0.5% (w/v) Tween 80, 0.5% (v/v) ethanol and incubated either aerobically or in a hypoxic chamber for 2 days at 30°C.**C** Non-polar lipid extracts from 0.1 OD_{600} equivalents of logarithmically growing wt and *arv1*Δ cultures were separated by HPLC. Eluted sterols (*top*) and steryl esters (*bottom*) were detected by absorbance at 280 nm. erg, ergosterol; A, ergostatrienol (MW=396); B, Ergosta-5,7-dien-3β-ol (22-dihydroergosterol; MW=398). The identities of sterols A and B were confirmed by liquid chromatography-mass spectrometry. The likely molecular species of the steryl esters is indicated in the bottom panel. **D** Structure of ergosterol and 22,23-dihydroergosterol (sterol 'B' in panel C). **E** Ergosterol and 22,23-dihydroergosterol content of sucrose-gradient separated cellular membranes from wt and *arv1*Δ cell homogenates. Fractions were collected from the top, and aliquots were either extracted with hexane for ergosterol analysis or washed by centrifugation in 100 mM Tris-HCl pH 7.5 and analyzed by SDS-PAGE and immunoblotting using antibodies directed against organelle-specific marker proteins (ER, Sec61; vacuole, Vph1; PM, Gas1). Immunoblots were quantified by densitometry using the ImageJ program (http://rsb.info.nih.gov/ij/). Experiments were performed by A.G

Previous reports (Kajiwara et al., 2008; Swain et al., 2002) indicated that Arv1 is required for normal glycerophospholipid, sphingolipid, and sterol metabolism. We determined that a*rv1*Δ cells have a higher sterol, steryl ester, and phospholipid content than wild-type cells, but that the molar ratio of sterol to phospholipid is unaffected (Table 3.3S). HPLC analyses revealed that whereas the ergosterol content of *arv1*Δ was similar to that of wild-type cells, *arv1*Δ cells accumulated the ergosterol biosynthetic intermediate 22,23-dihydroergosterol (Fig. 3.2C, D and Table 3.3S). This increase may be caused by deficiency of the C-22 sterol desaturase (Erg5) (Kelly et al., 1995) or because the biosynthetic intermediate is mislocalized and unavailable to the enzyme. The high level of 22,23-dihydroergosterol results in ergosterol accounting for only ~60% of total sterol in *arv1*Δ cells compared with 77% in wild-type cells (Table 3.3S). The decreased fraction of ergosterol relative to total sterol in *arv1*Δ vs wild-type cells is similar to that reported previously by Swain et al. (Swain et al., 2002). However, whereas we find that *arv1*Δ cells accumulate 22,23-dihydroergosterol, Swain et al. (Swain et al., 2002) reported that the cells accumulate lanosterol and other uncharacterized sterol intermediates. It is possible that 22,23-dihydroergosterol was the main uncharacterized intermediate reported by these authors.

We next examined the intracellular distribution of ergosterol in *arv1*Δ cells by using a well-vetted sucrose gradient centrifugation procedure (De Craene et al., 2006; Georgiev et al., 2011; Pomorski et al., 2003) to separate the PM from intracellular

membranes (Fig. 3.2E, top panels). As Sec61 is distributed throughout the ER, including the cortical ER region that lies adjacent to the PM, it is clear from Fig. 3.2E (top panels) that the PM-enriched fractions are not contaminated by ER membranes. Fractionation profiles of *arv1*Δ cells and wild-type cells were similar (Fig. 3.2E, top panels). We found that the majority (~70%) of ergosterol is located in the PM in both *arv1*Δ and wild-type cells, whereas a large fraction (~50%) of 22,23-dihydroergosterol is recovered in intracellular fractions (Fig. 3.2E, bottom panels).

Previous reports used metabolic radiolabeling (in conjunction with thin layer chromatography) (Tinkelenberg et al., 2000) and filipin staining (Kajiwara et al., 2008) to conclude that sterols accumulate in intracellular membranes of *arv1*Δ cells. Our data suggest that this is primarily due to the increased level of 22,23-dihydroergosterol.

We conclude that *arv1*Δ cells display aberrant sterol metabolism exemplified by a ~2.5-fold accumulation of 22,23-dihydroergosterol, but that the distribution of sterols amongst cellular membranes (PM versus internal membranes) in *arv1*Δ is similar to that found in wild-type cells.

3.1.3. Dehydroergosterol (DHE) is transported from the PM to the ER and lipid droplets in arv1Δ cells

We recently described a fluorescence-based assay to visualize and quantify intracellular sterol transport in yeast (Georgiev et al., 2011). The assay exploits the fluorescence of DHE (Fig. 3.3A), a naturally occurring sterol. DHE is an excellent analog of ergosterol as it supports the growth of *hem1*Δ cells that require exogenous sterol for growth (Georgiev et al., 2011). In a typical experiment, cells are incubated with DHE under hypoxic conditions to enable the fluorescent sterol to enter the PM. Hypoxic incubation overcomes 'aerobic sterol exclusion' and is required for sterol loading (Georgiev et al., 2011). On chasing the cells under aerobic conditions, DHE is seen to move out of the PM and appear in LDs. DHE redistribution, scored by cell counting and the conversion of DHE to DHE-ester, occurs in an ATP-dependent manner that does not require vesicle-mediated transport (Georgiev et al., 2011).

Figure 3.3. DHE transport from PM to ER.

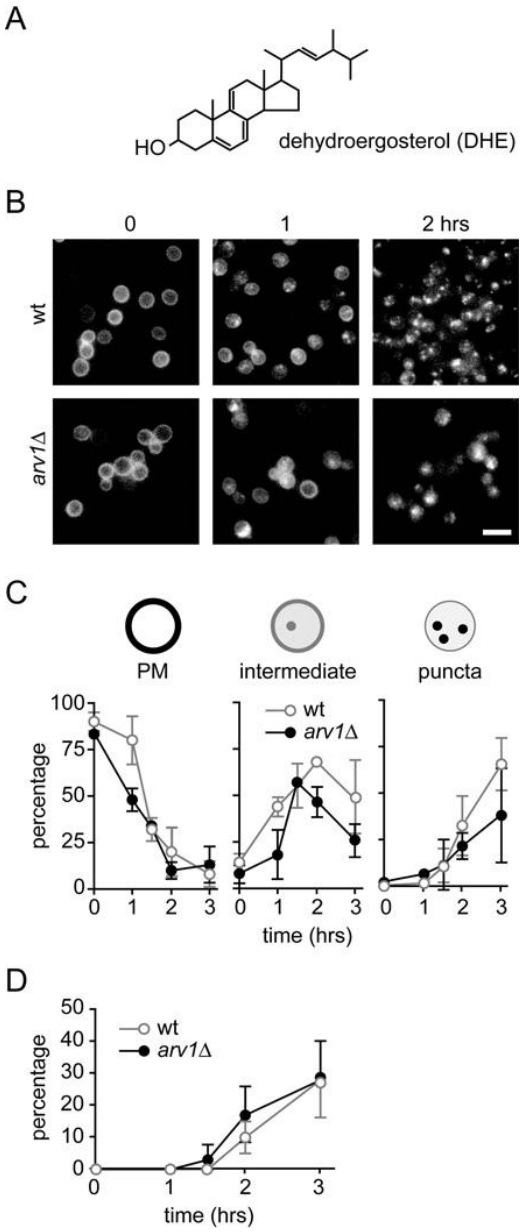

(A) Structure of dehydroergosterol (DHE). **(B)** Epifluorescence micrographs of wild-type (wt) and *arv1*Δ cells grown under hypoxic conditions for 36h at 30°C in yeast extract-peptone-dextrose (YPD) supplemented with 20 µg/mL DHE in 0.5% ethanol, 0.5% Tween-80, and chased under aerobic conditions for 0, 1 or 2h. Each of the square images is 100 µm on edge. **(C)** Quantification of images such as those recorded in panel B. The images were scored manually by assigning individual cells to one of the three categories (PM, intermediate, puncta) illustrated schematically above the graphs. Data are from three independent experiments; at least 200 cells were counted for each time-point in each experiment. **(D)** DHE-loaded cells were processed as in panels B and C, except that at each time-point an aliquot of the cells was taken for lipid extraction and HPLC analysis to resolve and quantify DHE and DHE esters. The graph shows the percentage of DHE recovered in the form of DHE-ester. Experiments were conducted by A.G

We applied the DHE redistribution assay to assess intracellular sterol transport in *arv1*Δ cells. As shown in Fig. 3.3B, both wild-type, and *arv1*Δ cells could be efficiently loaded with DHE and showed PM-localized fluorescence at the start of the chase period. After a 2h chase under aerobic conditions, fluorescence appeared in the form of discrete puncta corresponding to LDs. Redistribution was evident in both wild-type and *arv1*Δ cells, with the principal difference being in the size and number of puncta per cell. DHE-stained LDs were small and numerous in wild-type cells, whereas *arv1*Δ cells had fewer and larger LDs, consistent with previous observations (Shechtman et al., 2011). Thus, DHE is able to redistribute from the PM to intracellular compartments in *arv1*Δ cells.

We quantified DHE redistribution by scoring cells according to the categories depicted schematically in Fig. 3.3C: PM staining, intermediate staining, and puncta. The data (Fig. 3.3C) indicate that DHE moves out of the PM at a similar rate in wild-type and *arv1*Δ cells such that after 2 h there are essentially no cells with PM-localized DHE (Fig. 3.3C, left panel). Wild-type and *arv1*Δ cells differed somewhat in the rate at which DHE appeared in puncta (Fig. 3C, right panel). Puncta were discernible in both cell types after a ~1 h lag period but were more evident in wild-type than *arv1*Δ cells after 3 h. To provide an independent read-out of transport we extracted lipids from the cells at different time points and determined the percentage of DHE that had been converted to DHE ester. As shown in Fig. 3.3D, DHE esterification could be detected after a lag period of ~1.5 h and increased monotonically in both cell types over the 3 h period of the experiment. We conclude that sterol transport from the PM to the ER is unaffected by Arv1 deficiency as DHE moves out of the PM (visual scoring) and arrives at the ER (conversion to DHE ester) at a similar rate in both wild-type and *arv1*Δ cells. DHE internalization is unlikely to involve endocytosis as a parallel redundant route. The deletion of *ARV1* results in endocytosis defects (Christopher T Beh & Rine, 2004), which is consistent with synthetic growth defects observed when combining *arv1*Δ with *abp1*Δ*, sla1*Δ*, or sla2*Δ endocytosis mutations in a haploid cell (data not shown). Whether by nonvesicular or endocytic vesicular transport, the movement of DHE out of the PM was unaffected in *arv1*Δ cells.

3.1.4. Ergosterol is transported from the ER to the PM in arv1∆ cells

To examine anterograde sterol transport in *arv1*∆ cells we pulse-labeled the cells for 4 min at 30°C with [^{3}H-methyl]methionine to incorporate [^{3}H] into newly synthesized sterols and chased for 90 min at the same temperature. Cell samples taken at the end of the pulse-labeling period and after the chase were rapidly cooled, treated with energy poisons and homogenized by bead-beating. The resulting homogenate was fractionated by sucrose gradient centrifugation to resolve the PM from intracellular membranes as shown in Fig. 3.2E.

The specific radioactivity (SR = cpm ÷ absorbance units) of ergosterol was determined for subcellular fractions as well as for whole cells, and the relative specific radioactivity ($RSR_{frac} = SR_{frac} \div SR_{cell}$) of fractions pooled pair-wise from the top of the gradient was calculated. We first analyzed wild-type cells. At the end of the pulse period, intracellular membranes (fractions 1-8) had an $RSR_{frac} > 1$ whereas the PM (fractions 9-14) had an $RSR_{frac} < 1$ (Fig. 3.4A). At the end of the chase period, all gradient fractions had an $RSR_{frac} \sim 1$ (Fig. 3.4B). These data indicate that at the end of the labeling pulse [^{3}H]ergosterol is mainly located in the ER-enriched intracellular fractions as expected, but at the conclusion of the chase period, it equilibrated completely with the PM and other cellular membranes.

Figure 3.4. Ergosterol transport from ER to PM.

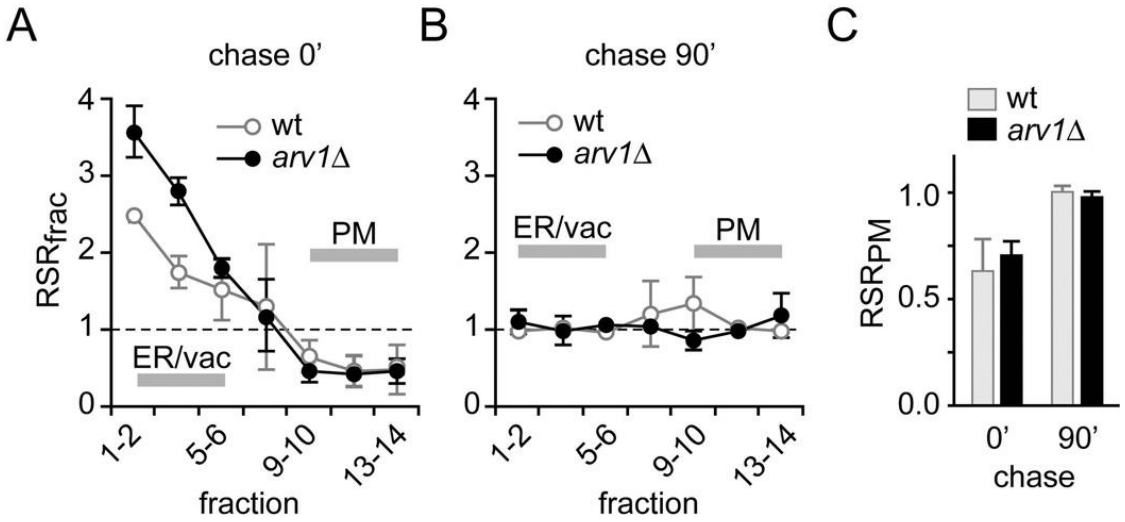

Wild-type (wt) and *arv1*Δ cells were pulse-labeled for 4 min and chased for 90 min at 30°C. Samples taken at the end of the pulse-labeling period (chase **=** 0 min) and at the end of the chase (chase **=** 90 min) were fractionated on sucrose gradients. The specific radioactivity (SR **=** cpm ÷ absorbance units) of ergosterol was determined for subcellular fractions as well as for whole cells by HPLC analysis, and the relative specific radioactivity (RSR_{frac} **=** SR_{frac} ÷ SR_{cell}) of fractions pooled pairwise from the top of the gradient was calculated. **(A)** RSR of fractions analyzed after the pulse-labeling period; **(B)** RSR of fractions analyzed after a 90 min chase; **(C)** Average RSR of the PM (fractions 9-14) after the pulse and chase periods. The fractionation protocol is the same as that characterized in Fig. 2E. Fractions containing ER (Sec61), vacuole (Vph1) and PM (Gas1) markers are indicated. Experiments were conducted by A.G

The spontaneous movement of ergosterol between membranes during the fractionation procedure is not expected to be a factor in our analyses as it is predicted to be very slow (Georgiev et al., 2011). Our data support this assertion. If ergosterol moved spontaneously between membranes at an appreciable rate during the fractionation procedure, then RSR_{frac} would equal 1 for all fractions in the end-of-pulse sample but we note that RSR_{frac} was ≠ 1 for almost all these samples. Also relevant is our observation that ergosterol and 22,23-dihydroergosterol fractionate differently (Fig. 3.2E, lower panels), indicating that sterol exchange during cell homogenization and fractionation is not a complicating factor in our analysis.

The RSR_{frac} profiles for Arv1-deficient and wild-type cells at the end of the pulse period and after a 90 min chase are essentially the same (Fig. 3.4A,B) indicating that Arv1-deficiency does not affect the movement of ergosterol from the ER to the PM.

Of note, RSR_{frac} of the PM was ≥ 0.5 at the end of the pulse period for both strains (Fig. 3.4C) indicating that the $t_{1/2}$ for ergosterol movement between the ER and PM is < 4 min, irrespective of Arv1 function.

3.1.5. Altered PM lipid organization in arv1Δ cells

Cells lacking Arv1 are hyper-sensitive to nystatin (Tinkelenberg et al., 2000), a polyene anti-fungal compound that manifests toxicity by binding ergosterol at the PM surface. We confirmed this phenotype in our strain background (Fig. 3.5, bottom panels). In addition, whereas only ~1.5 ± 0.4% of PM ergosterol was extracted by methyl-β-cyclodextrin from wild-type cells under our standard conditions, similar to data previously reported (Baumann et al., 2005; Georgiev et al., 2011), the efficiency of extraction from *arv1*Δ cells was 4.5-fold higher (6.8 ± 3.4%). The increased availability of PM ergosterol to methyl-β-cyclodextrin extraction and the nystatin-sensitivity of *arv1*Δ cells indicate that Arv1 influences the organization of sterols at the PM.

To determine whether the change in PM lipid organization was restricted to sterols, we tested whether *arv1*Δ cells were sensitive to papuamide B, a marine cyclodepsipeptide that is toxic to cells that expose phosphatidylserine (PS) at their surface (Parsons et al., 2006). As PS is normally not exposed at the cell surface, wild-type cells are relatively resistant to papuamide B. However, *drs2*Δ and *osh4*Δ strains are papuamide B-sensitive as reported previously (Muthusamy et al., 2009), and so we used these strains as controls. We found that *arv1*Δ cells were hypersensitive to papuamide B (Fig. 3.5, top panels), indicating a loss of PM lipid asymmetry.

Figure 3.5. Drug sensitivity tests.

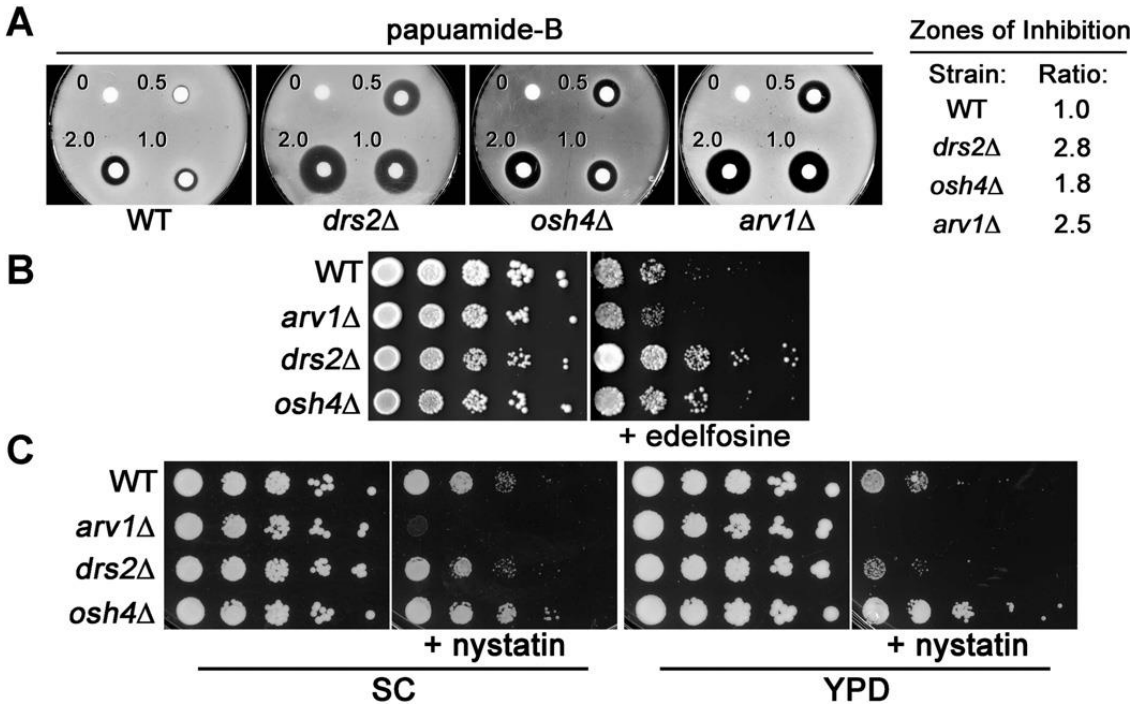

A Zone of inhibition assay comparing the growth of wt (BY4741), *drs2*Δ (CBY2317), *osh4*Δ (CBY5150) and *arv1*Δ (CBY994) cells in the presence of papuamide B. At the concentrations indicated, papuamide B was added to each disc and the diameters of the zones where cell growth was inhibited were measured. Average diameters of inhibition zones were determined from triplicate trials and tabulated for each strain as a ratio relative to wild type. **B** Ten-fold serial dilutions of wt, *arv1*Δ, *drs2*Δ and *osh4*Δ cultures spotted onto SC medium with and without the inhibitory PC analog, edelfosine (60 μM) and **C** spotted onto SC or YPD medium with or without 10 μM nystatin. Plates were incubated at 30°C for 48 hrs. Experiments were conducted by V.R

PS exposure at the surface of *arv1*Δ cells could be due to compromised phospholipid flippase activity. Preliminary experiments in which cells were labeled with NBD-PC, a fluorescent derivative of phosphatidylcholine (PC), indicated that this was not the case: NBD-PC was taken up by *arv1*Δ cells and distributed amongst internal membranes exactly as seen in wild-type cells (not shown). To examine this result more closely we tested the sensitivity of the cells to edelfosine, a toxic analog of PC. Edelfosine toxicity requires its import across the PM by lipid flippases of the P4-type ATPase class (Hanson, Malone, Birchmore, & Nichols, 2003; Riekhof & Voelker, 2009). Thus, wild-type cells are sensitive to edelfosine but *drs2*Δ cells that lack a major contributor to flippase activity (Sebastian, Baldridge, Xu, & Graham, 2012) are predicted to be resistant. As shown in Fig. 3.5 (middle panels), Drs2-deficient cells are relatively

resistant to the drug but *arv1*Δ and wild-type cells are similarly sensitive to edelfosine indicating that PS exposure in *arv1*Δ is not due to compromised PM lipid flippase activity. These results indicate that Arv1 has little impact on PC trafficking across the PM and between the PM and internal organelles. We conclude that the organization of ergosterol and PS within the PM is specifically affected by Arv1 deficiency.

3.1.6. Cortical and cytoplasmic ER defects in arv1Δ cells

Considering that GFP-Arv1 resides in the cortical ER (Fig. 3.1C) and *arv1*Δ cells exhibit PM defects (Fig. 3.5), we examined whether Arv1 deficiency affects the organization of cortical ER at its interface with the PM. In medial optical sections through wild-type cells, the ER-specific marker Sec61-GFP displays ring-like perinuclear fluorescence as well as discontinuous fluorescence along the cell cortex (Fig. 3.6A). However, the web-like lattice of the cortical ER organization is best observed through optical sections focused at the cell surface. Although perinuclear and cortical Sec61-GFP fluorescence was observed in *arv1*Δ cells, extraneous cytoplasmic fluorescence corresponding to ER tendrils was also seen and the cortical ER lattice was disorganized (Fig. 3.6B, C). After shifting *arv1*Δ cells cultured at 30ºC to 37ºC, which inhibits cell growth (Fig. 3.2A), the percentage of *arv1*Δ cells with ER defects increased (Fig. 3.6C). In *arv1*Δ cells expressing RFP-ER (a fusion of RFP with the C-terminal transmembrane domain of tail-anchored Scs2, an ER membrane protein (Schuldiner et al., 2008)), perinuclear and cortical fluorescence was also detected, though 5-fold longer exposures were required for visualization relative to wild-type cells (Fig. 3.6D, E). In medial sections, 86% of *arv1*Δ cells had extraneous cytoplasmic ER compared to only 7% in wild-type cells (at equal exposures) (N = 100) (Fig. 3.6D). At the cell surface, the regular lattice of cortical ER observed in 96% of wild-type cells was present in only 9% of *arv1*Δ cells (N = 100) (Fig. 3.6E). These results suggest that Arv1 affects ER structural organization at the cell cortex.

Figure 3.6. Cortical ER organization is disrupted in *arv1*Δ cells.

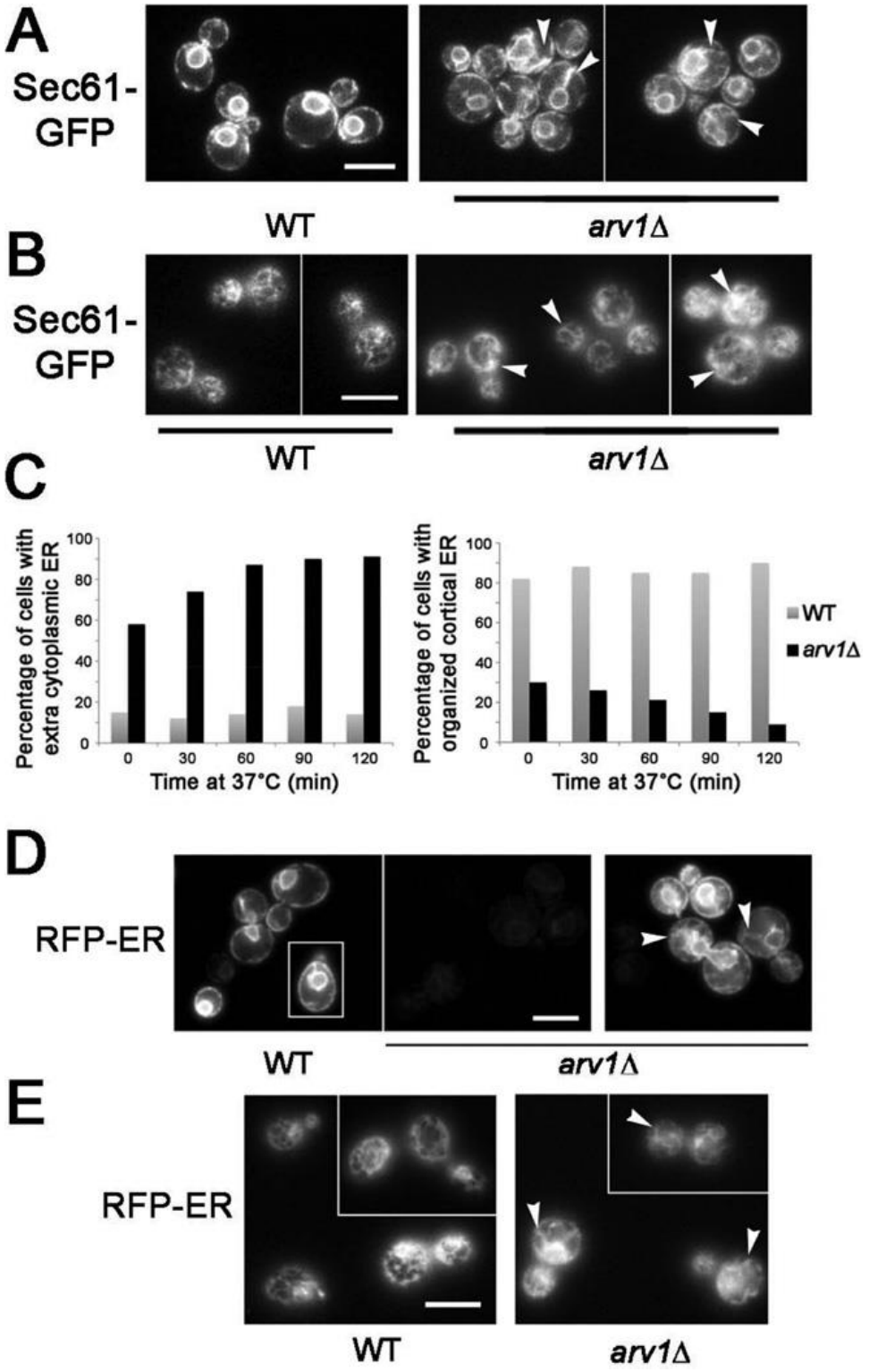

A Medial optical sections of wt (BY4742) and *arv1*Δ (CBY994) cells expressing the ER-localized marker Sec61-GFP. **B** Sec61-GFP localization shown in optical sections focused at the cell surface. To visualize cortical ER in *arv1*Δ cells, due to background fluorescence caused by the proliferation of cytoplasmic ER, contrast adjustments between wt and *arv1*Δ images were not equivalent. **C** Bar graphs quantify extraneous cytoplasmic ER and organization defects in cortical ER (N > 100 cells). **D** At equivalent exposures, RFP-ER (pCB1024) fluorescence cannot be visualized in *arv1*Δ cells (middle panel) unless relative to wt cells 5-fold longer exposures are performed (right panel). **E** Optical sections focused at the cell surface also show that the RFP-ER-marked cortical ER is disorganized in *arv1*Δ cells compared to wt. Arrowheads in all panels indicate examples of disorganized and extraneous peripheral/cortical ER observed in *arv1*Δ cells. Scale bars = 5 µm. Experiments were conducted by J.J

Because the tail-anchored RFP-ER was reduced in levels in *arv1*Δ cells, we tested whether the expression of another intact tail-anchored ER protein was affected. Sbh1 is a tail-anchored integral membrane protein inserted into the ER membrane by the GET complex (Schuldiner et al., 2008). In 85.5% wild-type cells, RFP-Sbh1 expressed from a low-copy plasmid localizes to the cortical and perinuclear ER. In contrast, this localization pattern is observed in only 8.5% *arv1*Δ cells, and overall fluorescence is diminished (N = 200 cells; Fig. 3.7A). Accordingly, a comparison of protein levels by immunoblot analysis indicated reduced expression of both RFP-ER and -Sbh1 in *arv1*Δ cell extracts relative to wild type, using actin as the loading control (Fig. 3.7B). Due to its low expression, RFP-Sbh1 was detected in wild-type extracts only when expressed from a high-copy plasmid. However, regardless of plasmid dosage RFP-Sbh1 could not be detected in *arv1*Δ cell extracts. These results implicate Arv1 in the targeting and expression of tail-anchored single C-terminal transmembrane domain proteins.

Figure 3.7. Tail-anchored ER integral membrane proteins in *arv1*Δ cells.

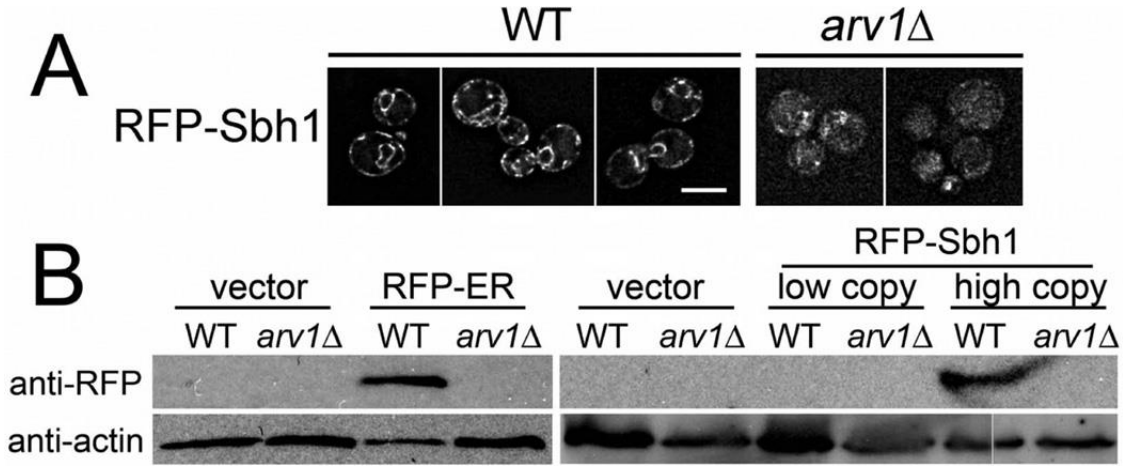

A Wt (BY4742) and *arv1*Δ (CBY994) cells expressing the ER tail-anchored protein RFP-Sbh1 from a low-copy plasmid (pCB1080). Scale bar, 5 µm. **B** In extracts isolated from wt and *arv1*Δ cells, expression of RFP-ER (pCB1024), and -Sbh1 expressed from a low *CEN* (pCB1080) and high 2µ (pCB1081) copy-number plasmids, were compared on immunoblots probed with an anti-RFP antibody. To show equivalent loading, equal amounts of sample were also probed on immunoblots with an anti-actin antibody that detects yeast Act1. Experiments were conducted by J.J

3.2. Summary

We examined intracellular sterol transport in *arv1*Δ cells using both a visual fluorescence-based assay to assess retrograde sterol transport from the PM to the ER and a subcellular fractionation approach to monitor anterograde transport of newly synthesized ergosterol from the ER to the PM. The assays revealed that transport between the PM and ER occurs normally in *arv1*Δ cells, eliminating a direct role for Arv1 in sterol movement between these membrane compartments. We note, however, that exogenously supplied DHE was esterified at the same rate in *arv1*Δ and wild-type cells but it took longer to appear in LDs in *arv1*Δ cells. The reason for this is unclear but as the morphology of LDs is affected by Arv1 deficiency (*arv1*Δ cells have fewer and larger LDs than wild-type cells, *e.g*. Fig. 3.3B and reference (Shechtman et al., 2011)), it is possible that the absence of Arv1 impacts the recruitment of steryl esters from the ER to LDs. Further work will be needed to investigate this phenomenon.

Our studies revealed that Arv1 provides an unusual functional link between the ER and PM. Arv1-deficient cells show defects in cortical and cytoplasmic ER and changes in the lipid organization of the PM such that sterol 'availability' increases and the transbilayer asymmetry of the PM phospholipid bilayer is altered. It is possible that these effects are mediated by interactions between the cytoplasmically oriented AHD (Arv1 Homology Domain) of Arv1 (Villasmil et al., 2011) (Fig. 3.1A) and one or more PM components. The nystatin sensitivity of *arv1*Δ cells is partially reversed by expression of the AHD consistent with the possibility that the AHD is a key element in the ability of Arv1 to regulate PM lipid organization in *trans*. Future work will determine if this possibility can be generalized to account for other observed changes in PM lipid organization in Arv1-deficient cells, as well as changes in ER morphology.

Distended cytoplasmic ER tendrils are observed in some mutants that perturb the retrieval of ER-resident proteins from the Golgi (Copic et al., 2009). In fact, *arv1*Δ cells also fail to retrieve the ER Hsp70 Kar2, which is secreted by default out of the cell (Copic et al., 2009). Defects in the ER retrieval pathway do not affect cell growth unless unfolded protein response (UPR)-mediated transcription is also inhibited. In cells where both ER retrieval and UPR transcription are inhibited, the loss of Kar2 and other ER proteins from the cell cannot be compensated by increased UPR-dependent expression, resulting in cell lethality (C T Beh & Rose, 1995). Likewise combining both *arv1*Δ and the deletion of the UPR-transcriptional activator *HAC1* is lethal in a haploid cell (Copic et al., 2009). *ARV1* exhibits interactions with some other genes that affect Kar2 retention, including all those representing the GET complex (Copic et al., 2009), which inserts tail-anchored proteins into the ER membrane (Chartron, Clemons, & Suloway, 2012). In *arv1*Δ cells, the polytopic transmembrane protein Sec61-GFP is unaffected but fluorescence and levels of the C-terminal transmembrane domain proteins RFP-ER and -Sbh1 are markedly reduced. This result suggests that Arv1 is involved in GET-mediated tail-end insertion into the ER. The role of Arv1 in ER structure and/or lipid droplet biogenesis might then simply reflect functional requirements for proper insertion of tail-end membrane proteins.

3.3. Materials and Methods

3.3.1. General

Yeast strains and plasmids are listed in Tables 1 and 2, respectively. All other materials were obtained as described previously (Georgiev et al., 2011). To generate *N*-terminal GFP-*ARV1* fusions, a stitch PCR approach was used in which 320 bp *ARV1* promoter was joined with the sequence encoding eGFP and in turn fused in-frame to the *ARV1* coding sequence with 97 bp downstream of the stop codon. The amplified fusion product was inserted into the *Bam*HI site of pRS315 and pRS325 and confirmed by sequencing. Procedures for hypoxic incubation of yeast cells, DHE fluorescence microscopy and quantification of DHE redistribution by analysis of fluorescence images, lipid extraction, HPLC analysis of lipids, ACAT assays and sucrose gradient fractionation to measure transport of ergosterol from the ER to the PM were carried out exactly as described previously (Georgiev et al., 2011).

3.3.2. Drug sensitivity tests

Papuamide B zone of inhibition assay: For each yeast strain tested, 2 ml of a saturated overnight culture was suspended in 3 ml of 1% molten agar and spread over the surface of solid medium plates. After agar hardening, a 6-mm disc of filter paper containing 12 µl of different concentrations of Papuamide B (Lynsey Huxham, University of British Columbia, Canada) in DMSO was placed on the surface. Plates were incubated at 30°C for 36 hr, and drug sensitivities were measured by comparing the diameter surrounding each disc within which growth was inhibited. Values reported represent an average of three independent trials.

Edelfosine and nystatin growth inhibition: Ten-fold serial dilutions of yeast cultures were spotted onto solid SC (Synthetic complete) or YPD (Yeast Peptone Dextrose) media containing 60 µM edelfosine (Cayman Chemicals, Ann Arbor, MI) or 10 µM nystatin (Sigma-Aldrich Chemicals, Oakville, ON) and incubated at 30°C for 48 hrs.

3.3.3. Fluorescence microscopy

Fluorescent cell images were observed on a Leica DMXRA2 microscope equipped with an X100/1.40 Plan-Apo objective using a GFP filter set. Images were captured with an Orca100ER digital camera (Hamamatsu Photonics, Hamamatsu-City, Japan). For GFP-Arv1 localization studies, log phase cells were imaged in filter-sterilized synthetic medium using 2 sec and 250 msec exposures at 55% arc lamp intensity for CEN (pCB1031) and 2µ (pCB1033) GFP-*ARV1* transformants, respectively. Deconvolution was performed using the deconvolution module in Volocity 6.0 (Perkin-Elmer, Waltham, MA) based on a theoretical point spread function (widefield, NA 1.40, emission 507 nm) with a confidence limit of 99%. All experiments were conducted on log phase cells with a 30% arc lamp intensity with a 500 msec exposure to visualize RFP-Sbh1, and 200 or 500 msec for RFP-ER as indicated. Images from RFP-Shb1 expressing cells were deconvolved using a 95% confidence limit and a theoretical point spread function (widefield, 1.40 NA, emission 607 nm). Cells expressing GFP and RFP fusions were visualized using GFP and Texas-Red filters, respectively (Chroma Technology, Bellows Falls, WT). GFP-Arv1/RFP-ER co-localization studies were performed on a Zeiss Axio Observer microscope modified with a Yokagawa CSU-10 spinning disk using a Hamamatsu 9100 EMCCD camera. A 491 nm laser was set for 80% power and 1 s exposures using a 230 analog gain for GFP fluorescence. Identical settings were used for RFP, but with a 561 nm laser. Confocal images were deconvolved using the Volocity deconvolution module based on theoretical point spread functions and a confidence of 95%. All image analyses were performed using Improvision software (Lexington, MA). Exposure times and contrast enhancement were constant for each series of images unless otherwise noted.

3.3.4. Immunoblot analysis

For analysis of protein expression, 10 OD of RFP-ER expressing cells were prepared as described by Ohashi et al. (Ohashi, Gibson, Gregor, & Schatz, 1982). Pellets were resuspended in SDS sample buffer and boiled for 5 min before SDS-PAGE. Protein transfer to nitrocellulose membranes and immunoblot conditions were as previously described (Christopher T. Beh, Brizzio, & Rose, 1997). To detect RFP-ER,

immunoblots were incubated with a 1:1000 titre of anti-RFP antibody (Thermo Fisher Scientific Inc., Rockford, IL) followed by a 1:10000 titer of anti-rabbit-HRP secondary antibody (Bio-Rad Laboratories, Hercules, CA). Actin was detected using a 1:1000 titer of anti-actin antibody (Cedarlane, Burlington, ON) followed with a 1:10000 titer of anti-mouse-HRP secondary antibody (Life Technologies Inc., Burlington, ON). Detection of RFP-Sbh1 by immunoblot required protein transfer to a polyvinylidene fluoride (PVDF) membrane, using conditions recommended by the manufacturer (Bio-Rad Laboratories, Hercules, CA). The PVDF immunoblot was probed with the same antibodies and titers as used for RFP-ER detection.

3.4. Acknowledgements

We thank David Sullivan and Michael Kersting for measuring the efficiency of cyclodextrin-mediated sterol extraction from wild-type and *arv1*Δ cells, Patty Kane and Tom Rapoport for antibodies, Christopher Loewen for plasmids, Harry Pearce for advice, Fred Maxfield for use of a fluorescence microscope, and Ziwei Ding for technical assistance. This work was supported by NIH grant GM71041 (A.K.M.) and the NSERC (C.T.B.).

Table 3.1S. Yeast strains used in this study.

Strain	Genotype	Source
BY4741	*MAT*a *his3*Δ*1 leu2*Δ*0 met15*Δ*0 ura3*Δ*0*	(Winzeler et al., 1999)
BY4742	*MAT*α *his3*Δ*1 leu2*Δ*0 lys2*Δ*0 ura3*Δ*0*	(Winzeler et al., 1999)
CBY994	BY4741 *arv1*Δ::kan-MX4	(Winzeler et al., 1999)
CBY2317	BY4741 *drs2*Δ::kan-MX4	(Winzeler et al., 1999)
CBY5150	BY4741 *osh4*Δ::kan-MX4	(Winzeler et al., 1999)
CBY5194	BY4742 *lem3*Δ::kan-MX4	(Winzeler et al., 1999)
CBY5303	BY4742 *SEC61*-GFP::*HIS3*	This study
CBY5307	CBY994 *SEC61*-GFP::*HIS3*	This study

Table 3.2S. Plasmids used in this study.

Plasmid	Markers	Source
pCB1024	P^{PHO5}-dsRED-$SCS2^{220-244}$ CEN *URA3*	(Loewen, Young, Tavassoli, & Levine, 2007)
pCB1031	GFP-*ARV1* CEN *LEU2*	This study
pCB1033	GFP-*ARV1* 2µ *LEU2*	This study
pCB1080	mRFP-*SBH1 CEN URA3*	This study
pCB1081	mRFP-*SBH1* 2µ *URA3*	This study
pRS315	CEN *LEU2*	(Sikorski & Hieter, 1989)
pRS325	2µ *LEU2*	(Sikorski & Hieter, 1989)

Table 3.3S. Sterol, steryl ester and phospholipid content of wild-type and *arv1*Δ cells

	ergosterol[a]	22,23-dihydroergosterol[a]	steryl ester[a]	PL[a,b]	Sterol/PL[b,c]
BY4742	1.33 ± 0.09	0.40 ± 0.01	0.056 ± 0.005	18.1 ± 1.3	~0.096
*arv1*Δ	1.53 ± 0.04	1.00 ± 0.14	0.138 ± 0.013	27.5 ± 5.1	~0.092

anmol per OD unit, i.e., per 2 x 107 cells

bPL, phospholipid

cmolar ratio

Overnight cultures were diluted to OD_{600}=0.5 in YPD and grown for 4h at 30°C before harvesting. Non-polar lipids (including sterols and steryl esters) were extracted from glass-bead disrupted yeast cells with hexane. Phospholipids were extracted from an aliquot of the same lysate using methanol:chloroform (1:2, by volume). The organic solvent was evaporated in a speed-vac and an aliquot of the non-polar extract corresponding to 0.1 OD units of cells was analyzed by HPLC, while 2.0 OD equivalents of the polar extract was analyzed by measuring the phosphate content of the hydrolyzed lipids. Standard curves were generated with pure ergosterol (Sigma) or sodium

phosphate. The numbers are from 3 (sterol) or 2 (phospholipid) independent measurements for each strain.

Chapter 4. Polarized Exocytosis Induces Compensatory Endocytosis by Sec4p-Regulated Cortical Actin Polymerization

Johansen J, Alfaro G, Beh CT Published in PLoS Biology Aug 2016 doi: 10.1371/journal.pbio.1002534. K Kozminski, KG and Dighe , SA contributed to figure 4.4 denoted as KK in figure legends

4.1. Abstract

Polarized growth is maintained by both polarized exocytosis, which transports membrane components to specific locations on the cell cortex, and endocytosis, which retrieves these components before they can diffuse away. Despite functional links between these two transport pathways, they are generally considered to be separate events. Using live cell imaging, *in vivo* and *in vitro* protein binding assays, and *in vitro* pyrene-actin polymerization assays, we show that the yeast Rab GTPase Sec4p couples polarized exocytosis with cortical actin polymerization, which induces endocytosis. After polarized exocytosis to the plasma membrane, Sec4p binds Las17/Bee1p (yeast WASp) in a complex with Sla1p and Sla2p during actin patch assembly. Mutations that inactivate Sec4p, or its guanine nucleotide exchange factor (GEF) Sec2p, inhibit actin patch formation, whereas the activating *sec4-Q79L* mutation accelerates patch assembly. *in vitro* assays of Arp2/3-dependent actin polymerization established that GTPγS-Sec4p overrides Sla1p inhibition of Las17p-dependent actin nucleation. These results support a model where Sec4p relocates along the plasma membrane from polarized sites of exocytic vesicle fusion to nascent sites of endocytosis. Activated Sec4p then promotes actin polymerization and triggers compensatory endocytosis, which controls surface expansion and kinetically refines cell polarization.

4.2. Introduction

In specific secretory cell types, endocytosis compensates for the expansion of cell surface area caused by vesicular transport to the plasma membrane (PM) (Schafer, 2003). The coupling of endocytosis with exocytosis controls membrane expansion in Xenopus oocytes during cortical granule exocytosis (Anna Marie Sokac et al., 2003), and after vesicle transport to the PM in both neurons and non-neuronal cells (Gundelfinger, Kessels, & Qualmann, 2003). In polarized cell types, polarized exocytosis is also linked to a reciprocal endocytic event where membrane traffic to-and-from adherens junctions maintain epithelial apical-basal polarity by recycling junctional proteins (Mara C. Duncan & Peifer, 2008). These examples raise the more general question of whether cycles of exocytosis and endocytosis are directly coupled in all cell types.

In *Saccharomyces cerevisiae*, the first indication that vesicular transport to-and-from the PM is coupled was the finding that mutations in late secretory (*SEC*) genes, required for the final stages of exocytosis, also disrupt uptake of lucifer yellow by endocytosis (Riezman, 1985). More puzzling was the finding that *SEC* genes required for earlier events in exocytosis had weak or variable effects on endocytic uptake, suggesting that any block in exocytosis does not result in a commensurate inhibition of endocytosis. Although there are notable exceptions in which early *SEC* mutants do impact endocytosis (S. Y. Carroll et al., 2012; Jose et al., 2015; Payne et al., 1988), a recent phenomics analysis of trafficking mutants generally supports the notion that the late stage of exocytosis is particularly important for regulating endocytosis (Jose et al., 2015). Specifically, the exocyst complex, which tethers post-Golgi vesicles to the PM during exocytosis, was described as a "network hub" for coordinating the two trafficking pathways at the cell surface (Jose et al., 2015). These results suggest the possibility of a direct regulatory mechanism for integrating the late stages of post-Golgi exocytosis with endocytic internalization.

Like other late *SEC* genes, *SEC4* appears to affect both exocytosis and endocytosis (Riezman, 1985). *SEC4* encodes a Rab GTPase that moves with exocytic vesicles along actomyosin cables from the Golgi to sites of polarized growth on the PM

within the budding daughter cell (Boyd et al., 2004; D. H. Schott et al., 2002). The dynamic movement of GFP-Sec4p particles during exocytosis has been tracked in living cells and involves two distinct patterns of motion: the first corresponds to the actomyosin-directed polarized transport of vesicles into the bud; the second follows membrane fusion of exocytic vesicles with the PM, during which GFP-Sec4p particles dwell briefly at the cell cortex making small random movements before disappearing (Donovan & Bretscher, 2015; D. H. Schott et al., 2002). At first glance, Sec4p and its regulation of exocytosis appears to be completely independent from mechanisms controlling endocytosis. Given that the GDP dissociation inhibitor Gdi1p mediates Sec4p removal from the PM and trafficking back to the Golgi, even the recycling and internalization of Sec4p does not require endocytosis (Calero et al., 2003; C. Z. Chen et al., 2004; Garrett et al., 1994). Nonetheless, it has been shown that Sec4p localizes to recycling endomembranes involved in establishing cell polarization (Mukherjee et al., 2013). This result hints that Sec4p might have an involvement in some aspect of endocytosis, apart from its established role in polarized exocytosis.

In budding yeast, the polarized sites where exocytic vesicles dock at the PM partially overlap with nascent sites of endocytosis, which correspond to cortical actin patches (Adams & Pringle, 1984; Goode, Eskin, & Wendland, 2015; Kilmartin & Adams, 1984). The maintenance of polarized growth at these sites is dependent on both polarized exocytosis and endocytosis (Valdez-Taubas & Pelham, 2003). Classic yeast ultrastructural studies showed that exocytic vesicles are in close proximity to cortical actin but do not directly associate (Adams & Pringle, 1984; Kilmartin & Adams, 1984). However, as polarized cell growth proceeds during the yeast cell cycle, exocytic docking sites and actin patches relocate in lockstep; first from the incipient bud site in unbudded cells to the bud tip in small-budded cells, then around the entire bud cortex in medium-budded cells, and finally to the mother/bud neck in large-budded cells. Even though exocytic vesicles do not directly interact with nascent sites of endocytosis, a specific regulator of exocytosis (like Sec4p) could laterally diffuse through the PM to interact with endocytic components at actin patches.

The generation of cortical actin patches for endocytic membrane internalization involves a series of distinct events, each punctuated by the formation and

dissolution of specific protein complexes (Goode et al., 2015). The duration of the initiating event is variable and relatively long (~1-2 min), which might represent a stochastic activation. During this phase, early coat proteins such as clathrin, Ede1p, and Syp1p are recruited and computational modeling suggests that the packaging of membrane cargo helps drive this event forward (Jose, Tollis, Nair, Sibarita, & McCusker, 2013; Layton et al., 2011). Over the next 20-30 s, Sla1p, Sla2p, and Las17p are recruited during the slow coat assembly phase, which lays the groundwork for the subsequent dynamic phase of actin network assembly (Goode et al., 2015). Sla1p and the yeast HIP1r homolog Sla2p represent conserved clathrin adaptors, whereas Las17p is the yeast Wiskott-Aldrich syndrome protein (N-WASp) homolog (Feliciano & Di Pietro, 2012; Goode et al., 2015; R. Li, 1997; Moseley & Goode, 2006). Las17p is a potent activator of Arp2/3-dependent actin polymerization, but it is kept inactive during this period in part by an inhibitory interaction with Sla1p (Feliciano & Di Pietro, 2012). In this way, Sla1p plays dual roles during endocytic internalization where it acts both an activator required for coat assembly and an inhibitor by regulating the timing of subsequent steps in actin patch maturation (Feliciano & Di Pietro, 2012; Moseley & Goode, 2006; A. A. Rodal et al., 2003). The regulatory mechanism that frees Las17p from Sla1p inhibition is unknown, but it represents a key transitional mechanism for unleashing the rapid sequence of final events. In effect, this pause helps coordinate the completion of coated pit maturation with the onset of actin nucleation. Finally, during the next actin patch assembly phase, the inward force for membrane internalization is provided. This step is characterized by rapid patch dynamics, as reflected in the motility of Abp1p (Marko Kaksonen, Toret, & Drubin, 2005), a mediator of Arp2/3-dependent F-actin branching (Goode, Rodal, Barnes, & Drubin, 2001). Inward PM deformation is quickly followed by membrane scission, which completes membrane internalization and the biogenesis of endocytic vesicles.

Here we investigate if a direct regulatory mechanism exists to integrate polarized exocytosis with endocytosis. We show that the polarized delivery of Sec4p regulates the stage-specific assembly of actin patches by promoting actin polymerization. In addition to being a well-established regulator of exocytosis, Sec4p met all the expectations for a regulator of endocytosis: (*i*) Sec4p transiently localized to endocytic sites at a specific period during their formation; (*ii*) *SEC4* mutations disrupted

actin patch assembly; (*iii*) Sec4p physically interacted *in vitro* and *in vivo* with Las17p, which is required for cortical actin nucleation; (*iv*) in the presence of Las17p and Sla1p, Sec4p induced Arp2/3-dependent actin polymerization in vitro; (*v*) Sec4p polarization led to the polarized assembly of actin patches. These results indicated that Sec4p overrides a limiting step in actin patch formation and thereby directly couples transport cycles to-and-from the cell cortex.

4.3. Results

4.3.1. Sec4p is Recruited to Nascent Cortical Actin Patches to Promote Their Assembly

Targeting and docking of exocytic vesicles to the PM is mediated by the multi-protein exocyst complex. Sec4p anchors a subset of exocyst complex subunits, including Sec5p, to the vesicle membrane (Guo et al., 1999). Even though Sec4p and Sec5p travel together to the PM (Boyd et al., 2004), we observed that at the cortex the actin patch marker Sla1p-RFP co-localized 4-times more often with GFP-Sec4p particles than with Sec5p-3xGFP particles ($N > 340$; $p < 0.0001$). This result suggested a link between Sec4p and nascent sites of endocytosis as defined by actin patches, distinct from other subunits of the exocyst complex and exocytic vesicles. However, there are several criteria to be met if Sec4p is proposed to play a direct role coordinating actin patch assembly with its established role during the late stages of exocytosis. First, because of the hierarchal addition of actin patch subunits, if Sec4p is a direct regulator of patch assembly it must exhibit both a specific spatial and temporal co-localization with nascent endocytic sites. Second, as read-outs of actin nucleation and network formation at patches, actin patch dynamics and/or morphology would be disrupted as a result of a genetic defect in any regulator of endocytic internalization. If Sec4p co-ordinates endocytic internalization with exocytosis, then we also predict that Sec4p motility at the PM would be affected by defects in actin patch assembly and vice versa. If Sec4p represents the mechanism by which polarized exocytosis promotes actin patch polarization, then changes in Sec4p activity and distribution would be predicted to affect the asymmetric formation of actin patches within budding cells. Finally, a direct role in

endocytic internalization necessitates that Sec4p physically interacts with specific actin patch subunits to regulate a particular mechanistic event during patch assembly.

As both a test of our criteria and to establish if Sec4p directly regulates endocytosis, GFP-Sec4p localization at the PM was analyzed and the effect of inactivating *SEC4* on actin patch assembly was examined. Because of the fleeting nature of actin patch dynamics, the temporal and spatial overlap between GFP-Sec4p and actin patches was most evident when individual GFP-Sec4p particles were tracked on the cell cortex (Fig. 4.1). The GFP-Sec4p fusion construct used for these analyses is an established reporter of Sec4p in yeast, as shown by immunofluorescence and immunoelectron microscopy (D. H. Schott et al., 2002). Nevertheless, individual GFP-Sec4p particles are difficult to visualize in living cells because of the continuous transport of exocytic vesicles to the PM, where GFP-Sec4p appears at the bud cortex as a "churning mass" (D. H. Schott et al., 2002). To track individual GFP-Sec4p particles, we focused our analysis on medium-to-large budded cells in which GFP-Sec4p particles were less densely distributed on the PM. We also used fluorescence photobleaching to track newly transported GFP-Sec4p particles on the cell cortex (Movie S1). In these experiments, actin patch assembly and vesicle trafficking, which are inherently read-outs of cell growth, continued as normal. Moreover, there were no adverse effects on cell viability even when the laser intensity and the duration of photobleaching were both increased 10-fold beyond that used in these experiments (see Materials and Methods). For all fluorescent markers tested (GFP-Sec4p, and Abp1p-, Sla1p-, and Las17p-RFP), particle lifetimes were equivalent in photobleached cells as compared to those that were not (by one-way analysis of variance at a 95% confidence limit; $N \geq 36$ cells). Thus, both the photobleaching conditions and the GFP-Sec4p reporter itself were suitable for examining dynamic associations between individual GFP-Sec4p particles and assembling actin patches.

Figure 4.1. Spatial and temporal co-localization of Sec4p with actin patch subunits during actin patch assembly.

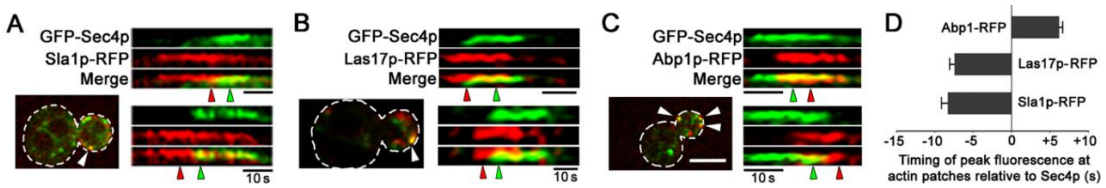

A-C. Images of wild-type cells (WT; BY4741) showing the co-localization (arrowheads) of newly transported GFP-Sec4p particles after FRAP with Sla1p-, Las17-, and Abp1-RFP (bar = 2 μm). Duplicate examples of kymographs are shown comparing the relative timing of GFP-Sec4p co-localization with each actin patch subunit. For each kymograph shown, green (GFP-Sec4p) and red (RFP fusions) arrowheads indicate maximum voxel fluorescence intensities. **D.** Bar graph reporting average differences in time for the maximum fluorescence of each RFP-marked actin patch subunit relative to GFP-Sec4p (N = 22 particles/strain; kymographs from ≥ 11 independent cells). In all graphs, data is shown as mean values with error bars representing S.E.M. Experiments were conducted by J.J

To analyze GFP-Sec4p particles during endocytic site formation, GFP-Sec4p was visualized by confocal fluorescence microscopy relative to the defined timing of subunit recruitment during actin patch assembly (Goode et al., 2015; Marko Kaksonen et al., 2005). After their transport into photobleached zones at the bud cortex, > 64% of individual GFP-Sec4p particles co-localized with Abp1p-, Sla1p-, and Las17p-RFP foci (N > 90). Kymograph analysis of GFP-Sec4p localization during actin patch assembly also showed an invariant timing; Sec4p always associated after Sla1p and Las17p recruitment, and then Sec4p disappeared immediately following the arrival of Abp1p (Fig. 4.1A-D, Movies S2-S4). In short, this analysis showed that Sec4p and proteins involved in endocytic internalization concurrently localize during a specific stage in actin patch assembly.

The functional significance of Sec4p co-localization with Abp1p, Sla1p, and Las17p was apparent when analyzing characteristic properties of actin-patch assembly in a *SEC4* conditional mutant. The dynamics and morphology of actin patches provide several experimental read-outs for the kinetic events before and during cortical actin polymerization that ultimately result in PM internalization (Marko Kaksonen et al., 2005): (*i*) subunit lifetimes indicate proper recruitment and turnover of actin patch components involved in endocytic site formation; (*ii*) as measured by particle velocity, the rapid motility of Sla1p and Abp1p provide a read-out for active actin polymerization during initial membrane invagination and inward membrane internalization, respectively; (*iii*) the

density of actin patches is also a measure of proper subunit recruitment and stability of the internalization machinery; (*iv*) Abp1p accumulation on “actin comets” also indicates morphological defects in cortical actin organization. At 23˚C, polarized exocytosis is unaffected in *sec4-8*^{ts} cells and comparable to wild type (Harsay & Bretscher, 1995). However, after incubation at 37˚C for 60 min, the *sec4-8*^{ts} mutation disrupts polarized exocytosis (Harsay & Bretscher, 1995). Using the motility and lifetime of actin patch components as readouts, we found that after the temperature shift the formation of endocytic sites in these cells was also affected (Fig. 4.2, Movie S5); measured defects in actin patch dynamics in *sec4-8*^{ts} cells matched in magnitude the defects observed in established endocytosis mutants (Marko Kaksonen et al., 2005). At 37˚C, Sla1p-RFP- and GFP-Abp1p-marked actin patches persisted 1.6- and 2-fold longer in *sec4-8*^{ts} cells than in wild type, respectively (Fig. 4.2A, B). Even as early as 30 min after the temperature shift to 37˚C, statistically significant increases in Sla1p-RFP and GFP-Abp1p lifetimes ($p < 0.0001$; N = 55 cells) were detectable in *sec4-8*^{ts} cells. Actin patch dynamics and the timing of subunit recruitment were also defective in *sec4-8*^{ts} cells. In *sec4-8*^{ts} cells incubated at 37˚C for 60 min, the recruitment of GFP-Abp1p to nascent actin patches was delayed 3-fold after Sla1p-RFP was first detected, relative to what was observed in wild-type cells (Fig. 4.2A), and the dynamic movement of GFP-Abp1p along the PM was 44% slower (Fig. 4.2C). Because Sec4p GTPase activation requires its GEF, Sec2p, we also tested if actin patches are affected in *sec2-41*^{ts} cells. Like *sec4-8*^{ts} cells, Sla1p-RFP lifetime (Fig. 4.2B) and GFP-Abp1p motility (Fig. 4.2C) were also disrupted in *sec2-41*^{ts} cells at 37˚C. Moreover, the overall density of actin patches in buds declined in both *SEC4* and *SEC2* mutant cells. For *sec2-41*^{ts} and *sec4-8*^{ts} cells incubated at 37˚C, there was a > 70% reduction in GFP-Abp1p particles and > 50% fewer Sla1p-RFP particles within buds as compared to wild type (Fig. 4.2D). These reductions in actin patch dynamics and density within buds clearly establish that Sec4p and its regulator Sec2p affect the proper formation of endocytic sites.

Figure 4.2. Mutations in *SEC4* and *SEC2* disrupt actin patches assembly and proper endocytic internalization.

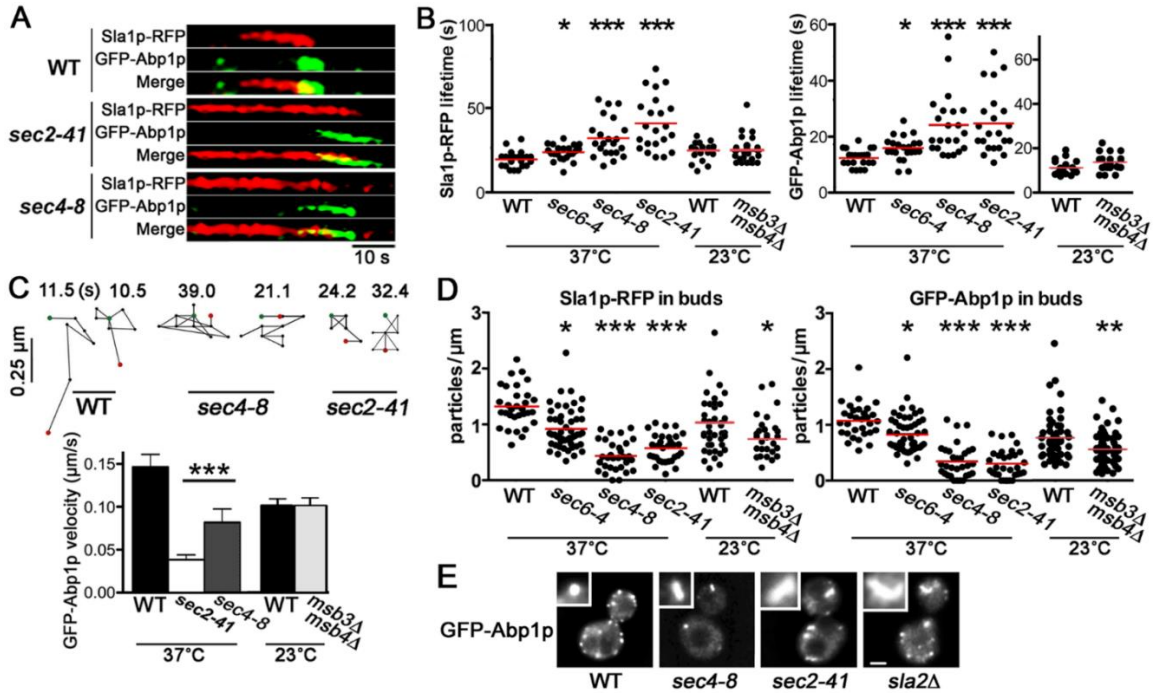

A. Kymographs show coincident localization of single Sla1p-RFP and GFP-Abp1p particles during actin patch assembly in buds from WT (BY4741), *sec2-41* (CBY4710) and *sec4-8* (CBY4711) cells incubated at 37˚C for 60 min. **B.** Scatterplots quantifying increased average lifetime of individual Sla1p-RFP and GFP-Abp1p particles in *sec4-8* and *sec2-41* cells relative to WT, with modest lifetime increases in *sec6-4* (CBY4712) cells, and no change detected in *msb3*Δ *msb4*Δ cells (CBY1981). **C.** Two representative tracings of GFP-Abp1p particles moving at the cell cortex in WT, *sec4-8*, and *sec2-41* cells at 37˚C, as tracked using confocal video microscopy (green and red dots mark the first and last positions of the particles, respectively); tracings are oriented so that the bud cortex is up and the cell interior is down. Differences between positions (black dots) are 1 s and total elapsed times are shown above each tracing and, below, the average velocities for GFP-Abp1p particles are plotted in the bar graph (N > 50 tracings). **D.** Scatterplots show total numbers of GFP-Abp1p and Sla1p-RFP particles in buds of *sec6-4*, *sec4-8* and *sec2-41* cells relative to WT after incubation at 37˚C, and in buds of *msb3*Δ *msb4*Δ and WT cells (N > 20 buds). **E.** Representative actin patch internalization defects observed in *sec4-8*, *sec2-41*, and *sla2*Δ (CBY4863) cells as shown by Abp1p-GFP “comet tails” (inserts), compared to Abp1p-GFP spots in WT (bar = 2 µm). Unless stated otherwise, for all plots statistical differences relative to congenic WT control strains are shown by single, double, and triple asterisks indicating $p < 0.05$, 0.0015, and 0.0001, respectively. Panel C was conducted by G.A the remainder was performed by J.J

Similar to what is seen in actin patch mutants, the morphology of actin patches was also aberrant in *SEC4* and *SEC2* mutant cells. In *sla2*Δ cells, for instance, instead

of normal punctate GFP-Abp1p-marked actin patches, “comet tails” are observed when nucleated actin protrudes into the cytoplasm (Marko Kaksonen, Sun, & Drubin, 2003). Although the deletion of *SLA2* results in a greater number of larger actin comets, we detected small comets in 31% of *sec4-8*^{ts} cells and 48% of *sec2-41*^{ts} cells at 37˚C, as compared to 88% of *sla2*Δ cells and 0% of wild-type cells (N > 70) (Fig. 4.2E). All told, as indicated by defects in actin patch dynamics and morphology, the proper formation of endocytic sites requires Sec4p and its GEF, Sec2p.

A rapid onset of actin patch assembly defects has also been reported for temperature-conditional *SEC* mutants after incubation at elevated temperatures (S. Y. Carroll et al., 2012; Riezman, 1985). To determine the specificity of *SEC4* and *SEC2* effects on actin patches, we tested Sla1p and Abp1p dynamics in another late-acting *SEC* mutant. In *sec6-4*^{ts} cells, containing a conditional mutation in the Sec6p exocyst complex subunit, there was a minor 1.2-fold and 1.3-fold increase in GFP-Abp1p and Sla1p-RFP particle lifetimes, respectively, relative to wild type after incubation at 37˚C for 60 min (Fig. 4.2B). Although Sec2p affects Sec4p activity in endocytosis, other regulators of Sec4p affect its role during exocytosis but not endocytosis. Several genes encode Sec4p GAPs (GTPase-Activating Proteins) including *MSB3* and *MSB4*, and the combined deletions of *MSB3* and *MSB4* disrupt polarized exocytosis by affecting the GTP/GDP-cycle of Sec4p (Gao et al., 2003). However, actin patch assembly was unaffected in *msb3*Δ *msb4*Δ cells given that GFP-Abp1p motility and Sla1p-RFP/GFP-Abp1p lifetimes were relatively normal (though patch depolarization was observed [see below]) (Fig. 4.2B-D). These findings suggested that among genes required for polarized exocytosis, *SEC4* and *SEC2* have a specific role in actin patch assembly.

4.3.2. Sec4p Interacts *in vitro* and *in vivo* With Actin Patch Subunits

The close temporal and spatial relationship between Sec4p and actin patch subunits, Las17p in particular, suggested a possible direct physical interaction. Indeed, radiolabeled Las17p synthesized in a cell-free transcription/translation system directly interacted *in vitro* with GTPγS-bound GST-Sec4p, expressed and purified from bacteria (Fig. 4.3A). GST-Sec4p binding to Las17p was enhanced 2.8 fold in the presence of

GTPγS as compared to GDP. In negative control assays, Las17p did not bind to GST or GST-Ypt1p, whether or not GTPγS or GDP was added. Because Ypt1p is an ER/Golgi-localized small GTPase and a close Sec4p sequence homolog, we conclude that the interaction between Las17p and Sec4p represents a specific association. Using the same binding conditions, we failed to detect an interaction between bacterially expressed GST-Sec4p and *in vitro* translated Sla1p. These findings indicated that Sec4p specifically and directly interacts with Las17p in vitro.

Figure 4.3. Physical interaction of Sec4p with actin patch subunits.

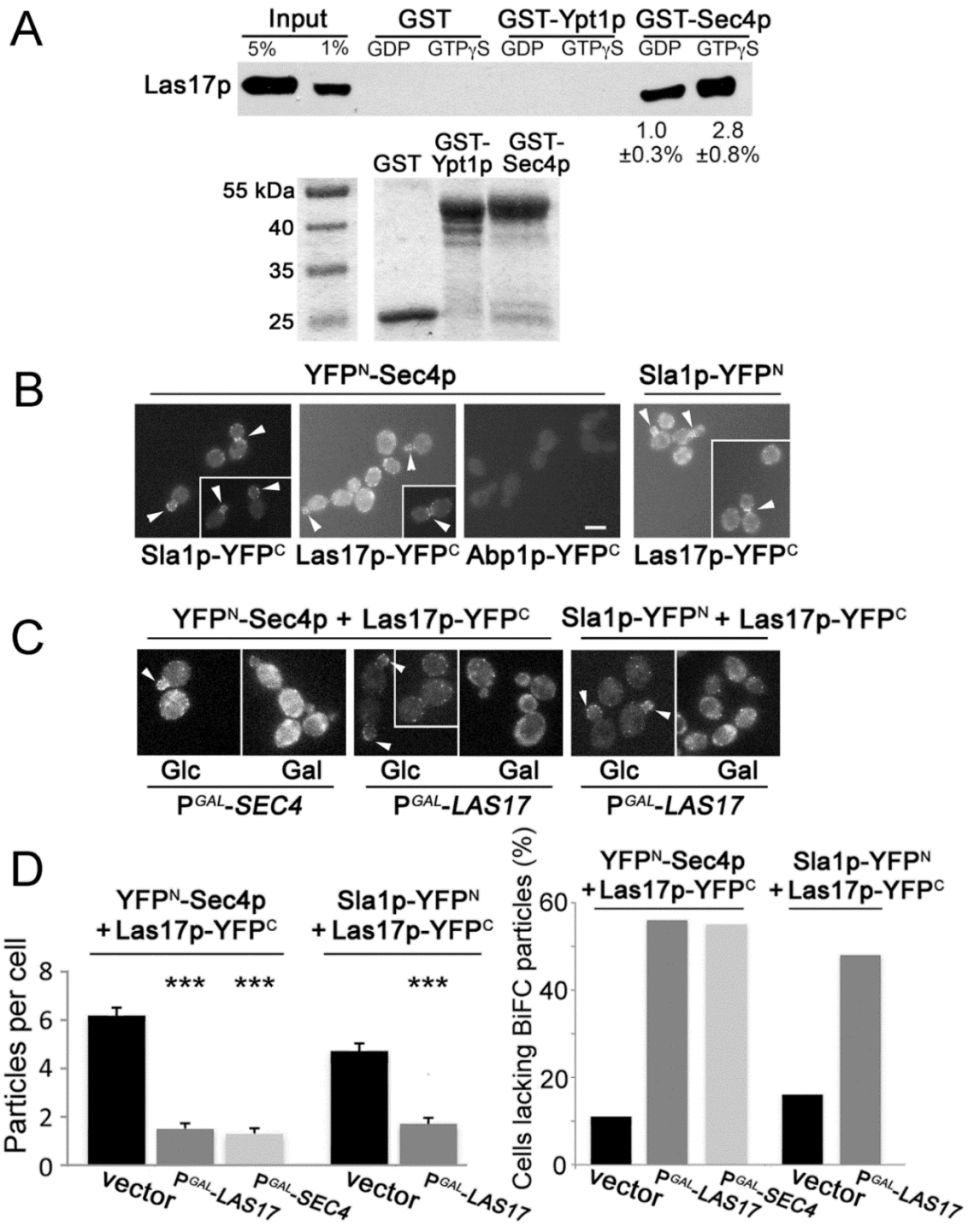

A. Top panel: representative *in vitro* binding assay showing *in vitro* transcribed and translated ^{35}S-Las17p binding to bacterially expressed GST-Sec4p purified and immobilized on beads prior to SDS-PAGE and autoradiography. Average percentage of input Las17p interacting with GDP- or GTPγS-bound GST-Sec4p as shown (N = 3). Bottom panel: SDS-PAG showing equal amounts (1 µg) of GST-Sec4p, GST and GST-Ypt1p preloaded with GDP or GTPγS prior to ^{35}S-Las17p addition. **B.** BiFC assays for cells expressing Sla2p-YFP^{N} (CBY4625) or YFP^{N}-Sec4p (CBY4629) when mated with cells expressing Las17p-YFP^{C} (CBY4660), Sla2p-YFP^{C} (CBY4661), or Abp1p-YFP^{C} (CBY4632). Fluorescence at the cell cortex (arrowheads) indicates *in vivo* interactions at actin patches (bar = 5 µm). **C.** Competition of BiFC binding following overnight P^{GAL}-*LAS17* induction or 6 h P^{GAL}-*SEC4* induction with galactose (Gal), compared to no induction in glucose (Glc) medium, in cells expressing YFP^{N}-Sec4p and Las17p-YFP^{C} (CBY4638). In all cells observed (including controls), non-specific cytoplasmic fluorescence increased after transfer to galactose-containing medium. **D.** Bar graphs quantifying reductions in BiFC particles within cells corresponding to images shown in panels **B** and **C** (N > 100 cells). Experiments were conducted by J.J

To determine if the Sec4p/Las17p *in vitro* binding is relevant in vivo, Sec4p interactions with actin patch subunits were visualized in living cells by bimolecular fluorescence complementation (BiFC) assays (Kerppola, 2008; Miller, Kim, Huh, & Park, 2015) (Fig. 4.3B-D). In BiFC, putative interaction partners are fused with non-functional halves of a fluorescent protein (*i.e*. YFP-Venus) and if they associate in a complex within ~50 Å of each other, the fused YFP^{N} amino- and YFP^{C} carboxy- halves reconstitute an intact fluorescent protein (Kerppola, 2008). Consistent with previous findings (R. Li, 1997), co-expression of Las17p-YFP^{N} and Sla1p-YFP^{C} generated fluorescence at cortical actin patches in all cells counted (N = 100), indicative of a Las17p/Sla1p interaction (Fig. 4.3B). This same fluorescent distribution was seen in all cells (N = 100) when YFP^{N}-Sec4p was co-expressed with Las17p-YFP^{C} or Sla1p-YFP^{C} (Fig. 4.3B, D). None of the fusion proteins generated fluorescence when expressed alone. Because YFP^{N}-Sec4p co-expression in cells with Abp1p-YFP^{C} also produced no fluorescence (N = 100 cells), we conclude that Sec4p does not interact with just any actin patch subunit, even if they briefly co-localize (Fig. 4.3B, D). The YFP^{N}-Sec4p BiFC interaction with Las17p-YFP^{C} was competed away by increased expression of wild-type Las17p or Sec4p (Fig. 4.3C, D). P^{GAL}-*LAS17* or -*SEC4* overexpression reduced the number of YFP^{N}-Sec4p/Las17p-YFP^{C} particles, comparable to the competition observed of Las17p-YFP^{N}/Sla1p-YFP^{C} BiFC interaction upon P^{GAL}-*LAS17* overexpression (Fig. 4.3C, D). As confirmed by BiFC assays, both *in vivo* and *in vitro* binding experiments indicated that Sec4p associates with the actin-patch coat complex by a direct interaction with Las17p.

4.3.3. Actin Patch Subunits Have Reciprocal Effects on Sec4p and Polarized Exocytosis

If Sec4p regulates exo- and endocytosis in a coupled cycle, then we predicted that mutations disrupting endocytosis would have a corresponding impact on Sec4p dynamics, activity, and/or expression. Having established that *SEC4* mutations affect Sla1p and Abp1p dynamics we tested the reciprocal, namely, whether GFP-Sec4p motility is affected by actin patch defects. In wild-type cells, the vectorial path of GFP-Sec4p changes when it arrives in the bud, making brief translational movements along the PM before disappearing (Donovan & Bretscher, 2015; D. H. Schott et al., 2002). We conducted photobleaching experiments on medium- and large-sized buds in endocytosis mutants to track individual GFP-Sec4p particles by three-dimensional time-lapse (4D) confocal microscopy (Fig. 4.4). Specifically, we examined mutants that disrupted *BBC1* (myosin-interacting SH3 domain protein), *LAS17*, *RVS167* (amphiphysin homolog), or *SLA2* (Moseley & Goode, 2006). In general, we found an inverse correlation between GFP-Sec4p particle lifetimes and particle motility in these mutants. For most these mutants, GFP-Sec4p particles persisted longer but remained static. In both *rvs167*Δ cells and *sla2*/*end4-1*^{ts} cells, GFP-Sec4p particle velocity was reduced by more than half as compared to wild type, whereas the velocity of GFP-Sec4p actually increased 67% in *bbc1*Δ cells (Fig. 4.4A), which is consistent with the inhibitory role of Bbc1p on Las17p-dependent actin polymerization (A. A. Rodal et al., 2003). At 37˚C, moderate velocity decreases were also evident in *las17-1*^{ts} and *-13*^{ts} cells (Fig. 4.4A). To our surprise, in *las17*Δ cells grown at 30˚C or in *las17-14*^{ts} cells shifted to 37˚C for 60 min, GFP-Sec4p membrane localization was completely disrupted (Fig. 4.4B). In *las17-1*, *las17-13*, and *sla2/end4-1*^{ts} cells GFP-Sec4p particle lifetime increased by > 50%, whereas it remained unchanged in *rvs167*Δ cells, and decreased by 53% in *bbc1*Δ cells. As an additional assay of to test how polarized exocytosis and endocytosis are inter-connected, Bgl2p secretion was analyzed in endocytosis-defective cells (Fig. 4.4C). Bgl2p serves as a marker for polarized exocytosis because its vesicular transport is targeted to sites of polarized growth from where it is secreted out of the cell (Harsay & Bretscher, 1995). As shown for *sec6-4*^{ts} cells grown at 37˚C, Bgl2p accumulated internally when polarized exocytosis is blocked (Fig. 4.4C). Likewise, Bgl2p exocytosis was inhibited in *las17*Δ, *las17-13*, and *sla2*Δ endocytosis mutants. Because the endocytosis defect in *rvs167*Δ

cells is relatively weak (Lombardi & Riezman, 2001), we predicted that any coupled defect in exocytosis would also be weak. Consistent with this prediction, no Bgl2p secretion defect was detected in *rvs167*Δ cells (Fig. 4.4C). Overall these results support the conclusion that polarized exocytosis and endocytosis constitute a coupled transport cycle in budding yeast.

Figure 4.4. Reciprocal effects of endocytosis on polarized exocytosis.

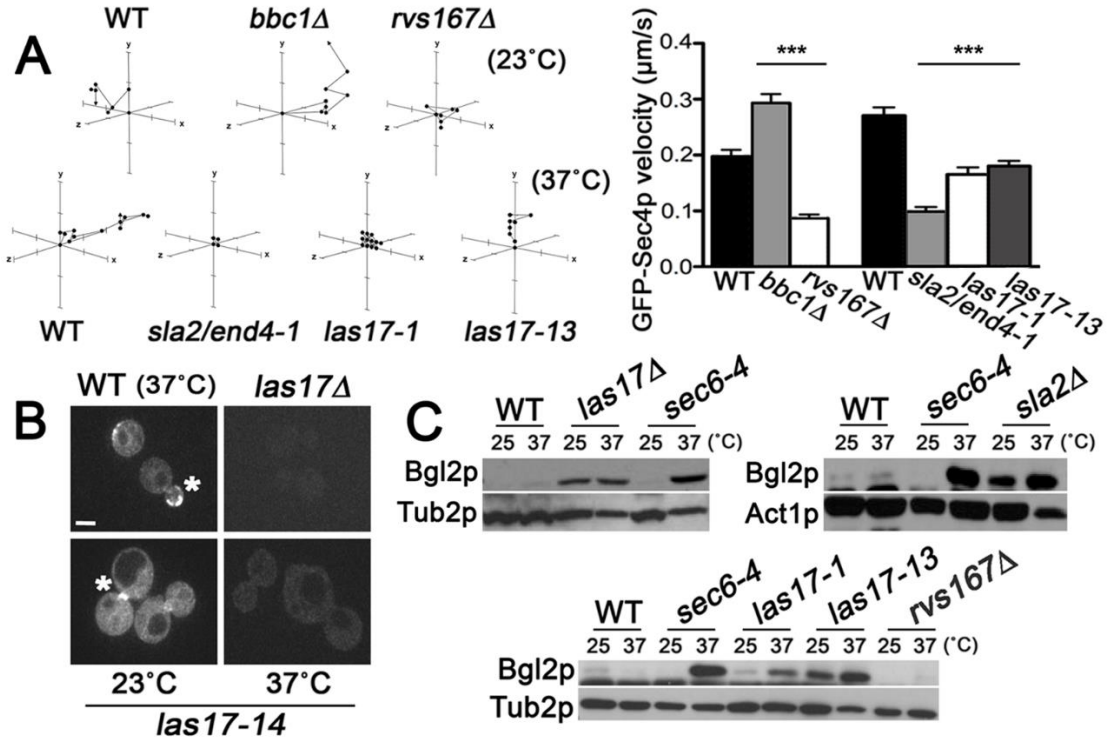

Sec4p motility is dependent on actin patch assembly. **A.** Representative tracings from three-dimensional time-lapse confocal microscopy showing GFP-Sec4p movement after its transport into photobleached zones at the bud cortex in *las17-1*^{ts} (CBY4356), *las17-13*^{ts} (CBY4357), *rvs167*Δ (CBY4733), *bbc1*Δ (CBY4373), *sla2/end4-1*^{ts} (CBY4452) endocytosis-defective cells, relative to WT (CBY4741). Temperature-conditional mutations were incubated at 37˚C for 2 h, whereas motility in deletion mutants was assessed at 23˚C. On each axis, 0.5 µm intervals are indicated. The bar graph quantifies GFP-Sec4p particle motility at the PM for each strain (N > 30 particles). **B.** Images of GFP-Sec4p localization at sites of polarized growth (asterisk) in WT (BY4741), *las17*Δ (CBY1024), and *las17-14* (CBY4358) cells. Under these conditions, GFP-Sec4p was not detected on any membrane in *las17*Δ cells grown at 30˚C (as shown), or in *las17-14* cells incubated at 37˚C for 2 h (bar = 2 µm). **C.** Immunoblots assaying Bgl2p polarized exocytosis showing defective Bgl2p internalization in *sla2*Δ (DDY1980), *las17*Δ (DDY1709), *las17-13* (CBY4357), *las17-1* (CBY4356) endocytosis mutants, compared to the *sec6-4* exocytosis-defective control (NY17) and congenic WT strains (BY4741 and DDY130). Bgl2p exocytosis was not defective in *rvs167*Δ cells (CBY4372). The same blots were probed for tubulin (Tub2p) or actin (Act1p) as internal loading controls. Panel A and B were conducted by G.A while panel C was conducted by K.K

4.3.4. Sec4p Polarization Affects Actin Patch Polarization

Actin patches are predominantly associated with PM regions surrounding sites of polarized growth (D. Pruyne & Bretscher, 2000). The proximity of actin patches to these sites helps maintain the polarized distribution of proteins in buds by recycling them before they diffuse throughout the membrane into the mother cell (Jose et al., 2013; Valdez-Taubas & Pelham, 2003). In *sec2-41*^{ts} and *sec4-8*^{ts} cells at 37˚C, the density of actin patches within buds sharply declined (Fig. 4.2D) but, as observed by confocal microscopy, the total number of Sla1p- and Abp1p-RFP particles in both mother cells and their buds was equivalent to that in wild-type cells (an average of 8.4 – 9.9 particles/cell; N = 50). To determine if this discrepancy reflects a change in actin patch polarization, we analyzed the ratio of actin patches within buds relative to those within mother cells in *SEC4* and *SEC2* mutants. In *sec4-8*^{ts} and *sec2-41*^{ts} cells incubated at 37˚C for 60 min, the bud-to-mother ratio of Sla1p-RFP and GFP-Abp1p was at least 10-fold less than in wild-type cells, indicating a significant loss in actin patch polarization (Fig. 4.5A). If Sec4p polarization promotes the polarization of endocytic sites, we predicted that distributing Sec4p more uniformly around the PM would have the opposite effect and cause actin patch depolarization. As previously described, *msb3*Δ *msb4*Δ mutations affect Sec4p activity during exocytosis but combined they have modest effects on actin patch assembly and motility (Fig. 4.2C-E). Nonetheless, we observed in *msb3*Δ *msb4*Δ cells that GFP-Sec4p localization spread beyond the bud and was distributed more evenly along the mother cell PM (Fig. 4.5B). We exploited this finding to determine how Sec4p depolarization affected actin patch polarization. In these cells, Sec4p depolarization correlated with a loss in Sla1p-RFP and GFP-Abp1p asymmetry where there was a ~3-fold reduction in the normal cluster of particles in buds versus mother cells (Fig. 4.5C). Because Msb3/4p are GAPs for some Rab GTPases other than Sec4p (Albert & Gallwitz, 2000; Walworth et al., 1992), we tested if Sec4p depolarization by another mechanism would also result in actin patch depolarization. The *sec4-Q79L* mutation mimics a Ras oncogenic mutation that lowers intrinsic GTPase activity and shifts more of the protein into the activated GTP-bound form, similar to what is predicted when Sec4p GAPs are deleted (Lachmann, Barr, & Ungermann, 2012). It is important to

note that the *sec4-Q79L* mutation only affects exocytosis if cells are incubated for prolonged periods (24 h) at 13˚C (Lachmann et al., 2012). Despite its modest effects on exocytosis, the activated *sec4-Q79L* mutation had significant effects on actin patches even at normal growth temperatures. In all cells observed (N = 100), GFP-sec4-Q79Lp on the PM was depolarized into the mother cell (Fig. 4.5D), and in *sec4-Q79L* cells, a corresponding depolarization of the actin patch subunits Sla1p and Abp1p was observed (Fig. 4.5E). To determine if the depolarization of actin patches in *sec4-Q79L* cells impacts the polarized recycling of endocytic cargo, we analyzed the distribution of RFP-Snc1p. Snc1p is an exocytic SNARE protein that is immediately recycled after polarized exocytosis via endocytosis (Lewis, Nichols, Prescianotto-Baschong, Riezman, & Pelham, 2000). In 93% of wild-type cells (N = 100), RFP-Snc1p is concentrated at the PM in small and medium buds with little or no fluorescence in mother cells (Fig. 4.5F). In *sec4-Q79L* cells, some increase in internal RFP-Snc1p was observed but in a majority of these cells (87%; N = 100) the fluorescence was depolarized, where RFP-Snc1p was localized on the PM in mother cells on the side opposite from the bud (Fig. 4.5F). In *msb3*Δ *msb4*Δ cells, internal GFP-Snc1p accumulation obscured assessment of its depolarization at the PM. Nonetheless, these findings suggested that the polarized enrichment of actin patches and endocytic cargo within buds is dependent on Sec4p polarization.

Figure 4.5. Actin patch polarization is affected by Sec4p polarization.

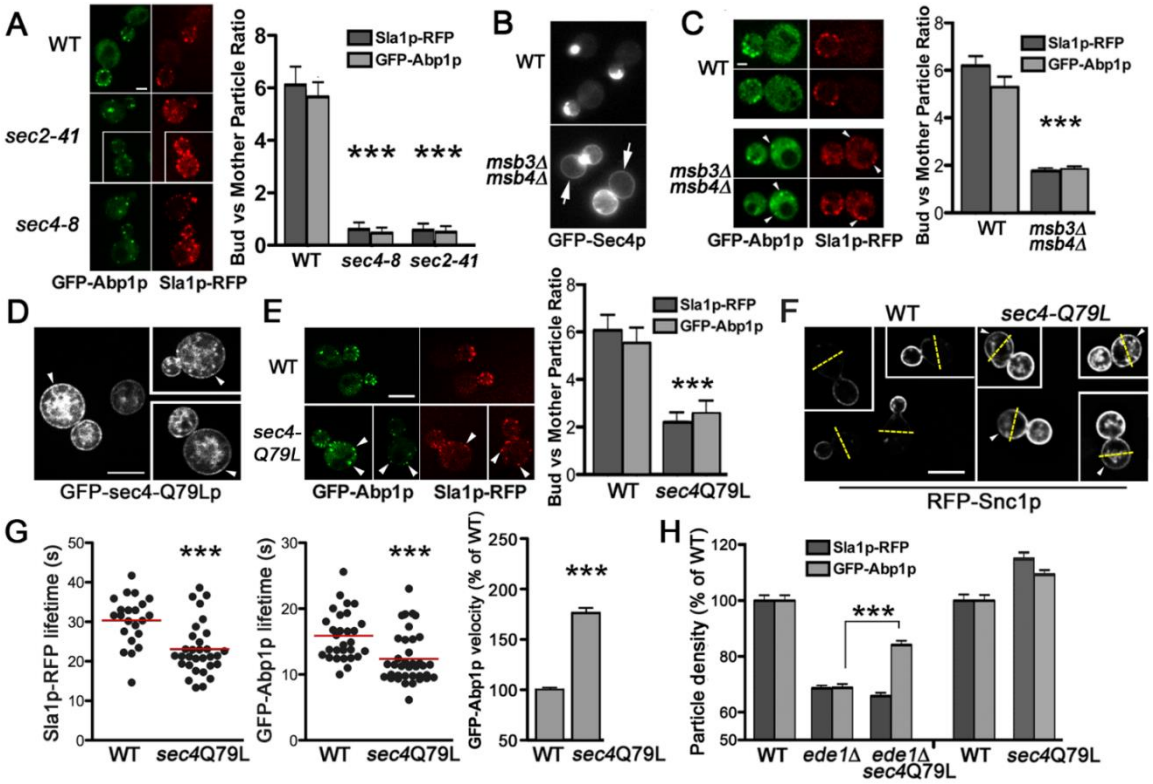

A. Deconvolved medial images of Sla1p-RFP and GFP-Abp1p in WT (BY4741), *sec4-8*^{ts} (CBY4711), and *sec2-41*^{ts} (CBY4710) cells incubated at 37˚C for 60 min as acquired by confocal microscopy (bar = 2 µm). Ratios of Sla1p-RFP and GFP-Abp1p localization in buds versus mother cells for WT, *sec4-8*^{ts}, and *sec2-41*^{ts} cells are quantified in the bar graph (N > 50). **B.** Images of GFP-Sec4p fluorescence in WT (BY4741) and the corresponding depolarized GFP-Sec4p in *msb3*Δ *msb4*Δ (CBY1980) cells. GFP-Sec4p is dispersed around the bud and mother cell cortex (arrows) in 78% of *msb3*Δ *msb4*Δ cells compared to 0% in WT (N > 100). **C.** Images from a wide-field fluorescence microscope showing Sla1p-RFP and GFP-Abp1p expressed in *msb3*Δ *msb4*Δ cells showing actin patch depolarization within mother cells (arrowheads), as compared to wild type. The bar graph quantifies the ratio of Sla1p-RFP and GFP-Abp1p particle localization in buds versus mother cells for WT and *msb3*Δ *msb4*Δ cells (N > 20). **D.** Deconvolved wide-field microscopy images of WT (BY4741) cells expressing GFP-sec4-Q79Lp (bar = 5 µm). Arrowheads indicate depolarized distribution of GFP-sec4-Q79Lp at the PM in mother cells. **E.** Deconvolved medial images of Sla1p-RFP and GFP-Abp1p in WT (BY4741) and *sec4-Q79L* (CBY4793) cells as acquired by confocal microscopy (bar = 2 µm). Ratios of Sla1p-RFP and GFP-Abp1p localization in buds versus mother cells for WT and *sec4-Q79L* cells are quantified in the bar graph (N = 31). **F.** Depolarization of RFP-Snc1p cargo recycling in *sec4-Q79L* cells as compared to WT, as visualized by deconvolved wide-field microscopy (bar = 5 µm). Superimposed dashed yellow lines are drawn through the middle of mother cells and arrowheads indicate PM fluorescence in the back half of mother cells furthest from the bud. **G.** Scatterplots showing lifetimes for Sla1p-RFP and GFP-Abp1p particles in WT and *sec4-Q79L* cells incubated at 23˚C and, as quantified in the bar graph (right) (N > 30), GFP-Abp1p particle velocity increases in *sec4-Q79L* (JGY73) cells relative to its congenic WT control (KEF473A) (N > 70 particles). **H.** Bar graph showing Sla1p-RFP and GFP-Abp1p particle density per µm of the cell surface in *ede1*Δ (CBY4775), *ede1*Δ *sec4-Q79L* (CBY4846), and *sec4-Q79L* (CBY4793) cells cultured at 23˚C as a percentage of the particle density in WT (BY4741) cells (N > 50 medium- and large-budded cells). Triple asterisks (as defined in Fig. 1) denote a statistically significant density increase in *ede1*Δ *sec4-Q79L* cells as compared to *ede1*Δ cells. Experiments were conducted by J.J

Because loss of Sec4p function disrupted actin patch assembly and polarization, we tested if constitutive Sec4p activation might enhance actin patch assembly and/or motility. At 23˚C, Sla1p-RFP lifetime in *sec4-Q79L* cells was 24% less than in wild type, similar to reductions in Sla1p-RFP lifetime reported for clathrin and *EDE1* endocytosis mutants (Marko Kaksonen et al., 2005; Stimpson et al., 2009). Unlike clathrin and *EDE1* mutants, however, in *sec4-Q79L* cells GFP-Abp1p lifetime was also reduced by 35% (Fig. 4.5G), and in the original *sec4-Q79L* strain (JGY73) the dynamic movement of GFP-Abp1p increased by 86% relative to its congenic wild-type control (Fig. 4.5G; this effect was not observed when *sec4-Q79L* was integrated into the BY4741 wild-type strain). Thus, Sec4-Q79Lp constitutive activation appeared to accelerate actin patch formation, which was the reciprocal effect of inactivating Sec4p (*i.e*. Fig. 4.2A-C). As predicted, because Abp1p is recruited after Sec4p, *SEC4* mutations had a greater downstream impact on Abp1p lifetime as compared to Sla1p (Fig. 4.5G, scatterplot). The effects of the constitutively active *sec4-Q79L* mutation on

actin patches, and the fact that GTPγS enhanced Sec4p binding to Las17p *in vitro* (Fig. 4.3A), suggested that GTP binding by Sec4p promotes actin patch assembly through Las17p.

If Sec4p interacts *in vivo* with Las17p and Sla1p during the slow coat assembly phase of actin patch formation, then Sec4p would act downstream after the recruitment of the early coat protein Ede1p (Gagny et al., 2000; Miliaras & Wendland, 2004). Based on this pathway order, we predict that the accelerated formation of actin patches caused by the *sec4-Q79L* mutation would be epistatic to *ede1*Δ defects. In *ede1*Δ cells, the decrease in actin patch density and motility are moderate but comparable to the endocytic defects in clathrin mutants (Gagny et al., 2000; Marko Kaksonen et al., 2005; Miliaras & Wendland, 2004; A. A. Rodal et al., 2003). We found, however, that the reduction in GFP-Abp1p particles in *ede1*Δ cells was in fact partially suppressed by *sec4-Q79L* expression (Fig. 4.5H). These experiments suggested *SEC4* stimulates the actin patch assembly pathway downstream of *EDE1*, consistent with our other findings.

4.3.5. Sec4p Overrides Sla1p Inhibition of Las17p-Dependent Actin Polymerization in vitro

Given that Sec4p is recruited at the same time as Sla1p and Las17p during endocytic site formation, we tested whether Sec4p is also involved in the important step of Arp2/3-dependent actin nucleation, which is activated by Las17p (Goode et al., 2015). During these time-course assays, the assembly of actin filaments involves three distinct phases (Carlier, Pernier, Montaville, Shekhar, & Kühn, 2015; Pollard, 2007): (*i*) an initial nucleation lag phase, in which monomeric G-actin associates as trimers and in conjunction with the Arp2/3 complex forms a stable core for the addition of more actin subunits (this phase is nearly instantaneous when Las17p is added [Fig. 4.6A]); (*ii*) an elongation growth phase, as denoted by the middle linear region of the sigmoidal curves, during which actin monomers are added primarily to the plus-end of growing filaments; (*iii*) the final equilibrium or steady-state phase, when addition and dissociation of monomers from the respective ends of the actin filament reach a balance. To compare effects of adding additional regulatory components into these assembly reactions,

polymerization rates can be calculated from the slopes of the linear regions of each plot during the filament growth phase. Both *in vitro* and in vivo, Sla1p inhibits Las17p nucleation activity, serving as a “checkpoint” during actin patch assembly prior to actin polymerization and membrane internalization (Feliciano & Di Pietro, 2012; A. A. Rodal et al., 2003). To test if Sec4p affects this Sla1p-Las17p regulatory event, we performed *in vitro* pyrene actin polymerization assays at the physiological temperature of 30˚C (Fig. 4.6A-E). As previously reported (Feliciano & Di Pietro, 2012), we found that GST-Las17p stimulates Arp2/3-dependent actin polymerization but this activity was inhibited when GST-Sla1p was added to the assay (Fig. 4.6A). However, in a concentration-dependent manner, addition of GTPγS-GST-Sec4p counteracted Sla1p inhibition of Las17p (Fig. 4.6B). In the presence of Sla1p, GST-Sec4p incubated with GTPγS restored actin polymerization to roughly half the maximal rate measured for assays with Las17p and Arp2/3 complex without Sla1p (Fig. 4.6B). Although GTPγS-GST-Sec4p significantly increased the rate of actin polymerization in the presence of Sla1p, polymerization did not reach the same maximum as in assays with Las17p and Arp2/3 alone (Fig. 4.6B). Sec4p activity in these assays was nucleotide specific given that only GTPγS-GST-Sec4p stimulated polymerization, whereas GDP-bound GST-Sec4p had no effect on Sla1p inhibition of Las17p (Fig. 4.6C). The ability of GTPγS-Sec4p to override Sla1p inhibition was also GTPase-specific because GST-Ypt1p had no effect on Sla1p-Las17p regulation of actin polymerization, whether GDP or GTPγS was added (Fig. 4.6D). In the absence of Las17p, GTPγS-Sec4p had no significant effect on the rate of actin polymerization with added Arp2/3 complex (Fig. 4.6E), indicating that Sec4p has no inherent actin nucleation activity and only acts as a regulator of Las17p. These data give further support to the conclusion that Sec4p directly interacts with the endocytic machinery to override a rate-limiting step in actin patch polymerization.

Figure 4.6. GTPγS-Sec4p overrides Sla1p inhibition of Las17p-dependent actin nucleation *in vitro*.

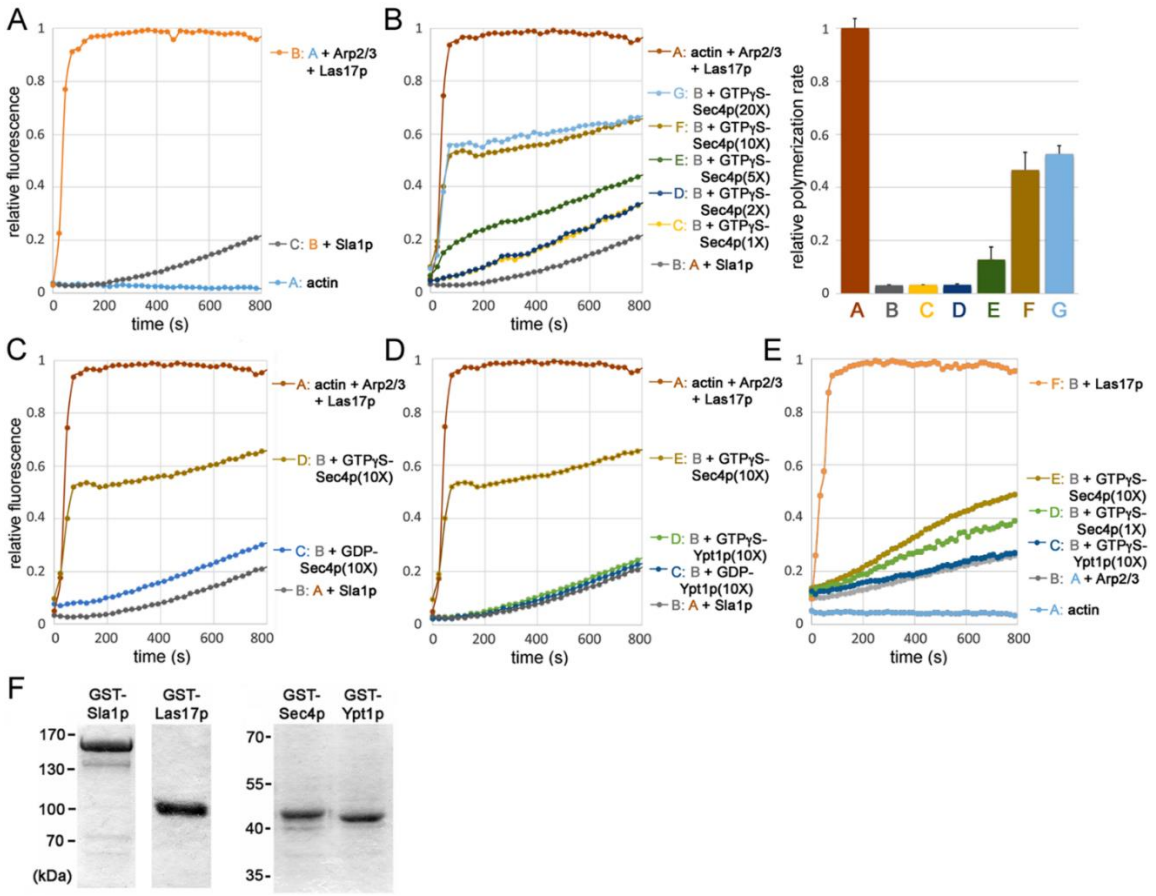

All assays contained 1.5 µM actin (99% pyrene-labeled) polymerized at 30˚C in the presence 75 nM Arp2/3 complex. **A.** Actin polymerization was induced upon addition of 75 nM bacterially expressed GST-Las17p, but this activation was inhibited by the addition of 75 nM full-length Sla1p (expression and purified as a GST-fusion protein). **B.** Time-course (left) showing concentration-dependent effects of GTPγS-Sec4p (fused to GST) on Sla1p inhibition of Las17p, in which a 1, 2, 5, 10, or 20 X molar excess of GTPγS-Sec4p was added (relative to Las17p, Arp2/3, and Sla1p) into each actin polymerization reaction. Based on the accompanying graph, the bar graph (right) shows calculated rates of actin polymerization with increasing concentrations of GTPγS-Sec4p (rates were calculated from slopes of the linear segment of curves corresponding to half maximal polymerization). **C.** GTPγS versus GDP nucleotide dependence of Sec4p for activating actin polymerization in the presence of Sla1p and Las17p (Sec4p was added in 10 X molar excess as indicated). **D.** In contrast to the effect of GTPγS-Sec4p, GTPγS- or GDP-bound Ypt1p fails to counteract Sla1p inhibition of Las17p (Sec4p and Ypt1p were added in 10 X molar excess). **E.** In the absence of Las17p, GTPγS-Sec4p had negligible actin nucleation activity (as indicated, Sec4p was added in 1 and 10 X molar excess, and 10 X molar excess of Ypt1p was added). **F.** Affinity-purified GST fusion proteins (1 µg) used in actin polymerization assays, separated by SDS-PAGE and stained with Coomassie. All plots shown represent averages of 6-10 independent trials. Experiments were conducted by J.J

4.4. Discussion

In addition to its role in exocytosis, the Sec4p Rab GTPase also fulfills criteria expected of a direct regulator of actin patch assembly and endocytic internalization. Analysis of individual GFP-Sec4p particles in living cells after their arrival at the cell cortex indicated that Sec4p shares a brief but specific spatial and temporal co-localization with the actin patch subunits Sla1p, Las17p, and Abp1p. Akin to mutations in known actin patch components, conditional mutations in both *SEC4* and its activator *SEC2* disrupted actin patch assembly, dynamics, structure and polarization. As shown by both *in vitro* and *in vivo* binding assays, Sec4p directly interacts with Las17p and associates in a complex with Sla1p/Las17p at nascent actin patches. Sec4p polarization was also an important determinant for polarized actin patch assembly in budding cells. Most importantly, *in vitro* pyrene actin polymerization assays revealed the mechanism by which Sec4p regulates actin patch formation. By overriding Sla1p inhibition of Las17p, activated Sec4p promotes actin nucleation and thereby drives forward a key regulatory step in endocytic internalization (Fig. 4.7).

Figure 4.7. Sec4p overrides the inhibition of cortical actin polymerization to induce compensatory endocytosis.

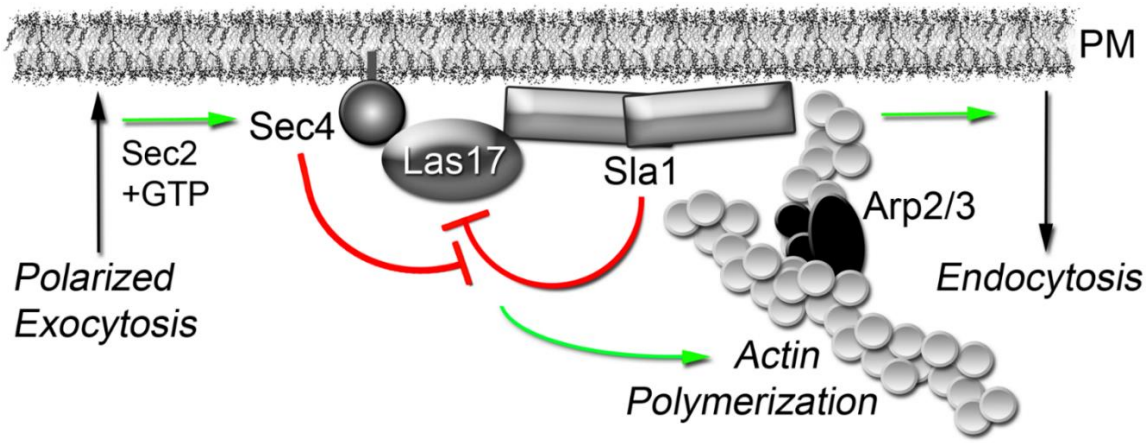

Our results supported the model in which, after the completion of polarized exocytosis, activated GTP-Sec4p deposited on the plasma membrane (PM) physically interacts with Las17p. GTP-bound Sec4p then overrides Sla1p inhibition of Las17p to promote both Arp2/3-dependent actin polymerization and the ensuing steps of endocytic membrane internalization. In the immediate vicinity around polarized sites where exocytic vesicles fuse with the PM, Sec4p directly integrates membrane transport to-and-from the cell surface by inducing compensatory endocytosis. Model was made by C.B

The rate-limiting step in actin filament assembly is nucleation, which involves the Arp2/3 complex and nucleation-promoting factors, the most robust being Las17p (Padrick & Rosen, 2010; A. A. Rodal et al., 2003). As a clathrin adaptor, Sla1p is required for the endocytic internalization of membrane protein cargo. However, Sla1p and other inhibitors also restrain Las17p activity and thereby regulate the final burst of cortical actin polymerization, which ultimately provides the force needed for membrane internalization (Boettner et al., 2009; Feliciano & Di Pietro, 2012; A. A. Rodal et al., 2003). Sec4p arrives at nascent endocytic sites during this brief period, and Sec4p relieved the inhibition of Las17p nucleation by Sla1p in vitro. Sec4p largely restores actin polymerization rates but, even at saturating concentrations, Sec4p did not completely reverse Sla1p inhibitory effects. Under these assay conditions, the relative maximum level of actin polymerization was not attained, suggesting that the monomer-polymer equilibrium was affected, perhaps due to an increased rate of filament depolymerization or treadmilling. Sla1p is also not the only inhibitor to keep Las17p in an inactive state. Although Syp1p binds to Sla1p, Syp1p also inhibits Las17p activity possibly in a Sla1p-independent manner (Boettner et al., 2009; Feliciano & Di Pietro, 2012; A. A. Rodal et al., 2003). Nonetheless, in our *in vitro* assays Sec4p counteracted Sla1p inhibition without Syp1p, suggesting that Sec4p inhibition of Sla1p does not involve Syp1p. Because Sec4p directly binds Las17p, Sec4p might directly interfere or compete with the physical interaction between Sla1p and Las17p. Although *in vitro* activated Sec4p was required in molar excess to effectively override Sla1p inhibition, *in vivo* the effective concentration of Sec4p is likely to be significantly greater given that Sec4p particles are concentrated on the membrane. We note that bacterially expressed Sec4p is not post-translationally lipidated, which might also reduce its activity in these assays. Previous *in vitro* reconstitution of actin assembly from yeast extracts did not identify Sec4p as a contributing factor in Las17p-dependent actin nucleation (Michelot et al., 2010). However, this biochemical approach would have excluded membranes and membrane-bound regulators, such as Sec4p. Apart from Las17p-dependent nucleation of cortical actin, other activators also contribute to the initial seeding events for actin polymerization. In fission yeast, it is proposed that cofilin-severed actin filaments bind specific adapter proteins at nascent sites of endocytosis to provide the initial filaments from which the Arp2/3 branched actin network grow (M C Duncan, Cope, Goode, Wendland, & Drubin, 2001). We conclude that Sec4p plays an important role in the

Sla1p/Las17p regulation of Arp2/3-dependent actin polymerization, but this mechanism likely works in parallel with other regulators that independently promote cortical actin formation.

The initial formation of nascent endocytic sites appears to be largely dictated by cargo-adapter interactions (Goode et al., 2015), but downstream events in actin patch assembly also regulate the rate of endocytosis (S. Y. Carroll et al., 2012; Q. Chen & Pollard, 2013; Chi et al., 2012; Feliciano & Di Pietro, 2012; Kaminska et al., 2011; Spiess et al., 2013). At the PM, the most rapidly maturing actin patches coincide with the immediate regions around newly delivered exocytic vesicles (Layton et al., 2011). One interpretation of this result is that the concentration of endocytic cargo at these regions triggers adaptor packaging and endocytic site formation. Although this proposal is consistent with computational modeling, it has been noted that major cargo-binding adaptors arrive later in the process of actin patch assembly (Goode et al., 2015). If general cargo delivery by exocytosis were the general cue for initiating endocytosis, then any mutation in exocytic trafficking would be predicted to disrupt endocytosis, which is not the case (Riezman, 1985). Alternatively, a specific regulator of exocytic vesicle trafficking could be the trigger. We propose that Sec4p is that trigger, which couples transport to-and-from the PM. In this way, Sec4p is the last of many GTPases in a Rab cascade (Hutagalung & Novick, 2011) that sequentially regulate membrane trafficking out to the cell cortex, and back again, to ensure a directional flow of membrane traffic throughout the cell. Because Sec4p is first recruited to the secretory pathway at the Golgi, this model also explains why endocytosis is generally more affected by late *SEC* genes as compared to early *SEC* genes, which affect the exocytic pathway before the Golgi (Jose et al., 2015; Riezman, 1985). We also observed that the reciprocal was true, namely, that the cellular distribution of Sec4p was dependent on Las17p. The severe mislocalization of GFP-Sec4p in *las17*Δ and *las17-14* cells was particularly surprising. Although other alleles of *LAS17* affected GFP-Sec4p motility on the PM, at high temperatures *las17-14* specifically reduced all membrane-bound GFP-Sec4p. Given that the *las17-14* allele is synthetically lethal with a deletion mutation that removes the proline-rich carboxy-terminal region of Pan1p (*pan1*ΔPRD) (Barker et al., 2007), the specific effect of *las17-14* on Sec4p localization might involve Pan1p and the broader Las17p regulatory network. Pan1p interacts in an endocytic scaffolding/signaling

complex with End3p and Sla1p (Tang et al., 2000), which together might modulate Sec4p activity and localization. Alternatively, Las17p binding contributes to Sec4p stability and this physical interaction is abolished in *las17*Δ or *las17-14* cells, but not in *las17-13* or *las17-1* cells. Based on our results, Sec4p is a bi-functional regulator of both polarized exocytosis and endocytosis.

A convergence of exocytosis and endocytosis has also been described in filamentous fungi, in which the "Spitzenkörper" serves as a recycling compartment at the apical tip of hyphae that maintains polarized growth (L. A. Jones & Sudbery, 2010; Riquelme et al., 2014; Taheri-Talesh et al., 2008). This specialized compartment contains recycled PM proteins, polarisome components, and exocyst subunits as well as Sec4p. In *S. cerevisiae*, a Spitzenkörper-like membrane structure containing both Sec4p and the Cdc42p repressor Bem3p has been reported (Mukherjee et al., 2013). In addition to Sec4p and Bem3p, this compartment contains both endocytic and exocytic markers and is only observed early during bud emergence at polarized tips, close to but not directly associated with the PM. In contrast, our measurements were restricted to Sec4p particles on the PM and only involved later-staged medium/large-budded cells. Based on these facts, the Sec4p-actin patch interactions we analyzed are independent of any Spitzenkörper-related recycling compartment. Nonetheless, Sec4p polarization did have a significant impact on the polarization of nascent endocytic sites on the PM. The inactivation of Sec4p reduced density of actin patches but those that remained were no longer concentrated within the bud. Sec4p depolarization observed in *msb3*Δ *msb4*Δ cells correlated with depolarization of actin patches even though otherwise patch assembly was only mildly affected. The depolarized localization of activated sec4-Q79Lp also correlated with actin patch depolarization and the loss of polarized recycling of endocytic membrane cargo. Of course, other mechanisms also exist to promote actin patch polarization, including processes that act downstream of Cdc42p polarization (Howell & Lew, 2012). However, our data suggest that polarized exocytosis deposits Sec4p at sites on the PM where it can stimulate cortical actin polymerization nearby. By internalizing material adjacent to sites of polarized growth, before extensive lateral diffusion can occur, we propose this mechanism prevents the escape of membrane proteins from the bud and reinforces the separation between mother and daughter cells provided by the septin barrier (Caudron & Barral, 2009; Orlando et al., 2011).

In metazoans, Cdc42 plays a central role in integrating exocytosis and endocytosis, for example in the endocytic recycling of junctional proteins (Mara C. Duncan & Peifer, 2008; Harris & Tepass, 2010). In Xenopus eggs, Cdc42 binds N-WASp and facilitates filamentous actin assembly around vesicles docked at the PM, which reconfigures cortical granules for compensatory endocytic internalization after exocytosis (Anna Marie Sokac et al., 2003). Unlike metazoan N-WASp, however, the yeast homolog Las17p does not directly interact with Cdc42p (Park & Bi, 2007) and the inter-relationship between Cdc42p and transport cycles involving polarized exocytosis and endocytosis are unclear (Layton et al., 2011). Thus, the "kiss-and-coat" mode of compensatory endocytosis in Xenopus (Anna M. Sokac & Bement, 2006), or "kiss-and-run" recycling of presynaptic exocytic vesicles (Gundelfinger et al., 2003), do not appear to apply to budding yeast. Our results are, however, consistent with findings in *C. elegans* implicating the Sec4p homolog Rab3 in coordinating the exocytosis/endocytosis cycle of synaptic vesicles (Bai et al., 2010). We, therefore, propose by this mechanism of compensatory endocytosis that Sec4p homologs in other polarized cell types might augment or supplant Cdc42p in maintaining a balance of membrane going to-and-from the PM.

4.5. Materials and Methods

4.5.1. Strains and Plasmids

Yeast strains used are listed in the S1 Table and plasmids in S2 Table. All fusions were functional as tested by complementation of corresponding mutant defects.

4.5.2. Fluorescence microscopy

Wide-field fluorescence microscopy was performed as previously described (Keith G. Kozminski et al., 2006) [66]. Confocal images were captured on a Zeiss Axio Observer.Z1 microscope (Carl Zeiss International, Oberkochen, Germany) equipped with a CSU-10 Nipkow spinning disc (Yokogawa Electronic Corp., Tokyo, Japan), and Z-stacks were acquired using an Improvision Piezo Focus Drive. Z-stacks were separated by 0.5 μm and spanned, at minimum, the entire cell width. Images were acquired using a

Zeiss 100 X 1.4 NA plan-apochromat oil immersion lens and a Hamamatsu EM-CCD C9100-13 camera (Hamamatsu Photonics, Hamamatsu-city, Japan) mounted on a 1.5 X C-mount and digital analysis and deconvolution was done using Volocity software (Improvision Inc., Lexington, MA). GFP and RFP fluorophores were excited with a 491 nm and 561 nm lasers respectively; emitted light was filtered with GFP ET520/40M or RFP ET593/40M emission filters (Chroma Technology Corp., Rockingham, VT). Cells were mounted directly onto glass slides in synthetic medium and images were acquired with equivalent exposures and laser power unless specified otherwise.

To track newly generated individual GFP-Sec4p particles after entering the daughter bud, the entire bud was first photobleached using a 300 mW solid-state 405 nm laser (Lasiris ColdRay Laser, Stockeryale Inc., Salem, NH). The FRAP laser was used at maximum power for 250 ms when analyzing GFP-Sec4p colocalization with Sla1p-RFP and Abp1p-RFP, and 40 ms for FRAP of GFP-Sec4p/Las17p-RFP-containing cells. The exposure time was 61 ms (71% laser power) and 1.0 s (67% power) for colocalization experiments involving GFP-Sec4p and Sla1p-RFP, respectively; 51 ms (65% power) and 505 ms (69% power) for GFP-Sec4p and Abp1p-RFP, respectively; and 500 ms (35% power) and 1 s (40% power) for Las17p-RFP, respectively. GFP-sec4-Q79L was imaged on the confocal microscope at 300 ms exposure at 70% power. Actin comet tails were detected by observing actin patch formation in cells over a 90 s period using widefield video microscopy. Abp1p-GFP comet-tail images were captured with a 400 ms exposure at 17% arc lamp intensity and full gain. RFP-Snc1p was visualized by widefield microscopy using 50 ms exposures at 17% arc lamp intensity.

4.5.3. Image analysis

The following guidelines were used for the quantification of particle tracking and co-localization in movies and captured images: (*i*) for tracking reliability in movies, only new GFP-Sec4p particles transported to the bud cortex, and whose entire lifespan was captured, were analyzed; (*ii*) only particles in medium and large buds were analyzed because within smaller buds particles crossed paths due to high density; (*iii*) for movies of all cells analyzed, fluorescent particles that crossed paths were excluded from

analysis; (*iv*) Sec4p particles were followed immediately after FRAP as each Sec4p particle arrived at the bud cortex, and ended after the particle was no longer visible at any focal plane within the cell; (*v*) actin patch subunits were tracked when particles first appeared on the PM and ended when they were no longer detectable within any focal plane; (*vi*) in movies and still images, individual particles that could not be completely distinguished from local fluorescence background were excluded from analysis; (*vii*) only those particles where fluorescence overlap persisted over three or more movie frames were counted as being co-localized; (*viii*) given that slight positional changes between acquisition of each fluorescence image might cause particles to appear juxtaposed, co-localization was defined as when the majority of fluorescence pixels overlapped between two individual particles.

Particles were tracked using the manual tracking function of the visualization and quantification module in Volocity. The manual tracking function was also used for 4D-confocal microscopy analysis of particle movement. Particle tracings and velocity data were generated using the Volocity visualization and quantification module. Kymographs were generated using the multiple kymograph module of ImageJ (http://rsb.info.nih.gov/ij/). To determine the peak particle fluorescence at the PM on kymographs, Voxel Spy from Volocity was used to determine the frame with highest voxel pixel intensity from videos recording the entire lifetime of each particle; if peak voxel intensity remained constant for multiple frames, then the frame with the highest area of peak intensity was chosen. Images of actin comet tails were deconvolved by iterative restoration with a 95% confidence threshold using Volocity 3D deconvolution based on a theoretical PSF calculated from emissions at 509 nm with a 1.40 NA. All images were equivalently processed using Photoshop (Adobe Systems, San Jose, CA). Movies were rendered and characters were added using Sony Vegas Pro 8.0 (Sony, Tokyo, Japan).

4.5.4. BiFC protein interaction assays

BiFC was performed as previously described (Manderson, Malleshaiah, & Michnick, 2008) with modifications. For constant expression levels, YFP^N- and YFP^C-fusion constructs were integrated using the modified vectors pHVF1-CT, pUVF2-CT, and

pHVF2-NT (gifts from Dr. Christopher Loewen, UBC). Haploid transformants expressing YFP^N- and YFP^C-fusions, respectively, were mated and BiFC assays were conducted by wide-field fluorescence microscopy on the resulting diploid cells. For each image, a single optical section was acquired using a YFP filter as previously described (Manderson et al., 2008). Exposure times were 500 ms at full gain using an arc lamp intensity set at 55%, except for YFP^N-Sec4p/Abp1p-YFP^C and Las17p-YFP^N/Sla1p-YFP^C analysis where the intensity was set at 100%. The images were deconvolved using the Volocity 3D deconvolution theoretical point spread function and calculated based on emissions at 520 nm with a 1.40 NA.

4.5.5. *in vitro* protein binding assays and Bgl2p polarized exocytosis assay

For affinity purification, GST-Sec4p, GST-Ypt1p, and GST were expressed in BL21(DE3) RIL cells (Agilent Technologies, Santa Clara, CA) following induction with 1 mM IPTG for 14-16 h at 23˚C. Cells were lysed by sonication in purification buffer (125 mM Tris pH 8.0 150 mM NaCl) and the GST-fusion proteins were immobilized on magnetic glutathione beads (Pierce Biotechnologies Inc., Rockford, IL) after overnight incubation at 4°C. Protein-bound beads were washed 3 times with purification buffer and, after Bradford analysis of protein content, 250 µg of bound protein was washed 3 times with 150 mM Tris pH 7.5, 10 mM EDTA, 250 mM NaCl, 0.5% [v/v] Triton X-100 to remove any GTP or GDP already bound by the isolated GST-Sec4p and GST-Ypt1p. Then, after 3 washes with binding buffer (150 mM Tris pH 7.5, 1.5 mM $MgCl_2$, 250 mM NaCl, 0.5% [v/v] Triton X-100), beads were resuspended in binding buffer containing either 1.5 mM GDP or 1.5 mM GTPγS and incubated for 30 min at 23˚C. ^{35}[S]-labeled Las17p-Myc, corresponding to 10 µl of product from the TNT T7 Coupled Reticulocyte Lysate System (Promega, Madison, WI), was added to 1 µg of each immobilized GST-fusion sample and incubated for 1 h at 23˚C. After 6 x 5 min washes with binding buffer containing 1.5 mM GDP or GTPγS, respectively, bound ^{35}[S]-Las17p-Myc was eluted by boiling in SDS sample buffer, separated by SDS-PAGE, and gels were fixed, dried, and exposed on film. Bgl2p polarized exocytosis was assayed as previously described.

4.5.6. *in vitro* pyrene-actin polymerization assay and affinity purification of fusion proteins

For purification of GST-fusion proteins from bacterial extracts, and their subsequent use in actin polymerization assays, coding sequences for *SLA1*, *LAS17*, *SEC4,* and *YPT1* were sub-cloned into *Bam*HI and *Sal*I sites in pGEX-4T-1 (GE Healthcare Life Sciences, Pittsburg, PA). For protein expression, plasmids were transformed into the *E. coli* strain BL21 (DE3) RIL. To induce GST-fusion protein expression, 250 ml of early log-phase cultures grown in LB at 37˚C were treated with 1 mM IPTG and, after an additional 2 h of growth at 23˚C, cells were pelleted by centrifugation at 5,000 x *g* for 30 mins at 4˚C. After re-suspension in 20 ml binding buffer (125 mM Tris pH 8.0, 150 mM NaCl) containing EDTA-free protease inhibitors (Roche, Basel, CH), cells were lysed by sonication using a digital sonifier (Branson Ultrasonics Co., Danbury, CT) at 20% amplitude for 3 mins with cycle bursts of 1 s on and 3 s off. Cell debris was pelleted by centrifugation at 25,000 x *g* for 1 h at 4˚C and GST-fusion proteins were purified from the supernatant by binding overnight to glutathione magnetic beads (Pierce Biotechnology Inc., Rockford, IL) at 4˚C. Beads were washed 6 times with binding buffer, and fusion proteins were eluted after a 30 min incubation in elution buffer (125 mM Tris pH 8.0, 150 mM NaCl, 50 mM glutathione) containing HALT protease inhibitor (Pierce Biotechnologies Inc. Rockford, IL) at 4˚C. The elutions were repeated 4 times and eluents were pooled. Before addition to pyrene-actin polymerization assays, fusion proteins were concentrated using Amplicon size exclusion spin columns (100k for GST-Sla1p, 50K for GST-Las17p and 35k for GST-Sec4p and GST-Ypt1p) by centrifugation at 7,000 x *g* for 30 mins at 4˚C. Concentrated fusion protein was diluted in G buffer for actin polymerization assays. Protein concentrations were determined by Bradford analysis (Sigma-Aldrich, St. Louis, MO).

Actin polymerization experiments were performed as previously described (Layton et al., 2011). Reaction mixtures contained 1.5 µM depolymerized rabbit actin (99% pyrene-labeled) (Cedarlane Labs, Burlington, ON), 75 nM bovine Arp2/3 complex (Hypermol EK, Bielefeld, Germany) and 75 nM GST-Sla1 and/or GST-Las17, along with varying concentrations of GST-Sec4 and GST-Ypt1 incubated with 1.5 mM GTPγS or GDP. Reactions were initiated upon addition of 1/10 volume of polymerization buffer (500 mM KCl, 20 mM $MgCl_2$, 10 mM ATP). Actin polymerization was measured at 30°C

using an Infinite 200M PRO microplate reader (Tecan Mannedorf, CH) with excitation and emission wavelengths of 365 nm and 406 nm, respectively. Actin polymerization rates were calculated from the slope of the linear portion of assembly curves.

4.5.7. Statistical Analysis

Statistical differences between datasets were analyzed with two-tailed unpaired Student *t*-tests from which *p*-values were derived. Scatterplots were generated using GraphPad Prism 5.0 (Graphpad Software, La Jolla, CA) where means are indicated with vertical lines. In bar graphs, statistical data is shown as mean values with error bars representing S.E.M. (Standard Error of the Mean).

4.6. Acknowledgements

Many thanks to Keith Kozminski and Shubha Dighe for performing the Bgl2p exocytosis assay. The authors thank Charles Boone, Elizabeth Conibear, David Drubin, Philip Hieter, Christopher Loewen, Peter Novick and Randy Schekman for plasmids and yeast strains. Thanks also to Lisa Craig, Nick Harden, Nancy Hawkins, Michel Leroux, Evan Quon, and Peter Stirling for comments on the work and manuscript. Technical assistance was provided by Ziwei Ding and Lauren Fullerton. This work was supported by the Canadian Cancer Society Research Institute (CCSRI grant 700492). G.A. was supported by MSFHR and NSERC studentship awards. This work is dedicated to R. Beh and A. Beh for their courageous battles with cancer.

4.7. Supporting Information

Table 4.1S: *S. cerevisiae* strains used in this study.

Strain	Genotype	Source
BY4741	*MAT***a** *his3Δ1 leu2Δ0 met15Δ0 ura3Δ0*	(Winzeler et al., 1999)
BY4742	*MAT*α *his3Δ1 leu2Δ0 lys2Δ0 ura3Δ0*	(Winzeler et al., 1999)
CBY31	*MAT***a** *leu2-3,122 lys2-801 ura3-52 his3Δ200 trp1Δ901 suc2Δ9*	
CBY1024	*MAT***a** *his3Δ1 leu2Δ0 lys2Δ0 ura3Δ0 las17Δ::kan-MX4*	

CBY1980	*MAT***a** *his3Δ1 leu2Δ0 met15Δ0 lys2Δ0 ura3Δ0 msb3Δ::kan-MX4 msb4Δ::kan-MX4*	
CBY1981	*MAT***a** *his3Δ1 leu2Δ0 ura3Δ0 msb3Δ::kan-MX4 msb4Δ::kan-MX4*	
CBY4356	BY4741 *las17-1:kan-MX4*	P. Hieter, UBC
CBY4357	BY4741 *las17-13:kan-MX4*	P. Hieter, UBC
CBY4358	BY4741 *las17-14:kan-MX4*	(Z. Li et al., 2011)
CBY4372	BY4741 *rvs167Δ::kan-MX4*	(Winzeler et al., 1999)
CBY4373	BY4742 *bbc1Δ::kan-MX4*	(Winzeler et al., 1999)
CBY4374	BY4741 *sla1Δ::kan-MX4*	(Winzeler et al., 1999)
CBY4621	SEY6210 *LAS17*-YFP^{N}*:HIS3*	
CBY4629	SEY6210 *HIS3*:P^{ADH1}-YFP^{N}-*SEC4*	
CBY4632	CBY31 *ABP1*-YFP^{C}*:URA3*	
CBY4635	CBY31 *HIS3*:P^{ADH1}-YFP^{N}-*SEC4*	
CBY4638	*MATα*/*MAT***a** *leu2-3,122/leu2-3,122 lys2-801/lys2-801 ura3-52/ura3-52 his3Δ200/his3Δ200 trp1Δ901/trp1Δ901 suc2Δ9/suc2Δ9 HIS3*:P^{ADH1}-YFP^{N}-*SEC4/SEC4 LAS17*-YFP^{C}*:URA3/LAS17*	
CBY4645	*MATα*/*MAT***a** *leu2-3,122/leu2-3,122 lys2-801/lys2-801 ura3-52/ura3-52 his3Δ200/his3Δ200 trp1Δ901/trp1Δ901 suc2Δ9/suc2Δ9 HIS3*:P^{ADH1}-YFP^{N}-*SEC4/SEC4 ABP1*-YFP^{C}*:URA3/ABP1*	
CBY4657	SEY6210 *LAS17*-YFP^{C}*:URA3*	
CBY4677	BY4741 *SLA1*-RFP*:HIS3*	
CBY4679	CBY31 *SLA1-YFP^{C}:URA3*	
CBY4681	SEY6210 *SLA1*-YFP^{C}*:URA3*	
CBY4686	BY4741 *ABP1*-RFP*:HIS3*	
CBY4689	BY4741 *LAS17*-RFP*:HIS3*	
CBY4710	*MAT***a** *his3Δ1 leu2Δ0 lys2Δ0 ura3Δ0 sec2-41:kan-MX4*	C. Boone, U. Toronto
CBY4711	*MAT***a** *his3Δ1 leu2Δ0 lys2Δ0 ura3Δ0 sec4-8:kan-MX4*	C. Boone, U. Toronto
CBY4712	*MAT***a** *his3Δ1 leu2Δ0 lys2Δ0 ura3Δ0 sec6-4:kan-MX4*	C. Boone, U. Toronto
CBY4742	*MATα*/*MAT***a** *leu2-3,122/leu2-3,122 lys2-801/lys2-801 ura3-52/ura3-52 his3Δ200/his3Δ200 trp1Δ901/trp1Δ901 suc2Δ9/suc2Δ9 LAS17-*YFP^{N}*:HIS3/LAS17 SLA1*-YFP^{C}*:URA3/SLA1*	
CBY4749	*MATα*/*MAT***a** *leu2-3,122/leu2-3,122 lys2-801/lys2-801 ura3-52/ura3-52 his3Δ200/his3Δ200 trp1Δ901/trp1Δ901 suc2Δ9/suc2Δ9 HIS3*:P^{ADH1}-YFP^{N}-*SEC4/SEC4 SLA1*-YFP^{C}*:URA3/SLA1*	
CBY4759	*MAT***a** *his3Δ1 leu2Δ0 lys2Δ0 ura3Δ0 sec4Δ::kan-MX4* [GFP-*SEC4 URA3 CEN*]	
CBY4768	*MAT***a** *his3Δ1 leu2Δ0 met15Δ0 ura3Δ0 sec2-41:kan-MX4 SLA1*-RFP:*HIS3* [P^{ACT1}-GFP-*ABP1 URA3 CEN*]	
CBY4775	BY4742 *ede1Δ::kan-MX4*	(Z. Li et al., 2011)
CBY4787	*MAT***a** *his3Δ1 leu2Δ0 lys2Δ0 ura3Δ0 sec4-Q79L:HIS3:sec4Δ::kan-MX4*	

	[P*ACT1*-GFP-*ABP1 URA3 CEN*]	
CBY4793	*MAT***a** *his3Δ1 leu2Δ0 lys2Δ0 ura3Δ0 sec4-Q79L:HIS3:sec4Δ::kan-MX4*	
CBY4805	BY4742 *SLA1-RFP:HIS3* [P*ACT1*-*GFP-ABP1 URA3 CEN*]	
CBY4810	*MAT*α *his3Δ1 leu2Δ0 ura3Δ0 ede1Δ::kan-MX4 SLA1*-RFP*:HIS3* [P*ACT1*-GFP-*ABP1 URA3 CEN*]	
CBY4846	*MAT*α *his3Δ1 leu2Δ0 ura3Δ0 ede1Δ::kan-MX4 SLA1*-RFP*:HIS3 sec4-Q79L:HIS3:sec4Δ::kan-MX4* [P*ACT1*-GFP-*ABP1 URA3 CEN*]	
CBY4863	BY4742 *sla2Δ::kan-MX4*	(Winzeler et al., 1999)
DDY130	*MAT***a** *his3Δ200 leu2-3,112 lys2-801 ura3-52*	D. Drubin, UC, Berkeley
DDY904	*MAT*α *his3Δ200 leu2-3,112 lys2-801 ura3-52*	D. Drubin, UC, Berkeley
DDY1438	*MAT*α *his3Δ200 leu2-3,112 lys2-801 ura3-52 las17Δ::URA3*	D. Drubin, UC, Berkeley
DDY1980	*MAT***a** *his3Δ200 leu2-3,112 lys2-801 ura3-52 sla2Δ::URA3*	D. Drubin, UC, Berkeley
JGY73	*MAT***a** *his3Δ200 leu2Δ1 lys2-801 trp1Δ63 ura3-52 sec4-Q79L*	(Goode et al., 2001)
KEF473A	*MAT***a** *his3Δ200 leu2Δ1 lys2-801 trp1Δ63 ura3-52*	(Goode et al., 2001)
NY17	*MAT***a** *sec6-4^{ts} ura3-52*	(Novick et al., 1980)
RH286-1C	*MAT*a *leu2 ura3 his4 bar1 end4-1(ts)*	(Raths, Rohrer, Crausaz, & Riezman, 1993)
RSY255	*MAT*α *ura3-52 leu2-3,112*	(Novick & Schekman, 1979)
SEY2102	*MAT*α *his4-519 leu2-3,112 ura3-52 bgl2::URA3*	(Klebl & Tanner, 1989)
SEY6210	*MAT*α *ura3-52 his3Δ200 lys2-801am leu2-3,112 trp1Δ901 suc2Δ9*	(J. S. Robinson et al., 1988)
W303-1A	*MAT*a *leu2-3,112 ura3-1 his3-11 can1-100 ade2-1*	

Unless otherwise referenced, all strains were created as part of this study.

Table 4.2S: Plasmids used in this study.

Plasmid	Description	Source
pAGX2	P*ACT1*-GFP *CEN URA3*	(Ozaki-Kuroda et al., 2001)
pCB591	GFP-*SEC4 CEN TRP1*	
pCB733	P*ACT1*-GFP-*ABP1 CEN LYS2*	
pCB768	P*ACT1*-GFP-*ABP1 CEN URA3*	
pCB871	*sec4^{Q79L} HIS3*	
pCB879	*SLA1*-mRFP:*HIS3-MX6 LEU2 CEN*	
pCB881	*SLA1*-mRFP:*HIS3-MX6 LEU2* 2μ	
pCB901	GFP-*SEC4-Q79L CEN URA3*	
pCB941	P*GAL1*-*SEC4* 2μ *TRP1*	
pCB942	P*GAL1*-*LAS17* 2μ *TRP1*	
pCB954	pCITE-4a(+) *LAS17-myc*	
pCB964	GST-*SEC4*	

pCITE-4a(+)	T7-promoter CITE	Novagen, Madison, WI
pDD1737	mRFP:*HIS3-MX6*	D. Drubin, UC, Berkeley
pFA6a-GFP-HIS3MX6	GFP:*HIS3-MX6*	(Wach, Brachat, Alberti-Segui, Rebischung, & Philippsen, 1997)
pGEX-4T-1	GST	GE Healthcare, UK
pHVF1-CT	YFP^{F1}:*HIS3-MX6*	C. Loewen, UBC
pHVF1-NT	*HIS3-MX6*:P^{ACT1}-YFP^{F1}	C. Loewen, UBC
pKT10-GAL-HA	P^{GAL}-HA 2µ *URA3*	(Misu et al., 2003)
pLC1330	HA-RFP-*SNC1 CEN URA3*	E. Conibear, UBC
pNB810	*SEC3*-GFP *URA3 CEN*	(Finger et al., 1998)
pPG5-SEC5-3xGFP	*SEC5*-3xGFP *URA3*	(Jose et al., 2015)
pPG5-SEC15-3xGFP	*SEC15*-3xGFP *URA3*	(Jose et al., 2015)
pRC2098	GFP-*SEC4 CEN URA3*	(Calero et al., 2003)
pRS303	*HIS3*	(Sikorski & Hieter, 1989)
pRS426	2µ *URA3*	(Sikorski & Hieter, 1989)
pUVF2-CT	YFP^{F2}:*URA3*	C. Loewen, UBC
YCplac22	*CEN TRP1*	(Gietz & Akio, 1988)
YCplac33	*CEN URA3*	(Gietz & Akio, 1988)
YCplac111	*CEN LEU2*	(Gietz & Akio, 1988)
YEplac181	2µ *LEU2*	(Gietz & Akio, 1988)
YEplac195	2µ *URA3*	(Gietz & Akio, 1988)

Unless otherwise referenced, all plasmids were created as part of this study.

Supplemental Movies and Legends

S1 Video. Photobleaching enables single particle tracking of GFP-Sec4p at the cell cortex. Time-lapse videos of two representative wild-type cells (BY4741) expressing both GFP-Sec4p and Abp1p-RFP. Large white circles indicate the photobleached region (bud membrane), and asterisks indicate the duration of the laser burst. Green arrowheads indicate cortical GFP-Sec4p particles, RFP-Abp1p is indicated by red arrowheads, and yellow arrowheads indicate the transitional overlap of GFP-Sec4p and RFP-Abp1p fluorescence. Total acquisition time is 90 s edited and compressed to play at 5 frames/s (for technical reasons 3 frames during laser photobleaching were excluded). Made by J.J

S2 Video. Las17p-RFP and GFP-Sec4p particles co-localize at cortical actin patches. Time-lapse video of a wild-type cell expressing RFP-Las17p and GFP-Sec4p, immediately after photobleaching. Particle co-localization at cortical actin patches is indicated by circles where red and green arrowheads indicate Las17p and cortical Sec4p, respectively, and yellow arrowheads indicate their temporal and spatial overlap. Total acquisition time is 2 min, compressed into 5 frames/s. Made by J.J

S3 Video. Sla1p-RFP and GFP-Sec4p co-localize at cortical actin patches. Time-lapse video of a representative wild-type cell expressing Sla1p and GFP-Sec4p, immediately after photobleaching. Particle co-localization at cortical actin patches is indicated by circles where red and green arrowheads indicate Sla1p and cortical Sec4p, respectively, and yellow arrowheads indicate their temporal and spatial overlap. Total acquisition time is 1 min, compressed into 4 frames/s. Made by J.J

S4 Video. GFP-Sec4p particles co-localize with Abp1p-RFP at cortical actin patches. Time-lapse video of a wild-type cell expressing GFP-Sec4p and Abp1-RFP, immediately after photobleaching. Particle co-localization at cortical actin patches is indicated by circles where green and red arrows indicate cortical GFP-Sec4p and Abp1p-RFP, respectively, and yellow arrowheads indicate their coincident overlap. Note that GFP-Sec4p precedes Abp1p-RFP at actin patches, whereas Las17p and Sla1p precede the appearance of GFP-Sec4p particles. Total acquisition time is 2 min, compressed into 5 frames/s. Made by J.J

S5 Video. *SEC4* and *SEC2* function are required for normal actin patch polarization and dynamics. WT (BY4741), *sec2-41* (CBY4710), and *sec4-8* (CBY4711) cells expressing Sla1p-RFP and Abp1-GFP after an incubation at 37˚C for 60 min. Particles are tracked immediately after photobleaching where circles indicate examples of co-localization. Red arrowheads indicate Sla1p-RFP particles, green

arrowheads indicate Abp1p particles, and yellow arrowheads indicate temporal and spatial overlap. Total acquisition time is 2 min compressed into 5 frames/s. Made by J.J

Chapter 5. Discussion

Integration of transport pathways to balance the flux of membrane material to and from the PM is of vital importance. The work presented here presents new mechanisms and understanding as to how yeast achieves balance, not only between vesicular transport pathways that were considered mechanistically separate but also by providing evidence that links non-vesicular and vesicular transport through possible mechanistic integration. These discoveries introduce new complexities into our understanding of how membrane homeostasis is regulated and have sparked new fields of research since their respective discoveries.

5.1. ORPs are regulators of vesicular and non-vesicular transport but mechanisms remain elusive

Since the discovery that Osh4p binds directly to exocytic vesicles it has been speculated that Osh4p's role on vesicles is to sequester local PI(4)P, allowing for efficient association of Sec2p with Sec4p on the vesicle, thus promoting exocyst complex assembly (Christopher T Beh et al., 2012). Ling et al. investigated this claim and while they showed that Osh4p does associate with exocytic vesicles in a PI(4)P-dependent manner, their argument that Osh4p mediated PI(4)P sequestration is required for Sec2p association with Sec15p is troublesome. As the authors determined, PI(4)P distribution is severely affected in *OSH4* deletion strains, making any interpretation of co-immunoprecipitation experiments involving PI(4)P sensitive protein complexes performed in this strain background problematic (Ling et al., 2014). Furthermore, a model where Osh4p is required Sec2p-Sec15p complex formation would imply severe exocytic defects in *osh4Δ*, however, exocytic defects are only observed when all Osh proteins are deleted (Christopher T Beh & Rine, 2004). While the data presented in this thesis did establish that Osh4p co-immunoprecipitated with the exocyst complex, it remains unknown which of the exocyst complex proteins make direct

physical contact with Osh4p. To get a better understanding of Osh4p's role during vesicle transport one could perform *in vitro* interaction studies on single exocyst components to pinpoint what proteins Osh4p physically bind and potentially regulate. This approach has the added advantage that one can control PI(4)P levels independently of strain background variations as it was demonstrated in (Mizuno-Yamasaki et al., 2010). One interesting possibility is that Osh4p acts as a direct regulator of Sec4p during exocytosis. This claim is not completely unfounded as Sec4p did co-immunoprecipitate with Osh4p and evidence from mammalian cells have shown that OSBP, ORP3 and ORP1L interact physically with the small GTPases, Arf1, R-Ras and Rab7 respectively (Johansson et al., 2005; Mesmin, Bigay, et al., 2013; Weber-Boyvat et al., 2015), suggesting that ORPs may regulate the activity of small GTPases directly in response to lipid environment. Additional analysis will be required to validate such a hypothesis.

Another line of evidence that links Osh4p to the regulation of exocytosis in yeast was the discovery that Osh4p physically interacts with Cdc42p and Rho1p at the PM. If Osh4p's role on exocytic vesicles solely was to sequester PI(4)P from the vesicle to promote exocyst complex assembly, then physical interactions with Cdc42p and Rho1p, which are both restricted to the PM in the bud tip (Fujiwara et al., 1998; Ziman et al., 1993), would not be expected. This indicates that Osh4p may be involved in regulating the function of the Rho GTPases at the PM. This is supported by the finding that Osh4p overexpression partially suppressed specific temperature sensitive *CDC42* alleles, while it exacerbated *RHO1* temperature sensitive alleles to a point where they were no longer viable at room temperature (Keith G. Kozminski et al., 2006). This genetic analysis strongly suggests that Osh4p is involved in regulating Rho1p and Cdc42p function upon arrival at the PM, but further analysis of the interactions is required to establish the mechanism involved.

Since their discovery, ORPs have been implicated in PM sterol homeostasis, exemplified by the hypothesis that OSBP and Osh4p function as cytosolic sterol/ PI(4)P shuttles that pick up sterols at the ER, translocate to the PM where they deposit the sterol in the PM in exchange for PI(4)P, and finally return to the ER to repeat the cycle (de Saint-Jean et al., 2011; Mesmin, Bigay, et al., 2013). In both papers, the authors rely

on *in vitro* data to establish the ability of OSBP/Osh4p to transfer lipids directly between liposomes, and while a correlation between OSBP/Osh4p function and PI(4)P transfer was observed in vivo, the *in vivo* evidence linking OSBP/Osh4p to sterol transport was less convincing since an assay testing rate of sterol uptake into lipid droplets would rely more on sterol esterification rates than non-vesicular transfer (Mesmin, Bigay, et al., 2013). This does not exclude that OSBP/Osh4p are involved in sterol transfer in vivo, but it does question the transfer model presented. Furthermore, combining the observation that sterol transfer was unaffected in Osh protein depleted cells (Georgiev et al., 2011; Keith G. Kozminski et al., 2003) with the finding that Osh4^{Y97F}p, which cannot bind sterols (Im et al., 2005), is hyperactivated rather than inactivated, as would have been predicted for a putative sterol transfer protein, disputes that ORPs are sterol transfer proteins *in vivo* and indicates that sterol binding regulates the activity of Osh4p (Alfaro et al., 2011). Interestingly, studies have shown that mutants abolishing Osh4p PI(4)P-binding resulted in loss of Osh4p function (de Saint-Jean et al., 2011; Ling et al., 2014). This observation together with the finding that deletion of *SAC1* rescued lethality caused by hyperactivated Osh4^{Y97F}p (Alfaro et al., 2011) indicates that Osh4p function is dependent on PI(4)P-binding. To test this further analysis of *OSH4* mutants incapable of binding mutants should be performed. Investigating how these mutations affect Osh4p function in proposed sterol transfer and vesicular trafficking alike should be assayed. These studies would help improve the understanding of the importance of PI(4)P-binding in regulating ORP function.

Increasing evidence has linked ORP function to the regulation of membrane contact site function, however, the molecular mechanism remains unknown. In yeast, it was shown Osh6p and Osh7p are required for PS-PI(4)P exchange between the ER and PM in the absence of vesicular transport (Maeda et al., 2013). A similar observation was made in HeLa cells, where ORP5 and ORP8 mediated non-vesicular PM-ER PS-PI(4)P exchange (Chung et al., 2015). The finding that ORPs are required for PS-PI(4)P transfer implies that ORPs may serve as direct lipid transfer proteins, however, an alternative model states that ORPs act as protein regulators at membrane contact sites in response to local lipid environment, and that lipid transfer is a result of this regulation (Christopher J. Stefan et al., 2011; Tavassoli et al., 2013). Such a model is supported by the findings that the cortical ER bound protein Osh3p can recruit Sac1p to PM-ER

contact sites. Here Osh3p stimulates the activity of Sac1p which dephosphorylates PI(4)P in the PM (Christopher J. Stefan et al., 2011). A similar mechanism has been reported for the PE N-methyltransferase, Opi3p, which similarly to Sac1p, is recruited to PM-ER contact sites by Osh3p, stimulating Opi3p to convert PE to PC in the PM (Tavassoli et al., 2013). Further support for Osh proteins acting as physical regulators of membrane contact sites was provided by the fact that both Osh2p and Osh3p make physical contact with Scs2p, which is a key component of the protein machinery regulating PM-ER membrane contact sites (Riekhof et al., 2014). To try to elucidate which of these models are correct, one could knock out Osh proteins in strains lacking PM-ER membrane contact sites and investigate lipid composition of the PM. If Osh proteins affect PM lipid composition through membrane contact sites, then one would not expect deletions of *OSH*s to show any effects in strains lacking membrane contact sites. However, if Osh proteins can act independently of contact sites then an effect could be observed.

5.2. Arv1p potentially regulates proper lipid raft formation by maintaining ER ultrastructure.

ARV1 was originally identified in yeast as a sterol transporter based on nystatin sensitivity and sterol accumulation in ER as well as Golgi fractions in cell fractionation experiments when *ARV1* was mutated, indicating that Arv1p might function as an ER to PM sterol transfer protein (Tinkelenberg et al., 2000). Later studies showed that deleting *ARV1* caused a drop in complex sphingolipid synthesis, implicating Arv1p in complex sphingolipid synthesis regulation (Swain et al., 2002). Together these studies indicate that that Arv1p plays a role in the regulation of lipid raft generation and/or function in the ER. This hypothesis is supported by the finding that Arv1p is required for efficient insertion of GPI-anchored proteins into the ER membrane during vesicle biogenesis, a process that has been linked to the formation of lipid rafts (Bagnat et al., 2000; Kajiwara et al., 2008; Lee et al., 2002; Markham et al., 2011). Furthermore, it was shown that deletion of *ARV1* caused mislocalization of the lipid raft-associated scaffold protein, Ste5p, during pheromone-dependent MAP kinase signaling (H. Jin, McCaffery, & Grote, 2008; Villasmil et al., 2011). More recently a study showed that Arv1p could be a

regulator of the unfolded protein response pathway (UPR), which targets unfolded proteins for degradation at the ER during cellular stress. However, since it has been shown that UPR stimulation is dependent on membrane composition, it is possible that disorganization of lipid rafts in *ARV1* deleted cells stimulates the UPR (Hou et al., 2014; Volmer & Ron, 2015). Our findings that Arv1p is required for maintaining ER ultrastructure could help explain the observed phenotypes since it has been shown that structural integrity of the local membrane environment is a prerequisite for membrane raft formation. (Bagatolli et al., 2010). A loss of local structure integrity could have detrimental effects on lipid raft generation causing them to disperse and cause sterol accumulation in the intracellular membranes as recorded (Tinkelenberg et al., 2000). Since the structural requirements for lipid raft synthesis are universal, it would also explain why the phenotypes observed in mammalian tissue and mice models echo sterol defects observed in yeast. (Lagor et al., 2015; F. Tong et al., 2010). If the ultrastructural organization of the ER does regulate lipid raft formation, then it would be predicted that deletions of other proteins required for maintaining structural integrity would also result in lipid raft defects. To test this hypothesis one could investigate lipid raft formation in *ice2Δ* and *lnp51Δ* which display ER structural defects similar to *Arv1*Δ (Shuliang Chen, Novick, & Ferro-Novick, 2012; Estrada de Martin, Du, Novick, & Ferro-Novick, 2005).

In yeast, non-vesicular transport has been shown to regulate sterol transfer from the ER to the PM. Since non-vesicular transport occurs at membrane contact sites and *arv1*Δ displays both sterol transfer defects and loss of structural integrity of the ER, it is possible that membrane contact site function is dependent on proper ER ultrastructure. If this is the case, then sterol defects seen in *arv1*Δ might be due to loss of membrane contact sites. To test this one could perform microscopy experiments to investigate the abundance of membrane contact sites in *arv1*Δ cells. If a reduction in PM-ER contact sites is observed, then a prediction would be that artificially tethering the PM to the ER would rescue sterol defects observed in *arv1*Δ. Ultimately the function of Arv1p remains poorly defined and further analysis is required to establish a well-defined role.

5.3. Implications of the discovery of yeast compensatory endocytosis and open questions

The existence of a functional link between exocytosis and endocytosis in yeast has been known for many years (Riezman, 1985). However, that the two processes are mechanistically linked through the activity of Sec4p presents a completely new understanding of the coordination of vesicular transport. Amongst the many questions, this discovery raises the perhaps most interesting is if small Rab GTPases could mechanistically link the two processes in all cell types? Before attempting to answer such a question one needs to be aware of the fundamental differences between yeast and mammalian endocytosis. While most of the proteins involved in regulating endocytosis are very well conserved throughout evolution, there are striking differences between the yeast WASp, Las17p, and its mammalian homolog, N-WASp. In mammals, the activity of N-WASp during endocytosis is partially regulated through its interaction with the Rho GTPase Cdc42 (Bu et al., 2010; Anna Marie Sokac et al., 2003). The interaction between N-WASp and Cdc42 is dependent on the N-WASp CRIB (Cdc42 Rac interactive binding) region and binding of $PI(4,5)P_2$ in the PM. Upon binding to Cdc42, N-WASp recruits and stimulates the function of the Arp2/3 complex leading to actin polymerization (Prehoda, Scott, Mullins, & Lim, 2000). This could imply that Cdc42 regulates N-WASp activity similarly to Sec4p regulation of Las17p during yeast compensatory endocytosis. If so, a general mechanism for compensatory endocytosis in mammals would have to be distinct from what is presented in yeast. However, recent evidence suggests that the situation is more complex, since the small Rab GTPase, Rab3, was found to be required for endophilin mediated endocytosis in *C. elegans* (Bai et al., 2010). Further support for Rab GTPases regulating endocytosis has been provided by the discovery that depletion of Rabin 8, a metazoan homolog of Sec2p, by RNAi dramatically reduced endocytosis efficiency in nTERT-RPE cells (J. Wang et al., 2015). Also, it was recently discovered that a Rab8, metazoan Sec4p homolog, isotype, Rab8B, is required for Wnt-stimulated endocytosis in *C.elegans* (Demir et al., 2013). Together these studies show that Rab GTPase-dependent endocytosis has been described in the literature, but how common it is and if Rab stimulated endocytosis does work as a general form of compensatory endocytosis must be proven experimentally in the future.

Another aspect of compensatory endocytosis that remains unknown is how do cells establish sites of endocytosis during the process? Establishment of endocytic sites is generally thought to be stimulated by ubiquitination of receptor proteins on the PM, tagging them for endocytosis (Lu, Drubin, & Sun, 2016). However, our proposed model states that Sec4p stimulation of compensatory endocytosis is independent of receptor proteins. How can actin patch assembly be initiated in absence of receptor stimuli? One possibility is that mixing of the PM with the vesicular membrane stimulates the assembly of actin patches in zones adjacent to sites of exocytosis. Such a model would be similar to the proposed models of compensatory endocytosis in synapses and Xenopus oocytes (Anna Marie Sokac et al., 2003; Takamori et al., 2006). In synapses, it is proposed that cholesterol-rich lipid rafts, deposited in the PM during exocytosis, diffuse out of the active zones, which stimulates clustering of proteins like the v-SNARE Syp2, the synaptotagmin, Syt1, and the synaptic vesicle-associated glycoprotein, SV2. This clustering allows for AP-2 to associate with the proteins stimulating assembly of the endocytic machinery (Haucke, Wenk, Chapman, Farsad, & De Camilli, 2000; Mitter et al., 2003; Mutch et al., 2011; Takamori et al., 2006; Yao, Nowack, Kensel-Hammes, Gardner, & Bajjalieh, 2010). Since AP-2 is dispensable for actin patch formation in yeast it seems unlikely that yeast would rely on AP-2 playing a major role in establishing endocytic sites during yeast compensatory endocytosis (Susheela Y. Carroll et al., 2009; Payne et al., 1988). An alternative model is found in Xenopus where it is believed that, $PI(4,5)P_2$ from the PM mix with the PI(4)P-rich membrane of the cortical granule upon fusion. This mixing recruits Cdc42 which stimulates actin polymerization, leading to stabilization of the partly fused cortical granule at the PM and allows for subsequent compensatory endocytosis (Anna M. Sokac & Bement, 2006; Anna Marie Sokac et al., 2003). Since yeast exocytic vesicles contain high levels of PI(4)P it is possible that local increases in PI(4)P levels due to membrane mixing is what stimulates assembly of actin patches. Interestingly, it was recently shown that the ENTH domain of GlENTHp bound PI(4)P with high affinity (Feliziani et al., 2015). Since the ENTH domain is highly conserved throughout evolution and that Ent1p depends on its ENTH domain to regulate actin patch maturation and coordinates assembly of the patches with Sla2p (Aguilar et al., 2003; Baggett et al., 2003; Sun et al., 2005), it is possible that increases in local PI(4)P levels, due to exocytic vesicle fusion, stimulates assembly at endocytic sites. This hypothesis is supported by the finding that mammalian ANTH domains also have the

ability to bind PI(4)P *in vitro* (Di Paolo & De Camilli, 2006).Testing this hypothesis *in vivo* is challenging due to mutations changing PM phosphoinositide composition generally having severe impacts on cellular viability and causing widespread effects making analysis difficult (A. Audhya et al., 2000; Desrivières, Cooke, Morales-Johansson, Parker, & Hall, 2002; Tahirovic et al., 2005). Therefore, *in vitro* analysis of potential PI(4)P-binding capacity of proteins involved in actin patch establishment would be required to assess if PI(4)P could be a potential stimulator of actin patch assembly during yeast compensatory endocytosis.

Las17p is the major actin nucleation-promoting factor during yeast endocytosis and its activation constitutes the strongest stimulation of Arp2/3 complex-dependent F-actin formation during endocytosis. As a result, its activity is highly regulated by interactions with suppressors and activators alike. The strongest inhibitor of Las17 is Sla1p and it is believed that the interaction between Las17p and Sla1p serves as the final checkpoint before the recruitment of the Arp2/3 complex during endocytosis (Feliciano & Di Pietro, 2012). The interaction between Las17p and Sla1p depends on two polyproline regions in Las17p and two SH3 domains in Sla1p (Feliciano & Di Pietro, 2012). While we show that Sec4p can relieve the inhibition of Las17p by Sla1p in vitro, we do not know how Sec4p regulates this interaction. One possibility is that Sec4p competes with Sla1p for the binding of the polyproline region in Las17p. Once bound to this region Sec4p could promote the release of Las17p from Sal1p. However, since Sec4p does not contain SH3 domains (Dunn, Stearns, & Botstein, 1993; Sato, Fukai, Ishitani, & Nureki, 2007) direct competition for Las17p binding seems unlikely. Another possibility is that Sec4p acts as an allosteric regulator of Las17p causing a conformational shift in the Las17p-Sla1p complex, allowing for Las17p activation of the Arp2/3 complex. Domain binding analysis between Sec4p and Las17p could be performed *in vitro* to help gain a better understanding of the mechanism involved.

One interesting observation made during our experimentation was that the relative maximum level of actin polymerization was never attained when Sla1p inhibition of Las17p was relieved by Sec4p (figure 4.6). This observation suggests that equilibrium between actin polymerization with actin cable degradation occurs sooner in samples where Las17p function is affected by Sec4p and Sla1p compared to samples with

Las17p alone. One explanation for this observation is that the degree of actin cable branching is reduced in samples where Sla1p and Sec4p are added to the experiment, resulting in a 1:1 ratio of actin monomer addition to actin monomer degradation. If this is the case, then actin polymer branching should be affected by addition of Sla1p and Sec4p to the experiment. To investigate this claim one could perform electron microscopy experiments on the actin polymers formed to directly assay the structure. If branching is indeed affected, then it is possible that other factors are required to fully relieve Sla1p inhibition of Las17 in vitro. One candidate for this Bzz1p, an SH3 domain containing protein, shown to stimulate actin polymerization upon binding to Las17p (Soulard et al., 2002). To test this hypothesis one could add purified Bzz1p to the reaction mixture and investigate if full activation is obtained. Another possibility is that Sec4p requires N-terminal di-geranylgeranylation (Garrett et al., 1994; Y. Jiang, Rossi, & Ferro-Novick, 1993) and PM association to achieve optimal activity. Since bacterially purified Sec4p remains unmodified and no PM analog was included in the experimental setup, it is possible that optimal activity was never obtained. To test this hypothesis, Sec4p would need to be purified from yeast and the actin polymerization experiment would have to be conducted with liposomes supplemented to the reaction mixture.

5.4. Concluding remarks

This thesis has provided important new insights into how PM homeostasis is achieved through the mechanistic integration of membrane transport pathways (figure 5.1). While the exact role of Osh4p remains controversial, the discovery that Osh4p associates with the exocyst complex and may act as a direct regulator of exocytosis provides a new potential line of communication between vesicular and non-vesicular transport. Arv1p, while not a direct sterol transporter, is important for maintaining proper ER structural organization and may indirectly provide the foundation for transport communication hubs through lipid rafts and/or membrane contact sites. Finally, finding a direct mechanistic link between endocytosis and exocytosis may prove important in establishing a completely new level of integration of transport pathways in *Saccharomyces cerevisiae*

Figure 5.1 Schematic of current understanding of transport pathway integration in yeast

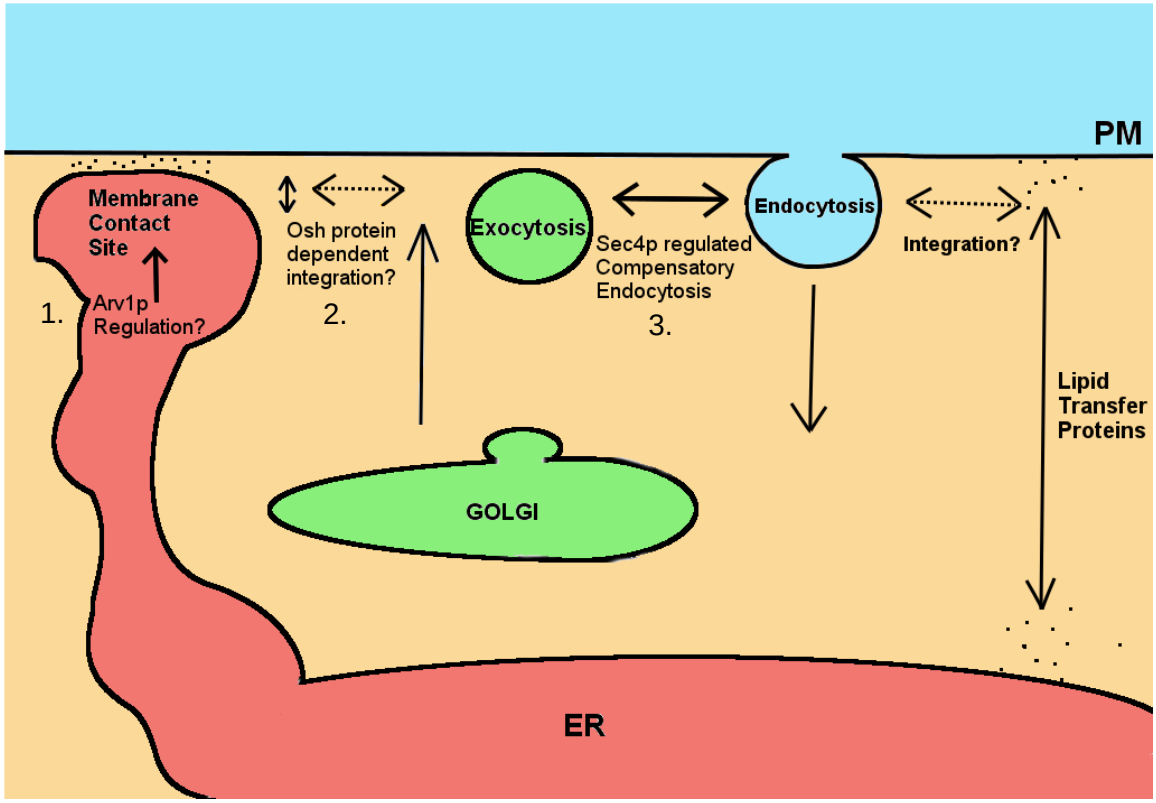

1. Arv1p is a conserved ER protein that regulates ER structure, potentially affecting PM-ER membrane contact sites. **2.** Osh4p has been implicated in both non-vesicular transport and as a potential regulator of exocytosis, potentially integrating non-vesicular and vesicular transport **3.** The small Rab GTPase Sec4p is a mechanistic link between exocytosis and endocytosis integrating these processes in yeast compensatory endocytosis

References

Adamo, J. E., Moskow, J. J., Gladfelter, A. S., Viterbo, D., Lew, D. J., & Brennwald, P. J. (2001). Yeast Cdc42 functions at a late step in exocytosis, specifically during polarized growth of the emerging bud. *The Journal of Cell Biology*, *155*(4), 581–592. http://doi.org/10.1083/jcb.200106065

Adamo, J. E., Rossi, G., & Brennwald, P. (1999). The Rho GTPase Rho3 has a direct role in exocytosis that is distinct from its role in actin polarity. *Molecular Biology of the Cell*, *10*(12), 4121–4133. Retrieved from http://www.ncbi.nlm.nih.gov/entrez/query.fcgi?cmd=Retrieve&db=PubMed&dopt=Citation&list_uids=10588647

Adams, A. E. M., & Pringle, J. R. (1984). Relationship of actin and tubulin distribution to bud growth in wild-type and morphogenetic-mutant Saccharomyces cerevisiae. *Journal of Cell Biology*, *98*(3), 934–945. http://doi.org/10.1083/jcb.98.3.934

Aguilar, R. C., Watson, H. A., & Wendland, B. (2003). The yeast epsin Ent1 is recruited to membranes through multiple independent interactions. *Journal of Biological Chemistry*, *278*(12), 10737–10743. http://doi.org/10.1074/jbc.M211622200

AhYoung, A. P., Jiang, J., Zhang, J., Khoi Dang, X., Loo, J. A., Zhou, Z. H., & Egea, P. F. (2015). Conserved SMP domains of the ERMES complex bind phospholipids and mediate tether assembly. *Proceedings of the National Academy of Sciences of the United States of America*, *112*(25), E3179-88. http://doi.org/10.1073/pnas.1422363112

Albert, S., & Gallwitz, D. (2000). Msb4p, a protein involved in Cdc42p-dependent organization of the actin cytoskeleton, is a Ypt/Rab-specific GAP. *Biological Chemistry*, *381*(5–6), 453–6. http://doi.org/10.1515/BC.2000.059

Alés, E., Tabares, L., Poyato, J. M., Valero, V., Lindau, M., & Alvarez de Toledo, G. (1999). High calcium concentrations shift the mode of exocytosis to the kiss-and-run mechanism. *Nature Cell Biology*, *1*, 40–44. http://doi.org/10.1038/9012

Alfaro, G., Johansen, J., Dighe, S. A., Duamel, G., Kozminski, K. G., & Beh, C. T. (2011). The sterol-binding protein Kes1/Osh4p is a regulator of polarized exocytosis. *Traffic*, *12*(11), 1521–1536. http://doi.org/10.1111/j.1600-0854.2011.01265.x

Allen, D., Thomas, P., & Michell, R. H. (1978). Rapid transbilayer diffusion of 1,2-diacylglycerol and its relevance to control of membrane curvature. *Nature*, *276*,

289–290.

Alory, C., & Balch, W. E. (2003). Molecular evolution of the Rab-escort-protein/guanine-nucleotide-dissociation-inhibitor superfamily. *Molecular Biology of the Cell*, *14*(9), 3857–67. http://doi.org/10.1091/E03-04-0227

Alpy, F., & Tomasetto, C. (2005). Give lipids a START: the StAR-related lipid transfer (START) domain in mammals. *Journal of Cell Science*, *118*(Pt 13), 2791–2801. http://doi.org/10.1242/jcs.02485

Alpy, F., & Tomasetto, C. (2014). START ships lipids across interorganelle space. *Biochimie*. http://doi.org/10.1016/j.biochi.2013.09.015

Amberg, D. C., Burke, D. J., & Strathern, J. N. (2005). *Methods in Yeast Genetics: A Cold Spring Harbor Laboratory Course Manual, 2005 Edition*. *A Cold Spring Harbor Laboratory Course Manual*. Retrieved from http://www.amazon.com/Methods-Yeast-Genetics-Spring-Laboratory/dp/0879697288

Audhya, A., & Emr, S. D. (2002). Stt4 PI 4-kinase localizes to the plasma membrane and functions in the Pkc1-mediated MAP kinase cascade. *Developmental Cell*, *2*(5), 593–605. http://doi.org/10.1016/S1534-5807(02)00168-5

Audhya, A., Foti, M., & Emr, S. D. (2000). Distinct Roles for the Yeast Phosphatidylinositol 4-Kinases, Stt4p and Pik1p, in Secretion, Cell Growth, and Organelle Membrane Dynamics. *Mol Biol Cell.*, *11*(8), 2673–2689. http://doi.org/10.1091/mbc.11.8.2673

Avinoam, O., Schorb, M., Beese, C. J., Briggs, J. A. G., & Kaksonen, M. (2015). Endocytic sites mature by continuous bending and remodeling of the clathrin coat. *Science (New York, N.Y.)*, *348*(6241), 1369–72. http://doi.org/10.1126/science.aaa9555

Babu, M., Vlasblom, J., Pu, S., Guo, X., Graham, C., Bean, B. D. M., … Greenblatt, J. F. (2012). Interaction landscape of membrane-protein complexes in Saccharomyces cerevisiae. *Nature*, *489*(7417), 585–589. http://doi.org/10.1038/nature11354

Bagatolli, L. A., Ipsen, J. H., Simonsen, A. C., & Mouritsen, O. G. (2010). An outlook on organization of lipids in membranes: Searching for a realistic connection with the organization of biological membranes. *Progress in Lipid Research*. http://doi.org/10.1016/j.plipres.2010.05.001

Baggett, J. J., D'Aquino, K. E., & Wendland, B. (2003). The Sla2p Talin Domain Plays a Role in Endocytosis in Saccharomyces cerevisiae. *Genetics*, *165*(4), 1661–1674.

Bagnat, M., Chang, A., & Simons, K. (2001). Plasma membrane proton ATPase Pma1p requires raft association for surface delivery in yeast. *Molecular Biology of the Cell*, *12*(12), 4129–4138. http://doi.org/10.1091/mbc.12.12.4129

Bagnat, M., Keränen, S., Shevchenko, a, Shevchenko, a, & Simons, K. (2000). Lipid rafts function in biosynthetic delivery of proteins to the cell surface in yeast. *Proceedings of the National Academy of Sciences of the United States of America*, *97*(7), 3254–3259. http://doi.org/10.1073/pnas.97.7.3254

Bai, J., Hu, Z., Dittman, J. S., Pym, E. C. G., & Kaplan, J. M. (2010). Endophilin functions as a membrane-bending molecule and is delivered to endocytic zones by exocytosis. *Cell*, *143*(3), 430–441. http://doi.org/10.1016/j.cell.2010.09.024

Balla, A., & Balla, T. (2006). Phosphatidylinositol 4-kinases: old enzymes with emerging functions. *Trends in Cell Biology*. http://doi.org/10.1016/j.tcb.2006.05.003

Balla, T., Szentpetery, Z., & Kim, Y. J. (2009). Phosphoinositide signaling: new tools and insights. *Physiology (Bethesda, Md.)*, *24*, 231–244. http://doi.org/10.1152/physiol.00014.2009

Bankaitis, V. A., Aitken, J. R., Cleves, A. E., & Dowhan, W. (1990). An essential role for a phospholipid transfer protein in yeast Golgi function. *Nature*, *347*(6293), 561–562. http://doi.org/10.1038/347561a0

Bankaitis, V. A., Malehorn, D. E., Emr, S. D., & Greene, R. (1989). The Saccharomyces cerevisiae SEC14 gene encodes a cytosolic factor that is required for transport of secretory proteins from the yeast Golgi complex. *Journal of Cell Biology*, *108*(4), 1271–1281. http://doi.org/10.1083/jcb.108.4.1271

Barker, S. L., Lee, L., Pierce, B. D., Maldonado-Báez, L., Drubin, D. G., & Wendland, B. (2007). Interaction of the endocytic scaffold protein Pan1 with the type I myosins contributes to the late stages of endocytosis. *Molecular Biology of the Cell*, *18*(8), 2893–2903. http://doi.org/10.1091/mbc.E07

Baumann, N. A., Sullivan, D. P., Ohvo-Rekil??, H., Simonot, C., Pottekat, A., Klaassen, Z., … Menon, A. K. (2005). Transport of newly synthesized sterol to the sterol-enriched plasma membrane occurs via nonvesicular equilibration. *Biochemistry*, *44*(15), 5816–5826. http://doi.org/10.1021/bi048296z

Becker, K. a, & Hart, N. H. (1999). Reorganization of filamentous actin and myosin-II in zebrafish eggs correlates temporally and spatially with cortical granule exocytosis. *Journal of Cell Science*, *112 (Pt 1*, 97–110.

Beh, C. T., Alfaro, G., Duamel, G., Sullivan, D. P., Kersting, M. C., Dighe, S., … Menon, A. K. (2009). Yeast oxysterol-binding proteins: Sterol transporters or regulators of cell polarization? In *Molecular and Cellular Biochemistry* (Vol. 326, pp. 9–13). http://doi.org/10.1007/s11010-008-9999-7

Beh, C. T., Brizzio, V., & Rose, M. D. (1997). KAR5 encodes a novel pheromone-inducible protein required for homotypic nuclear fusion. *Journal of Cell Biology*, *139*(5), 1063–1076. http://doi.org/10.1083/jcb.139.5.1063

Beh, C. T., Cool, L., Phillips, J., & Rine, J. (2001). Overlapping functions of the yeast oxysterol-binding protein homologues. *Genetics*, *157*(3), 1117–1140.

Beh, C. T., McMaster, C. R., Kozminski, K. G., & Menon, A. K. (2012). A Detour for Yeast Oxysterol-Binding Proteins. *The Journal of Biological Chemistry*, *287*(14), 11481–11488. http://doi.org/10.1074/jbc.R111.338400

Beh, C. T., & Rine, J. (2004). A role for yeast oxysterol-binding protein homologs in endocytosis and in the maintenance of intracellular sterol-lipid distribution. *Journal of Cell Science*, *117*(Pt 14), 2983–2996. http://doi.org/10.1242/jcs.01157

Beh, C. T., & Rose, M. D. (1995). Two redundant systems maintain levels of resident proteins within the yeast endoplasmic reticulum. *Proceedings of the National Academy of Sciences of the United States of America*, *92*(21), 9820–3. http://doi.org/10.1073/pnas.92.21.9820

Beitel, G. J., Clark, S. G., & Horvitz, H. R. (1990). Caenorhabditis elegans ras gene let-60 acts as a switch in the pathway of vulval induction. *Nature*. http://doi.org/10.1038/348503a0

Bement, W. M., Benink, H., Mandato, C. A., & Swelstad, B. B. (2000). Evidence for direct membrane retrieval following cortical granule exocytosis in exocytosis in Xenopus oocytes and eggs. *Journal of Experimental Zoology*, *286*(7), 767–775. http://doi.org/10.1002/(SICI)1097-010X(20000601)286:7<767::AID-JEZ11>3.0.CO;2-L

Benjamin, J. J. R., Poon, P. P., Lewis, S. M., Auger, A., Wong, T. A., Singer, R. A., & Johnston, G. C. (2011). The yeast Arf GTPase-activating protein Age1 is regulated by phospholipase D for post-Golgi vesicular transport. *Journal of Biological Chemistry*, *286*(7), 5187–5196. http://doi.org/10.1074/jbc.M110.185108

Berchtold, D., & C.Walther, T. (2009). TORC2 Plasma Membrane Localization Is Essential for Cell Viability and Restricted to a Distinct Domain. *Molecular Biology of the Cell*, *20*, 1565–1575. http://doi.org/10.1091/mbc.E08

Boettner, D. R., D'Agostino, J. L., Torres, O. T., Daugherty-Clarke, K., Uygur, A., Reider, A., … Goode, B. L. (2009). The F-BAR Protein Syp1 Negatively Regulates WASp-Arp2/3 Complex Activity during Endocytic Patch Formation. *Current Biology*, *19*(23), 1979–1987. http://doi.org/10.1016/j.cub.2009.10.062

Boyd, C., Hughes, T., Pypaert, M., & Novick, P. (2004). Vesicles carry most exocyst subunits to exocytic sites marked by the remaining two subunits, Sec3p and Exo70p. *Journal of Cell Biology*, *167*(5), 889–901. http://doi.org/10.1083/jcb.200408124

Bu, W., Lim, K. B., Yu, Y. H., Chou, A. M., Sudhaharan, T., & Ahmed, S. (2010). Cdc42 interaction with N-WASP and Toca-1 regulates membrane tubulation, vesicle

formation and vesicle motility: Implications for endocytosis. *PLoS ONE*, *5*(8). http://doi.org/10.1371/journal.pone.0012153

Burston, H. E., Maldonado-Báez, L., Davey, M., Montpetit, B., Schluter, C., Wendland, B., & Conibear, E. (2009). Regulators of yeast endocytosis identified by systematic quantitative analysis. *Journal of Cell Biology*, *185*(6), 1097–1110. http://doi.org/10.1083/jcb.200811116

Calero, M., Chen, C. Z., Zhu, W., Winand, N., Havas, K. A., Gilbert, P. M., … Collins, R. N. (2003). Dual prenylation is required for Rab protein localization and function. *Molecular Biology of the Cell*, *14*(5), 1852–67. http://doi.org/10.1091/mbc.E02-11-0707

Carlier, M. F., Pernier, J., Montaville, P., Shekhar, S., & Kühn, S. (2015). Control of polarized assembly of actin filaments in cell motility. *Cellular and Molecular Life Sciences*. http://doi.org/10.1007/s00018-015-1914-2

Carroll, S. Y., Stimpson, H. E. M., Weinberg, J., Toret, C. P., Sun, Y., & Drubin, D. G. (2012). Analysis of yeast endocytic site formation and maturation through a regulatory transition point. *Molecular Biology of the Cell*, *23*(4), 657–668. http://doi.org/10.1091/mbc.E11-02-0108

Carroll, S. Y., Stirling, P. C., Stimpson, H. E. M., Gießelmann, E., Schmitt, M. J., & Drubin, D. G. (2009). A Yeast Killer Toxin Screen Provides Insights into A/B Toxin Entry, Trafficking, and Killing Mechanisms. *Developmental Cell*, *17*(4), 552–560. http://doi.org/10.1016/j.devcel.2009.08.006

Caudron, F., & Barral, Y. (2009). Septins and the Lateral Compartmentalization of Eukaryotic Membranes. *Developmental Cell*. http://doi.org/10.1016/j.devcel.2009.04.003

Chartron, J. W., Clemons, W. M., & Suloway, C. J. M. (2012). The complex process of GETting tail-anchored membrane proteins to the ER. *Current Opinion in Structural Biology*. http://doi.org/10.1016/j.sbi.2012.03.001

Chen, C. Y., & Graham, T. R. (1998). An arf1Δ synthetic lethal screen identifies a new clathrin heavy chain conditional allele that perturbs vacuolar protein transport in Saccharomyces cerevisiae. *Genetics*, *150*(2), 577–589.

Chen, C. Z., Calero, M., DeRegis, C. J., Heidtman, M., Barlowe, C., & Collins, R. N. (2004). Genetic analysis of yeast Yip1p function reveals a requirement for Golgi-localized Rab proteins and Rab-guanine nucleotide dissociation inhibitor. *Genetics*, *168*(4), 1827–1841. http://doi.org/10.1534/genetics.104.032888

Chen, G. C., Kim, Y. J., & Chan, C. S. M. (1997). The Cdc42 GTPase-associated proteins Gic1 and Gic2 are required for polarized cell growth in Saccharomyces cerevisiae. *Genes and Development*, *11*(22), 2958–2971.

http://doi.org/10.1101/gad.11.22.2958

Chen, Q., & Pollard, T. D. (2013). Actin filament severing by cofilin dismantles actin patches and produces mother filaments for new patches. *Current Biology*, *23*(13), 1154–1162. http://doi.org/10.1016/j.cub.2013.05.005

Chen, S., Novick, P., & Ferro-Novick, S. (2012). ER network formation requires a balance of the dynamin-like GTPase Sey1p and the Lunapark family member Lnp1p. *Nature Cell Biology*, *14*(7), 707–16. http://doi.org/10.1038/ncb2523

Chen, S., Wang, J., Muthusamy, B. P., Liu, K., Zare, S., Andersen, R. J., & Graham, T. R. (2006). Roles for the Drs2p-Cdc50p complex in protein transport and phosphatidylserine asymmetry of the yeast plasma membrane. *Traffic*, *7*(11), 1503–1517. http://doi.org/10.1111/j.1600-0854.2006.00485.x

Chi, R. J., Torres, O. T., Segarra, V. a, Lansley, T., Chang, J. S., Newpher, T. M., & Lemmon, S. K. (2012). Role of Scd5, a protein phosphatase-1 targeting protein, in phosphoregulation of Sla1 during endocytosis. *Journal of Cell Science*, *125*(Pt 20), 4728–39. http://doi.org/10.1242/jcs.098871

Chung, J., Torta, F., Masai, K., Lucast, L., Czapla, H., Tanner, L. B., … De Camilli, P. (2015). PI4P/phosphatidylserine countertransport at ORP5- and ORP8-mediated ER-plasma membrane contacts. *Science*, *349*(6246), 428–32. http://doi.org/10.1126/science.aab1370

Clark, B. J. (2012). The mammalian START domain protein family in lipid transport in health and disease. *Journal of Endocrinology*. http://doi.org/10.1530/JOE-11-0313

Cleves, A. E., McGee, T. P., Whitters, E. A., Champlon, K. M., Altken, J. R., Dowhan, W., … Bankaitis, V. A. (1991). Mutations in the CDP-choline pathway for phospholipid biosynthesis bypass the requirement for an essential phospholipid transfer protein. *Cell*, *64*(4), 789–800. http://doi.org/10.1016/0092-8674(91)90508-V

Cleves, A. E., Novick, P. J., & Bankaitis, V. A. (1989). Mutations in the SAC1 gene suppress defects in yeast Golgi and yeast actin function. *Journal of Cell Biology*, *109*(6 I), 2939–2950. http://doi.org/10.1083/jcb.109.6.2939

Cockcroft, S. (2001). Phosphatidylinositol transfer proteins couple lipid transport to phosphoinositide synthesis. *Seminars in Cell {&} Developmental Biology*, *12*(2), 183–191. http://doi.org/10.1006/scdb.2000.0235

Copic, A., Dorrington, M., Pagant, S., Barry, J., Lee, M. C. S., Singh, I., … Miller, E. A. (2009). Genomewide analysis reveals novel pathways affecting endoplasmic reticulum homeostasis, protein modification and quality control. *Genetics*, *182*(3), 757–769. http://doi.org/10.1534/genetics.109.101105

Cremona, O., & De Camilli, P. (1997). Synaptic vesicle endocytosis. *Current Opinion in*

Neurobiology. http://doi.org/10.1016/S0959-4388(97)80059-1

Creutz, C. E., Snyder, S. L., & Schulz, T. A. (2004). Characterization of the yeast tricalbins: Membrane-bound multi-C2-domain proteins that form complexes involved in membrane trafficking. *Cellular and Molecular Life Sciences*, *61*(10), 1208–1220. http://doi.org/10.1007/s00018-004-4029-8

Curwin, A. J., Fairn, G. D., & McMaster, C. R. (2009). Phospholipid transfer protein Sec14 is required for trafficking from endosomes and regulates distinct trans-golgi export pathways. *Journal of Biological Chemistry*, *284*(11), 7364–7375. http://doi.org/10.1074/jbc.M808732200

D'Agostino, J. L., & Goode, B. L. (2005). Dissection of Arp2/3 complex actin nucleation mechanism and distinct roles for its nucleation-promoting factors in Saccharomyces cerevisiae. *Genetics*, *171*(1), 35–47. http://doi.org/10.1534/genetics.105.040634

Das, A., Slaughter, B. D., Unruh, J. R., Bradford, W. D., Alexander, R., Rubinstein, B., & Li, R. (2012). Flippase-mediated phospholipid asymmetry promotes fast Cdc42 recycling in dynamic maintenance of cell polarity. *Nature Cell Biology*, *14*(3), 304–310. http://doi.org/10.1038/ncb2444

De Craene, J.-O., Coleman, J., de Martin, P. E., Pypaert, M., Anderson, S., Yates, III, J. R., … *Department. (2006). Rtn1p is involved in structuring the cortical endoplasmic reticulum. *Molecular Biology of the Cell*, *17*(August), 3009–3020. http://doi.org/10.1091/mbc.E06

de Saint-Jean, M., Delfosse, V., Douguet, D., Chicanne, G., Payrastre, B., Bourguet, W., … Drin, G. (2011). Osh4p exchanges sterols for phosphatidylinositol 4-phosphate between lipid bilayers. *Journal of Cell Biology*, *195*(6), 965–978. http://doi.org/10.1083/jcb.201104062

Deleu, M., Crowet, J. M., Nasir, M. N., & Lins, L. (2014). Complementary biophysical tools to investigate lipid specificity in the interaction between bioactive molecules and the plasma membrane: A review. *Biochimica et Biophysica Acta - Biomembranes*, *1838*(12), 3171–3190. http://doi.org/10.1016/j.bbamem.2014.08.023

Demir, K., Kirsch, N., Beretta, C. A., Erdmann, G., Ingelfinger, D., Moro, E., … Boutros, M. (2013). RAB8B Is Required for Activity and Caveolar Endocytosis of LRP6. *Cell Reports*, *4*(6), 1224–1234. http://doi.org/10.1016/j.celrep.2013.08.008

Desrivières, S., Cooke, F. T., Morales-Johansson, H., Parker, P. J., & Hall, M. N. (2002). Calmodulin controls organization of the actin cytoskeleton via regulation of phosphatidylinositol (4,5)-bisphosphate synthesis in Saccharomyces cerevisiae. *The Biochemical Journal*, *366*(Pt 3), 945–951. http://doi.org/10.1042/BJ20020429

Desrivières, S., Cooke, F. T., Parker, P. J., & Hall, M. N. (1998). MSS4, a

phosphatidylinositol-4-phosphate 5-kinase required for organization of the actin cytoskeleton in Saccharomyces cerevisiae. *Journal of Biological Chemistry*, *273*(25), 15787–15793. http://doi.org/10.1074/jbc.273.25.15787

Di Paolo, G., & De Camilli, P. (2006). Phosphoinositides in cell regulation and membrane dynamics. *Nature*, *443*(7112), 651–657. http://doi.org/10.1038/nature05185

Dickson, R. C., Sumanasekera, C., & Lester, R. L. (2006). Functions and metabolism of sphingolipids in Saccharomyces cerevisiae. *Progress in Lipid Research*. http://doi.org/10.1016/j.plipres.2006.03.004

Dighe, S. A., & Kozminski, K. G. (2008). Swf1p, a member of the DHHC-CRD family of palmitoyltransferases, regulates the actin cytoskeleton and polarized secretion independently of its DHHC motif. *Molecular Biology of the Cell*, *Akinleye,*(10), 4454–68. http://doi.org/10.1091/mbc.E08-03-0252

Diril, M. K., Wienisch, M., Jung, N., Klingauf, J., & Haucke, V. (2006). Stonin 2 is an AP-2-dependent endocytic sorting adaptor for synaptotagmin internalization and recycling. *Developmental Cell*, *10*(2), 233–244. http://doi.org/10.1016/j.devcel.2005.12.011

Donovan, K. W., & Bretscher, A. (2015). Tracking individual secretory vesicles during exocytosis reveals an ordered and regulated process. *Journal of Cell Biology*, *210*(2), 181–189. http://doi.org/10.1083/jcb.201501118

Dores, M. R., Schnell, J. D., Maldonado-Baez, L., Wendland, B., & Hicke, L. (2010). The function of yeast Epsin and Ede1 ubiquitin-binding domains during receptor internalization. *Traffic*, *11*(1), 151–160. http://doi.org/10.1111/j.1600-0854.2009.01003.x

Drin, G., von Filseck, J. M., & Čopič, A. (2016). New molecular mechanisms of inter-organelle lipid transport. *Biochemical Society Transactions*, *44*(2), 486–92. http://doi.org/10.1042/BST20150265

Dudley, A. M., Janse, D. M., Tanay, A., Shamir, R., & Church, G. M. (2005). A global view of pleiotropy and phenotypically derived gene function in yeast. *Molecular Systems Biology*, *1*, 2005.0001. http://doi.org/10.1038/msb4100004

Duncan, M. C., Cope, M. J., Goode, B. L., Wendland, B., & Drubin, D. G. (2001). Yeast Eps15-like endocytic protein, Pan1p, activates the Arp2/3 complex. *Nature Cell Biology*, *3*(7), 687–90. http://doi.org/10.1038/35083087

Duncan, M. C., & Peifer, M. (2008). Regulating polarity by directing traffic: Cdc42 prevents adherens junctions from Crumblin' aPart. *Journal of Cell Biology*. http://doi.org/10.1083/jcb.200811057

Dunn, B., Stearns, T., & Botstein, D. (1993). Specificity domains distinguish the Ras-related GTPases Ypt1 and Sec4. *Nature*, *362*(6420), 563–565. http://doi.org/10.1038/362563a0

Ercan, E., Momburg, F., Engel, U., Temmerman, K., Nickel, W., & Seedorf, M. (2009). A conserved, lipid-mediated sorting mechanism of yeast Ist2 and mammalian STIM proteins to the peripheral ER. *Traffic*, *10*(12), 1802–1818. http://doi.org/10.1111/j.1600-0854.2009.00995.x

Estrada de Martin, P., Du, Y., Novick, P., & Ferro-Novick, S. (2005). Ice2p is important for the distribution and structure of the cortical ER network in Saccharomyces cerevisiae. *Journal of Cell Science*, *118*(Pt 1), 65–77. http://doi.org/10.1242/jcs.01583

Faini, M., Beck, R., Wieland, F. T., & Briggs, J. A. G. (2013). Vesicle coats: Structure, function, and general principles of assembly. *Trends in Cell Biology*. http://doi.org/10.1016/j.tcb.2013.01.005

Fairn, G. D., Curwin, A. J., Stefan, C. J., & McMaster, C. R. (2007). The oxysterol binding protein Kes1p regulates Golgi apparatus phosphatidylinositol-4-phosphate function. *Proceedings of the National Academy of Sciences of the United States of America*, *104*(39), 15352–7. http://doi.org/10.1073/pnas.0705571104

Fairn, G. D., Hermansson, M., Somerharju, P., & Grinstein, S. (2011). Phosphatidylserine is polarized and required for proper Cdc42 localization and for development of cell polarity. *Nat. Cell Biol.*, *13*(12), 1424–1430. http://doi.org/10.1038/ncb2351

Fairn, G. D., Hermansson, M., Somerharju, P., & Grinstein, S. (2011). Phosphatidylserine polarization is required for proper Cdc42 localization and for development of cell polarity. *Febs Journal*, *278*, 142.

Fairn, G. D., & McMaster, C. R. (2008). Emerging roles of the oxysterol-binding protein family in metabolism, transport, and signaling. *Cellular and Molecular Life Sciences*. http://doi.org/10.1007/s00018-007-7325-2

Fang, M., Kearns, B. G., Gedvilaite, A., Kagiwada, S., Kearns, M., Fung, M. K., & Bankaitis, V. A. (1996). Kes1p shares homology with human oxysterol binding protein and participates in a novel regulatory pathway for yeast Golgi-derived transport vesicle biogenesis. *The EMBO Journal*, *15*(23), 6447–59. Retrieved from http://www.pubmedcentral.nih.gov/articlerender.fcgi?artid=452470&tool=pmcentrez&rendertype=abstract

Faulhammer, F., Kanjilal-Kolar, S., Kn??dler, A., Lo, J., Lee, Y., Konrad, G., & Mayinger, P. (2007). Growth control of golgi phosphoinositides by reciprocal localization of sac1 lipid phosphatase and pik1 4-kinase. *Traffic*, *8*(11), 1554–1567. http://doi.org/10.1111/j.1600-0854.2007.00632.x

Feliciano, D., & Di Pietro, S. M. (2012). SLAC, a complex between Sla1 and Las17, regulates actin polymerization during clathrin-mediated endocytosis. *Molecular Biology of the Cell*, *23*, 4256–4272. http://doi.org/10.1091/mbc.E11-12-1022

Feliziani, C., Zamponi, N., Gottig, N., Rópolo, A. S., Lanfredi-Rangel, A., & Touz, M. C. (2015). The giardial ENTH protein participates in lysosomal protein trafficking and endocytosis. *Biochimica et Biophysica Acta - Molecular Cell Research*, *1853*(3), 646–659. http://doi.org/10.1016/j.bbamcr.2014.12.034

Ferguson, S., & De Camilli, P. (2012). Dynamin, a membrane remodelling GTPase. *Nat Rev Mol Cell Biol*, *13*(2), 75–88. http://doi.org/10.1038/nrm3266

Fernández-Alfonso, T., Kwan, R., & Ryan, T. A. (2006). Synaptic Vesicles Interchange Their Membrane Proteins with a Large Surface Reservoir during Recycling. *Neuron*, *51*(2), 179–186. http://doi.org/10.1016/j.neuron.2006.06.008

Fernández-Murray, J. P., & McMaster, C. R. (2005). Glycerophosphocholine catabolism as a new route for choline formation for phosphatidylcholine synthesis by the Kennedy pathway. *Journal of Biological Chemistry*, *280*(46), 38290–38296. http://doi.org/10.1074/jbc.M507700200

Ferrell, J. E., Lee, K. J., & Huestis, W. H. (1985). Lipid transfer between phosphatidylcholine vesicles and human erythrocytes: exponential decrease in rate with increasing acyl chain length. *Biochemistry*, *24*(12), 2857–2864. http://doi.org/10.1021/bi00333a007

Fesce, R., Grohovaz, F., Valtorta, F., & Meldolesi, J. (1994). Neurotransmitter release: fusion or “kiss-and-run”? *Trends in Cell Biology*, *4*(1), 1–4. http://doi.org/10.1016/0962-8924(94)90025-6

Finger, F. P., Hughes, T. E., & Novick, P. (1998). Sec3p is a spatial landmark for polarized secretion in budding yeast. *Cell*, *92*(4), 559–571. http://doi.org/10.1016/S0092-8674(00)80948-4

Fischer, M. A., Temmerman, K., Ercan, E., Nickel, W., & Seedorf, M. (2009). Binding of plasma membrane lipids recruits the yeast integral membrane protein Ist2 to the cortical ER. *Traffic*, *10*(8), 1084–1097. http://doi.org/10.1111/j.1600-0854.2009.00926.x

Flanagan, C. a, Schnieders, E. a, Emerick, a W., Kunisawa, R., Admon, a, & Thorner, J. (1993). Phosphatidylinositol 4-kinase: gene structure and requirement for yeast cell viability. *Science (New York, N.Y.)*, *262*(5138), 1444–1448. http://doi.org/10.1126/science.8248783

Foti, M., Audhya, A., & Emr, S. D. (2001). Sac1 lipid phosphatase and Stt4 phosphatidylinositol 4-kinase regulate a pool of phosphatidylinositol 4-phosphate that functions in the control of the actin cytoskeleton and vacuole morphology.

Molecular Biology of the Cell, *12*(8), 2396–411. http://doi.org/10.1091/mbc.12.8.2396

Friesen, H., Humphries, C., Ho, Y., Schub, O., Colwill, K., & Andrews, B. (2006). Characterization of the yeast amphiphysins Rvs161p and Rvs167p reveals roles for the Rvs heterodimer in vivo. *Molecular Biology of the Cell*, *17*(3), 1306–21. http://doi.org/10.1091/mbc.E05-06-0476

Fröhlich, F., Moreira, K., Aguilar, P. S., Hubner, N. C., Mann, M., Walter, P., & Walther, T. C. (2009). A genome-wide screen for genes affecting eisosomes reveals Nce102 function in sphingolipid signaling. *Journal of Cell Biology*, *185*(7), 1227–1242. http://doi.org/10.1083/jcb.200811081

Fujiwara, T., Tanaka, K., Mino, a, Kikyo, M., Takahashi, K., Shimizu, K., & Takai, Y. (1998). Rho1p-Bni1p-Spa2p interactions: implication in localization of Bni1p at the bud site and regulation of the actin cytoskeleton in Saccharomyces cerevisiae. *Molecular Biology of the Cell*, *9*(5), 1221–1233. http://doi.org/10.1091/mbc.9.5.1221

Gagny, B., Wiederkehr, a, Dumoulin, P., Winsor, B., Riezman, H., & Haguenauer-Tsapis, R. (2000). A novel EH domain protein of Saccharomyces cerevisiae, Ede1p, involved in endocytosis. *Journal of Cell Science*, *113 (Pt 1*, 3309–19. Retrieved from http://www.ncbi.nlm.nih.gov/pubmed/10954428

Gall, W. E., Geething, N. C., Hua, Z., Ingram, M. F., Liu, K., Chen, S. I., & Graham, T. R. (2002). Drs2p-dependent formation of exocytic clathrin-coated vesicles in vivo. *Current Biology*, *12*(18), 1623–1627. http://doi.org/10.1016/S0960-9822(02)01148-X

Gallo-Ebert, C., McCourt, P. C., Donigan, M., Villasmil, M. L., Chen, W., Pandya, D., … Nickels, J. T. (2012). Arv1 lipid transporter function is conserved between pathogenic and nonpathogenic fungi. *Fungal Genetics and Biology*, *49*(2), 101–113. http://doi.org/10.1016/j.fgb.2011.11.006

Gao, X. D., Albert, S., Tcheperegine, S. E., Burd, C. G., Gallwitz, D., & Bi, E. (2003). The GAP activity of Msb3p and Msb4p for the Rab GTPase Sec4p is required for efficient exocytosis and actin organization. *Journal of Cell Biology*, *162*(4), 635–646. http://doi.org/10.1083/jcb.200302038

Garrenton, L. S., Stefan, C. J., McMurray, M. A., Emr, S. D., & Thorner, J. (2010). Pheromone-induced anisotropy in yeast plasma membrane phosphatidylinositol-4,5-bisphosphate distribution is required for MAPK signaling. *Proceedings of the National Academy of Sciences of the United States of America*, *107*(26), 11805–11810. http://doi.org/10.1073/pnas.1005817107

Garrett, M. D., Zahner, J. E., Cheney, C. M., & Novick, P. J. (1994). GDI1 encodes a GDP dissociation inhibitor that plays an essential role in the yeast secretory pathway. *The EMBO Journal*, *13*(7), 1718–1728.

Gatta, A. T., Wong, L. H., Sere, Y. Y., Calderón-Noreña, D. M., Cockcroft, S., Menon, A. K., & Levine, T. P. (2015). A new family of StART domain proteins at membrane contact sites has a role in ER-PM sterol transport. *eLife*, *4*(MAY), 1–21. http://doi.org/10.7554/eLife.07253

Gauthier-Kemper, A., Kahms, M., & Klingauf, J. (2015). Restoring synaptic vesicles during compensatory endocytosis. *Essays in Biochemistry*, *57*(1), 121–134. http://doi.org/10.1042/bse0570121

Gavin, A.-C., Aloy, P., Grandi, P., Krause, R., Boesche, M., Marzioch, M., … Superti-Furga, G. (2006). Proteome survey reveals modularity of the yeast cell machinery. *Nature*, *440*(7084), 631–6. http://doi.org/10.1038/nature04532

Gavin, A.-C., Bösche, M., Krause, R., Grandi, P., Marzioch, M., Bauer, A., … Superti-Furga, G. (2002). Functional organization of the yeast proteome by systematic analysis of protein complexes. *Nature*, *415*(6868), 141–147. http://doi.org/10.1038/415141a

Georgiev, A. G., Sullivan, D. P., Kersting, M. C., Dittman, J. S., Beh, C. T., & Menon, A. K. (2011). Osh proteins regulate membrane sterol organization but are not required for sterol movement between the ER and PM. *Traffic*, *12*(10), 1341–1355. http://doi.org/10.1111/j.1600-0854.2011.01234.x

Gietz, R. D., & Akio, S. (1988). New yeast-Escherichia coli shuttle vectors constructed with in vitro mutagenized yeast genes lacking six-base pair restriction sites. *Gene*, *74*(2), 527–534. http://doi.org/10.1016/0378-1119(88)90185-0

Goñi, F. M., & Alonso, A. (2009). Effects of ceramide and other simple sphingolipids on membrane lateral structure. *Biochimica et Biophysica Acta - Biomembranes*. http://doi.org/10.1016/j.bbamem.2008.09.002

Goode, B. L., Eskin, J. A., & Wendland, B. (2015). Actin and endocytosis in budding yeast. *Genetics*, *199*(2), 315–58. http://doi.org/10.1534/genetics.112.145540

Goode, B. L., Rodal, A. A., Barnes, G., & Drubin, D. G. (2001). Activation of the Arp2/3 complex by the actin filament binding protein Abp1p. *Journal of Cell Biology*, *152*(3), 627–634. http://doi.org/10.1083/jcb.153.3.627

Grosshans, B. L., & Novick, P. (2008). Identification and Verification of Sro7p as an Effector of the Sec4p Rab GTPase. *Methods in Enzymology*. http://doi.org/10.1016/S0076-6879(07)38007-5

Gundelfinger, E. D., Kessels, M. M., & Qualmann, B. (2003). Temporal and spatial coordination of exocytosis and endocytosis. *Nature Reviews. Molecular Cell Biology*, *4*(2), 127–139. http://doi.org/10.1038/nrm1016

Guo, W., Roth, D., Walch-Solimena, C., & Novick, P. (1999). The exocyst is an effector

for Sec4P, targeting secretory vesicles to sites of exocytosis. *EMBO Journal*, *18*(4), 1071–1080. http://doi.org/10.1093/emboj/18.4.1071

Hama, H., Schnieders, E. A., Thorner, J., Takemoto, J. Y., & DeWald, D. B. (1999). Direct involvement of phosphatidylinositol 4-phosphate in secretion in the yeast Saccharomyces cerevisiae. *Journal of Biological Chemistry*, *274*(48), 34294–34300. http://doi.org/10.1074/jbc.274.48.34294

Hamburger, Z. A., Hamburger, A. E., West, A. P. J., & Weis, W. I. (2006). Crystal structure of the S.cerevisiae exocyst component Exo70p. *Journal of Molecular Biology*, *356*(1), 9–21. http://doi.org/10.1016/j.jmb.2005.09.099

Hammond, G. R. V, Schiavo, G., & Irvine, R. F. (2009). Immunocytochemical techniques reveal multiple, distinct cellular pools of PtdIns4P and PtdIns(4,5)P(2). *The Biochemical Journal*, *422*(1), 23–35. http://doi.org/10.1042/BJ20090428

Han, G. S., Audhya, A., Markley, D. J., Emr, S. D., & Carman, G. M. (2002). The Saccharomyces cerevisiae LSB6 gene encodes phosphatidylinositol 4-kinase activity. *Journal of Biological Chemistry*, *277*(49), 47709–47718. http://doi.org/10.1074/jbc.M207996200

Hanada, K., Kumagai, K., Tomishige, N., & Yamaji, T. (2009). CERT-mediated trafficking of ceramide. *Biochimica et Biophysica Acta - Molecular and Cell Biology of Lipids*. http://doi.org/10.1016/j.bbalip.2009.01.006

Hanson, P. K., Malone, L., Birchmore, J. L., & Nichols, J. W. (2003). Lem3p is essential for the uptake and potency of alkylphosphocholine drugs, edelfosine and miltefosine. *Journal of Biological Chemistry*, *278*(38), 36041–36050. http://doi.org/10.1074/jbc.M305263200

Harris, K. P., & Tepass, U. (2010). Cdc42 and Vesicle Trafficking in Polarized Cells. *Traffic*. http://doi.org/10.1111/j.1600-0854.2010.01102.x

Harsay, E., & Bretscher, a. (1995). Parallel Secretory Pathways to the Cell-Surface In Yeast. *Journal Of Cell Biology*, *131*(2), 297–310.

Hashizume, K., Cheng, Y.-S., Hutton, J. L., Chiu, C. -h., & Carr, C. M. (2009). Yeast Sec1p Functions before and after Vesicle Docking. *Molecular Biology of the Cell*, *20*(22), 4673–4685. http://doi.org/10.1091/mbc.E09-02-0172

Hattendorf, D. a, Andreeva, A., Gangar, A., Brennwald, P. J., & Weis, W. I. (2007). Structure of the yeast polarity protein Sro7 reveals a SNARE regulatory mechanism. *Nature*, *446*(7135), 567–571. http://doi.org/10.1038/nature05635

Haucke, V., Wenk, M. R., Chapman, E. R., Farsad, K., & De Camilli, P. (2000). Dual interaction of synaptotagmin with µ2- and α-adaptin facilitates clathrin-coated pit nucleation. *Embo J*, *19*(22), 6011–6019. http://doi.org/10.1093/emboj/19.22.6011

He, B., & Guo, W. (2009). The exocyst complex in polarized exocytosis. *Current Opinion in Cell Biology*. http://doi.org/10.1016/j.ceb.2009.04.007

He, B., Xi, F., Zhang, X., Zhang, J., & Guo, W. (2007). Exo70 interacts with phospholipids and mediates the targeting of the exocyst to the plasma membrane. *The EMBO Journal*, *26*(18), 4053–4065. http://doi.org/10.1038/sj.emboj.7601834

Hearn, J. D., Lester, R. L., & Dickson, R. C. (2003). The uracil transporter Fur4p associates with lipid rafts. *Journal of Biological Chemistry*, *278*(6), 3679–3686. http://doi.org/10.1074/jbc.M209170200

Helfrich, W. (1973). Elastic Properties of Lipid Bilayers: Theory and Possible Experiments. *Zeitschrift Fur Naturforschung - Section C Journal of Biosciences*, *28*(11–12), 693–703. http://doi.org/10.1515/znc-1973-11-1209

Henne, W. M., Liou, J., & Emr, S. D. (2015). Molecular mechanisms of inter-organelle ER-PM contact sites. *Current Opinion in Cell Biology*. http://doi.org/10.1016/j.ceb.2015.05.001

Henneberry, A. L., Lagace, T. A., Ridgway, N. D., & McMaster, C. R. (2001). Phosphatidylcholine synthesis influences the diacylglycerol homeostasis required for SEC14p-dependent Golgi function and cell growth. *Molecular Biology of the Cell*, *12*(3), 511–20. Retrieved from http://www.pubmedcentral.nih.gov/articlerender.fcgi?artid=30960&tool=pmcentrez&rendertype=abstract

Homma, K., Terui, S., Minemurall, M., Qadota, H., Anraku, Y., Kanaho, Y., & Ohya, Y. (1998). Phosphatidylinositol-4-phosphate 5-kinase localized on the plasma membrane is essential for yeast cell morphogenesis. *Journal of Biological Chemistry*, *273*(25), 15779–15786. http://doi.org/10.1074/jbc.273.25.15779

Höning, S., Ricotta, D., Krauss, M., Späte, K., Spolaore, B., Motley, A., … Owen, D. J. (2005). Phosphatidylinositol-(4,5)-bisphosphate regulates sorting signal recognition by the clathrin-associated adaptor complex AP2. *Molecular Cell*, *18*(5), 519–531. http://doi.org/10.1016/j.molcel.2005.04.019

Hou, N. S., Gutschmidt, A., Choi, D. Y., Pather, K., Shi, X., Watts, J. L., … Taubert, S. (2014). Activation of the endoplasmic reticulum unfolded protein response by lipid disequilibrium without disturbed proteostasis in vivo. *Proceedings of the National Academy of Sciences of the United States of America*, *111*(22), E2271-80. http://doi.org/10.1073/pnas.1318262111

Houy, S., Croisé, P., Gubar, O., Chasserot-Golaz, S., Tryoen-Tóth, P., Bailly, Y., … Gasman, S. (2013). Exocytosis and endocytosis in neuroendocrine cells: Inseparable membranes! *Frontiers in Endocrinology*. http://doi.org/10.3389/fendo.2013.00135

Howell, A. S., & Lew, D. J. (2012). Morphogenesis and the cell cycle. *Genetics*. http://doi.org/10.1534/genetics.111.128314

Hua, Y., Woehler, A., Kahms, M., Haucke, V., Neher, E., & Klingauf, J. (2013). Blocking endocytosis enhances short-term synaptic depression under conditions of normal availability of vesicles. *Neuron*, *80*(2), 343–349. http://doi.org/10.1016/j.neuron.2013.08.010

Hutagalung, A. H., & Novick, P. J. (2011). Role of Rab GTPases in membrane traffic and cell physiology. *Physiological Reviews*, *91*(1), 119–49. http://doi.org/10.1152/physrev.00059.2009

Ile, K. E., Schaaf, G., & Bankaitis, V. a. (2006). Phosphatidylinositol transfer proteins and cellular nanoreactors for lipid signaling. *Nature Chemical Biology*, *2*(11), 576–583. http://doi.org/10.1038/nchembio835

Im, Y. J., Raychaudhuri, S., Prinz, W. a, & Hurley, J. H. (2005). Structural mechanism for sterol sensing and transport by OSBP-related proteins. *Nature*, *437*(7055), 154–158. http://doi.org/10.1038/nature03923

Insall, R. H., & Machesky, L. M. (2004). Regulation of WASP: PIP2 pipped by Toca-1? *Cell*. http://doi.org/10.1016/j.cell.2004.07.005

Itoh, T., Koshiba, S., Kigawa, T., Kikuchi, A., Yokoyama, S., & Takenawa, T. (2001). Role of the ENTH domain in phosphatidylinositol-4,5-bisphosphate binding and endocytosis. *Science*, *291*(5506), 1047–1051. http://doi.org/10.1126/science.291.5506.1047

Jacquier, N., & Schneiter, R. (2012). Mechanisms of sterol uptake and transport in yeast. *Journal of Steroid Biochemistry and Molecular Biology*. http://doi.org/10.1016/j.jsbmb.2010.11.014

Jean, S., & Kiger, A. a. (2012). Coordination between RAB GTPase and phosphoinositide regulation and functions. *Nature Reviews Molecular Cell Biology*, *13*(7), 463–470. http://doi.org/10.1038/nrm3379

Jedd, G., Mulholland, J., & Segev, N. (1997). Two new Ypt GTPases are required for exit from the yeast trans-Golgi compartment. *Journal of Cell Biology*. http://doi.org/10.1083/jcb.137.3.563

Jeong, H., Park, J., & Lee, C. (2016). Crystal structure of Mdm12 reveals the architecture and dynamic organization of the ERMES complex. *EMBO Reports*, *17*, 1857–1871. http://doi.org/10.15252/embr

Jiang, B., Brown, J. L., Sheraton, J., Fortin, N., & Bussey, H. (1994). A new family of yeast genes implicated in ergosterol synthesis is related to the human oxysterol binding protein. *Yeast (Chichester, England)*, *10*(3), 341–53.

http://doi.org/10.1002/yea.320100307

Jiang, Y., Rossi, G., & Ferro-Novick, S. (1993). Bet2p and Mad2p are components of a prenyltransferase that adds geranylgeranyl onto Ypt1p and Sec4p. *Nature*, *366*(6450), 84–86. http://doi.org/10.1038/366084a0

Jin, H., McCaffery, J. M., & Grote, E. (2008). Ergosterol promotes pheromone signaling and plasma membrane fusion in mating yeast. *Journal of Cell Biology*, *180*(4), 813–826. http://doi.org/10.1083/jcb.200705076

Jin, Y., Sultana, A., Gandhi, P., Franklin, E., Hamamoto, S., Khan, A. R., … Weisman, L. S. (2011). Myosin V transports secretory vesicles via a Rab GTPase cascade and interaction with the exocyst complex. *Developmental Cell*, *21*(6), 1156–1170. http://doi.org/10.1016/j.devcel.2011.10.009

Johansen, J., Ramanathan, V., & Beh, C. T. (2012). Vesicle trafficking from a lipid perspective: Lipid regulation of exocytosis in Saccharomyces cerevisiae. *Cell Logist.*, *2*(3), 151–160. http://doi.org/10.4161/cl.20490

Johansson, M., Lehto, M., Tanhuanpa, K., Cover, T. L., & Olkkonen, V. M. (2005). The Oxysterol-binding Protein Homologue ORP1L Interacts with Rab7 and Alters Functional Properties of Late Endocytic Compartments. *Molecular Biology of the Cell*, *16*, 5480–5492. http://doi.org/10.1091/mbc.E05

Johansson, M., Rocha, N., Zwart, W., Jordens, I., Janssen, L., Kuijl, C., … Neefjes, J. (2007). Activation of endosomal dynein motors by stepwise assembly of Rab7-RILP-p150Glued, ORP1L, and the receptor βIII spectrin. *Journal of Cell Biology*, *176*(4), 459–471. http://doi.org/10.1083/jcb.200606077

Johnson, C. M., & Rodgers, W. (2008). Spatial Segregation of Phosphatidylinositol 4,5-Bisphosphate (PIP2) Signaling in Immune Cell Functions. *Immunology, Endocrine & Metabolic Agents - Medicinal Chemistry*, *8*(4), 349–357. http://doi.org/10.2174/187152208787169233

Jones, L. A., & Sudbery, P. E. (2010). Spitzenkörper, exocyst, and polarisome components in Candida albicans hyphae show different patterns of localization and have distinct dynamic properties. *Eukaryotic Cell*, *9*(10), 1455–1465. http://doi.org/10.1128/EC.00109-10

Jones, S., Newman, C., Liu, F., & Segev, N. (2000). The TRAPP complex is a nucleotide exchanger for Ypt1 and Ypt31/32. *Molecular Biology of the Cell*, *11*(12), 4403–4411. Retrieved from papers3://publication/uuid/AD1A2B48-3C25-40EE-BA84-1A6FFC19456F

Jose, M., Tollis, S., Nair, D., Mitteau, R., Velours, C., Massoni-Laporte, A., … McCusker, D. (2015). A quantitative imaging-based screen reveals the exocyst as a network hub connecting endocytosis and exocytosis. *Molecular Biology of the Cell*, *26*(13),

2519–34. http://doi.org/10.1091/mbc.E14-11-1527

Jose, M., Tollis, S., Nair, D., Sibarita, J. B., & McCusker, D. (2013). Robust polarity establishment occurs via an endocytosis-based cortical corralling mechanis. *Journal of Cell Biology*, *200*(4), 407–418. http://doi.org/10.1083/jcb.201206081

Kagiwada, S., & Hashimoto, M. (2007). The yeast VAP homolog Scs2p has a phosphoinositide-binding ability that is correlated with its activity. *Biochemical and Biophysical Research Communications*, *364*(4), 870–876. http://doi.org/10.1016/j.bbrc.2007.10.079

Kajiwara, K., Watanabe, R., Pichler, H., Ihara, K., Murakami, S., Riezman, H., & Funato, K. (2008). Yeast ARV1 Is Required for Efficient Delivery of an Early GPI Intermediate to the First Mannosyltransferase during GPI Assembly and Controls Lipid Flow from the Endoplasmic Reticulum. *Molecular Biology of the Cell*, *19*(5), 2069–2082. http://doi.org/10.1091/mbc.E07-08-0740

Kaksonen, M., Sun, Y., & Drubin, D. G. (2003). A Pathway for Association of Receptors, Adaptors, and Actin during Endocytic Internalization. *Cell*, *115*(4), 475–487. http://doi.org/10.1016/S0092-8674(03)00883-3

Kaksonen, M., Toret, C. P., & Drubin, D. G. (2005). A modular design for the clathrin- and actin-mediated endocytosis machinery. *Cell*, *123*(2), 305–320. http://doi.org/10.1016/j.cell.2005.09.024

Kaksonen, M., Toret, C. P., & Drubin, D. G. (2005). A modular design for the clathrin-and actin-mediated endocytosis machinery. *Cell*, *123*(2), 305–320. Retrieved from http://linkinghub.elsevier.com/retrieve/pii/S0092867405009785

Kaksonen, M., Toret, C. P., & Drubin, D. G. (2006). Harnessing actin dynamics for clathrin-mediated endocytosis. *Nature Reviews. Molecular Cell Biology*, *7*(6), 404–414. http://doi.org/10.1038/nrm1940

Kaminska, J., Spiess, M., Stawiecka-Mirota, M., Monkaityte, R., Haguenauer-Tsapis, R., Urban-Grimal, D., … Zoladek, T. (2011). Yeast Rsp5 ubiquitin ligase affects the actin cytoskeleton in vivo and in vitro. *European Journal of Cell Biology*, *90*(12), 1016–1028. http://doi.org/10.1016/j.ejcb.2011.08.002

Kandutsch, A. A., & Shown, E. P. (1981). Assay of oxysterol-binding protein in a mouse fibroblast, cell-free system. Dissociation constant and other properties of the system. *Journal of Biological Chemistry*, *256*(24), 13068–13073.

Kearns, B. G., Alb Jr, J. G., & Bankaitis, V. (1998). Phosphatidylinositol transfer proteins: the long and winding road to physiological function. *Trends in Cell Biology*, *8*(7), 276–282.

Kearns, B. G., McGee, T. P., Mayinger, P., Gedvilaite, a, Phillips, S. E., Kagiwada, S., &

Bankaitis, V. a. (1997). Essential role for diacylglycerol in protein transport from the yeast Golgi complex. *Nature*, *387*(6628), 101–105. http://doi.org/10.1038/387101a0

Keith G. Kozminski, †‡, Laure Beven, §¶, Angerman, E., Amy Hin Yan Tong, #, Charles Boone, #, Park§, and H.-O., & **. (2003). Interaction between a Ras and a Rho GTPase Couples Selection of a Growth Site to the Development of Cell Polarity in Yeast. *Molecular Biology of the Cell*, *14*(4), 4958–4970. http://doi.org/10.1091/mbc.E03

Kelly, S. L., Lamb, D. C., Corran, A. J., Baldwin, B. C., Parks, L. W., & Kelly, D. E. (1995). Purification and reconstitution of activity of Saccharomyces cerevisiae P450 61, a sterol Δ22-desaturase. *FEBS Letters*, *377*(2), 217–220. http://doi.org/10.1016/0014-5793(95)01342-3

Kerppola, T. K. (2008). Bimolecular fluorescence complementation (BiFC) analysis as a probe of protein interactions in living cells. *Annu Rev Biophys*, *37*, 465–87. http://doi.org/10.1146/annurev.biophys.37.032807.125842.BIMOLECULAR

Kilmartin, J. V., & Adams, A. E. M. (1984). Structural rearrangements of tubulin and actin during the cell cycle of the yeast Saccharomyces. *Journal of Cell Biology*, *98*(3), 922–933. http://doi.org/10.1083/jcb.98.3.922

Kim, K., Galletta, B. J., Schmidt, K. O., Chang, F. S., Blumer, K. J., & Cooper, J. A. (2006). Actin-based Motility during Endocytosis in Budding Yeast. *Molecular Biology of the Cell*, *17*(3), 1354–1363. http://doi.org/10.1091/mbc.E05

Kim, S. H., & Ryan, T. a. (2009). Synaptic vesicle recycling at CNS snapses without AP-2. *The Journal of Neuroscience : The Official Journal of the Society for Neuroscience*, *29*(12), 3865–74. http://doi.org/10.1523/JNEUROSCI.5639-08.2009

Kishimoto, T., Sun, Y., Buser, C., Liu, J., Michelot, A., & Drubin, D. G. (2011). Determinants of endocytic membrane geometry, stability, and scission. *Proceedings of the National Academy of Sciences*, *108*(44), E979–E988. http://doi.org/10.1073/pnas.1113413108

Klebl, F., & Tanner, W. (1989). Molecular cloning of a cell wall exo-beta-1,3-glucanase from Saccharomyces cerevisiae. *Journal of Bacteriology*, *171*(11), 6259–6264.

Klemm, R. W., Ejsing, C. S., Surma, M. A., Kaiser, H. J., Gerl, M. J., Sampaio, J. L., … Simons, K. (2009). Segregation of sphingolipids and sterols during formation of secretory vesicles at the trans-Golgi network. *Journal of Cell Biology*, *185*(4), 601–612. http://doi.org/10.1083/jcb.200901145

Kline, D., & Nuccitelli, R. (1985). The wave of activation current in the Xenopus egg. *Developmental Biology*, *111*(2), 471–487. http://doi.org/10.1016/0012-1606(85)90499-3

Kornmann, B., Currie, E., Collins, S. R., Schuldiner, M., Nunnari, J., Weissman, J. S., & Walter, P. (2009). An ER-mitochondria tethering complex revealed by a synthetic biology screen. *Science (New York, N.Y.)*, *325*(5939), 477–481. http://doi.org/10.1126/science.1175088

Kozminski, K. G., Alfaro, G., Dighe, S., & Beh, C. T. (2006). Homologues of oxysterol-binding proteins affect Cdc42p- and Rho1p-mediated cell polarization in Saccharomyces cerevisiae. *Traffic*, *7*(9), 1224–1242. http://doi.org/10.1111/j.1600-0854.2006.00467.x

Kozminski, K. G., Chen, a J., Rodal, a a, & Drubin, D. G. (2000). Functions and functional domains of the GTPase Cdc42p. *Molecular Biology of the Cell*, *11*(1), 339–54. Retrieved from http://www.pubmedcentral.nih.gov/articlerender.fcgi?artid=14778&tool=pmcentrez&rendertype=abstract

Krauss, M., & Haucke, V. (2007). Phosphoinositide-metabolizing enzymes at the interface between membrane traffic and cell signalling. *EMBO Reports*, *8*(3), 241–6. http://doi.org/10.1038/sj.embor.7400919

Kukulski, W., Picco, A., Specht, T., Briggs, J. A. G., & Kaksonen, M. (2016). Clathrin modulates vesicle scission, but not invagination shape, in yeast endocytosis. *eLife*, *5*(JUN2016). http://doi.org/10.7554/eLife.16036

Kumano, Y., & Nikawa, J. ichi. (1995). Functional analysis of mutations in the PIS gene, which encodes Saccharomyces cerevisiae phosphatidylinositol synthase. *FEMS Microbiology Letters*, *126*(1), 81–84. http://doi.org/10.1016/0378-1097(94)00530-5

Kvam, E., & Goldfarb, D. S. (2004). Nvj1p is the outer-nuclear-membrane receptor for oxysterol-binding protein homolog Osh1p in Saccharomyces cerevisiae. *Journal of Cell Science*, *117*(Pt 21), 4959–4968. http://doi.org/10.1242/jcs.01372

Lachmann, J., Barr, F. A., & Ungermann, C. (2012). The Msb3/Gyp3 GAP controls the activity of the Rab GTPases Vps21 and Ypt7 at endosomes and vacuoles. *Molecular Biology of the Cell*, *23*(13), 2516–26. http://doi.org/10.1091/mbc.E11-12-1030

Lagor, W. R., Tong, F., Jarrett, K. E., Lin, W., Conlon, D. M., Smith, M., … Rader, D. J. (2015). Deletion of murine Arv1 results in a lean phenotype with increased energy expenditure. *Nutrition & Diabetes*, *5*(June), e181. http://doi.org/10.1038/nutd.2015.32

Lauwers, E., & André, B. (2006). Association of yeast transporters with detergent-resistant membranes correlates with their cell-surface location. *Traffic*, *7*(8), 1045–1059. http://doi.org/10.1111/j.1600-0854.2006.00445.x

Laux, T., Fukami, K., Thelen, M., Golub, T., Frey, D., & Caroni, P. (2000). GAP43,

MARCKS, and CAP23 modulate PI(4,5)P2 at plasmalemmal rafts, and regulate cell cortex actin dynamics through a common mechanism. *Journal of Cell Biology*, *149*(7), 1455–1471. http://doi.org/10.1083/jcb.149.7.1455

Layton, A. T., Savage, N. S., Howell, A. S., Carroll, S. Y., Drubin, D. G., & Lew, D. J. (2011). Modeling vesicle traffic reveals unexpected consequences for Cdc42p-mediated polarity establishment. *Current Biology*, *21*(3), 184–194. http://doi.org/10.1016/j.cub.2011.01.012

Leber, A., Hrastnik, C., & Daum, G. (1995). Phospholipid-synthesizing enzymes in Golgi membranes of the yeast, Saccharomyces cerevisiae. *FEBS Letters*, *377*(2), 271–274. http://doi.org/10.1016/0014-5793(95)01361-X

LeBlanc, M. A., Fairn, G. D., Russo, S. B., Czyz, O., Zaremberg, V., Cowart, L. A., & McMaster, C. R. (2013). The Yeast Oxysterol Binding Protein Kes1 Maintains Sphingolipid Levels. *PLoS ONE*, *8*(4). http://doi.org/10.1371/journal.pone.0060485

LeBlanc, M. A., & McMaster, C. R. (2010). Lipid binding requirements for oxysterol-binding protein Kes1 inhibition of autophagy and endosome-trans-Golgi trafficking pathways. *Journal of Biological Chemistry*, *285*(44), 33875–33884. http://doi.org/10.1074/jbc.M110.147264

Lee, M. C. S., Hamamoto, S., & Schekman, R. (2002). Ceramide biosynthesis is required for the formation of the oligomeric H+-ATPase Pma1p in the yeast endoplasmic reticulum. *Journal of Biological Chemistry*, *277*(25), 22395–22401. http://doi.org/10.1074/jbc.M200450200

Lehto, M., & Olkkonen, V. M. (2003). The OSBP-related proteins: a novel protein family involved in vesicle transport, cellular lipid metabolism, and cell signalling. *Biochimica et Biophysica Acta (BBA) - Molecular and Cell Biology of Lipids*, *1631*(1), 1–11. http://doi.org/10.1016/S1388-1981(02)00364-5

Lev, S. (2010). Non-vesicular lipid transport by lipid-transfer proteins and beyond. *Nature Reviews. Molecular Cell Biology*, *11*(10), 739–750. http://doi.org/10.1038/nrm2971

Lev, S. (2012). Nonvesicular lipid transfer from the endoplasmic reticulum. *Cold Spring Harbor Perspectives in Biology*, *4*(10). http://doi.org/10.1101/cshperspect.a013300

Levental, I., Lingwood, D., Grzybek, M., Coskun, Ü., & Simons, K. (2010). Palmitoylation regulates raft affinity for the majority of integral raft proteins. *Proceedings of the National Academy of Sciences of the United States of America*, *107*(51), 22050–22054. http://doi.org/10.1073/pnas.1016184107

Leventis, P. A., & Grinstein, S. (2010). The Distribution and Function of Phosphatidylserine in Cellular Membranes. *Annual Review of Biophysics, Vol 39*, *39*, 407–427. http://doi.org/DOI 10.1146/annurev.biophys.093008.131234

Levine, T. (2004). Short-range intracellular trafficking of small molecules across endoplasmic reticulum junctions. *Trends in Cell Biology*. http://doi.org/10.1016/j.tcb.2004.07.017

Levine, T. P., & Munro, S. (2001). Dual targeting of Osh1p, a yeast homologue of oxysterol-binding protein, to both the Golgi and the nucleus-vacuole junction. *Molecular Biology of the Cell*, *12*(6), 1633–44. http://doi.org/10.1091/mbc.12.6.1633

Lewis, M. J., Nichols, B. J., Prescianotto-Baschong, C., Riezman, H., & Pelham, H. R. (2000). Specific retrieval of the exocytic SNARE Snc1p from early yeast endosomes. *Molecular Biology of the Cell*, *11*(1), 23–38. http://doi.org/10.1091/mbc.11.1.23

Li, R. (1997). Bee1, a yeast protein with homology to Wiscott-Aldrich syndrome protein, is critical for the assembly of cortical actin cytoskeleton. *Journal of Cell Biology*, *136*(3), 649–658. http://doi.org/10.1083/jcb.136.3.649

Li, X., Rivas, M. P., Fang, M., Marchena, J., Mehrotra, B., Chaudhary, A., … Bankaitis, V. A. (2002). Analysis of oxysterol binding protein homologue Kes1p function in regulation of Sec14p-dependent protein transport from the yeast Golgi complex. *Journal of Cell Biology*, *157*(1), 63–77. http://doi.org/10.1083/jcb.200201037

Li, X., Routt, S. M., Xie, Z., Cui, X., Fang, M., Kearns, M. a, … Bankaitis, V. a. (2000). Identification of a novel family of nonclassic yeast phosphatidylinositol transfer proteins whose function modulates phospholipase D activity and Sec14p-independent cell growth. *Molecular Biology of the Cell*, *11*(6), 1989–2005.

Li, Z., Vizeacoumar, F. J., Bahr, S., Li, J., Warringer, J., Vizeacoumar, F. S., … Boone, C. (2011). Systematic exploration of essential yeast gene function with temperature-sensitive mutants. *Nature Biotechnology*, *29*(4), 361–7. http://doi.org/10.1038/nbt.1832

Ling, Y., Hayano, S., & Novick, P. (2014). Osh4p is needed to reduce the level of phosphatidylinositol-4-phosphate on secretory vesicles as they mature. *Molecular Biology of the Cell*, *25*(21), 3389–400. http://doi.org/10.1091/mbc.E14-06-1087

Lipatova, Z., Hain, A. U., Nazarko, V. Y., & Segev, N. (2015). Ypt/Rab GTPases: Principles learned from yeast. *Critical Reviews in Biochemistry and Molecular Biology*, *9238*, 1–9. http://doi.org/10.3109/10409238.2015.1014023

Lipatova, Z., Tokarev, A. A., Jin, Y., Mulholland, J., Weisman, L. S., & Segev, N. (2008). Direct interaction between a myosin V motor and the Rab GTPases Ypt31/32 is required for polarized secretion. *Molecular Biology of the Cell*, *19*(11), 4177–4187. http://doi.org/10.1091/mbc.E08

Lipowsky, R. (1993). Domain-induced budding of fluid membranes. *Biophysical Journal*, *64*(4), 1133–1138. http://doi.org/10.1016/S0006-3495(93)81479-6

Liu, J., Zuo, X., Yue, P., & Guo, W. (2007). Phosphatidylinositol 4,5-bisphosphate mediates the targeting of the exocyst to the plasma membrane for exocytosis in mammalian cells. *Molecular Biology of the Cell*, *18*, 4483–4492. http://doi.org/10.1091/mbc.E07

Liu, M. (2011). The biology and dynamics of mammalian cortical granules. *Reproductive Biology and Endocrinology*, *9*(1), 149. http://doi.org/10.1186/1477-7827-9-149

Liu, Y., & Bankaitis, V. A. (2010). Phosphoinositide phosphatases in cell biology and disease. *Progress in Lipid Research*. http://doi.org/10.1016/j.plipres.2009.12.001

Loerke, D., Mettlen, M., Yarar, D., Jaqaman, K., Jaqaman, H., Danuser, G., & Schmid, S. L. (2009). Cargo and Dynamin Regulate Clathrin-Coated Pit Maturation. *PLoS Biology*, *7*(3). http://doi.org/10.1371/journal.pbio.1000057

Loewen, C. J. R., Roy, A., & Levine, T. P. (2003). A conserved ER targeting motif in three families of lipid binding proteins and in Opi1p binds VAP. *EMBO Journal*, *22*(9), 2025–2035. http://doi.org/10.1093/emboj/cdg201

Loewen, C. J. R., Young, B. P., Tavassoli, S., & Levine, T. P. (2007). Inheritance of cortical ER in yeast is required for normal septin organization. *Journal of Cell Biology*, *179*(3), 467–483. http://doi.org/10.1083/jcb.200708205

Lombardi, R., & Riezman, H. (2001). Rvs161p and Rvs167p, the Two Yeast Amphiphysin Homologs, Function Together in Vivo. *Journal of Biological Chemistry*, *276*(8), 6016–6022. http://doi.org/10.1074/jbc.M008735200

London, E. (2002). Insights into lipid raft structure and formation from experiments in model membranes. *Current Opinion in Structural Biology*. http://doi.org/10.1016/S0959-440X(02)00351-2

Longtine, M. S., McKenzie, A., Demarini, D. J., Shah, N. G., Wach, A., Brachat, A., … Pringle, J. R. (1998). Additional modules for versatile and economical PCR-based gene deletion and modification in Saccharomyces cerevisiae. *Yeast*, *14*(10), 953–961. http://doi.org/10.1002/(SICI)1097-0061(199807)14:10<953::AID-YEA293>3.0.CO;2-U

Losev, E., Reinke, C. a, Jellen, J., Strongin, D. E., Bevis, B. J., & Glick, B. S. (2006). Golgi maturation visualized in living yeast. *Nature*, *441*(7096), 1002–1006. http://doi.org/10.1038/nature04717

Lu, R., Drubin, D. G., & Sun, Y. (2016). Clathrin-mediated endocytosis in budding yeast at a glance. *Journal of Cell Science*, *129*(8), 1531–6. http://doi.org/10.1242/jcs.182303

Luo, Y., Li, T., Yu, F., Kramer, T., & Cristea, I. M. (2010). Resolving the Composition of Protein Complexes Using a MALDI LTQ Orbitrap. *Journal of the American Society*

for Mass Spectrometry, *21*(1), 34–46. http://doi.org/10.1016/j.jasms.2009.08.026

Maeda, K., Anand, K., Chiapparino, A., Kumar, A., Poletto, M., Kaksonen, M., & Gavin, A.-C. C. (2013). Interactome map uncovers phosphatidylserine transport by oxysterol-binding proteins. *Nature*, *501*(7466), 257–261. http://doi.org/10.1038/nature12430

Maléth, J., Choi, S., Muallem, S., & Ahuja, M. (2014). Translocation between PI(4,5)P2-poor and PI(4,5)P2-rich microdomains during store depletion determines STIM1 conformation and Orai1 gating. *Nature Communications*, *5*, 5843. http://doi.org/10.1038/ncomms6843

Malinska, K., Malinska, J., Operakova, M., & Tanner, W. (2003). Visualization of Protein Compartmentation within the Plasma Membrane of Living Yeast Cells. *Molecular Biology of the Cell*, *14*(November), 4427–4436. http://doi.org/10.1091/mbc.E03-04-0221

Malinsky, J., Opekarová, M., & Tanner, W. (2010). The lateral compartmentation of the yeast plasma membrane. *Yeast*. http://doi.org/10.1002/yea.1772

Manderson, E. N., Malleshaiah, M., & Michnick, S. W. (2008). A novel genetic screen implicates Elm1 in the inactivation of the yeast transcription factor SBF. *PLoS ONE*, *3*(1). http://doi.org/10.1371/journal.pone.0001500

Manford, A. G., Stefan, C. J., Yuan, H. L., MacGurn, J. A., & Emr, S. D. (2012). ER-to-Plasma Membrane Tethering Proteins Regulate Cell Signaling and ER Morphology. *Developmental Cell*, *23*(6), 1129–1140. http://doi.org/10.1016/j.devcel.2012.11.004

Manning, B. D., Padmanabha, R., & Snyder, M. (1997). The Rho-GEF Rom2p localizes to sites of polarized cell growth and participates in cytoskeletal functions in Saccharomyces cerevisiae. *Molecular Biology of the Cell*, *8*(10), 1829–1844.

Marco, E., Wedlich-Soldner, R., Li, R., Altschuler, S. J., & Wu, L. F. (2007). Endocytosis Optimizes the Dynamic Localization of Membrane Proteins that Regulate Cortical Polarity. *Cell*, *129*(2), 411–422. http://doi.org/10.1016/j.cell.2007.02.043

Maritzen, T., Podufall, J., & Haucke, V. (2010). Stonins--specialized adaptors for synaptic vesicle recycling and beyond? *Traffic (Copenhagen, Denmark)*, *11*(1), 8–15. http://doi.org/10.1111/j.1600-0854.2009.00971.x

Markham, J. E., Molino, D., Gissot, L., Bellec, Y., Hématy, K., Marion, J., … Faure, J.-D. (2011). Sphingolipids containing very-long-chain fatty acids define a secretory pathway for specific polar plasma membrane protein targeting in Arabidopsis. *The Plant Cell*, *23*(6), 2362–78. http://doi.org/10.1105/tpc.110.080473

Maxfield, F. R., & Menon, A. K. (2006). Intracellular sterol transport and distribution. *Current Opinion in Cell Biology*. http://doi.org/10.1016/j.ceb.2006.06.012

Maxfield, F. R., & van Meer, G. (2010). Cholesterol, the central lipid of mammalian cells. *Current Opinion in Cell Biology*. http://doi.org/10.1016/j.ceb.2010.05.004

McDermott, H., & Kim, K. (2015). Molecular dynamics at the endocytic portal and regulations of endocytic and recycling traffics. *European Journal of Cell Biology*. http://doi.org/10.1016/j.ejcb.2015.04.003

McLaughlin, S., & Murray, D. (2005). Plasma membrane phosphoinositide organization by protein electrostatics. *Nature*, *438*(December), 605–611. http://doi.org/10.1038/nature04398

Mesmin, B., Antonny, B., & Drin, G. (2013). Insights into the mechanisms of sterol transport between organelles. *Cellular and Molecular Life Sciences*. http://doi.org/10.1007/s00018-012-1247-3

Mesmin, B., Bigay, J., Moser Von Filseck, J., Lacas-Gervais, S., Drin, G., & Antonny, B. (2013). A four-step cycle driven by PI(4)P hydrolysis directs sterol/PI(4)P exchange by the ER-Golgi Tether OSBP. *Cell*, *155*(4). http://doi.org/10.1016/j.cell.2013.09.056

Mesmin, B., & Maxfield, F. R. (2009). Intracellular sterol dynamics. *Biochimica et Biophysica Acta - Molecular and Cell Biology of Lipids*. http://doi.org/10.1016/j.bbalip.2009.03.002

Mesmin, B., Pipalia, N. H., Lund, F. W., Ramlall, T. F., Sokolov, A., Eliezer, D., & Maxfield, F. R. (2011). STARD4 abundance regulates sterol transport and sensing. *Molecular Biology of the Cell*, *22*(21), 4004–15. http://doi.org/10.1091/mbc.E11-04-0372

Michelot, A., Costanzo, M., Sarkeshik, A., Boone, C., Yates, J. R., & Drubin, D. G. (2010). Reconstitution and protein composition analysis of endocytic actin patches. *Current Biology*, *20*(21), 1890–1899. http://doi.org/10.1016/j.cub.2010.10.016

Miki, H., Miura, K., & Takenawa, T. (1996). N-WASP, a novel actin-depolymerizing protein, regulates the cortical cytoskeletal rearrangement in a PIP2-dependent manner downstream of tyrosine kinases. *The EMBO Journal*, *15*(19), 5326–5335.

Miliaras, N. B., & Wendland, B. (2004). EH proteins: multivalent regulators of endocytosis (and other pathways). *Cell Biochemistry and Biophysics*, *41*(2), 295–318. http://doi.org/10.1385/CBB:41:2:295

Miller, K. E., Kim, Y., Huh, W. K., & Park, H. O. (2015). Bimolecular Fluorescence Complementation (BiFC) Analysis: Advances and Recent Applications for Genome-Wide Interaction Studies. *Journal of Molecular Biology*, *427*(11), 2039–2055. http://doi.org/10.1016/j.jmb.2015.03.005

Mioka, T., Fujimura-Kamada, K., & Tanaka, K. (2014). Asymmetric distribution of

phosphatidylserine is generated in the absence of phospholipid flippases in Saccharomyces cerevisiae. *MicrobiologyOpen*, *3*(5), 803–821. http://doi.org/10.1002/mbo3.211

Mirey, G., Soulard, A., Orange, C., Friant, S., & Winsor, B. (2005). SH3 domain-containing proteins and the actin cytoskeleton in yeast. *Biochemical Society Transactions*, *33*(Pt 6), 1247–9. http://doi.org/10.1042/BST20051247

Misu, K., Fujimura-Kamada, K., Ueda, T., Nakano, A., Katoh, H., & Tanaka, K. (2003). Cdc50p, a conserved endosomal membrane protein, controls polarized growth in Saccharomyces cerevisiae. *Molecular Biology of the Cell*, *14*(2), 730–747. http://doi.org/10.1091/mbc.E02-06-0314

Mitter, D., Reisinger, C., Hinz, B., Hollmann, S., Yelamanchili, S. V., Treiber-Held, S., … Ahnert-Hilger, G. (2003). The synaptophysin/synaptobrevin interaction critically depends on the cholesterol content. *Journal of Neurochemistry*, *84*(1), 35–42. http://doi.org/10.1046/j.1471-4159.2003.01258.x

Mizuno-Yamasaki, E., Medkova, M., Coleman, J., & Novick, P. (2010). Phosphatidylinositol 4-phosphate controls both membrane recruitment and a regulatory switch of the Rab GEF Sec2p. *Developmental Cell*, *18*(5), 828–840. http://doi.org/10.1016/j.devcel.2010.03.016

Morgera, F., Sallah, M. R., Dubuke, M. L., Gandhi, P., Brewer, D. N., Carr, C. M., & Munson, M. (2012). Regulation of exocytosis by the exocyst subunit Sec6 and the SM protein Sec1. *Molecular Biology of the Cell*, *23*(2), 337–346. http://doi.org/10.1091/mbc.E11-08-0670

Moseley, J. B., & Goode, B. L. (2006). The yeast actin cytoskeleton: from cellular function to biochemical mechanism. *Microbiology and Molecular Biology Reviews : MMBR*, pp. 605–645. http://doi.org/10.1128/MMBR.00013-06

Moser von Filseck, J., Čopič, A., Delfosse, V., Vanni, S., Jackson, C. L., Bourguet, W., & Drin, G. (2015). Phosphatidylserine transport by ORP/Osh proteins is driven by phosphatidylinositol 4-phosphate. *Science (New York, N.Y.)*, *349*(6246), 432–6. http://doi.org/10.1126/science.aab1346

Mousley, C. J., Tyeryar, K., Ile, K. E., Schaaf, G., Brost, R. L., Boone, C., … Bankaitis, V. A. (2008). Trans-Golgi Network and Endosome Dynamics Connect Ceramide Homeostasis with Regulation of the Unfolded Protein Response and TOR Signaling in Yeast. *Mol. Biol. Cell*, *19*(11), 4785–4803. http://doi.org/10.1091/mbc.E08-04-0426

Mousley, C. J., Tyeryar, K. R., Vincent-Pope, P., & Bankaitis, V. A. (2007). The Sec14-superfamily and the regulatory interface between phospholipid metabolism and membrane trafficking. *Biochimica et Biophysica Acta - Molecular and Cell Biology of Lipids*. http://doi.org/10.1016/j.bbalip.2007.04.002

Mukherjee, D., Sen, A., Boettner, D. R., Fairn, G. D., Schlam, D., Bonilla Valentin, F. J., … Claudio Aguilar, R. (2013). Bem3, a Cdc42 GTPase-activating protein, traffics to an intracellular compartment and recruits the secretory Rab GTPase Sec4 to endomembranes. *Journal of Cell Science*, *126*(Pt 20), 4560–71. http://doi.org/10.1242/jcs.117663

Muller, H. J. (1932). Further studies on the nature and causes of gene mutations. *International Congress of Genetics*, *6*(1), 213–255. Retrieved from http://darwin.amnh.org/bib/bibtexbrowser.php?key=muller1932yu83j&bib=EvoLit.bib &

Munn, A. L., & Riezman, H. (1994). Endocytosis is required for the growth of vacuolar H+-ATPase-defective yeast: Identification of six new END genes. *Journal of Cell Biology*, *127*(2), 373–386. http://doi.org/10.1083/jcb.127.2.373

Muralidharan-Chari, V., Clancy, J. W., Sedgwick, A., & D'Souza-Schorey, C. (2010). Microvesicles: mediators of extracellular communication during cancer progression. *Journal of Cell Science*, *123*(Pt 10), 1603–1611. http://doi.org/10.1242/jcs.064386

Mutch, S. A., Kensel-Hammes, P., Gadd, J. C., Fujimoto, B. S., Allen, R. W., Schiro, P. G., … Chiu, D. T. (2011). Protein quantification at the single vesicle level reveals that a subset of synaptic vesicle proteins are trafficked with high precision. *The Journal of Neuroscience*, *31*(4), 1461–1470. http://doi.org/10.1523/JNEUROSCI.3805-10.2011

Muthusamy, B. P., Raychaudhuri, S., Natarajan, P., Abe, F., Liu, K., Prinz, W. A., & Graham, T. R. (2009). Control of Protein and Sterol Trafficking by Antagonistic Activities of a Type IV P-type ATPase and Oxysterol Binding Protein Homologue. *Molecular Biology of the Cell*, *20*(12), 2920–2931. http://doi.org/DOI 10.1091/mbc.E08-10-1036

Nemoto, T., Kimura, R., Ito, K., Tachikawa, a, Miyashita, Y., Iino, M., & Kasai, H. (2001). Sequential-replenishment mechanism of exocytosis in pancreatic acini. *Nature Cell Biology*, *3*(3), 253–258. http://doi.org/10.1038/35060042

Nemoto, T., Kojima, T., Oshima, A., Bito, H., & Kasai, H. (2004). Stabilization of exocytosis by dynamic F-actin coating of zymogen granules in pancreatic acini. *Journal of Biological Chemistry*, *279*(36), 37544–37550. http://doi.org/10.1074/jbc.M403976200

Newpher, T. M., & Lemmon, S. K. (2006). Clathrin is important for normal actin dynamics and progression of Sla2p-containing patches during endocytosis in yeast. *Traffic*, *7*(5), 574–588. http://doi.org/10.1111/j.1600-0854.2006.00410.x

Nicholson, K. L., Munson, M., Miller, R. B., Filip, T. J., Fairman, R., & Hughson, F. M. (1998). Regulation of SNARE complex assembly by an N-terminal domain of the t-SNARE Sso1p. *Nature Structural Biology*, *5*(9), 793–802.

http://doi.org/10.1038/1834

Nordmann, M., Cabrera, M., Perz, A., Bröcker, C., Ostrowicz, C., Engelbrecht-Vandré, S., & Ungermann, C. (2010). The Mon1-Ccz1 complex is the GEF of the late endosomal Rab7 homolog Ypt7. *Current Biology*, *20*(18), 1654–1659. http://doi.org/10.1016/j.cub.2010.08.002

Novick, P., Field, C., & Schekman, R. (1980). Identification of 23 complementation groups required for post-translational events in the yeast secretory pathway. *Cell*, *21*(1), 205–215. http://doi.org/10.1016/0092-8674(80)90128-2

Novick, P., Medkova, M., Dong, G., Hutagalung, A., Reinisch, K., & Grosshans, B. (2006). Interactions between Rabs, tethers, SNAREs and their regulators in exocytosis. *Biochemical Society Transactions*, *34*(Pt 5), 683–6. http://doi.org/10.1042/BST0340683

Novick, P., Osmond, B. C., & Botstein, D. (1989). Suppressors of yeast actin mutations. *Genetics*, *121*(4), 659–674.

Novick, P., & Schekman, R. (1979). Secretion and cell-surface growth are blocked in a temperature-sensitive mutant of Saccharomyces cerevisiae. *Proceedings of the National Academy of Sciences of the United States of America*, *76*(4), 1858–1862. http://doi.org/10.1073/pnas.76.4.1858

Ohashi, A., Gibson, J., Gregor, I., & Schatz, G. (1982). Import of proteins into mitochondria. The precursor of cytochrome c1 is processed in two steps, one of them heme-dependent. *Journal of Biological Chemistry*, *257*(21), 13042–13047.

Olkkonen, V. V. M., & Levine, T. T. P. (2004). Oxysterol binding proteins: in more than one place at one time? *Biochemistry and Cell Biology*, *98*(1), 87–98. http://doi.org/10.1139/O03-088

Orlando, K., Sun, X., Zhang, J., Lu, T., Yokomizo, L., Wang, P., & Guo, W. (2011). Exo-endocytic trafficking and the septin-based diffusion barrier are required for the maintenance of Cdc42p polarization during budding yeast asymmetric growth. *Molecular Biology of the Cell*, *22*(5), 624–633. http://doi.org/10.1091/mbc.E10-06-0484

Orlando, K., Zhang, J., Zhang, X., Yue, P., Chiang, T., Bi, E., & Guo, W. (2008). Regulation of Gic2 localization and function by phosphatidylinositol 4,5-bisphosphate during the establishment of cell polarity in budding yeast. *Journal of Biological Chemistry*, *283*(21), 14205–14212. http://doi.org/10.1074/jbc.M708178200

Ortiz, D., Medkova, M., Walch-Solimena, C., & Novick, P. (2002). Ypt32 recruits the Sec4p guanine nucleotide exchange factor, Sec2p, to secretory vesicles; evidence for a Rab cascade in yeast. *Journal of Cell Biology*, *157*(6), 1005–1015.

http://doi.org/10.1083/jcb.200201003

Ozaki-Kuroda, K., Yamamoto, Y., Nohara, H., Kinoshita, M., Fujiwara, T., Irie, K., & Takai, Y. (2001). Dynamic localization and function of Bni1p at the sites of directed growth in Saccharomyces cerevisiae. *Molecular and Cellular Biology*, *21*(3), 827–39. http://doi.org/10.1128/MCB.21.3.827-839.2001

Paczkowski, J. E., Richardson, B. C., & Fromme, J. C. (2015). Cargo adaptors: Structures illuminate mechanisms regulating vesicle biogenesis. *Trends in Cell Biology*, *25*(7), 408–416. http://doi.org/10.1016/j.tcb.2015.02.005

Padrick, S. B., & Rosen, M. K. (2010). Physical mechanisms of signal integration by WASP family proteins. *Annual Review of Biochemistry*, *79*, 707–35. http://doi.org/10.1146/annurev.biochem.77.060407.135452

Park, H.-O., & Bi, E. (2007). Central Roles of Small GTPases in the Development of Cell Polarity in Yeast and Beyond. *Microbiology and Molecular Biology Reviews*, *71*(1), 48–96. http://doi.org/10.1128/MMBR.00028-06

Parsons, A. B., Lopez, A., Givoni, I. E., Williams, D. E., Gray, C. A., Porter, J., … Boone, C. (2006). Exploring the Mode-of-Action of Bioactive Compounds by Chemical-Genetic Profiling in Yeast. *Cell*, *126*(3), 611–625. http://doi.org/10.1016/j.cell.2006.06.040

Payne, G. S., Baker, D., Van Tuinen, E., & Schekman, R. (1988). Protein transport to the vacuole and receptor-mediated endocytosis by clathrin heavy chain-deficient yeast. *Journal of Cell Biology*, *106*(5), 1453–1461. http://doi.org/10.1083/jcb.106.5.1453

Pearse, B. M. F. (1975). Coated vesicles from pig brain: Purification and biochemical characterization. *Journal of Molecular Biology*, *97*(1). http://doi.org/10.1016/S0022-2836(75)80024-6

Peter, B. J., Kent, H. M., Mills, I. G., Vallis, Y., Butler, P. J. G., Evans, P. R., & McMahon, H. T. (2004). BAR domains as sensors of membrane curvature: the amphiphysin BAR structure. *Science (New York, N.Y.)*, *303*(5657), 495–499. http://doi.org/10.1126/science.1092586

Petkovic, M., Jemaiel, A., Daste, F., Specht, C. G., Izeddin, I., Vorkel, D., … Galli, T. (2014). The SNARE Sec22b has a non-fusogenic function in plasma membrane expansion. *Nature Cell Biology*, *16*(5), 434–44. http://doi.org/10.1038/ncb2937

Phillips, S. E., Sha, B., Topalof, L., Xie, Z., Alb, J. G., Klenchin, V. A., … Bankaitis, V. A. (1999). Yeast Sec14p deficient in phosphatidylinositol transfer activity is functional in vivo. *Molecular Cell*, *4*(2), 187–197. http://doi.org/10.1016/S1097-2765(00)80366-4

Pike, L. J., & Miller, J. M. (1998). Cholesterol depletion delocalizes phosphatidylinositol

bisphosphate and inhibits hormone-stimulated phosphatidylinositol turnover. *Journal of Biological Chemistry*, *273*(35), 22298–22304. http://doi.org/10.1074/jbc.273.35.22298

Pollard, T. D. (2007). Regulation of actin filament assembly by Arp2/3 complex and formins. *Annual Review of Biophysics and Biomolecular Structure*, *36*, 451–477. http://doi.org/10.1146/annurev.biophys.35.040405.101936

Pomorski, T., Lombardi, R., Riezman, H., Devaux, P. F., van Meer, G., & Holthuis, J. C. M. (2003). Drs2p-related P-type ATPases Dnf1p and Dnf2p are required for Phospholipid Translocation across the Yeast Plasma Membrane and Serve a Role in Endocytosis. *Molecular Biology of the Cell*, *14*(February), 1240–1254. http://doi.org/10.1091/mbc.E02

Poon, P. P., Nothwehr, S. F., Singer, R. A., & Johnston, G. C. (2001). The Gcs1 and Age2 ArfGAP proteins provide overlapping essential function for transport from the yeast trans-Golgi network. *Journal of Cell Biology*, *155*(7), 1239–1250. http://doi.org/10.1083/jcb.200108075

Prehoda, K. E., Scott, J. A., Mullins, R. D., & Lim, W. A. (2000). Integration of multiple signals through cooperative regulation of the N-WASP-Arp2/3 complex. *Science*, *290*(5492), 801–806. http://doi.org/10.1126/science.290.5492.801

Prinz, W. A. (2010). Lipid trafficking sans vesicles: Where, why, how? *Cell*. http://doi.org/10.1016/j.cell.2010.11.031

Proszynski, T. J., Klemm, R. W., Gravert, M., Hsu, P. P., Gloor, Y., Wagner, J., … Walch-Solimena, C. (2005). A genome-wide visual screen reveals a role for sphingolipids and ergosterol in cell surface delivery in yeast. *Proc Natl Acad Sci U.S.A.*, *102*(50), 17981–17986. http://doi.org/10.1073/pnas.0509107102

Pruyne, D., & Bretscher, a. (2000). Polarization of cell growth in yeast. *Journal of Cell Science*, *113 (Pt 4*, 571–585.

Pruyne, D. W., Schott, D. H., & Bretscher, A. (1998). Tropomyosin-containing actin cables direct the Myo2p-dependent polarized delivery of secretory vesicles in budding yeast. *Journal of Cell Biology*, *143*(7), 1931–1945. http://doi.org/10.1083/jcb.143.7.1931

Quon, E., & Beh, C. T. (2015). Membrane Contact Sites: Complex Zones for Membrane Association and Lipid Exchange. *Lipid Insights*, *8*(Suppl. 1), 55–63. http://doi.org/10.4137/LPI.S37190

Raths, S., Rohrer, J., Crausaz, F., & Riezman, H. (1993). end3 and end4: Two mutants defective in receptor-mediated and fluid-phase endocytosis in Saccharomyces cerevisiae. *Journal of Cell Biology*, *120*(1), 55–65. http://doi.org/10.1083/jcb.120.1.55

Raychaudhuri, S., Im, Y. J., Hurley, J. H., & Prinz, W. A. (2006). Nonvesicular sterol movement from plasma membrane to ER requires oxysterol-binding protein-related proteins and phosphoinositides. *Journal of Cell Biology*, *173*(1), 107–119. http://doi.org/10.1083/jcb.200510084

Reider, A., Barker, S. L., Mishra, S. K., Im, Y. J., Maldonado-Báez, L., Hurley, J. H., … Wendland, B. (2009). Syp1 is a conserved endocytic adaptor that contains domains involved in cargo selection and membrane tubulation. *The EMBO Journal*, *28*(20), 3103–3116. http://doi.org/10.1038/emboj.2009.248

Ridgway, N. D., Dawson, P. A., Ho, Y. K., Brown, M. S., & Goldstein, J. L. (1992). Translocation of oxysterol binding protein to Golgi apparatus triggered by ligand binding. *Journal of Cell Biology*, *116*(2), 307–319.

Riegelhaupt, J. J., Waase, M. P., Garbarino, J., Cruz, D. E., & Breslow, J. L. (2010). Targeted disruption of steroidogenic acute regulatory protein D4 leads to modest weight reduction and minor alterations in lipid metabolism. *Journal of Lipid Research*, *51*(5), 1134–43. http://doi.org/10.1194/jlr.M003095

Riekhof, W. R., & Voelker, D. R. (2009). The yeast plasma membrane P4-ATPases are major transporters for lysophospholipids. *Biochimica et Biophysica Acta - Molecular and Cell Biology of Lipids*. http://doi.org/10.1016/j.bbalip.2009.02.013

Riekhof, W. R., Wu, W. I., Jones, J. L., Nikrad, M., Chan, M. M., Loewen, C. J. R., & Voelker, D. R. (2014). An assembly of proteins and lipid domains regulates transport of phosphatidylserine to phosphatidylserine decarboxylase 2 in Saccharomyces cerevisiae. *Journal of Biological Chemistry*, *289*(9), 5809–5819. http://doi.org/10.1074/jbc.M113.518217

Riezman, H. (1985). Endocytosis in yeast: Several of the yeast secretory mutants are defective in endocytosis. *Cell*, *40*(4), 1001–1009. http://doi.org/10.1016/0092-8674(85)90360-5

Rink, J., Ghigo, E., Kalaidzidis, Y., & Zerial, M. (2005). Rab conversion as a mechanism of progression from early to late endosomes. *Cell*, *122*(5), 735–749. http://doi.org/10.1016/j.cell.2005.06.043

Riquelme, M., Bredeweg, E. L., Callejas-Negrete, O., Roberson, R. W., Ludwig, S., Beltran-Aguilar, A., … Freitag, M. (2014). The Neurospora crassa exocyst complex tethers Spitzenkorper vesicles to the apical plasma membrane during polarized growth. *Molecular Biology of the Cell*, *25*(8), 1312–1326. http://doi.org/10.1091/mbc.E13-06-0299

Rivas, M. P., Kearns, B. G., Xie, Z., Guo, S., Sekar, M. C., Hosaka, K., … Bankaitis, V. A. (1999). Pleiotropic alterations in lipid metabolism in yeast sac1 mutants: relationship to “bypass Sec14p” and inositol auxotrophy. *Molecular Biology of the Cell*, *10*(7), 2235–50. Retrieved from

http://www.pubmedcentral.nih.gov/articlerender.fcgi?artid=25439&tool=pmcentrez&rendertype=abstract

Rivera-Molina, F. E., & Novick, P. J. (2009). A Rab GAP cascade defines the boundary between two Rab GTPases on the secretory pathway. *Proceedings of the National Academy of Sciences of the United States of America*, *106*(34), 14408–13. http://doi.org/10.1073/pnas.0906536106

Rizzoli, S. O., & Jahn, R. (2007). Kiss-and-run, collapse and "readily retrievable" vesicles. *Traffic*. http://doi.org/10.1111/j.1600-0854.2007.00614.x

Roberts, T. M., Kobor, M. S., Bastin-Shanower, S. A., Ii, M., Horte, S. A., Gin, J. W., … Brown, G. W. (2006). Slx4 regulates DNA damage checkpoint-dependent phosphorylation of the BRCT domain protein Rtt107/Esc4. *Molecular Biology of the Cell*, *17*(1), 539–48. http://doi.org/10.1091/mbc.E05-08-0785

Robinson, J. S., Klionsky, D. J., Banta, L. M., & Emr, S. D. (1988). Protein sorting in Saccharomyces cerevisiae: isolation of mutants defective in the delivery and processing of multiple vacuolar hydrolases. *Molecular and Cellular Biology*, *8*(11), 4936–4948. http://doi.org/10.1128/MCB.8.11.4936.Updated

Robinson, M., Poon, P. P., Schindler, C., Murray, L. E., Kama, R., Gabriely, G., … Gerst, J. E. (2006). The Gcs1 Arf-GAP mediates Snc1,2 v-SNARE retrieval to the Golgi in yeast. *Mol Biol Cell*, *17*(4), 1845–1858. http://doi.org/10.1091/mbc.E05-09-0832

Robinson, N. G., Guo, L., Imai, J., Toh, E. A., Matsui, Y., & Tamanoi, F. (1999). Rho3 of Saccharomyces cerevisiae, which regulates the actin cytoskeleton and exocytosis, is a GTPase which interacts with Myo2 and Exo70. *Molecular and Cellular Biology*, *19*(5), 3580–3587. Retrieved from http://www.ncbi.nlm.nih.gov/pubmed/10207081

Rodal, A. A., Manning, A. L., Goode, B. L., & Drubin, D. G. (2003). Negative regulation of yeast WASp by two SH3 domain-containing proteins. *Current Biology*, *13*(12), 1000–1008. http://doi.org/10.1016/S0960-9822(03)00383-X

Rodal, A. a, Sokolova, O., Robins, D. B., Daugherty, K. M., Hippenmeyer, S., Riezman, H., … Goode, B. L. (2005). Conformational changes in the Arp2/3 complex leading to actin nucleation. *Nature Structural & Molecular Biology*, *12*(1), 26–31. http://doi.org/10.1038/nsmb870

Rodriguez-Agudo, D., Calderon-Dominguez, M., Medina, M. A., Ren, S., Gil, G., & Pandak, W. M. (2012). ER stress increases StarD5 expression by stabilizing its mRNA and leads to relocalization of its protein from the nucleus to the membranes. *J Lipid Res*, *53*(12), 2708–2715. http://doi.org/10.1194/jlr.M031997

Rodriguez-Agudo, D., Ren, S., Hylemon, P. B., Redford, K., Natarajan, R., Del Castillo, A., … Pandak, W. M. (2005). Human StarD5, a cytosolic StAR-related lipid binding protein. *Journal of Lipid Research*, *46*(8), 1615–1623.

http://doi.org/10.1194/jlr.M400501-JLR200

Rohatgi, R., Ma, L., Miki, H., Lopez, M., Kirchhausen, T., Takenawa, T., & Kirschner, M. W. (1999). The interaction between N-WASP and the Arp2/3 complex links Cdc42-dependent signals to actin assembly. *Cell*, *97*(2), 221–231. http://doi.org/10.1016/S0092-8674(00)80732-1

Romanowski, M. J., Soccio, R. E., Breslow, J. L., & Burley, S. K. (2002). Crystal structure of the Mus musculus cholesterol-regulated START protein 4 (StarD4) containing a StAR-related lipid transfer domain. *Proceedings of the National Academy of Sciences of the United States of America*, *99*(10), 6949–54. http://doi.org/10.1073/pnas.052140699

Routt, S. M., & Bankaitis, V. a. (2004). Biological functions of phosphatidylinositol transfer proteins. *Biochemistry and Cell Biology = Biochimie et Biologie Cellulaire*, *82*(1), 254–262. http://doi.org/10.1139/o03-089

Roy, A., & Levine, T. P. (2004). Multiple pools of phosphatidylinositol 4-phosphate detected using the pleckstrin homology domain of Osh2p. *Journal of Biological Chemistry*, *279*(43), 44683–44689. http://doi.org/10.1074/jbc.M401583200

Saito, K., Fujimura-Kamada, K., Hanamatsu, H., Kato, U., Umeda, M., Kozminski, K. G., & Tanaka, K. (2007). Transbilayer Phospholipid Flipping Regulates Cdc42p Signaling during Polarized Cell Growth via Rga GTPase-Activating Proteins. *Developmental Cell*, *13*(5), 743–751. http://doi.org/10.1016/j.devcel.2007.09.014

Salminen, A., & Novick, P. J. (1989). The Sec15 protein responds to the function of the GTP binding protein, Sec4, to control vesicular traffic in yeast. *Journal of Cell Biology*, *109*(3), 1023–1036. http://doi.org/10.1083/jcb.109.3.1023

Santiago-Tirado, F. H., & Bretscher, A. (2011). Membrane-trafficking sorting hubs: Cooperation between PI4P and small GTPases at the trans-Golgi network. *Trends in Cell Biology*. http://doi.org/10.1016/j.tcb.2011.05.005

Santiago-Tirado, F. H., Legesse-Miller, A., Schott, D., & Bretscher, A. (2011). PI4P and Rab Inputs Collaborate in Myosin-V-Dependent Transport of Secretory Compartments in Yeast. *Developmental Cell*, *20*(1), 47–59. http://doi.org/10.1016/j.devcel.2010.11.006

Sato, Y., Fukai, S., Ishitani, R., & Nureki, O. (2007). Crystal structure of the Sec4p.Sec2p complex in the nucleotide exchanging intermediate state. *Proceedings of the National Academy of Sciences of the United States of America*, *104*(20), 8305–10. http://doi.org/10.1073/pnas.0701550104

Schaaf, G., Ortlund, E. A., Tyeryar, K. R., Mousley, C. J., Ile, K. E., Garrett, T. A., … Bankaitis, V. A. (2008). Functional Anatomy of Phospholipid Binding and Regulation of Phosphoinositide Homeostasis by Proteins of the Sec14 Superfamily. *Molecular*

Cell, *29*(2), 191–206. http://doi.org/10.1016/j.molcel.2007.11.026

Schafer, D. A. (2003). Actin puts on the squeezeNo Title. *Nature Cell Biology*, *5*, 693–694.

Schauder, C. M., Wu, X., Saheki, Y., Narayanaswamy, P., Torta, F., Wenk, M. R., … Reinisch, K. M. (2014). Structure of a lipid-bound extended synaptotagmin indicates a role in lipid transfer. *Nature*, *510*(7506), 552–5. http://doi.org/10.1038/nature13269

Schorr, M., Then, A., Tahirovic, S., Hug, N., & Mayinger, P. (2001). The phosphoinositide phosphatase Sac1p controls trafficking of the yeast Chs3p chitin synthase. *Current Biology*, *11*(18), 1421–1426. http://doi.org/10.1016/S0960-9822(01)00449-3

Schott, D. H., Collins, R. N., & Bretscher, A. (2002). Secretory vesicle transport velocity in living cells depends on the myosin-V lever arm length. *Journal of Cell Biology*, *156*(1), 35–39. http://doi.org/10.1083/jcb.200110086

Schott, D., Ho, J., Pruyne, D., & Bretscher, A. (1999). The COOH-terminal domain of Myo2p, a yeast myosin V, has a direct role in secretory vesicle targeting. *Journal of Cell Biology*, *147*(4), 791–807. http://doi.org/10.1083/jcb.147.4.791

Schuldiner, M., Metz, J., Schmid, V., Denic, V., Rakwalska, M., Schmitt, H. D., … Weissman, J. S. (2008). The GET Complex Mediates Insertion of Tail-Anchored Proteins into the ER Membrane. *Cell*, *134*(4), 634–645. http://doi.org/10.1016/j.cell.2008.06.025

Schulz, T. A., Choi, M. G., Raychaudhuri, S., Mears, J. A., Ghirlando, R., Hinshaw, J. E., & Prinz, W. A. (2009). Lipid-regulated sterol transfer between closely apposed membranes by oxysterol-binding protein homologues. *Journal of Cell Biology*, *187*(6), 889–903. http://doi.org/10.1083/jcb.200905007

Schulz, T. A., & Creutz, C. E. (2004). The Tricalbin C2 Domains: Lipid-Binding Properties of a Novel, Synaptotagmin-Like Yeast Protein Family. *Biochemistry*, *43*(13), 3987–3995. http://doi.org/10.1021/bi036082w

Sebastian, T. T., Baldridge, R. D., Xu, P., & Graham, T. R. (2012). Phospholipid flippases: Building asymmetric membranes and transport vesicles. *Biochimica et Biophysica Acta - Molecular and Cell Biology of Lipids*. http://doi.org/10.1016/j.bbalip.2011.12.007

Sengupta, P., Hammond, A., Holowka, D., & Baird, B. (2008). Structural determinants for partitioning of lipids and proteins between coexisting fluid phases in giant plasma membrane vesicles. *Biochimica et Biophysica Acta - Biomembranes*, *1778*(1), 20–32. http://doi.org/10.1016/j.bbamem.2007.08.028

Sharifai, N., Samarajeewa, H., Kamiyama, D., Deng, T. C., Boulina, M., & Chiba, A. (2014). Imaging dynamic molecular signaling by the Cdc42 GTPase within the developing CNS. *PLoS ONE*, *9*(2). http://doi.org/10.1371/journal.pone.0088870

Shechtman, C. F., Henneberry, A. L., Seimon, T. A., Tinkelenberg, A. H., Wilcox, L. J., Lee, E., … Sturley, S. L. (2011). Loss of subcellular lipid transport due to ARV1 deficiency disrupts organelle homeostasis and activates the unfolded protein response. *Journal of Biological Chemistry*, *286*(14), 11951–11959. http://doi.org/10.1074/jbc.M110.215038

Sheetz, M. P., & Singer, S. J. (1974). Biological Membranes as Bilayer Couples. A Molecular Mechanism of Drug-Erythrocyte Interactions. *Proceedings of the National Academy of Sciences*, *71*(11), 4457–4461. http://doi.org/10.1073/pnas.71.11.4457

Sikorski, R. S., & Hieter, P. (1989). A system of shuttle vectors and yeast host strains designed for efficient manipulation of DNA in Saccharomyces cerevisiae. *Genetics*, *122*(1), 19–27. http://doi.org/0378111995000377 [pii]

Simons, K., & Sampaio, J. L. (2011). Membrane organization and lipid rafts. *Cold Spring Harbor Perspectives in Biology*. http://doi.org/10.1101/cshperspect.a004697

Sivadon, P., Bauer, F., Aigle, M., & Crouzet, M. (1995). Actin cytoskeleton and budding pattern are altered in the yeast rvs161 mutant: the Rvs161 protein shares common domains with the brain protein amphiphysin. *MGG Molecular & General Genetics*, *246*(4), 485–495. http://doi.org/10.1007/BF00290452

Skinner, H. B., McGee, T. P., McMaster, C. R., Fry, M. R., Bell, R. M., & Bankaitis, V. a. (1995). The Saccharomyces cerevisiae phosphatidylinositol-transfer protein effects a ligand-dependent inhibition of choline-phosphate cytidylyltransferase activity. *Proceedings of the National Academy of Sciences of the United States of America*, *92*(1), 112–116. http://doi.org/10.1073/pnas.92.1.112

Skruzny, M., Brach, T., Ciuffa, R., Rybina, S., Wachsmuth, M., & Kaksonen, M. (2012). Molecular basis for coupling the plasma membrane to the actin cytoskeleton during clathrin-mediated endocytosis. *Proceedings of the National Academy of Sciences*, *109*(38), E2533–E2542. http://doi.org/10.1073/pnas.1207011109

Skruzny, M., Desfosses, A., Prinz, S., Dodonova, S. O., Gieras, A., Uetrecht, C., … Kaksonen, M. (2015). An Organized Co-assembly of Clathrin Adaptors Is Essential for Endocytosis. *Developmental Cell*, *33*(2), 150–162. http://doi.org/10.1016/j.devcel.2015.02.023

Slepnev, V. I., & De Camilli, P. (2000). Accessory factors in clathrin-dependent synaptic vesicle endocytosis. *Nature Reviews. Neuroscience*, *1*(3), 161–72. http://doi.org/10.1038/35044540

Smaczynska-de Rooij, I. I., Allwood, E. G., Aghamohammadzadeh, S., Hettema, E. H.,

Goldberg, M. W., Ayscough, K. R., … Cai, M. J. (2010). A role for the dynamin-like protein Vps1 during endocytosis in yeast. *Journal of Cell Science*, *123*(Pt 20), 3496–506. http://doi.org/10.1242/jcs.070508

Smaczynska-de Rooij, I. I., Allwood, E. G., Mishra, R., Booth, W. I., Aghamohammadzadeh, S., Goldberg, M. W., & Ayscough, K. R. (2012). Yeast Dynamin Vps1 and Amphiphysin Rvs167 Function Together During Endocytosis. *Traffic*, *13*(2), 317–328. http://doi.org/10.1111/j.1600-0854.2011.01311.x

Soccio, R. E., Adams, R. M., Romanowski, M. J., Sehayek, E., Burley, S. K., & Breslow, J. L. (2002). The cholesterol-regulated StarD4 gene encodes a StAR-related lipid transfer protein with two closely related homologues, StarD5 and StarD6. *Proceedings of the National Academy of Sciences of the United States of America*, *99*(10), 6943–8. http://doi.org/10.1073/pnas.052143799

Soffientini, U., Dolan, S., & Graham, A. (2015). Cytosolic Lipid Trafficking Proteins STARD4 and STARD5 Modulate Hepatic Neutral Lipid Metabolism: Implications for Diabetic Dyslipidaemia and Steatosis. *Journal of Diabetes and Metabolism*, *6*(6). http://doi.org/10.4172/2155-6156.1000558

Sokac, A. M., & Bement, W. M. (2006). Kiss-and-Coat and Compartment Mixing: Coupling Exocytosis to Signal Generation and Local Actin Assembly. *Molecular Biology of the Cell*, *17*(4), 1495–502. http://doi.org/10.1091/mbc.E05-10-0908

Sokac, A. M., Co, C., Taunton, J., & Bement, W. (2003). Cdc42-dependent actin polymerization during compensatory endocytosis in Xenopus eggs. *Nature Cell Biology*, *5*(8), 727–732. http://doi.org/10.1038/ncb1025

Songer, J. A., & Munson, M. (2009). Sec6p Anchors the Assembled Exocyst Complex at Sites of Secretion. *Molecular Biology of the Cell*, *20*, 973–982. http://doi.org/10.1091/mbc.E08

Soulard, A., Lechler, T., Spiridonov, V., Shevchenko, A., Shevchenko, A., Li, R., & Winsor, B. (2002). Saccharomyces cerevisiae Bzz1p is implicated with type I myosins in actin patch polarization and is able to recruit actin-polymerizing machinery in vitro. *Molecular and Cellular Biology*, *22*(22), 7889–7906. http://doi.org/10.1128/MCB.22.22.7889-7906.2002

Spiess, M., de Craene, J. O., Michelot, A., Rinaldi, B., Huber, A., Drubin, D. G., … Friant, S. (2013). Lsb1 Is a Negative Regulator of Las17 Dependent Actin Polymerization Involved in Endocytosis. *PLoS ONE*, *8*(4). http://doi.org/10.1371/journal.pone.0061147

Springer, S., Spang, A., & Schekman, R. (1999). A primer on vesicle budding. *Cell*, *97*(2), 145–148.

Sreenivas, A., Patton-Vogt, J. L., Bruno, V., Griac, P., & Henry, S. A. (1998). A role for

phospholipase D (Pld1p) in growth, secretion, and regulation of membrane lipid synthesis in yeast. *Journal of Biological Chemistry*, *273*(27), 16635–16638. http://doi.org/10.1074/jbc.273.27.16635

Stefan, C. J., Audhya, A., & Emr, S. D. (2002). The yeast synaptojanin-like proteins control the cellular distribution of phosphatidylinositol (4,5)-bisphosphate. *Mol Biol Cell*, *13*(2), 542–557. http://doi.org/10.1091/mbc.01-10-0476

Stefan, C. J., Manford, A. G., Baird, D., Yamada-Hanff, J., Mao, Y., & Emr, S. D. (2011). Osh proteins regulate phosphoinositide metabolism at ER-plasma membrane contact sites. *Cell*, *144*(3), 389–401. http://doi.org/10.1016/j.cell.2010.12.034

Stevens, C. F., & Williams, J. H. (2000). "Kiss and run" exocytosis at hippocampal synapses. *Proceedings of the National Academy of Sciences of the United States of America*, *97*(23), 12828–33. http://doi.org/10.1073/pnas.230438697

Stimpson, H. E. M., Toret, C. P., Cheng, A. T., Pauly, B. S., & Drubin, D. G. (2009). Early-arriving Syp1p and Ede1p function in endocytic site placement and formation in budding yeast. *Molecular Biology of the Cell*, *20*(22), 4640–51. http://doi.org/10.1091/mbc.E09-05-0429

Stock, S. D., Hama, H., DeWald, D. B., & Takemoto, J. Y. (1999). SEC14-dependent secretion in Saccharomyces cerevisiae. Nondependence on sphingolipid synthesis-coupled diacylglycerol production. *Journal of Biological Chemistry*, *274*(19), 12979–12983. http://doi.org/10.1074/jbc.274.19.12979

Stolz, L. E., Huynh, C. V., Thorner, J., & York, J. D. (1998). Identification and characterization of an essential family of inositol polyphosphate 5-phosphatases (INP51, INP52 and INP53 gene products) in the yeast Saccharomyces cerevisiae. *Genetics*, *148*(4), 1715–1729.

Stolz, L. E., Kuo, W. J., Longchamps, J., Sekhon, M. K., & York, J. D. (1998). INP51, a yeast inositol polyphosphate 5-phosphatase required for phosphatidylinositol 4,5-bisphosphate homeostasis and whose absence confers a cold-resistant phenotype. *Journal of Biological Chemistry*, *273*(19), 11852–11861. http://doi.org/10.1074/jbc.273.19.11852

Stott, B. M., Vu, M. P., McLemore, C. O., Lund, M. S., Gibbons, E., Brueseke, T. J., … Bell, J. D. (2008). Use of fluorescence to determine the effects of cholesterol on lipid behavior in sphingomyelin liposomes and erythrocyte membranes. *Journal of Lipid Research*, *49*(October 2015), 1202–1215. http://doi.org/10.1194/jlr.M700479-JLR200

Strahl, T., Hama, H., DeWald, D. B., & Thorner, J. (2005). Yeast phosphatidylinositol 4-kinase, Pik1, has essential roles at the Golgi and in the nucleus. *Journal of Cell Biology*, *171*(6), 967–979. http://doi.org/10.1083/jcb.200504104

Strahl, T., & Thorner, J. (2007). Synthesis and function of membrane phosphoinositides in budding yeast, Saccharomyces cerevisiae. *Biochimica et Biophysica Acta - Molecular and Cell Biology of Lipids*. http://doi.org/10.1016/j.bbalip.2007.01.015

Sturley, S. L. (2000). Conservation of eukaryotic sterol homeostasis: New insights from studies in budding yeast. *Biochimica et Biophysica Acta - Molecular and Cell Biology of Lipids*. http://doi.org/10.1016/S1388-1981(00)00145-1

Sullivan, D. P., Ohvo-Rekilä, H., Baumann, N. a, Beh, C. T., & Menon, a K. (2006). Sterol trafficking between the endoplasmic reticulum and plasma membrane in yeast. *Biochemical Society Transactions*, *34*(Pt 3), 356–358. http://doi.org/10.1042/BST0340356

Sun, Y., Kaksonen, M., Madden, D. T., Schekman, R., & Drubin, D. G. (2005). Interaction of Sla2p's ANTH domain with PtdIns(4,5)P2 is important for actin-dependent endocytic internalization. *Molecular Biology of the Cell*, *16*(2), 717–730. http://doi.org/10.1091/mbc.E04-08-0740

Surma, M. A., Klose, C., Klemm, R. W., Ejsing, C. S., & Simons, K. (2011). Generic Sorting of Raft Lipids into Secretory Vesicles in Yeast. *Traffic*, *12*(9), 1139–1147. http://doi.org/10.1111/j.1600-0854.2011.01221.x

Swain, E., Stukey, J., McDonough, V., Germann, M., Liu, Y., Sturley, S. L., & Nickels, J. T. (2002). Yeast cells lacking the ARV1 gene harbor defects in sphingolipid metabolism: Complementation by human ARV1. *Journal of Biological Chemistry*, *277*(39), 36152–36160. http://doi.org/10.1074/jbc.M206624200

Symons, M., Derry, J. M. J., Karlak, B., Jiang, S., Lemahieu, V., McCormick, F., … Abo, A. (1996). Wiskott-Aldrich syndrome protein, a novel effector for the GTPase CDC42Hs, is implicated in actin polymerization. *Cell*, *84*(5), 723–734. http://doi.org/10.1016/S0092-8674(00)81050-8

Taheri-Talesh, N., Horio, T., Araujo-Baza, L., Dou, X., Espeso, E. A., Penalva, M. A., … Oakley, B. R. (2008). The Tip Growth Apparatus of Aspergillus nidulans. *Molecular Biology of the Cell*, *19*, 1439–1449. http://doi.org/10.1091/mbc.E07

Tahirovic, S., Schorr, M., & Mayinger, P. (2005). Regulation of intracellular phosphatidylinositol-4-phosphate by the Sac1 lipid phosphatase. *Traffic*, *6*(2), 116–130. http://doi.org/10.1111/j.1600-0854.2004.00255.x

Takamori, S., Holt, M., Stenius, K., Lemke, E. A., Grønborg, M., Riedel, D., … Jahn, R. (2006). Molecular Anatomy of a Trafficking Organelle. *Cell*, *127*(4), 831–846. http://doi.org/10.1016/j.cell.2006.10.030

Takei, K., Mundigl, O., Daniell, L., & De Camilli, P. (1996). The synaptic vesicle cycle: A single vesicle budding step involving clathrin and dynamin. *Journal of Cell Biology*, *133*(6), 1237–1250. http://doi.org/10.1083/jcb.133.6.1237

Tang, H. Y., Xu, J., & Cai, M. (2000). Pan1p, End3p, and S1a1p, three yeast proteins required for normal cortical actin cytoskeleton organization, associate with each other and play essential roles in cell wall morphogenesis. *Molecular and Cellular Biology*, *20*(1), 12–25. http://doi.org/10.1128/MCB.20.1.12-25.2000

Tarassov, K., Messier, V., Landry, C. R., Radinovic, S., Serna Molina, M. M., Shames, I., … Shames, I. (2008). An in vivo map of the yeast protein interactome. *Science (New York, N.Y.)*, *320*(5882), 1465–70. http://doi.org/10.1126/science.1153878

Taunton, J., Rowning, B. A., Coughlin, M. L., Wu, M., Moon, R. T., Mitchison, T. J., & Larabell, C. A. (2000). Actin-dependent propulsion of endosomes and lysosomes by recruitment of N-WASP. *Journal of Cell Biology*, *148*(3), 519–530. http://doi.org/10.1083/jcb.148.3.519

Tavassoli, S., Chao, J. T., Young, B. P., Cox, R. C., Prinz, W. A., de Kroon, A. I., & Loewen, C. J. (2013). Plasma membrane--endoplasmic reticulum contact sites regulate phosphatidylcholine synthesis. *{EMBO} Rep.*, *14*(5), 434–440. http://doi.org/10.1038/embor.2013.36

TerBush, D. R., & Novick, P. (1995). Sec6, Sec8, and Sec15 are components of a multisubunit complex which localizes to small bud tips in Saccharomyces cerevisiae. *Journal of Cell Biology*, *130*(2), 299–312. http://doi.org/10.1083/jcb.130.2.299

Thorsell, A.-G., Lee, W. H., Persson, C., Siponen, M. I., Nilsson, M., Busam, R. D., … Lehtiö, L. (2011). Comparative structural analysis of lipid binding START domains. *PloS One*, *6*(6), e19521. http://doi.org/10.1371/journal.pone.0019521

Tinkelenberg, A. H., Liu, Y., Alcantara, F., Khan, S., Guo, Z., Bard, M., & Sturley, S. L. (2000). Mutations in yeast ARV1 alter intracellular sterol distribution and are complemented by human ARV1. *Journal of Biological Chemistry*, *275*(52), 40667–40670. http://doi.org/10.1074/jbc.C000710200

Tong, F., Billheimer, J., Shechtman, C. F., Liu, Y., Crooke, R., Graham, M., … Rader, D. J. (2010). Decreased expression of ARV1 results in cholesterol retention in the endoplasmic reticulum and abnormal bile acid metabolism. *Journal of Biological Chemistry*, *285*(44), 33632–33641. http://doi.org/10.1074/jbc.M110.165761

Tong, J., Yang, H., Yang, H., Eom, S. H., & Im, Y. J. (2013). Structure of Osh3 reveals a conserved mode of phosphoinositide binding in oxysterol-binding proteins. *Structure*, *21*(7), 1203–1213. http://doi.org/10.1016/j.str.2013.05.007

Torri-Tarelli, F., Haimann, C., & Ceccarelli, B. (1987). Coated vesicles and pits during enhanced quantal release of acetylcholine at the neuromuscular junction. *Journal of Neurocytology*, *16*, 205–214.

Toulmay, A., & Prinz, W. A. (2012). A conserved membrane-binding domain targets

proteins to organelle contact sites. *J. Cell. Sci.*, *125*(Pt 1), 49–58. http://doi.org/10.1242/jcs.085118

Tsujishita, Y., & Hurley, J. H. (2000). Structure and lipid transport mechanism of a StAR-related domain. *Nature Structural Biology*, *7*(5), 408–14. http://doi.org/10.1038/75192

Tuck, S. (2011). Extracellular vesicles: Budding regulated by a phosphatidylethanolamine translocase. *Current Biology*, *21*(24). http://doi.org/10.1016/j.cub.2011.11.009

Umebayashi, K., & Nakano, A. (2003). Ergosterol is required for targeting of tryptophan permease to the yeast plasma membrane. *Journal of Cell Biology*, *161*(6), 1117–1131. http://doi.org/10.1083/jcb.200303088

Urbani, L., & Simoni, R. D. (1990). Cholesterol and vesicular stomatitis virus G protein take separate routes from the endoplasmic reticulum to the plasma membrane. *Journal of Biological Chemistry*, *265*(4), 1919–1923.

Valdez-Taubas, J., & Pelham, H. R. B. (2003). Slow diffusion of proteins in the yeast plasma membrane allows polarity to be maintained by endocytic cycling. *Current Biology*, *13*(18), 1636–1640. http://doi.org/10.1016/j.cub.2003.09.001

Van Leeuwen, W., Vermeer, J. E. M., Gadella, T. W. J., & Munnik, T. (2007). Visualization of phosphatidylinositol 4,5-bisphosphate in the plasma membrane of suspension-cultured tobacco BY-2 cells and whole Arabidopsis seedlings. *Plant Journal*, *52*(6), 1014–1026. http://doi.org/10.1111/j.1365-313X.2007.03292.x

van Meer, G., Voelker, D. R., & Feigenson, G. W. (2008). Membrane lipids: where they are and how they behave. *Nature Reviews. Molecular Cell Biology*, *9*(2), 112–124. http://doi.org/10.1038/nrm2330

Villasmil, M. L., Ansbach, A., & Nickels, J. T. (2011). The putative lipid transporter, Arv1, is required for activating pheromone-induced MAP kinase signaling in Saccharomyces cerevisiae. *Genetics*, *187*(2), 455–465. http://doi.org/10.1534/genetics.110.120725

Villasmil, M. L., & Nickels, J. T. (2011). Determination of the membrane topology of Arv1 and the requirement of the ER luminal region for Arv1 function in Saccharomyces cerevisiae. *FEMS Yeast Research*, *11*(6), 524–527. http://doi.org/10.1111/j.1567-1364.2011.00737.x

Volmer, R., & Ron, D. (2015). Lipid-dependent regulation of the unfolded protein response. *Current Opinion in Cell Biology*, *33*, 67–73. http://doi.org/10.1016/j.ceb.2014.12.002

Wach, A., Brachat, A., Alberti-Segui, C., Rebischung, C., & Philippsen, P. (1997).

Heterologous HIS3 marker and GFP reporter modules for PCR-targeting in Saccharomyces cerevisiae. *Yeast*, *13*(11), 1065–1075. http://doi.org/10.1002/(SICI)1097-0061(19970915)13:11<1065::AID-YEA159>3.0.CO;2-K

Wagner, W., Bielli, P., Wacha, S., & Ragnini-Wilson, A. (2002). Mlc1p promotes septum closure during cytokinesis via the IQ motifs of the vesicle motor Myo2p. *EMBO Journal*, *21*(23), 6397–6408. http://doi.org/10.1093/emboj/cdf650

Walch-Solimena, C., Collins, R. N., & Novick, P. J. (1997). Sec2p mediates nucleotide exchange on Sec4p and is involved in polarized delivery of post-Golgi vesicles. *Journal of Cell Biology*, *137*(7), 1495–1509. http://doi.org/10.1083/jcb.137.7.1495

Walch-Solimena, C., & Novick, P. (1999). The yeast phosphatidylinositol-4-OH kinase Pik1 regulates secretion at the Golgi. *Nature Cell Biology*, *1*, 523–525.

Walther, T. C., Brickner, J. H., Aguilar, P. S., Bernales, S., & Walter, P. (2006). Eisosomes mark static sites of endocytosis. *Nature*, *439*(7079), 998–1003. http://doi.org/Doi 10.1038/Nature04472

Walworth, N. C., Brennwald, P., Kabcenell, a K., Garrett, M., & Novick, P. (1992). Hydrolysis of GTP by Sec4 protein plays an important role in vesicular transport and is stimulated by a GTPase-activating protein in Saccharomyces cerevisiae. *Molecular and Cellular Biology*, *12*(5), 2017–2028. http://doi.org/10.1128/MCB.12.5.2017

Wang, D., Sletto, J., Tenay, B., & Kim, K. (2011). Yeast dynamin implicated in endocytic scission and the disassembly of endocytic components. *Communicative and Integrative Biology*, *4*(2), 178–181. http://doi.org/10.4161/cib.4.2.14257

Wang, J., Ren, J., Wu, B., Feng, S., Cai, G., Tuluc, F., … Guo, W. (2015). Activation of Rab8 guanine nucleotide exchange factor Rabin8 by ERK1/2 in response to EGF signaling. *Proceedings of the National Academy of Sciences of the United States of America*, *112*(1), 148–53. http://doi.org/10.1073/pnas.1412089112

Wang, P.-Y., Weng, J., & Anderson, R. G. W. (2005). OSBP is a cholesterol-regulated scaffolding protein in control of ERK 1/2 activation. *Science (New York, N.Y.)*, *307*(5714), 1472–1476. http://doi.org/10.1126/science.1107710

Watanabe, S., Rost, B. R., Camacho-Pérez, M., Davis, M. W., Söhl-Kielczynski, B., Rosenmund, C., & Jorgensen, E. M. (2013). Ultrafast endocytosis at mouse hippocampal synapses. *Nature*, *504*(7479), 242–7. http://doi.org/10.1038/nature12809

Watt, S. A., Kular, G., Fleming, I. N., Downes, C. P., & Lucocq, J. M. (2002). Subcellular localization of phosphatidylinositol 4,5-bisphosphate using the pleckstrin homology domain of phospholipase C delta1. *The Biochemical Journal*, *363*(Pt 3), 657–66.

http://doi.org/10.1074/jbc.M301418200

Weber-Boyvat, M., Aro, N., Chernov, K. G., Nyman, T., & Jäntti, J. (2011). Sec1p and Mso1p C-terminal tails cooperate with the SNAREs and Sec4p in polarized exocytosis. *Molecular Biology of the Cell*, *22*(2), 230–244. http://doi.org/10.1091/mbc.E10-07-0592

Weber-Boyvat, M., Chernov, K. G., Aro, N., Wohlfahrt, G., Olkkonen, V. M., & Jäntti, J. (2016). The Sec1/Munc18 Protein Groove Plays a Conserved Role in Interaction with Sec9p/SNAP-25. *Traffic*, *17*(2), 131–153. http://doi.org/10.1111/tra.12349

Weber-Boyvat, M., Kentala, H., Lilja, J., Vihervaara, T., Hanninen, R., Zhou, Y., … Olkkonen, V. M. (2015). OSBP-related protein 3 (ORP3) coupling with VAMP-associated protein A regulates R-Ras activity. *Experimental Cell Research*, *331*(2), 278–291. http://doi.org/10.1016/j.yexcr.2014.10.019

Weber-Boyvat, M., Zhong, W., Yan, D., & Olkkonen, V. M. (2013). Oxysterol-binding proteins: Functions in cell regulation beyond lipid metabolism. *Biochemical Pharmacology*. http://doi.org/10.1016/j.bcp.2013.02.016

Wen, K. K., & Rubenstein, P. A. (2005). Acceleration of yeast actin polymerization by yeast Arp2/3 complex does not require an Arp2/3-activating protein. *Journal of Biological Chemistry*, *280*(25), 24168–24174. http://doi.org/10.1074/jbc.M502024200

Wennerberg, K., Rossman, K. L., & Der, C. J. (2005). The Ras superfamily at a glance. *Journal of Cell Science*, *118*, 843–846.

Wesp, A., Hicke, L., Palecek, J., Lombardi, R., Aust, T., Munn, A. L., & Riezman, H. (1997). End4p/Sla2p interacts with actin-associated proteins for endocytosis in Saccharomyces cerevisiae. *Molecular Biology of the Cell*, *8*(11), 2291–2306. http://doi.org/10.1091/mbc.8.11.2291

West, M., Zurek, N., Hoenger, A., & Voeltz, G. K. (2011). A 3D analysis of yeast ER structure reveals how ER domains are organized by membrane curvature. *Journal of Cell Biology*, *193*(2), 333–346. http://doi.org/10.1083/jcb.201011039

Wilkie, A. O. (1994). The molecular basis of genetic dominance. *Journal of Medical Genetics*, *31*(2), 89–98. http://doi.org/10.1136/jmg.31.2.89

Willig, K. I., Rizzoli, S. O., Westphal, V., Jahn, R., & Hell, S. W. (2006). STED microscopy reveals that synaptotagmin remains clustered after synaptic vesicle exocytosis. *Nature*, *440*(7086), 935–939. http://doi.org/10.1038/nature04592

Willox, A. K., & Royle, S. J. (2012). Stonin 2 is a major adaptor protein for clathrin-mediated synaptic vesicle retrieval. *Current Biology*, *22*(15), 1435–1439. http://doi.org/10.1016/j.cub.2012.05.048

Winzeler, E. A., Shoemaker, D. D., Astromoff, A., Liang, H., Anderson, K., Andre, B., … Davis, R. W. (1999). Functional characterization of the S. cerevisiae genome by gene deletion and parallel analysis. *Science (New York, N.Y.)*, *285*(5429), 901–906. http://doi.org/10.1126/science.285.5429.901

Wiradjaja, F., Ooms, L. M., Tahirovic, S., Kuhne, E., Devenish, R. J., Munn, A. L., … Mitchell, C. A. (2007). Inactivation of the phosphoinositide phosphatases Sac1p and Inp54p leads to accumulation of phosphatidylinositol 4,5-bisphosphate on vacuole membranes and vacuolar fusion defects. *Journal of Biological Chemistry*, *282*(22), 16295–16307. http://doi.org/10.1074/jbc.M701038200

Wiradjaja, F., Ooms, L. M., Whisstock, J. C., McColl, B., Helfenbaum, L., Sambrook, J. F., … Mitchell, C. A. (2001). The yeast inositol polyphosphate 5-phosphatase Inp54p localizes to the endoplasmic reticulum via a C-terminal hydrophobic anchoring tail. Regulation of secretion from the endoplasmic reticulum. *Journal of Biological Chemistry*, *276*(10), 7643–7653. http://doi.org/10.1074/jbc.M010471200

Wong, T. a, Fairn, G. D., Poon, P. P., Shmulevitz, M., McMaster, C. R., Singer, R. a, & Johnston, G. C. (2005). Membrane metabolism mediated by Sec14 family members influences Arf GTPase activating protein activity for transport from the trans-Golgi. *Proceedings of the National Academy of Sciences of the United States of America*, *102*(36), 12777–82. http://doi.org/10.1073/pnas.0506156102

Wu, H., & Brennwald, P. (2010). The Function of Two Rho Family GTPases Is Determined by Distinct Patterns of Cell Surface Localization. *Molecular and Cellular Biology*, *30*(21), 5207–5217. http://doi.org/10.1128/MCB.00366-10

Wu, H., Turner, C., Gardner, J., Temple, B., & Brennwald, P. (2010). The Exo70 Subunit of the Exocyst Is an Effector for Both Cdc42 and Rho3 Function in Polarized Exocytosis. *Molecular Biology of the Cell*, *21*, 430–442. http://doi.org/10.1091/mbc.E09

Xie, Z., Fang, M., & Bankaitis, V. A. (2001). Evidence for an intrinsic toxicity of phosphatidylcholine to Sec14p-dependent protein transport from the yeast Golgi complex. *Molecular Biology of the Cell*, *12*(4), 1117–29. Retrieved from http://www.pubmedcentral.nih.gov/articlerender.fcgi?artid=32291&tool=pmcentrez&rendertype=abstract

Xie, Z., Fang, M., Rivas, M. P., Faulkner, a J., Sternweis, P. C., Engebrecht, J. a, & Bankaitis, V. a. (1998). Phospholipase D activity is required for suppression of yeast phosphatidylinositol transfer protein defects. *Proceedings of the National Academy of Sciences of the United States of America*, *95*(21), 12346–12351. http://doi.org/10.1073/pnas.95.21.12346

Xu, P., Baldridge, R. D., Chi, R. J., Burd, C. G., & Graham, T. R. (2013). Phosphatidylserine flipping enhances membrane curvature and negative charge required for vesicular transport. *Journal of Cell Biology*, *202*(6), 875–886.

http://doi.org/10.1083/jcb.201305094

Yakir-Tamang, L., & Gerst, J. E. (2009). A phosphatidylinositol-transfer protein and phosphatidylinositol-4-phosphate 5-kinase control Cdc42 to regulate the actin cytoskeleton and secretory pathway in yeast. *Molecular Biology of the Cell*, *20*(15), 3583–3597. http://doi.org/10.1091/mbc.E08

Yamashita, M., Kurokawa, K., Sato, Y., Yamagata, A., Mimura, H., Yoshikawa, A., … Fukai, S. (2010). Structural basis for the Rho- and phosphoinositide-dependent localization of the exocyst subunit Sec3. *Nature Structural & Molecular Biology*, *17*(2), 180–186. http://doi.org/10.1038/nsmb.1722

Yanagisawa, L. L., Marchena, J., Xie, Z., Li, X., Poon, P. P., Singer, R. a, … Bankaitis, V. a. (2002). Activity of specific lipid-regulated ADP ribosylation factor-GTPase-activating proteins is required for Sec14p-dependent Golgi secretory function in yeast. *Molecular Biology of the Cell*. http://doi.org/10.1091/mbc.01-11-0563.

Yang, S., Ayscough, K. R., & Drubin, D. G. (1997). A role for the actin cytoskeleton of Saccharomyces cerevisiae in bipolar bud-site selection. *Journal of Cell Biology*, *136*(1), 111–123. http://doi.org/10.1083/jcb.136.1.111

Yao, J., Nowack, A., Kensel-Hammes, P., Gardner, R. G., & Bajjalieh, S. M. (2010). Cotrafficking of SV2 and synaptotagmin at the synapse. *The Journal of Neuroscience : The Official Journal of the Society for Neuroscience*, *30*(16), 5569–78. http://doi.org/10.1523/JNEUROSCI.4781-09.2010

Youn, J.-Y., Friesen, H., Takuma, K., Henne, W. M., Kurat, C. F., Ye, W., … Andrews, B. J. (2010). Dissecting BAR Domain Function in the Yeast Amphiphysins Rvs161 and Rvs167 during Endocytosis. *Molecular Biology of the Cell*, *21*, 3054–3069. http://doi.org/10.1091/mbc.E10

Yu, H.-Y. E., & Bement, W. M. (2007). Multiple myosins are required to coordinate actin assembly with coat compression during compensatory endocytosis. *Molecular Biology of the Cell*, *18*(10), 4096–4105. http://doi.org/10.1091/mbc.E06-11-0993

Yu, J. W., Mendrola, J. M., Audhya, A., Singh, S., Keleti, D., DeWald, D. B., … Lemmon, M. A. (2004). Genome-wide analysis of membrane targeting by S. cerevisiae pleckstrin homology domains. *Molecular Cell*, *13*(5), 677–688. http://doi.org/10.1016/S1097-2765(04)00083-8

Zajac, A., Sun, X., Zhang, J., & Guo, W. (2005). Cyclical Regulation of the Exocyst and Cell Polarity Determinants for Polarized Cell Growth. *Molecular Biology of the Cell*, *16*(3), 1500–1512. http://doi.org/10.1091/mbc.E04-10-0896

Zanolari, B., Friant, S., Funato, K., Sütterlin, C., Stevenson, B. J., & Riezman, H. (2000). Sphingoid base synthesis requirement for endocytosis in Saccharomyces cerevisiae. *The EMBO Journal*, *19*(12), 2824–2833.

http://doi.org/10.1093/emboj/19.12.2824

Zeng, G., Yu, X., & Cai, M. (2001). Regulation of yeast actin cytoskeleton-regulatory complex Pan1p/Sla1p/End3p by serine/threonine kinase Prk1p. *Molecular Biology of the Cell*, *12*(12), 3759–3772.

Zhang, X., Bi, E., Novick, P., Du, L., Kozminski, K. G., Lipschutz, J. H., & Guo, W. (2001). Cdc42 Interacts with the Exocyst and Regulates Polarized Secretion. *Journal of Biological Chemistry*, *276*(50), 46745–46750. http://doi.org/10.1074/jbc.M107464200

Zhang, X., Orlando, K., He, B., Xi, F., Zhang, J., Zajac, A., & Guo, W. (2008). Membrane association and functional regulation of Sec3 by phospholipids and Cdc42. *Journal of Cell Biology*, *180*(1), 145–158. http://doi.org/10.1083/jcb.200704128

Ziman, M., Preuss, D., Mulholland, J., O'Brien, J. M., Botstein, D., & Johnson, D. I. (1993). Subcellular localization of Cdc42p, a Saccharomyces cerevisiae GTP-binding protein involved in the control of cell polarity. *Molecular Biology of the Cell*, *4*(12), 1307–1316.

Appendix A.

List of genes

Yeast gene name	Human homolog	Function	Associated disease(s)	References
ABP1	ABP1	Actin binding protein	Hepatitis B	(C. J. Huang, Chen, & Ting, 2000)
AGE1	ARFGAP1	Arf GTPase activating protein effector	Parkinson's Disease	(Stafa et al., 2012)
AGE2	ASAP2	Arf GTPase activating protein effector		
ARE1	SOAT1	Acyl-CoA:sterol acyltransferase	Atherosclerosis	(Chistiakov, Bobryshev, & Orekhov, 2016)
ARE2	SOAT1	Acyl-CoA:sterol acyltransferase	Atherosclerosis	(Chistiakov et al., 2016)
ARF1	ARF1	Ras GTPase. ADP-ribosylation factor	Oncogene	(Davis et al., 2016)
ARK1	AAK1	Serine/threonine protein kinase regulating the cortical actin	ALS	(Shi, Conner, & Liu, 2014)

		cytoskeleton		
ARV1	ARV1	ER transmembrane protein	Epilepsy	(Palmer et al., 2016)
BBC1		Putative regulator of actin patch assembly		
BEM3	CHN1	Rho GTPase activating protein	Neuropathy	(Miyake et al., 2008)
BGL2		Endo-beta-1,3-glucanase a major protein of the cell wall		
BZZ1	Syndapin	SH3 domain protein implicated in regulating actin polymerization	Oncogene	(Smid, Karas-Kuzelicki, Jazbec, & Mlinaric-Rascan, 2016)
CAN1	SLC7A	Plasma membrane arginine permease		
CDC42	CDC42	Rho GTPase regulating actin nucleation and cell polarity	Oncogene HIV	(Nikolic et al., 2011; Stengel & Zheng, 2011)
CDC50	TMEM30	Regulator of Drs2p catalytic activity	Cystic Fibrosis	(Muhlebach et al., 2016)

CHO1	PTDSS1	Phosphatidylserine synthase	Lenz-Majewski syndrome	(Sousa et al., 2014)
DNF1	ATP8B	Aminophospholipid translocase type 4 P-type ATPase	Liver disease	(Deng et al., 2012)
DNF2	ATP8B	Aminophospholipid translocase type 4 P-type ATPase	Liver disease	(Deng et al., 2012)
DRS2	ATP8A	Trans-Golgi network aminophospholipid translocase		
DYN2	DYNLL2	Cytoplasmic dynein light chain		
EDE1	EPS15	Scaffold protein involved in the formation of early endocytic sites	Oncogene	(Mendelsohn & Baselga, 2003)
END3		EH domain-containing protein involved in endocytosis		
ENT1	EPN1	Protein involved in endocytosis and actin patch assembly	Tumor Suppressor	(Chang et al., 2015)
ERG5	CYP26	C-22 sterol desaturase	Oncogene	(Sun et al., 2015)

ERG9	FDFT1	Squalene synthase	Cataract	(Mori et al., 2006)
EXO70	EXOC7	Subunit of the exocyst complex		
EXO84	EXOC8	Subunit of the exocyst complex		
FUR4		Plasma membrane localized uracil permease		
GAP1		General amino acid permease		
GAS1		Beta-1,3-glucanosyltransferase		
GDI1	GDI1	GDP dissociation inhibitor	Intellectual Disability	(Romero-Ramirez et al., 2004)
GIC1		Protein involved in initiation of budding and cellular polarization		
GSC1		Catalytic subunit of 1,3-beta-D-glucan synthase		
GYP1	TBC1D	Cis-golgi GTPase-activating protein	Obesity	(L. Chen et al., 2016)

		for Rabs		
HAC1	XBP1	Basic leucine zipper transcription factor	Oncogene	(Romero-Ramirez et al., 2004)
HEM1	ALAS1	5-aminolevulinate synthase	Porphyria	(Chan et al., 2015)
HSP70	HSP70	Heat shock protein	Oncogene	(Matokanovic, Barisic, Filipovic-Grcic, & Maysinger, 2013)
ICE2		Integral ER membrane protein involved in ER inheritance		
INP51	INPP5J	Synaptojanin-like hosphatidylinositol 4,5-bisphosphate 5-phosphatase	Tumor Suppressor	(Eramo & Mitchell, 2016)
INP52	SYNJ1	Polyphosphatidylinositol phosphatase involved in late endocytosis	Neurodegenerate Disease	(Drouet & Lesage, 2014)
INP53	INPP5E	Polyphosphatidylinositol phosphatase involved in late endocytosis	Tumor Suppressor	(Eramo & Mitchell, 2016)
INP54		Phosphatidylinositol 4,5-bisphosphate 5-		

		phosphatase		
IST2	TMEM16A	Cortical ER protein involved in ER-plasma membrane tethering	Oncogene	(Duvvuri et al., 2012)
KAR2		ATPase involved in protein import into the ER		
KEX2		Kexin protease		
KIP2		Kinesin-related motor protein involved in mitotic spindle positioning		
KRE11		Component of transport protein particle complex II		
LAM4	GRAMD1B	StART-like domain containing proteins potentially implicated in non-vesicular sterol transfer		
LAS17	N-WASP	Regulator of actin nucleation	Wiskott–Aldrich syndrome	(Rajmohan, Raodah, Wong, & Thanabalu, 2009)
LCB1	SPTLC1	Component of serine palmitoyltransferas	Neuropathy	(Güntert et al., 2016)

		e		
LEM3	TMEM30B	ER located regulator of Dnf1p and Dnf2p		
LSB6	PI4K2B	Type II phosphatidylinositol 4-kinase that binds WASp	Bipolar Disorder	(Houlihan et al., 2009)
MRS6	CHM/REP1	Rab escort protein	Oncogene	(Yun et al., 2017)
MSB3	TBC1D	Rab GTPase-activating protein	Obesity	(L. Chen et al., 2016)
MSB4	TBC1D	Rab GTPase-activating protein	Obesity	(L. Chen et al., 2016)
MSS4	PIP5K1B	PM associated phosphatidylinositol-4-phosphate 5-kinase	Chronic kidney disease	(Köttgen et al., 2010)
MYO2	MYO5A	Type V myosin motor	Griscelli disease	(Hurvitz et al., 1993)
MYO3	Myosin1	Type I myosin motor		
MYO5	Myosin1	Type I myosin motor		
NTE1	CES1	Serine esterase	Tumor Suppressor	(Verbrugge et al., 2016)

OPI3	PEMT	Transcriptional regulator		
OSH1	OSBP	Member of the oxysterol binding protein related protein family	Tumor Suppressor Ebola	(Burgett et al., 2011; Perreira, Chin, Feeley, & Brass, 2013)
OSH2	OSBP	Member of the oxysterol binding protein related protein family	Tumor Suppressor Ebola	(Burgett et al., 2011; Perreira et al., 2013)
OSH3	ORP3	Member of the oxysterol binding protein related protein family	Tumor Suppressor	(Burgett et al., 2011)
OSH4		Member of the oxysterol binding protein related protein family		
OSH5		Member of the oxysterol binding protein related protein family		
OSH6	ORP5	Member of the oxysterol binding protein related protein family	Tumor Suppressor	(Li, Zheng, Luo, Zhong, & Yan, 2016)
OSH7	ORP8	Member of the oxysterol binding	Tumor Suppressor	(Li et al., 2016)

		protein related protein family		
PAN1	ITSN1	Member of the Pan1p-Sla1p-End3p complex that promotes endocytosis	Down Syndrome	(Herrero-Garcia & O'Bryan, 2017)
PIK1	PI4KB	Golgi and ER associated phosphatidylinositol 4-kinase	Schizophrenia Bipolar disorder	(Houlihan et al., 2009)
PMA1	ATP2C2	Plasma membrane P2-type H+-ATPase		
PRK1	GAK	Serine/threonine protein kinase regulating the cortical actin cytoskeleton	Parkinson's Disease	(Y. P. Chen et al., 2013)
RGA1	CHN1	GTPase-activating protein for Cdc42p	Duane Syndrome	(Miyake et al., 2008)
RGA2	CHN1	GTPase-activating protein for Cdc42p	Duane Syndrome	(Miyake et al., 2008)
RHO1	RHOA	Rho GTPase regulating actin nucleation and cell polarity	Oncogene	(Schmidt et al., 2012)
RHO3	RHOB	Rho GTPase regulating cell polarity	Tumor suppressor	(M. Huang & Prendergast

				, 2006)
ROM2	NET1	Guanine nucleotide exchange factor for Rho1p	Oncogene	(Carr, Zuo, Oh, & Frost, 2013)
RVS161	Amphiphysin	N-BAR domain protein regulating final stages of endocytosis	Tumor Suppressor Alzheimer's Disease	(Prokic, Cowling, & Laporte, 2014)
RVS167	Amphiphysin	N-BAR domain protein regulating final stages of endocytosis	Tumor Suppressor Alzheimer's Disease	(Prokic et al., 2014)
SAC1	SAC1	ER bound Phosphatidylinositol phosphate phosphatase	Amyotrophic lateral sclerosis	(Forrest et al., 2013)
SBH1	SEC61B	Beta subunit of Sec61p ER translocation complex		
SCS2	VAPA	ER-plasma membrane tethering protein implicated in lipid metabolism	Tumor Suppressor	(Bruzzoni-Giovanelli et al., 2015)
SCS22	VAPB	ER-plasma membrane tethering protein implicated in lipid metabolism	ALS	(Teuling et al., 2007)

SEC1	MUNC18	Sm-like protein involved in exocytic vesicle docking	Epilepsy	(Chai et al., 2016)
SEC10	EXOC5	Subunit of the exocyst complex		
SEC14	SEC14-like family	Phosphatidylinositol/phosphatidylcholine transfer protein	Ataxia with vitamin E deficiency	(Mariotti et al., 2004)
SEC15	EXOC6	Subunit of the exocyst complex		
SEC2	RABIN8/ RAB3IP	GEF for Sec4p		
SEC3	EXOC1	Subunit of the exocyst complex		
SEC4	RAB8/ RAB3A	Rab GTPase regulating exocytosis	ADPKD Oncogene	(Bravo-Cordero et al., 2007; Charron, Bacallao, & Wandinger-Ness, 2000)
SEC5	EXOC2	Subunit of the exocyst complex		
SEC6	EXOC3	Subunit of the exocyst complex		
SEC61	SEC61	ER protein		

		translocation channel		
SEC7	ARFGEF1	Guanine nucleotide exchange factor for ADP ribosylation factors		
SEC8	EXOC4	Subunit of the exocyst complex		
SEC9	SNAP25	t-SNARE protein	Epilepsy Alzheimer's	(Noor & Zahid, 2016)
SFH5		Non-classical phosphatidylinositol transfer protein		
SLA1	CIN85	Cytoskeletal protein binding protein. Inhibitor of Las17p	Oncogene	(Samoylenko et al., 2012)
SLA2	HIP1R	Adaptor protein that links actin to sites of endocytosis	Parkinson's Disease	(Pihlstrøm et al., 2013)
SMY1		Kinesin-like protein		
SNC1	VAMP2	Exocytic v-SNARE		
SNC2	VAMP2	Exocytic v-SNARE		
SPO14	PLD2	Phospholipase D	Oncogene	(Su, Chen,

				& Frohman, 2009)
SRO7	LLGL1	Effector of Sec4p that forms a complex with Sec4p and t-SNARE Sec9p	Tumor Suppressor	(W. Yang et al., 2016)
SRO77	LLGL1	Effector of Sec4p that forms a complex with Sec4p and t-SNARE Sec9p	Tumor Suppressor	(W. Yang et al., 2016)
SSO1	STX4	PM t-SNARE		
SSO2	STX4	PM t-SNARE		
STE5		Pheromone-responsive MAPK scaffold protein		
STT4	PI4K2A	PM associated phosphatidylinositol-4-kinase	Schizophrenia	(Kaur et al., 2014)
SYP1	FCHO1/2	Negative regulator of WASp-Arp2/3 complex and involved in endocytic site formation		
SYT1	DAPP1	Guanine nucleotide exchange factor for Arf proteins		

TAT2		High affinity tryptophan and tyrosine permease		
TCB1	E-SYT1	ER-plasma membrane tethering protein		
TCB2	E-SYT2	ER-plasma membrane tethering protein		
TCB3	E-SYT3	ER-plasma membrane tethering protein		
TDH1	GAPDH	Glyceraldehyde-3-phosphate dehydrogenase		
VPH1		Subunit a of vacuolar-ATPase V0 domain		
VPS1	Dynamin	Dynamin motor involved in regulation of endocytosis	Neuropathy Oncogene	(Durieux, Prudhon, Guicheney, & Bitoun, 2010)
YPT1	RAB1	Rab family GTPase involved in ER to Golgi vesicular transport	Oncogene	(X.-Z. Yang et al., 2016)
YPT31	RAB11	Rab family GTPase regulating	Oncogene	(Xu et al., 2016)

		exocytosis		
YPT32	RAB11	Rab family GTPase regulating exocytosis	Oncogene	(Xu et al., 2016)
YSP2	GRAMD1B	StART-like domain containing proteins potentially implicated in non-vesicular sterol transfer		

Table 1. Complete list of genes discussed in this thesis along with known human homologs and associated diseases.

References for appendix list

Bravo-Cordero, J. J., Marrero-Diaz, R., Megías, D., Genís, L., García-Grande, A., García, M. a, … Montoya, M. C. (2007). MT1-MMP proinvasive activity is regulated by a novel Rab8-dependent exocytic pathway. *The EMBO Journal*, *26*(6), 1499–1510. http://doi.org/10.1038/sj.emboj.7601606

Bruzzoni-Giovanelli, H., González, J. R., Sigaux, F., Villoutreix, B. O., Cayuela, J. M., Guilhot, J., … Rousselot, P. (2015). Genetic polymorphisms associated with increased risk of developing chronic myelogenous leukemia. *Oncotarget*, *6*(34), 36269–77. http://doi.org/10.18632/oncotarget.5915

Burgett, A. W. G., Poulsen, T. B., Wangkanont, K., Anderson, D. R., Kikuchi, C., Shimada, K., … Shair, M. D. (2011). Natural products reveal cancer cell dependence on oxysterol-binding proteins. *Nature Chemical Biology*, *7*(9), 639–647. http://doi.org/10.1038/nchembio.625

Carr, H. S., Zuo, Y., Oh, W., & Frost, J. A. (2013). Regulation of focal adhesion kinase activation, breast cancer cell motility, and amoeboid invasion by the RhoA guanine nucleotide exchange factor Net1. *Mol Cell Biol*, *33*(14), 2773–2786. http://doi.org/10.1128/MCB.00175-13

Chai, Y. J., Sierecki, E., Tomatis, V. M., Gormal, R. S., Giles, N., Morrow, I. C., … Meunier, F. A. (2016). Munc 18-1 is a molecular chaperone for alpha-synuclein, controlling its self-replicating aggregation. *Journal of Cell Biology*,

214(6), 705–718. http://doi.org/10.1083/jcb.201512016

Chan, A., Liebow, A., Yasuda, M., Gan, L., Racie, T., Maier, M., … Querbes, W. (2015). Preclinical Development of a Subcutaneous ALAS1 RNAi Therapeutic for Treatment of Hepatic Porphyrias Using Circulating RNA Quantification. *Molecular Therapy. Nucleic Acids*, *4*, e263. http://doi.org/10.1038/mtna.2015.36

Chang, B., Tessneer, K. L., McManus, J., Liu, X., Hahn, S., Pasula, S., … Chen, H. (2015). Epsin is required for Dishevelled stability and Wnt signalling activation in colon cancer development. *Nature Communications*, *6*, 6380. http://doi.org/10.1038/ncomms7380

Charron, a J., Bacallao, R. L., & Wandinger-Ness, a. (2000). ADPKD: a human disease altering Golgi function and basolateral exocytosis in renal epithelia. *Traffic (Copenhagen, Denmark)*, *1*(8), 675–686. http://doi.org/10.1034/j.1600-0854.2000.010811.x

Chen, L., Chen, Q., Xie, B., Quan, C., Sheng, Y., Zhu, S., … Chen, S. (2016). Disruption of the AMPK–TBC1D1 nexus increases lipogenic gene expression and causes obesity in mice via promoting IGF1 secretion. *Proceedings of the National Academy of Sciences*, 201600581. http://doi.org/10.1073/pnas.1600581113

Chen, Y. P., Song, W., Huang, R., Chen, K., Zhao, B., Li, J., … Shang, H. F. (2013). GAK rs1564282 and DGKQ rs11248060 increase the risk for Parkinson's disease in a Chinese population. *J Clin Neurosci*, *20*(6), 880–883. http://doi.org/10.1016/j.jocn.2012.07.011\rS0967-5868(12)00546-2 [pii]

Chistiakov, D. A., Bobryshev, Y. V., & Orekhov, A. N. (2016). Macrophage-mediated cholesterol handling in atherosclerosis. *Journal of Cellular and Molecular Medicine*. http://doi.org/10.1111/jcmm.12689

Davis, J. E., Xie, X., Guo, J., Huang, W., Chu, W.-M., Huang, S., … Wu, G. (2016). ARF1 promotes prostate tumorigenesis via targeting oncogenic MAPK signaling. *Oncotarget*, *7*(26), 39834–39845. http://doi.org/10.18632/oncotarget.9405

Deng, B. C., Lv, S., Cui, W., Zhao, R., Lu, X., Wu, J., & Liu, P. (2012). Novel ATP8B1 mutation in an adult male with progressive familial intrahepatic cholestasis. *World Journal of Gastroenterology*, *18*(44), 6504–6509. http://doi.org/10.3748/wjg.v18.i44.6504

Drouet, V., & Lesage, S. (2014). Synaptojanin 1 mutation in Parkinson's disease brings further insight into the neuropathological mechanisms. *BioMed Research International*, *2014*, 289728. http://doi.org/10.1155/2014/289728

Durieux, A.-C., Prudhon, B., Guicheney, P., & Bitoun, M. (2010). Dynamin 2 and human diseases. *Journal of Molecular Medicine (Berlin, Germany)*, *88*(4), 339–350. http://doi.org/10.1007/s00109-009-0587-4

Duvvuri, U., Shiwarski, D. J., Xiao, D., Bertrand, C., Huang, X., Edinger, R. S., … Gollin, S. M. (2012). TMEM16A induces MAPK and contributes directly to tumorigenesis and cancer progression. *Cancer Research*, *72*(13), 3270–3281. http://doi.org/10.1158/0008-5472.CAN-12-0475-T

Eramo, M. J., & Mitchell, C. A. (2016). Regulation of PtdIns(3,4,5)P3/Akt signalling by inositol polyphosphate 5-phosphatases. *Biochemical Society Transactions*, *44*(1), 240–52. http://doi.org/10.1042/BST20150214

Forrest, S., Chai, A., Sanhueza, M., Marescotti, M., Parry, K., Georgiev, A., … Pennetta, G. (2013). Increased levels of phosphoinositides cause neurodegeneration in a Drosophila model of amyotrophic lateral sclerosis. *Human Molecular Genetics*, *22*(13), 2689–2704. http://doi.org/10.1093/hmg/ddt118

Güntert, T., Hänggi, P., Othman, A., Suriyanarayanan, S., Sonda, S., Zuellig, R. A., … Ogunshola, O. O. (2016). 1-Deoxysphingolipid-induced neurotoxicity involves N-methyl-D-aspartate receptor signaling. *Neuropharmacology*, *110*, 211–222. http://doi.org/10.1016/j.neuropharm.2016.03.033

Herrero-Garcia, E., & O'Bryan, J. P. (2017). Intersectin scaffold proteins and their role in cell signaling and endocytosis. *Biochimica et Biophysica Acta - Molecular Cell Research*. http://doi.org/10.1016/j.bbamcr.2016.10.005

Houlihan, L. M., Christoforou, A., Arbuckle, M. I., Torrance, H. S., Anderson, S. M., Muir, W. J., … Evans, K. L. (2009). A case-control association study and family-based expression analysis of the bipolar disorder candidate gene PI4K2B. *Journal of Psychiatric Research*, *43*(16), 1272–1277. http://doi.org/10.1016/j.jpsychires.2009.05.004

Huang, C. J., Chen, Y. H., & Ting, L. P. (2000). Hepatitis B virus core protein interacts with the C-terminal region of actin-binding protein. *J Biomed Sci*, *7*(2), 160–168. http://doi.org/10.1007/BF02256623

Huang, M., & Prendergast, G. C. (2006). RhoB in cancer suppression. *Histology and Histopathology*.

Hurvitz, H., Gillis, R., Klaus, S., Klar, A., Gross-Kieselstein, F., & Okon, E. (1993). A kindred with Griscelli disease: spectrum of neurological involvement. *European Journal of Pediatrics*, *152*(5), 402–405. http://doi.org/10.1007/BF01955897

Kaur, H., Jajodia, A., Grover, S., Baghel, R., Gupta, M., Jain, S., & Kukreti, R. (2014). Genetic variations of PIP4K2A confer vulnerability to poor antipsychotic response in severely ill schizophrenia patients. *PLoS ONE*, *9*(7). http://doi.org/10.1371/journal.pone.0102556

Köttgen, A., Pattaro, C., Böger, C. A., Fuchsberger, C., Olden, M., Glazer, N. L., … Fox, C. S. (2010). New loci associated with kidney function and chronic kidney disease. *Nature Genetics*, *42*(5), 376–84. http://doi.org/10.1038/ng.568

Li, J., Zheng, X., Luo, N., Zhong, W., & Yan, D. (2016). Oxysterol binding protein-related protein 8 mediates the cytotoxicity of 25-hydroxycholesterol. *Journal of Lipid Research*, *57*(10), 1845–1853.

Mariotti, C., Gellera, C., Rimoldi, M., Mineri, R., Uziel, G., Zorzi, G., … Di Donato, S. (2004). Ataxia with isolated vitamin E deficiency: neurological phenotype, clinical follow-up and novel mutations in TTPA gene in Italian families. *Neurological Sciences : Official Journal of the Italian Neurological Society and of the Italian Society of Clinical Neurophysiology*, *25*(3), 130–137. http://doi.org/10.1007/s10072-004-0246-z

Matokanovic, M., Barisic, K., Filipovic-Grcic, J., & Maysinger, D. (2013). Hsp70 silencing with siRNA in nanocarriers enhances cancer cell death induced by the inhibitor of Hsp90. *European Journal of Pharmaceutical Sciences*, *50*(1), 149–158. http://doi.org/10.1016/j.ejps.2013.04.001

Mendelsohn, J., & Baselga, J. (2003). Status of epidermal growth factor receptor antagonists in the biology and treatment of cancer. *Journal of Clinical Oncology : Official Journal of the American Society of Clinical Oncology*, *21*(14), 2787–99. http://doi.org/10.1200/JCO.2003.01.504

Miyake, N., Chilton, J., Psatha, M., Cheng, L., Andrews, C., Chan, W.-M., … Engle, E. C. (2008). Human CHN1 mutations hyperactivate alpha2-chimaerin and cause Duane's retraction syndrome. *Science*, *321*(5890),

839–43. http://doi.org/10.1126/science.1156121

Mori, M., Li, G., Abe, I., Nakayama, J., Guo, Z., Sawashita, J., … Shumiya, S. (2006). Lanosterol synthase mutations cause cholesterol deficiency-associated cataracts in the Shumiya cataract rat. *Journal of Clinical Investigation*, *116*(2), 395–404. http://doi.org/10.1172/JCI20797

Muhlebach, M. S., Clancy, J. P., Heltshe, S. L., Ziady, A., Kelley, T., Accurso, F., … Sagel, S. D. (2016). Biomarkers for cystic fibrosis drug development. *Journal of Cystic Fibrosis*. http://doi.org/10.1016/j.jcf.2016.10.009

Nikolic, D. S., Lehmann, M., Felts, R., Garcia, E., Blanchet, F. P., Subramaniam, S., & Piguet, V. (2011). HIV-1 activates Cdc42 and induces membrane extensions in immature dendritic cells to facilitate cell-to-cell virus propagation. *Blood*, *118*(18), 4841–4852. http://doi.org/10.1182/blood-2010-09-305417

Noor, A., & Zahid, S. (2016). A review of the role of synaptosomal-associated protein 25 (SNAP- 25) in neurological disorders. *International Journal of Neuroscience*, 01–23. http://doi.org/10.1080/00207454.2016.1248240

Palmer, E. E., Jarrett, K. E., Sachdev, R. K., Al Zahrani, F., Hashem, M. O., Ibrahim, N., … Lagor, W. R. (2016). Neuronal deficiency of ARV1 causes an autosomal recessive epileptic encephalopathy. *Human Molecular Genetics*, ddw157. http://doi.org/10.1093/hmg/ddw157

Perreira, J. M., Chin, C. R., Feeley, E. M., & Brass, A. L. (2013). IFITMs restrict the replication of multiple pathogenic viruses. *Journal of Molecular Biology*. http://doi.org/10.1016/j.jmb.2013.09.024

Pihlstrøm, L., Axelsson, G., Bjørnarå, K. A., Dizdar, N., Fardell, C., Forsgren, L., … Toft, M. (2013). Supportive evidence for 11 loci from genome-wide association studies in Parkinson's disease. *Neurobiology of Aging*, *34*(6). http://doi.org/10.1016/j.neurobiolaging.2012.10.019

Prokic, I., Cowling, B. S., & Laporte, J. (2014). Amphiphysin 2 (BIN1) in physiology and diseases. *Journal of Molecular Medicine*. http://doi.org/10.1007/s00109-014-1138-1

Rajmohan, R., Raodah, A., Wong, M. H., & Thanabalu, T. (2009). Characterization of Wiskott-Aldrich syndrome (WAS) mutants using Saccharomyces cerevisiae. *FEMS Yeast Research*, *9*(8), 1226–1235.

http://doi.org/10.1111/j.1567-1364.2009.00581.x

Romero-Ramirez, L., Cao, H., Nelson, D., Hammond, E., Lee, A. H., Yoshida, H., … Koong, A. C. (2004). XBP1 is essential for survival under hypoxic conditions and is required for tumor growth. *Cancer Research*, *64*(17), 5943–5947. http://doi.org/10.1158/0008-5472.CAN-04-1606

Samoylenko, A., Vynnytska-Myronovska, B., Byts, N., Kozlova, N., Basaraba, O., Pasichnyk, G., … Drobot, L. (2012). Increased levels of the HER1 adaptor protein Rukl/CIN85 contribute to breast cancer malignancy. *Carcinogenesis*, *33*(10), 1976–1984. http://doi.org/10.1093/carcin/bgs228

Schmidt, L. J., Duncan, K., Yadav, N., Regan, K. M., Verone, A. R., Lohse, C. M., … Heemers, H. V. (2012). RhoA as a mediator of clinically relevant androgen action in prostate cancer cells. *Molecular Endocrinology (Baltimore, Md.)*, *26*(5), 716–35. http://doi.org/10.1210/me.2011-1130

Shi, B., Conner, S. D., & Liu, J. (2014). Dysfunction of endocytic kinase AAK1 in ALS. *International Journal of Molecular Sciences*, *15*(12), 22918–22932. http://doi.org/10.3390/ijms151222918

Smid, A., Karas-Kuzelicki, N., Jazbec, J., & Mlinaric-Rascan, I. (2016). PACSIN2 polymorphism is associated with thiopurine-induced hematological toxicity in children with acute lymphoblastic leukaemia undergoing maintenance therapy. *Scientific Reports*, *6*, 30244. http://doi.org/10.1038/srep30244

Sousa, S. B., Jenkins, D., Chanudet, E., Tasseva, G., Ishida, M., Anderson, G., … Moore, G. E. (2014). Gain-of-function mutations in the phosphatidylserine synthase 1 (PTDSS1) gene cause Lenz-Majewski syndrome. *Nature Genetics*, *46*(1), 70–6. http://doi.org/10.1038/ng.2829

Stafa, K., Trancikova, A., Webber, P. J., Glauser, L., West, A. B., & Moore, D. J. (2012). GTPase activity and neuronal toxicity of parkinson's disease-associated LRRK2 is regulated by ArfGAP1. *PLoS Genetics*, *8*(2). http://doi.org/10.1371/journal.pgen.1002526

Stengel, K., & Zheng, Y. (2011). Cdc42 in oncogenic transformation, invasion, and tumorigenesis. *Cellular Signalling*. http://doi.org/10.1016/j.cellsig.2011.04.001

Su, W., Chen, Q., & Frohman, M. A. (2009). Targeting phospholipase D with small-molecule inhibitors as a potential therapeutic approach for cancer

metastasis. *Future Oncology (London, England)*, *5*(9), 1477–86. http://doi.org/10.2217/fon.09.110

Sun, B., Liu, K., Han, J., Zhao, L., Su, X., Lin, B., … Cheng, M.-S. (2015). Design, synthesis, and biological evaluation of amide imidazole derivatives as novel metabolic enzyme CYP26A1 inhibitors. *Bioorganic & Medicinal Chemistry*, *23*(20), 6763–6773. http://doi.org/10.1016/j.bmc.2015.08.019

Teuling, E., Ahmed, S., Haasdijk, E., Demmers, J., Steinmetz, M. O., Akhmanova, A., … Hoogenraad, C. C. (2007). Motor neuron disease-associated mutant vesicle-associated membrane protein-associated protein (VAP) B recruits wild-type VAPs into endoplasmic reticulum-derived tubular aggregates. *The Journal of Neuroscience : The Official Journal of the Society for Neuroscience*, *27*(36), 9801–9815. http://doi.org/10.1523/JNEUROSCI.2661-07.2007

Verbrugge, S. E., Al, M., Assaraf, Y. G., Kammerer, S., Chandrupatla, D. M. S. H., Honeywell, R., … Jansen, G. (2016). Multifactorial resistance to aminopeptidase inhibitor prodrug CHR2863 in myeloid leukemia cells: down-regulation of carboxylesterase 1, drug sequestration in lipid droplets and pro-survival activation ERK/Akt/mTOR. *Oncotarget*, *7*(5), 5240–57. http://doi.org/10.18632/oncotarget.6169

Xu, C. L., Wang, J. Z., Xia, X. P., Pan, C. W., Shao, X. X., Xia, S. L., … Zheng, B. (2016). Rab11-FIP2 promotes colorectal cancer migration and invasion by regulating PI3K/AKT/MMP7 signaling pathway. *Biochemical and Biophysical Research Communications*, *470*(2), 397–404. http://doi.org/10.1016/j.bbrc.2016.01.031

Yang, W., Zhou, C., Luo, M., Shi, X., Li, Y., Sun, Z., … He, J. (2016). MiR-652-3p is upregulated in non-small cell lung cancer and promotes proliferation and metastasis by directly targeting Lgl1. *ONCOTARGET*, *7*(13), 16703–16715. http://doi.org/10.18632/oncotarget.7697

Yang, X.-Z., Li, X.-X., Zhang, Y.-J., Rodriguez-Rodriguez, L., Xiang, M.-Q., Wang, H.-Y., & Zheng, X. F. S. (2016). Rab1 in cell signaling, cancer and other diseases. *Oncogene*, (November 2015), 1–6. http://doi.org/10.1038/onc.2016.81

Yun, U.-J., Sung, J. Y., Park, S.-Y., Ye, S.-K., Shim, J., Lee, J.-S., … Kim, Y.-N. (2017). Oncogenic role of rab escort protein 1 through EGFR and STAT3 pathway. *Cell Death & Disease*, *8*. http://doi.org/10.1038/cddis.2017.50

Appendix B.

List of Video Files

Full description of video files is found under **Supplemental Movies and Legends**, p. 156

supplementalmovies1.mp4
supplementalmovies2.mp4
supplementalmovies3.mp4
supplementalmovies4.mp4
supplementalmovies5.mp4